



1999 ANNUAL PROGRESS REPORT
ENERGY CONVERSION TEAM

U.S. Department of Energy

Energy Efficiency and
Renewable Energy

Office of Transportation
Technologies

Office of Advanced
Automotive Technologies

FUEL CELLS FOR TRANSPORTATION

A C K N O W L E D G E M E N T

We would like to express our sincere appreciation to Argonne National Laboratory and Computer Systems Management, Inc., for their artistic and technical contributions in preparing and publishing this report.

In addition, we would like to thank all our program participants for their contributions to the programs and all the authors who prepared the project abstracts that comprise this report.

This document highlights work sponsored by agencies of the U.S. Government. Neither the U.S. Government nor any agency thereof, nor any of their employees, makes any warranty, express or implied, or assumes any legal liability or responsibility for the accuracy, completeness, or usefulness of any information, apparatus, product, or process disclosed, or represents that its use would not infringe privately owned rights. Reference herein to any specific commercial product, process, or service by trade name, trademark, manufacturer, or otherwise does not necessarily constitute or imply its endorsement, recommendation, or favoring by the U.S. Government or any agency thereof. The views and opinions of authors expressed herein do not necessarily state or reflect those of the U.S. Government or any agency thereof.

**U.S. Department of Energy
Office of Advanced Automotive Technologies
1000 Independence Avenue, S.W.
Washington, DC 20585-0121**

FY 1999

Progress Report for Fuel Cells for Transportation

**Energy Efficiency and Renewable Energy
Office of Transportation Technologies
Office of Advanced Automotive Technologies
Energy Conversion Team**

Steven Chalk

Energy Conversion Team Leader

October 1999

CONTENTS

	<u>Page</u>
I. INTRODUCTION	1
II. FUEL CELL POWER SYSTEM DEVELOPMENT	9
A. Atmospheric Fuel Cell Power System for Transportation	9
B. Pressurized Fuel Cell Power System for Transportation	12
C. Cost Analyses of Fuel Cell Stack/Systems	16
D. PEM Systems Modeling and Analysis	19
III. FUEL PROCESSING SUBSYSTEM	23
A. Advanced Fuel-Flexible Fuel Processor Development SFAA for Next Millennium Fuel Processor™ for Transportation Fuel Cell Power System	23
B. Multifuel Processor for Fuel Cell Electric Vehicle Applications	28
C. Fuel-Flexible, UOB™ Fuel Processor System Development and Status	30
D. Integrated Fuel Processor Development	34
E. Microchannel Fuel Processor Components	37
F. On-Board Hydrogen Generation Technology	42
G. R&D on a Novel Breadboard Device Suitable for Carbon Monoxide Remediation in an Automotive PEM Fuel Cell Power Plant	48
H. Reformate Cleanup Technology	51
I. Evaluation of Partial Oxidation Fuel Cell Reformer Emissions	57
J. Catalytic Partial Oxidation Reforming Materials and Processes	60
K. Alternative Water-Gas Shift Catalyst Development	63
IV. FUEL CELL STACK SUBSYSTEM	67
A. R&D on a 50-kW, High-Efficiency, High-Power-Density, CO-Tolerant PEM Fuel Cell Stack System	67
B. Development of Advanced, Low-Cost PEM Fuel Cell Stack and System Design for Operation on Reformate Used in Vehicle Power Systems	71
C. Direct Methanol Fuel Cells	77
D. Efficient Fuel Cell Systems	80
V. PEM STACK COMPONENT COST REDUCTION	85
A. High-Performance, Low-Cost Membrane Electrode Assemblies for PEM Fuel Cells and Integrated Pilot Manufacturing Processes	85
B. Low-Cost, High Temperature, Solid Polymer Electrolyte Membrane for Fuel Cells	89

CONTENTS (Cont.)

	<u>Page</u>
C. Nanopore Inorganic Membranes as Electrolytes in Fuel Cells.....	94
D. Development and Optimization of Porous Carbon Papers Suitable for Gas Diffusion Electrodes	97
E. Optimized Electrodes for PEM Operation on Reformate/Air	100
F. New Alloy Electrocatalysts and Electrode Kinetics.....	104
G. Cathode Catalysts.....	107
H. Development of a \$10/kW Bipolar Separator Plate	110
I. Layered PEM Stack Development	113
J. Corrosion Test Cell for Metallic Bipolar Plate Materials	117
VI. AIR MANAGEMENT SUBSYSTEMS.....	121
A. Turbocompressor for PEM Fuel Cells	121
B. Development of a Scroll Compressor/Expander Module for Pressurization of 50-kW Automotive Fuel Cell Systems	124
C. Fuel Cell Power System - Critical Components for Transportation Development of Compact Air, Heat, and Water Management Systems: Variable Delivery Compressor/Expander Development.....	127
D. Electrically Boosted Gas-Bearing Turbocompressor for Fuel Cells	131
VII. HYDROGEN STORAGE	135
A. High-Pressure Conformable Hydrogen Storage for Fuel Cell Vehicles.....	135
B. Advanced Chemical Hydride Hydrogen Generation/Storage System for PEM Fuel Cell Vehicles	140
APPENDIX A: ACRONYMS, INITIALISMS, AND ABBREVIATIONS	145

I. INTRODUCTION

Developing Advanced PEM Fuel Cell Technologies for Transportation



Patrick Davis
Program Manager

On behalf of the Department of Energy’s Office of Advanced Automotive Technologies (OAAT), we are pleased to introduce the Fiscal Year (FY) 1999 Annual Progress Report for the Fuel Cells for Transportation Research and Development (R&D) Program. This introduction serves to briefly outline the nature, progress, and future directions of the program. The past year has been a very exciting one for fuel cell technology; major automotive and fuel cell companies have announced technology breakthroughs, development vehicles, partnerships, and new initiatives. The Department of Energy (DOE) continues to contribute to this progress in a significant way by supporting research and development activities that address the most critical barriers to the introduction of commercially viable proton-exchange-membrane (PEM) fuel cell systems.



Donna Lee Ho
Program Manager

The mission of the Fuel Cells for Transportation R&D Program is to develop highly efficient, low- or zero-emission automotive fuel cell propulsion systems. DOE has selected the PEM fuel cell as its leading technology candidate because of its high power density, quick start-up capability, and simplicity of construction.

The Program supports the Partnership for a New Generation of Vehicles (PNGV), a cooperative research and development partnership between the federal government and the United States Council for Automotive Research, which comprises Ford, General Motors, and DaimlerChrysler. One of the objectives of PNGV is to develop, by 2004, a mid-sized passenger vehicle capable of achieving a gasoline-equivalent fuel economy of 80 miles per gallon (mpg) while adhering to future emissions standards and maintaining such attributes as performance, comfort, and affordability. PNGV has targeted PEM fuel cell power systems as one of the promising technologies for achieving 80-mpg fuel economy in a light-weight, mid-size passenger vehicle.



JoAnn Milliken
Program Manager

While this report specifically documents the progress made by the Fuel Cells for Transportation R&D Program, we are pleased to note the many major and diverse fuel cell technology advancements that have received international

recognition throughout the year. These advancements have taken many forms – development cars (Ford’s Fuel Cell P2000, DaimlerChrysler’s NECAR 4, General

Zafira), stationary power advances, laboratory announcements, and even new business ventures. For instance, the California Fuel Cell Partnership, a program that was announced earlier this year, reflects the high level of interest by industry and state

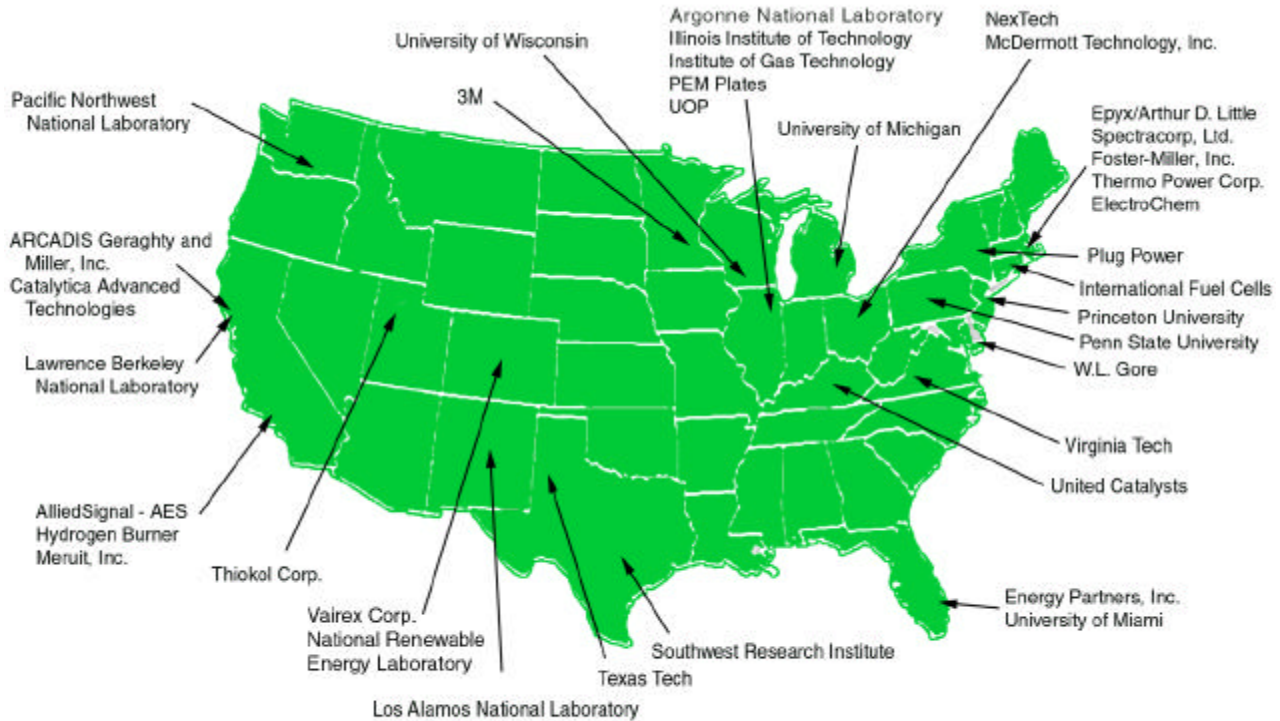


General Motors’ Zafira Fuel Cell Minivan

governments in accelerating the development of fuel cell vehicles. The Partnership's members represent the confluence of interested parties, including fuel cell and automotive concerns (Ballard, DaimlerChrysler, and Ford), the energy industry (ARCO, Shell Oil, and Texaco), and state government (California Energy Commission and the California Air Resources Board). The Partnership has plans to place about 50 fuel cell vehicles — cars and buses — on the road between 2000 and 2003. Aggressive plans like these demonstrate that fuel cell technology may play a major role in our nation's transportation future.



The Program is implemented through cost-shared contracts with automakers, automotive suppliers, and fuel cell and component developers. Furthermore, DOE National Laboratories and universities throughout the U.S. conduct research and development that increases the knowledge base of the emerging PEM fuel cell technology.



Fuel Cells for Transportation Program Participants

Meeting the Challenges

An extensive gasoline and petroleum-based fuels infrastructure exists in the United States today. The Department of Energy believes that the successful early introduction and acceptance of automotive fuel cells is dependent on fuel-flexible fuel cell systems, systems that run on both conventional and alternative fuels. However, to reach the goal of a commercially viable fuel-flexible fuel cell system, many technological challenges remain.

The commercial viability of the fuel-flexible fuel cell system remains closely associated with its cost competitiveness. Currently, the cost of the automotive fuel cell system is estimated at ten times higher than that needed to be competitive with the internal combustion engine. To meet the challenges of lowering system costs, the Fuel Cells for Transportation R&D Program strives to develop components with lower-cost materials, advanced manufacturing processes, and higher operating efficiency.

In addition, technologies associated with fuel cell systems (i.e., fuel-flexible fuel processors, low-cost bipolar plates, compact and efficient compressors, etc.) require that technological challenges be resolved. Fuel cell system performance must be the same as, if not better than, that of current automobile engines. The on-board fuel processor, for example, faces technological challenges in meeting response targets both for system start-up and during operation. Barriers associated with complete system integration include overall performance, weight, size, and durability.

R&D Highlights

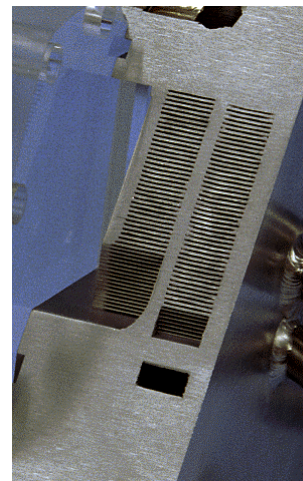
Researchers supporting the Fuel Cells for Transportation R&D Program made significant progress in meeting these challenges. In FY 1999, technological advances were made in systems development, in fuel-processing technology, and in the development of low-cost, high-volume manufacturing processes for key components. The following summaries represent a few selected highlights of the progress made under the program.

System Integration. To convert gasoline or other petroleum-based fuels into pure hydrogen, the fuel cell system must include a fuel processor. During FY 1999, Plug Power teamed with Epyx to successfully integrate and operate a 10-kW fuel cell stack, using an advanced, fuel-flexible fuel processor. The integration test achieved 10 kW_e of electrical output and met the project's interim system efficiency targets while operating on low-sulfur gasoline, methanol, ethanol, naphtha, and other fuels. Appropriate operational experience gained with this test can be incorporated into the next phases of the project. Seven different fuels were used in the test, and all demonstrated very low emissions. It is anticipated that Super Ultra Low Emission Vehicle (SULEV) standards should be achievable with a gasoline fuel cell power system.



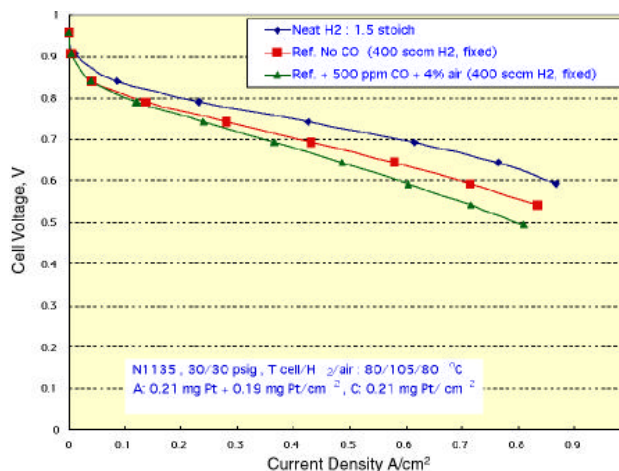
Fuel Cell Stack Subsystem

Microchannel Fuel Processor. At Pacific Northwest National Laboratory (PNNL), researchers are developing components for the onboard, automotive production of hydrogen from liquid hydrocarbons, using a newly developed microfabrication method to produce extremely compact hardware with high throughputs. During FY 1999, the PNNL researchers developed and conducted proof-of-concept demonstrations of a steam reforming microchannel reactor. This demonstration shows the feasibility of this concept of steam reforming of gasoline by yielding a hydrogen concentration in excess of 65%. It is anticipated that a complete microchannel fuel processing system could occupy less than 0.25 ft³ volume for a 50-kW application, one-tenth the size of conventional fuel processing technology.



Cutaway View of PNNL Microchannel Fuel Vaporizer

CO Tolerance Electrode. Los Alamos National Laboratory (LANL) is working on electrode optimization to achieve maximum performance in PEM fuel cells under conditions appropriate for reformat/air operation, using methods that meet cost and efficiency targets for transportation applications. One very important aspect of this work is the identification of new catalysts and operating conditions that improve the tolerance of the PEM fuel cell to CO in reformat fuel from a fuel processor. As little as 10 ppm CO in reformat fuel can poison conventional platinum catalysts in state-of-the-art fuel cells, putting very stringent performance requirements on the fuel processor. Using newly developed catalysts and a reconfigured anode, researchers at LANL were able to demonstrate nearly complete tolerance to 500 ppm CO in reformat fuels. They also demonstrated that the negative effects of 100 ppm CO in reformat on fuel cell performance could be eliminated with as little as 0.5% air bleed to the anode with an optimized membrane electrode assembly (reconfigured electrode, 0.6 mg/cm² anode Pt loading).



LANL Polarization Curves Showing Nearly Complete Tolerance to 500 ppm CO in Reformat

CO Cleanup Catalysts. Argonne National Laboratory is developing new catalysts for the water-gas shift reaction – an important fuel processing step that increases hydrogen content while lowering CO. Argonne researchers developed a breakthrough bifunctional catalyst that works effectively at a wide range of temperatures and is not damaged by exposure to air. Argonne also increased by a factor of three the catalyst’s ability to react at 230°C, while simultaneously reducing the expensive precious metal content by 50 percent. Comparing data obtained from Argonne’s catalyst testing with published data from commercial catalyst manufacturers indicates that this catalyst could reduce the total volume of the water-gas shift reactor by 30 percent.



3M's Three-Layer Catalyst-Coated Membrane

Low Cost MEA Manufacturing. 3M is developing an integrated pilot process for the low-cost manufacture of high-performance, high-quality membrane electrode assemblies (MEAs). In a major accomplishment, 3M demonstrated the feasibility of scaling up the fabrication of its proprietary thin-film catalyst and the continuous formation of three-layer catalyst-coated membrane material, producing 15 meters of material with 99.3% of the catalyst transferred and an excellent material uniformity.

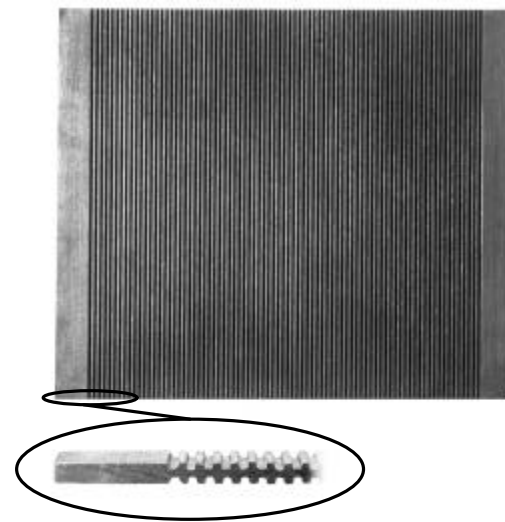
Low-Cost Bipolar Plate Manufacturing. Research at the Institute of Gas Technology (IGT) and subcontractor PEM Plates also contributed to reducing manufacturing costs through the development of a molded composite graphite

bipolar separator plate that achieves a projected manufacturing cost of less than \$10/kW while meeting all of the DOE performance specifications. To evaluate the various steps in the molding process, PEM Plates assembled a pilot production line with a molding capacity of five plates per hour. This pilot line will provide an understanding of the key steps in preparation of the composite blend, transferring the blend to the mold, forming the plates, releasing the plates from the molds, post-molding operations, and quality control. As a result of the molded graphite bipolar plate development, several fuel cell stack developers have requested plates molded to their design specifications.

Achievements and Awards

The Vice President's Partnership for a New Generation of Vehicles (PNGV) Medal.

Fifteen scientists from the DOE National Laboratories, the automobile industry, and automotive suppliers were honored at the White House on March 17, 1999, with the PNGV Medal. The research team was honored for several fuel processing accomplishments, including being the first to develop and demonstrate a system that would permit use of gasoline and other available fuels, such as methanol, ethanol, or natural gas, in fuel cell-powered vehicles. By developing and demonstrating a fuel-flexible system, the scientists removed a major barrier to the application of fuel cell technology in automobiles. The Medal winners were selected by a panel of five judges for research involving government-industry teamwork and resulting in a significant technical accomplishment in PNGV-related automotive technology.



Typical IGT Molded Composite Graphite Plate Flowfield

R&D 100 Award. Pacific Northwest National Laboratory received an R&D 100 Award from *R&D Magazine* during FY1999 for the microchannel gasoline vaporizer. Identified as one of the 100 most technologically significant new products of the year, this unit, which consists of a microchannel reactor and a microchannel heat exchanger, vaporizes the gasoline stream for a 50-kWe fuel processing/fuel-cell system. Heat for

vaporization is provided through the internal, catalytic combustion of low-concentration hydrogen from the fuel cell anode. The unit weighs only four pounds and occupies a volume of only 0.01 ft³, one-tenth the volume of conventional vaporizers.

Future Directions

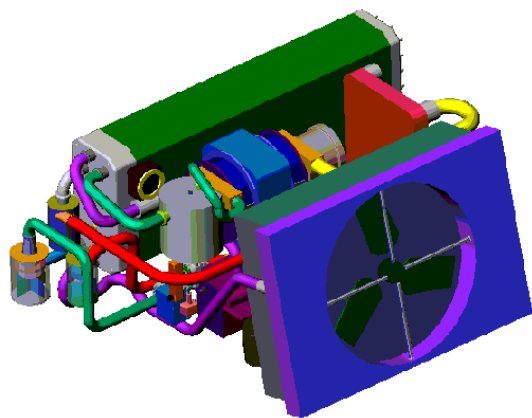
While we are very encouraged by the technical progress realized in FY 1999 under the Fuel Cells for Transportation R&D Program, we are also well aware of the significant challenges still ahead of us. We will continue to work diligently and steadfastly with our government and industry partners to address the technological barriers. In the forthcoming year, we will research the issues of cost, output, size, weight, and durability.



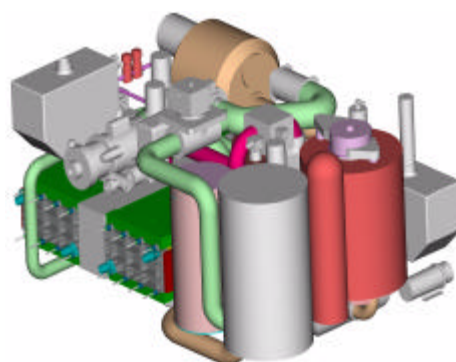
Researchers Honored for Fuel Cell Fuel-Processor Technology

During FY 2000, researchers at Argonne National Laboratory will continue to improve the performance of fuel-flexible fuel processors. Los Alamos National Laboratory will continue to develop improved electrodes for reformat/air fuel cells, as well as CO cleanup technology for fuel processors. We are also looking forward to the completion of stack subsystems from Energy Partners and AlliedSignal and integrated systems from Plug Power and International Fuel Cells.

The beginning of FY 2000 will also signal the start of 10 new projects. Work will begin in such areas as autothermal fuel processing, advanced high-volume MEA manufacturing, high-temperature membrane development, novel fuel cleanup devices, and compressor technology. Through these efforts and other related projects, researchers in the Fuel Cells for Transportation R&D Program will continue to achieve improvements in cost, durability, efficiency, and overall system performance, allowing us to move closer to the commercial availability of fuel cell vehicles.

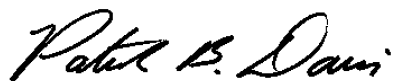


Energy Partners' 50-kW Fuel Cell Stack Subsystem

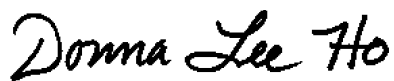


International Fuel Cells' 50-kW Integrated System

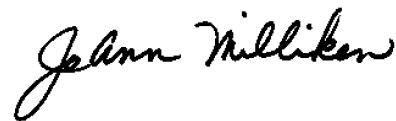
The remainder of this report presents project abstracts that highlight progress achieved during FY 1999 under the Fuel Cells for Transportation R&D Program. The abstracts summarize both industry and national laboratory projects, providing an overview of the work being conducted to overcome the technical barriers associated with the development of fuel cell power systems.



Patrick Davis
Energy Conversion Team
Office of Advanced Automotive
Technologies



Donna Lee Ho
Energy Conversion Team
Office of Advanced Automotive
Technologies



JoAnn Milliken
Energy Conversion Team
Office of Advanced Automotive
Technologies

II. FUEL CELL POWER SYSTEM DEVELOPMENT

A. Atmospheric Fuel Cell Power System for Transportation

Murdo J. Smith

International Fuel Cells

195 Governor's Highway

South Windsor, CT 06074

(860) 727-2269, fax: (860) 727-2399, e-mail: smithmu@ifc.utc.com

DOE Program Manager: Patrick Davis

(202) 586-8061, fax: (202) 586-9811, e-mail: patrick.davis@ee.doe.gov

ANL Technical Advisor: Walter Podolski

(630) 252-7558, fax: (630) 252-4176, e-mail: podolski@cmt.anl.gov

Contractor: International Fuel Cells, South Windsor, Connecticut

Prime Contract No. DE-AC02-99EE50567

Objective

The objective of this project is to deliver to DOE a 50-kW-equivalent gasoline fuel processing system and a fully integrated, gasoline-fueled 50-kW PEM power plant for functional demonstration testing. Although focused on gasoline operation, the fuel processing system will utilize fuel-flexible reforming technology that can be modified to accommodate such fuels as methanol, ethanol, and natural gas. The initial demonstration testing of each of the units will be performed at IFC. After IFC testing, each unit will be delivered to Argonne National Laboratory for additional operational tests by DOE.

OAAT R&D Plan: Tasks 5, 8, and 11; Barrier J

Approach

- Deliver and test autothermal fuel processor.
- Deliver and test ambient-pressure integrated power subsystem.

Accomplishments

New start in late FY 1999.

Future Directions

- Advanced PEM fuel cell power plant system capable of operation on gasoline or such alternative transportation fuels as methanol, ethanol, and natural gas
 - Integrated power subsystems meeting the physical and operational characteristics necessary for automobile applications
-

Introduction

International Fuel Cells (IFC) is committed to the commercialization of PEM fuel cell power plants for transportation applications. A program is in place that addresses technology development and the verification of each of the necessary components and subsystems and, ultimately, the fully integrated power plant itself. The focus of IFC's program is an ambient-pressure PEM power plant system operating on gasoline fuel and delivering 50 kW net dc power to the automotive electrical system.

Project Deliverables

Under the contract, IFC will deliver to DOE a 50-kW-equivalent gasoline fuel processing system and a 50-kW PEM power plant.

Planned Approach

Fuel Processing System

The gasoline fuel processing system (FPS) consists of an autothermal fuel reformer, a shift converter, a selective oxidizer, a fuel desulfurizer, and the balance-of-plant equipment and controls necessary to operate the system. The FPS is sized to provide sufficient hydrogen to meet the requirements of the PEM fuel cell to generate 50 kW of electrical dc power. The gas composition produced by the FPS will be consistent with the long-term operating requirements of the fuel cell, including CO levels of 50 parts per million or less.

Figure 1 shows a test article that integrates the autothermal reformer (ATR) with its associated process heat exchangers. ATR testing has demonstrated 98% fuel conversion with carbon-free operation. Figure 2 shows the low-temperature shift converter (LTSC) test article. The LTSC design is based on over 3 million hours of operation in IFC's stationary power plant. It is a low-temperature design with a CO output level of less than 1%. Several models of each of these components have been tested, confirming their operation while providing opportunities for reductions in both weight and volume. Similar development programs are under way for the fuel desulfurizer and selective oxidizer components.

Figure 3 shows a conceptual arrangement of the FPS as a stand-alone test unit. The objective is to maintain the physical arrangement of the

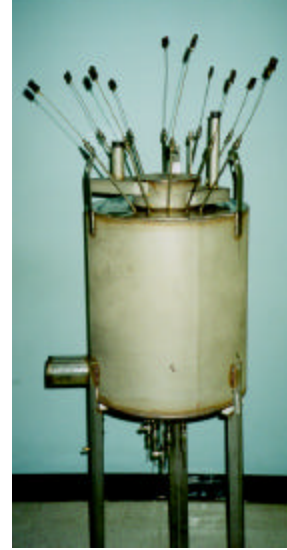


Figure 1. Integrated autothermal reformer test article.



Figure 2. Low-temperature shift converter test article.

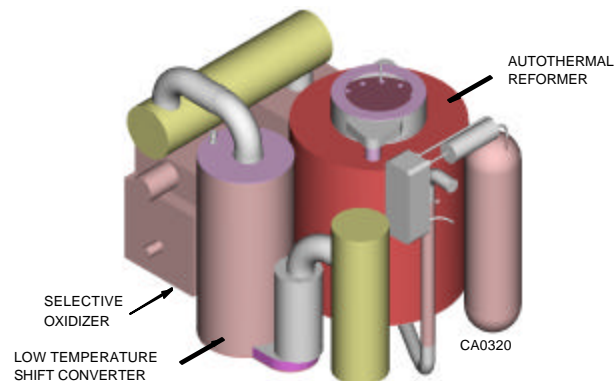


Figure 3. Conceptual 50-kWe fuel processor system.

components as close to the power plant arrangement as possible.

50-kW Power Plant

Figure 4 provides a schematic of the gasoline fuel cell power plant. The major subsystems include the Fuel Processing Subsystem, the Power Subsystem, and the Balance of Plant. The Balance of Plant includes the Thermal Management Subsystem, the Air and Water Subsystems, the Controller, and associated electrical equipment.

The 50-kW Power Subsystem comprises two 25-kW PEM ambient-pressure Cell Stack Assemblies (CSAs). Stack endurance tests on simulated reformat with CO have been completed,

with stack performance exceeding the program goals throughout the test period, as shown in Figure 5.

Figure 6 shows the 15% reduction in cell stack size that has been achieved. The greater portion of the advancement resulted from improved cell performance. A thinner cell design has also been developed and incorporated into the design base. Two 25-kW CSAs are joined to achieve the 50-kW rating of the Power Subsystem.

Figure 7 is a conceptual drawing of the fully integrated 50-kW power plant. As shown, the major gasoline processing system components are close-coupled on the right-hand side of the picture. The power subsystem and the thermal management and air supply systems are located on the left-hand side.

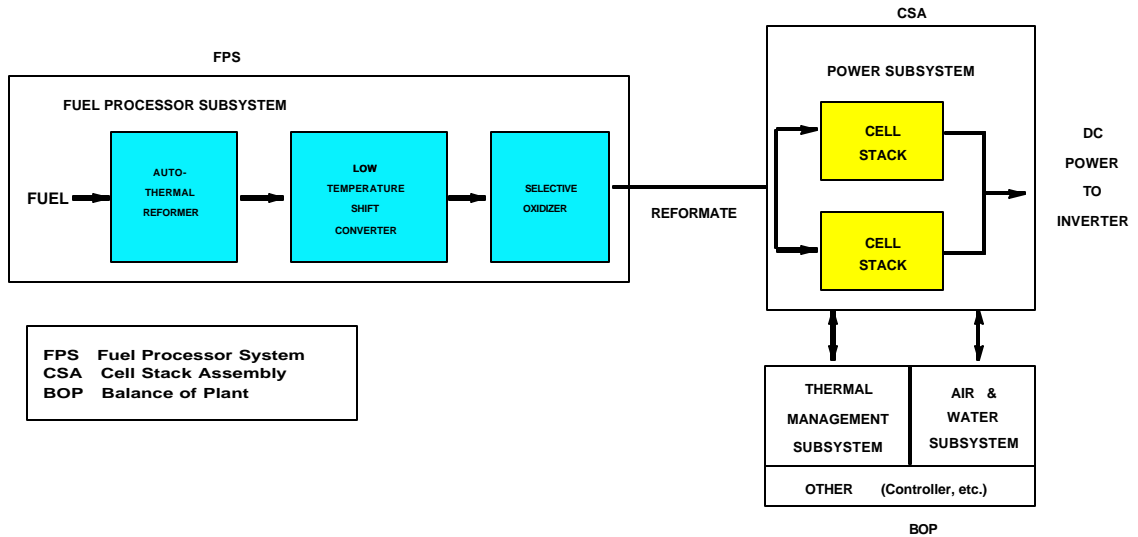


Figure 4. Power plant schematic.

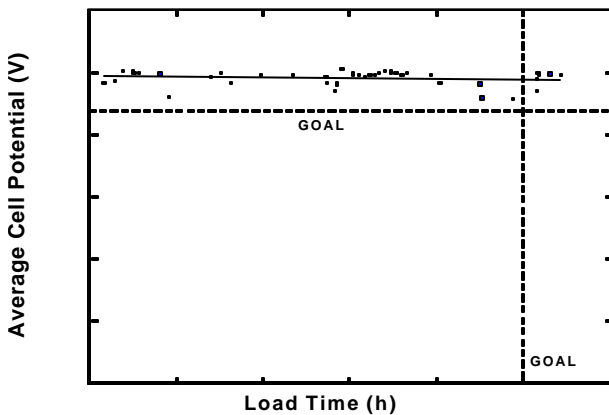


Figure 5. Cell stack endurance.

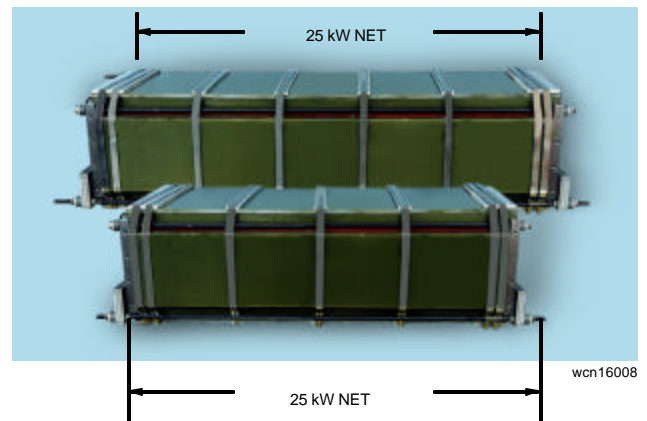


Figure 6. CSA advancement.

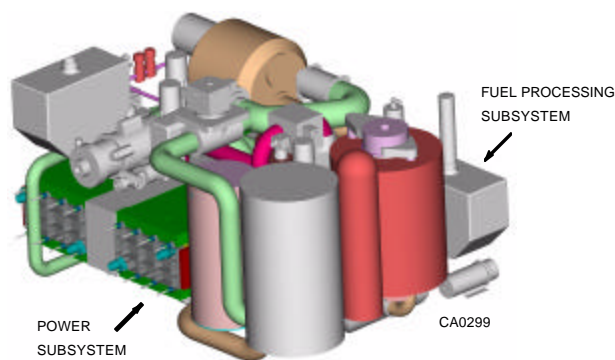


Figure 7. Conceptual 50-kW power plant.

Conclusions

IFC is committed to the commercialization of PEM fuel cell power plants for transportation applications. The focus of IFC's program is an ambient-pressure PEM power plant system operating on gasoline fuel. Under this new start, IFC will deliver to DOE a 50-kW-equivalent gasoline fuel processing system utilizing fuel-flexible reforming technology and a fully integrated gasoline-fueled 50-kW PEMFC power system for functional demonstration testing.

B. Pressurized Fuel Cell Power System for Transportation

William D. Ernst

Plug Power, LLC

Latham, NY 12110

(518) 782-7700, fax: (518) 782-7914

DOE Program Manager: Donna Lee Ho

(202) 586-8000, fax: (202) 586-9811, e-mail: donna.ho@ee.doe.gov

ANL Technical Advisor: Walter Podolski

(630) 252-7558, fax: (630) 252-4176, e-mail: podolski@cmt.anl.gov

Contractor: Plug Power, LLC, Latham, New York 12110

Prime Contract No. DE-FC02-97EE50472, September 30, 1997-August 30, 2000

Major Subcontractor: Epyx Corporation, Cambridge, MA 02140

Objectives

- Research and develop a fully integrated fuel cell system that operates on common transportation fuels (gasoline, methanol, ethanol, and natural gas) for automotive applications.
- Deliver a fully integrated 50-kW_e net polymer electrolyte membrane or proton exchange membrane (PEM) fuel cell stack with balance-of-plant (BOP) components, and a 50-kW_e (equivalent) fuel-flexible reformer.
- Provide test data evaluating the system for vehicle propulsion under driving cycle profiles.

OAAT R&D Plan: Tasks 5, 8, and 11; Barriers A, B, C, D, E, F, G, H, and J

Approach

- The integrated fuel cell system is being pursued in four phases:
 - Phase I: Define overall system; build and demonstrate a 10-kW_e system.
 - Phase II: Develop components for 50-kW_e system.
 - Phase III: Integrate all components into 50-kW_e brassboard system.

- Phase IV: Build and test integrated 50-kW_e power system in a test stand.

Accomplishments

- Successfully operated an integrated, multifuel-powered fuel cell (FC) system (at the 10-kW level) and obtained steady-state emissions data.
- Developed capability to build large fuel cell stacks.
- Built and tested 40-kW_e hydrogen-powered FC system. Demonstrated operation on Federal Urban Driving Standard (FUDS) cycle and rapid startup of stack from ambient temperature.

Fuel Cell Power System

(including fuel processor, stack and auxiliaries; excluding gasoline tank and DC-DC converter)

Characteristic	Status	DOE Technical Target
Net Power (kW _e)	50	50
Energy Efficiency @ 25% Peak Power (%)	40 (predicted)	40
Power Density (W/L)	250 (predicted)	250
Specific Power (W/kg)	250 (predicted)	250
Durability (hours)	2000 (predicted)	2000

Future Directions

- Develop an integrated system to increase fuel cell and fuel processor efficiency and to improve overall system power density.
 - Build and test a 50-kW_e, integrated gasoline-powered fuel cell system (brassboard level).
 - Build and test a tightly integrated 50-kW_e gasoline-powered fuel cell system.

Introduction

There are four phases to this program. Phase I is to develop fundamental knowledge regarding the individual components in the fuel cell system, culminating with the integration of a 10-kW_e net PEM fuel cell stack with a partial oxidation fuel processor. Phase II involves the development of components at the 50-kW_e level, followed by brassboard system integration of the various components in Phase III. In Phase IV, a completely integrated, compact 50-kW_e system will be built that incorporates the results of Phase III testing; this system will be used for performance and emissions testing.

Phase I was completed during FY 1998. Phase II was completed during FY 1999, and Phase III is currently in progress. In general, FY 1998 activities were focused on fundamental hardware development, while FY 1999 activities have been focused primarily on system operation and optimization.

While the fuel cells and subsystems will be designed and developed by Plug Power, Epyx, Inc., will provide the fuel processor. Plug Power will integrate the Epyx fuel processor into the overall fuel cell system.

Phase II Program Results

During FY 1999, Plug Power developed manufacturing techniques to enable construction of large (up to 50 kW) fuel cell stacks. Large stacks were built, using both stainless steel and carbon composite plates. Improved sealing techniques contributed significantly to the success of stack construction. Alternative stack clamping techniques were also developed in FY 1999.

Durability of stacks was proven out during FY 1999. Stacks built for this DOE program have been cycled thousands of times through pressure swings ranging from 1 to 3 atm. A 40-kW stack was started at room temperature and brought to 23 kW in less than a second (Figure 1).

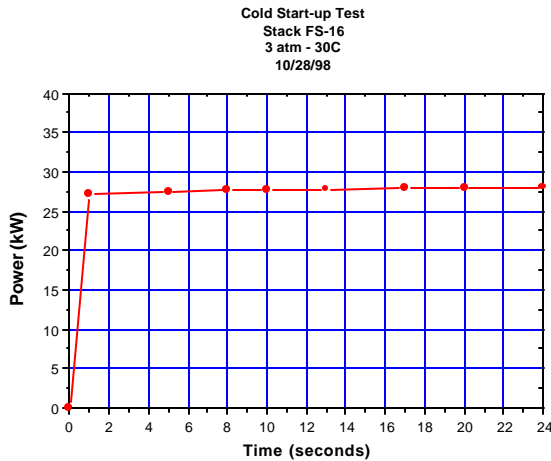


Figure 1. Startup of a 40-kW fuel cell stack.

Efforts were made during FY 1999 to optimize stack performance. An important step toward optimizing large stack performance is to accurately predict performance by using smaller stacks. Figure 2 compares the performance of several small stacks (operated on synthetic reformat) with that of a 10-kW stack that was operated on actual reformat produced by the Epyx fuel processor.

Significant gains were made during FY 1999 in the area of BOP and controls. In order for fuel cell systems to be efficient, reactants need to be delivered to the fuel cell stack at constant stoichiometries throughout the stack's operating range. The control system must be able to respond in a load following mode.

A major portion of FY 1999's effort was to build and test an automated test stand to deliver reactants at near-constant stoichiometries for a 40-kW_e stack.

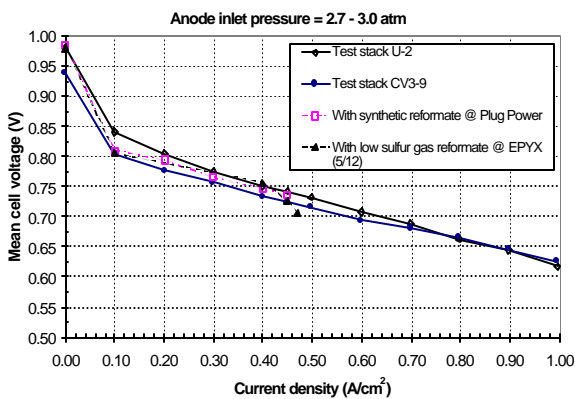


Figure 2. Comparison of stack performance with synthetic and real reformat.

This system successfully followed a FUDS cycle in load-following mode. The peak load transient, illustrated in Figure 3, shows excellent agreement between demanded and actual performance. The lag between load demand and actual output is due to a 0.62-second instrumentation lag.

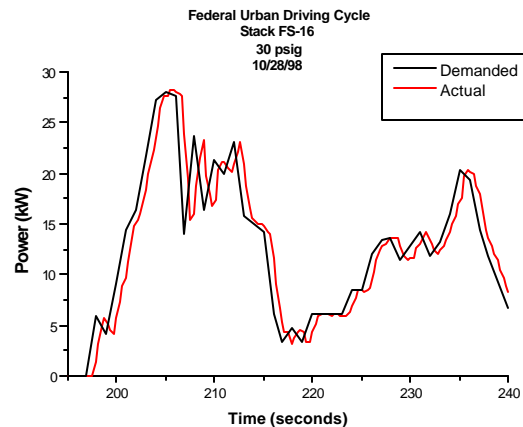


Figure 3. Peak load point on FUDS cycle.

Second 10-kW Integration

A second integrated test of a fuel cell and a gasoline-powered fuel processor was carried out in May 1999. This integration achieved all the intended goals: attain 10 kW_e output at design stoichiometry levels, meet interim system efficiency targets (low 30% range), demonstrate multifuel (7 fuels) operation, and gain operational experience that can be incorporated into the Phase III and Phase IV 50-kW_e systems. The fuels tested were ethanol, methanol, methane, Fischer-Tropsch synthetic gasoline, M-85, low-sulfur gasoline, and California Phase II gasoline.

The second 10-kW_e integration was successful due to the following:

- Extensive integration of the fuel cell and fuel processor systems,
- Improved fuel processor performance [higher H₂ concentration and very low CO levels (typically <10 ppm)], and
- Increased operational experience with both stacks and BOP.

Operational experience gained during the 10-kW_e integration included effects of operating pressures and temperatures, as well as humidification techniques.

Phase III

Components developed during Phases I and II are being integrated into a 50-kW_e brassboard system. In Phase III, the fuel cell and fuel processor will be built on individual skids and connected together. The interface points between the fuel cell stack subsystem and the Epyx fuel processor subsystem have been identified for the integrated system design. At each interface point, the necessary fluid state, flow, and thermal conditions have been defined. The overall system operating strategy has also been established. The key points are that (1) the operating pressure varies from 3.1 atm at maximum power to 2.2 atm at 1/4 power, (2) the water management system will be a closed loop, and (3) the reformate will be provided to the fuel cell stack fully saturated. The net effects of these conditions are better maintenance of water balance within the fuel cells and improved power density of the system.

Future Work

The remainder of this program will focus primarily on systems integration and operation. Stack development continues during Phase III in order to achieve higher power densities and reduced pressure drop across the stack. Two development approaches are being taken in these efforts.

Upon completion of Phase III testing, the Phase IV design will begin. Test results from Phase III will be used to optimize component selection for Phase IV. The Phase IV system will consist of a single design (one set of schematics) and will be built on one compact skid. Upon completion of qualification testing at Plug Power, the Phase IV system will be delivered to Argonne National Laboratory.

References

1. W.D. Ernst, "Plug Power Fuel Cell Development Program," DOE Automotive Technology Development Customers' Coordination Meeting, Dearborn, Mich., Oct. 27-30, 1997.
2. W.D. Ernst, "PEM Fuel Cell Stack Development for Automotive Applications," Fuel Cell Seminar, Orlando, Fla., Nov. 17-20, 1996.
3. W. Ernst, J. Law, J. Chen, and W. Acker, "PEM Fuel Cell Power Systems for Automotive Applications," Fuel Cell Seminar, Palm Springs, Calif., Nov. 1998.
4. W.D. Ernst, "Reformate-Fueled PEM Fuel Cells," SAE Fuel Cells for Transportation TOPTEC, Cambridge, Mass., March 18-19, 1998.

C. Cost Analyses of Fuel Cell Stack/Systems

Eric J. Carlson (Primary Contact) and Stephen A. Mariano

Arthur D. Little, Inc.

Acorn Park

Cambridge, MA 02140-2390

(617) 498-5903, fax: (617) 498-7012, e-mail: carlson.e@adlittle.com

DOE Program Manager: Donna Lee Ho

(202) 586-8000, fax: (202) 586-9811, e-mail: donna.ho@ee.doe.gov

ANL Technical Advisor: Robert Sutton

(630) 252-4321, fax: (630) 252-4176, e-mail: sutton@cmt.anl.gov

Contractor: Arthur D. Little, Inc., Cambridge, Massachusetts

Prime Contract No. DE-FC02-99EE50587, June 1999-June 2003

Objectives

- Develop an independent cost model for polymer electrolyte membrane (PEM) fuel cell systems for transportation applications.
- Assess cost reduction strategies for year 2000 to 2004 development programs.

OAAT R&D Plan: Task 8; Barrier J

Approach

This five-year, multitask program will develop (1) an independent cost estimate of 1999 potential PEM fuel cell system options and then (2) cost reduction strategies for year 2000 to 2004 PEMFC system development programs. Annual updates to the baseline cost estimate for the subsequent four years will be provided. Integrated into the system design and costing information will be feedback solicited from major system developers, as well as material and component suppliers, through structured interviews.

Accomplishments

New start in late FY 1999.

Future Directions

- In the first year, a baseline cost estimate will be developed, based on best available and projected technology and manufacturing practices. In addition, the impact of potential technology developments on system cost reduction will be assessed.
 - In the subsequent four years, annual updates to the baseline cost model and system scenarios will be made, based on assessments of developments in PEMFC system technologies and manufacturing processes.
-

Project tasks and the work breakdown by year are indicated in Figure 1.

The system cost model will be based on a realistic system model developed from Arthur D. Little's experience in fuel cell systems and through discussions with the DOE national laboratories and fuel cell system developers. We are currently working with a modeling group within Argonne National Laboratory to calculate the state parameters of system components, as well as energy and mass balances for each component. The model parameters will be selected to satisfy PNGV efficiency and fuel utilization goals. We will then scale the various components on the basis of technology available now. After scaling and integrating the components, we will then calculate the system weight and volume. At this time, the system parameters and model are calculated at full power. Such issues as transient response and startup are not specifically addressed in the design or model. As technology evolves, we will incorporate these advances into the system design and revise the system cost projections. Figure 2 shows the overall process of system design and cost modeling.

We will focus our attention on the fuel cell stack and fuel processor subsystems, while using suppliers to provide design and cost information for the balance-of-plant (BOP) components.

In Task 2, we will develop a technology-based cost model that starts with the system design and specifications and then defines the manufacturing processes, including development of materials and component databases and process and equipment databases. The manufacturing process will be scaled to automotive volumes and will use automotive financial and production factors. As part of the cost modeling, we will be able to separate materials and process costs. In Task 2, we will start the process of identifying major areas of uncertainty in costs of materials and process, as well as in design parameters. This will be assessed through sensitivity analyses and Monte Carlo simulations, as shown in the examples in Figure 3.

In Task 3, we will continue to analyze the impact of design parameters on cost (see Figure 4 for PNGV cost targets). For example, the impact of operation at higher temperatures (e.g., 150°C), allowed by new electrolyte membranes, on overall system cost will be assessed. Higher fuel cell temperatures will decrease heat-exchanger sizes, increase anode tolerance to CO, and increase performance. However, higher-temperature operation may require the use of more expensive stack materials. The impact of these potential impacts on system design and cost will be estimated.

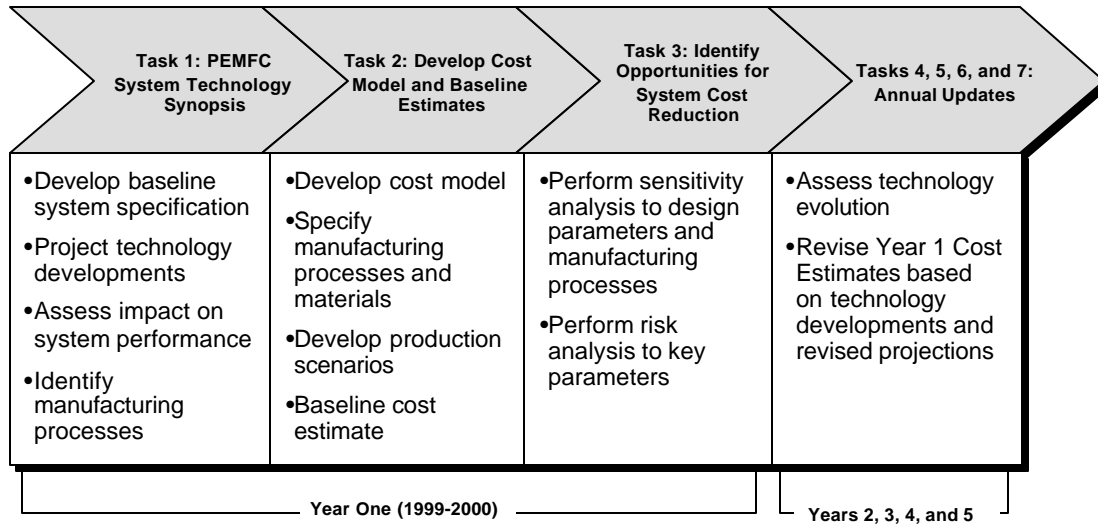


Figure 1. Project breakdown by task.

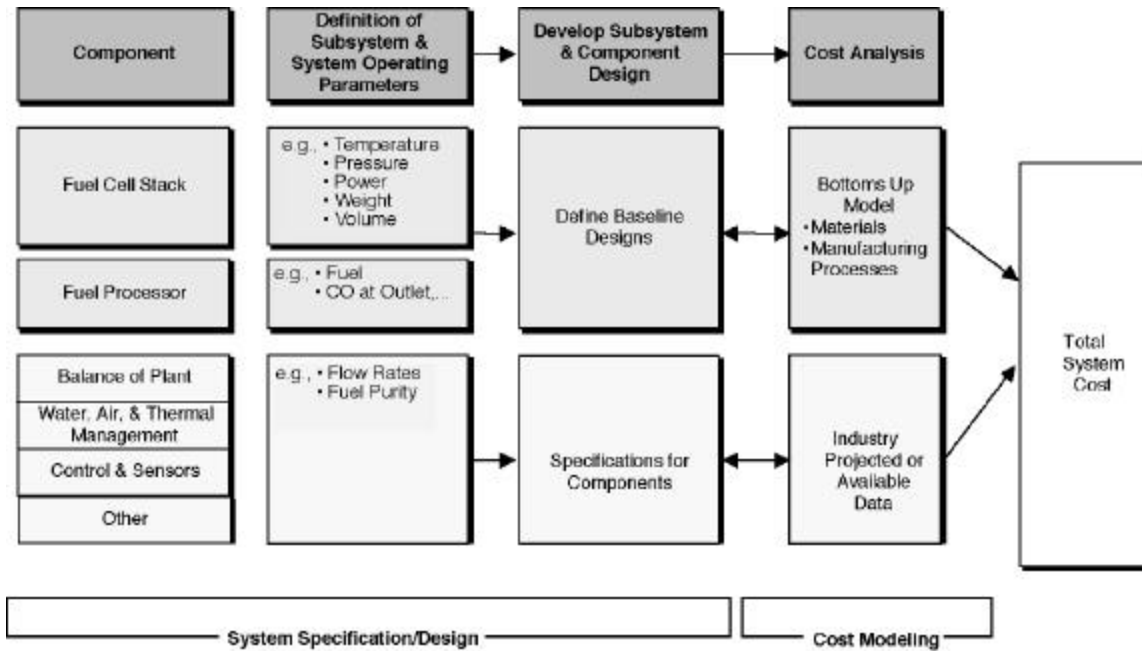


Figure 2. Approach to PEMFC system cost model.

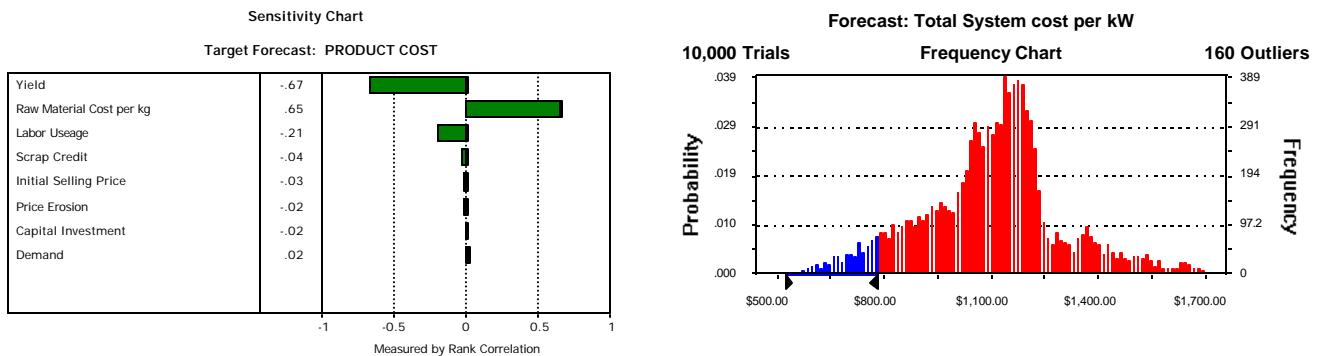


Figure 3. Examples of sensitivity analyses on cost and critical design parameters.

The following questions will be considered in the assessment of potential opportunities for cost reduction:

- What are the tradeoffs in stack performance and air management system complexity and cost arising from selection of operating pressure? Do the benefits of operating at lower pressure (e.g., increased blower system reliability and simplicity), while reducing the cost of air management, outweigh any negative impact on system performance?
- How do the type of liquid fuel (e.g., gasoline or methanol) and the specification of purity level affect the system design and cost?
- How do yields in individual process steps affect overall process yields and cost? Do certain designs, manufacturing processes, and measurements allow rework or recovery of valuable components, such as membrane electrode assemblies or separator plates?
- How do improvements in subsystem performance (e.g., stack power density per area) and manufacturing processes affect overall system cost? What are the critical materials, components, or subsystems to target for technology development?

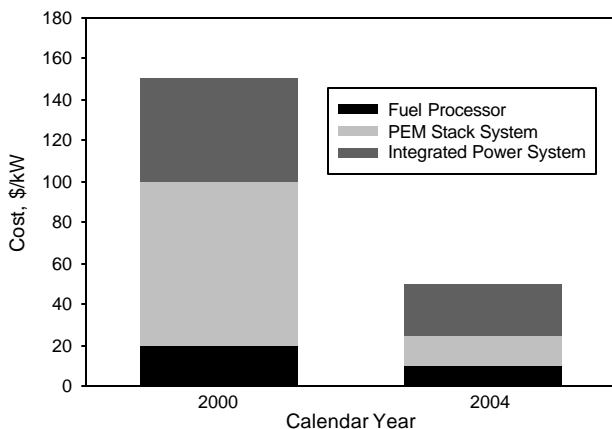


Figure 4 FY 2000 and FY 2004 PGMV High-Volume Cost Targets (500,000 units/yr) for PEMFC Power Systems for FY 2000 and FY 2004.

Deliverables

- Baseline PEMFC system configuration that reflects projected performance for the 2004/2005 timeframe.
- Matrix of system configurations that reflects uncertainties in performance projections, operating parameter options, and material developments.
- Development of cost model for PEMFC systems.
- Baseline cost estimate for 1999 technology.
- Definition of materials, design, performance, and manufacturing assumptions.
- Assessment of potential technology developments and their impact on PEMFC system cost.
- Annual updates of fuel cell stack, reformer, balance-of-plant components, and total system costs.

D. PEM Systems Modeling and Analysis

Rajesh Ahluwalia, E. Danial Doss, Howard Geyer, Romesh Kumar (Primary Contact), and Michael Krumpelt

Argonne National Laboratory, Argonne, IL 60439-4837
 (630) 252-4342, fax: (630) 252-4176

DOE Program Manager: JoAnn Milliken

(202) 586-2480, fax: (202) 586-9811, e-mail: joann.milliken@ee.doe.gov

Objectives

- Simulate automotive polymer electrolyte fuel cell systems and components to
 - identify key design parameters and operating efficiencies
 - model design, part-load, and dynamic performance
 - provide results and support to fuel cell developers, the Partnership for a New Generation of Vehicles (PNGV) technical teams, and others in the field

OAAT R&D Plan: Task 8; Barrier J

Approach

- Develop, document, and make available an efficient, versatile system design and analysis code
- Formulate component models of different fidelity
- Apply the models to issues of current interest
- Organize workshops as forums for interaction with other researchers

Accomplishments

- Documented GCtool with the National Energy Software Center and released Unix version for use on SUN workstations
- Modified GCtool for the PC Windows 98 platform and provided a beta version for testing
- Developed several additional models for GCtool:
 - a 2-D multinodal model of a polymer electrolyte fuel cell (PEFC)
 - a transient model for an integrated fuel processor (similar to Argonne Partial Oxidation Reformer, APOR)
 - a kinetic, finite-difference chemical reactor model
- Investigated the performance and efficiency of different fuel processor configurations
- Analyzed the influence of operating pressure on the design and performance of automotive fuel cell systems

Future Directions

- Release GCtool for the PC platform
- Include cost, weight, and volume in studies of pressurized versus atmospheric pressure systems
- Refine kinetic models for the fuel processor
- Analyze fuel processor configurations for highly active catalysts in which heat transfer effects dominate
- Conduct more detailed analyses of transient and startup issues
- Continue to work with PNGV and other developers

Introduction

This work addresses three of the major technical barriers that have been identified for the development of vehicles powered by fuel cells. These include fuel processor system integration and efficiency, thermal management, and fuel cell power system integration and management. The objective of the work is to develop system models that can be used to identify key design parameters and operating efficiencies; model design, part-load, and dynamic performance; and provide results and support to the fuel cell developers, the relevant PNGV technical teams, and other researchers. Modeling workshops were conducted to get input from fuel cell developers and disseminate the results of this work to researchers in the field.

The GCtool software package has been documented through the National Energy Software Center, and a Unix version of GCtool has been released for use on SUN workstations. GCtool is also being adapted to the PC platform, and a beta version is being tested internally with Windows 98 and Windows NT operating systems.

Enhancements to the model library of GCtool include a two-dimensional, multinodal model of the PEFC that can be used to investigate the effects of

pressure, temperature, fuel utilization, etc. in an internally consistent manner. A transient model of an integrated fuel processor, similar to APOR, has been developed. A kinetic, finite-difference model of chemical reactors of cylindrical geometry has also been developed. These enhancements and the analysis of the effects of operating pressure on system design and operation are described below.

The 2-D PEFC Model

We have developed a detailed, multinodal model of a polymer electrolyte fuel cell. This model takes into account the Nernst potential and the ohmic, activation, and concentration overpotentials. The model calculates the actual cell voltage as a function of current density, anode and cathode pressures and temperatures, fuel and oxidant gas compositions, and hydrogen and oxidant utilizations. By selecting appropriate values of the exchange current densities, membrane conductivity, and mass-transfer coefficients, the predicted model values were matched with experimental polarization curves. The model could then be used to simulate cell performance at any desired operating conditions. This enhanced model was used to assess

comparative performance at different pressures, temperatures, fuel and oxidant utilizations, etc.

The Integrated Fuel Processor Model

We have set up two fuel processor models, a low-fidelity one and a detailed kinetic one, for reactor geometries similar to those used in the APOR. The low-fidelity model can simulate steady-state or transient operation in a multi-annular geometry with arbitrary flow configurations and bed arrangements. The model incorporates up to ten axial nodes, with one radial node per annular channel. The model can be executed with chemical equilibrium, or with kinetic control of the approach to equilibrium. Heat transfer between channels and reactors, as well as pressure drops and heat losses, are included.

The detailed kinetic model is a two-dimensional (r-z) finite-difference model that can account for non-isothermal gas flows and catalyst beds. Processes simulated include fuel vaporization and dissociation, water vaporization and condensation, partial oxidation and steam reforming of the fuel, the water-gas shift reaction, combustion, and sulfidation. These models are being used to support the engineering development of the APOR.

Analysis of Atmospheric Pressure Systems

For an atmospheric pressure system, assuming equilibrium formation of methane and carbon, the fuel processor efficiency is highest at a partial-oxidation temperature (T_{POX}) of ~1100 K. At higher temperatures, the efficiency suffers because of the need for lower fuel equivalence ratios. At lower T_{POX} , efficiency suffers from the excess formation of methane.

A high-performance atmospheric pressure system has a reforming temperature of 1100 K, a fuel equivalence ratio of 3.4, and a water-to-fuel mass ratio in the fuel processor of 2.2 (this may be less than current practice), yielding a hydrogen concentration of 44.4% in the reformat (dry basis). For a net system efficiency of 45% at the rated power level, the fuel cell stack must be operated with a cell voltage of 0.8 V and with 90% hydrogen and 50% oxygen utilizations (these utilizations may be higher than those used in current practice).

Internal Humidification for an Adiabatic PEFC

Under these conditions, the radiator and condenser heat loads are about equal; 65% of the condenser cooling load is for the condensing of water from the cathode exhaust. If the fuel cell is internally humidified (i.e., operated as an adiabatic stack, removing the stack waste heat by vaporizing water), the radiator heat load shifts to the condenser. Table 1 shows this shift in heat duties as the water-to-fuel mass ratio in the feed to the PEFC is increased from 0.6 to 5.3.

Table 1. Effect of increasing internal humidification on radiator and condenser heat duties and sizes.

PEFC m_w/m_f	Radiator		Condenser	
	Q (kW)	Relative Size	Q (kW)	Relative Size
0.6	28.4	1.0	25.9	1.0
2.0	20.2	0.4	34.3	1.4
5.0	2.0	0.1	53.0	2.2
5.3	0.0	0.0	55.0	2.3

The Tail-Gas Burner (Catalytic Combustor)

Depending on the level of PEFC humidification, 15–35% of the condenser duty is due to sensible cooling of the combustor exhaust. The condenser duty can be decreased by 15–20% by directly cooling the depleted cathode air in the condenser and recovering the process water. The burner exhaust can then be discharged directly to the atmosphere without cooling.

Furthermore, fresh air (rather than depleted cathode air) can be used to burn the H_2 in the spent anode gas. The combination of the lower water content and the higher oxygen concentration can raise the combustor temperature above 575 K, thereby improving burner performance. A side benefit of this approach would be higher preheat for the vaporized fuel and/or process water for the reformer.

Ambient-Temperature Effects

The condenser is a critical component of the adiabatic PEFC system. It must reject >50% of the lower heating value of the fuel, and it must recover all of the process water used in fuel reforming. Because this condenser operates with rather small log-mean temperature differences between the

process gas and the ambient air, higher ambient temperatures would require a larger condenser for the same duty.

A condenser designed for an ambient temperature of 320 K (47°C, 116°F) would need to be 60% larger than one sized for an ambient temperature of 300 K (27°C, 81°F). Conversely, if a system is designed for an ambient temperature of 300 K, the maximum steady-state power rating would be decreased by 25% if the ambient temperature rose from 300 K to 320 K. In addition, water recovery would be inadequate for water balance on-board the vehicle.

Startup Times for the Fuel Processor

In the relatively simplistic startup scenario analyzed, the water-to-fuel ratio was maintained constant, but the air-to-fuel ratio was varied to obtain the highest heat generation, subject to maximum allowable temperatures in the partial-oxidation reactor. Since the fuel reformer consists of various catalytic processing steps, nominal gas hourly space velocities (GHSV) were used to represent the different catalyst beds. Not including sulfur removal, the startup times for the various catalysts are summarized in Table 2 for a "base" case (with GHSV comparable to today's commercial practice for the chemical process industry), as well as for much more active catalysts that can be operated with much higher GHSV. Table 2 also shows the effects of increasing the startup fuel flow rates beyond the full-power feed rates. It is evident from Table 2 that much more active catalysts (or highly improved reactor designs) are required than those in common use today.

Table 2. Startup times (in seconds) for the various catalyst beds in a gasoline fuel processor.

	POX	HTS	LTS	PROX
Base Case	>1200	>1200	>1200	>1200
2 * GHSV	938	>1200	>1200	>1200
4 * GHSV	565	646	758	>800
10 * GHSV	351	276	320	440
20 * GHSV	285	146	172	235
10 * GHSV, 1.5 * fuel flow	47	73	108	144
10 * GHSV, 2.0 * fuel flow	28	50	77	102

Pressure Effects

Extensive analyses were conducted to investigate the effects of pressurized versus ambient-pressure system design and operation. These effects were discussed at a workshop held in December 1998. Some of the major results of these analyses are summarized in Table 3.

Table 3. Comparison of system design and performance for operating pressures of 1 atm and 3 atm

	3-atm System	1-atm System
Compressor/ expander	Critical component	Not needed
Methane and carbon formation	Higher potential, need higher T _{POX}	Lower potential, need lower T _{POX}
Fuel processor components, relative sizes	POX = 0.33, HTS = 0.5, LTS = 0.5, PROX = 0.2	POX = 1.0, HTS = 1.0, LTS = 1.0, PROX = 1.0
PEFC stack	Needs active cooling; in-cell condensation adds to cooling load; cathode channels prone to flooding	25% larger cell active area; potential for membrane dry-out; stack cooling load decreased by water evaporation
Heat rejection, water balance	1/3 process water recovered in inertial separator, 2/3 in condenser	Condenser 2.8 times larger, smaller radiator
Response to high ambient temperatures	Power reduction determined by radiator size, ~35% reduction at 320 K	Power reduction determined by stack temperature rise, 25% reduction at 320 K

III. FUEL PROCESSING SUBSYSTEM

A. Advanced Fuel-Flexible Fuel Processor Development SFAA for Next Millennium Fuel Processor™ for Transportation Fuel Cell Power System

William L. Mitchell, P.E.

Epyx Corporation/Arthur D. Little

20 Acorn Park, Cambridge, MA 02140

(617) 498-6149, fax: (617) 498-6655, e-mail: mitchell.william@adlittle.com

DOE Program Manager: Patrick Davis

(202) 586-8061, fax: (202) 586-9811, e-mail: patrick.davis@ee.doe.gov

ANL Technical Advisor: Walter Podolski

(630) 252-7558, fax: (630) 252-4176, e-mail: podolski@cmt.anl.gov

Contractor: Epyx Corporation/Arthur D. Little, Cambridge, Massachusetts

Prime Contract Nos. DE-RA02-97EE50443 and DE-FC02-99EE50580

Subcontractors/Partners: Modine Manufacturing (PRDA); Energy Partners (SFAA); United Catalysts, Inc (SFAA); Corning, Inc (SFAA); STC Catalysts, Inc. (SFAA); and Dana Corporation (SFAA)

Objectives

Epyx/ Arthur D. Little, Inc. (Epyx/ADL), is developing a 50-kWe fuel-flexible fuel reformer capable of processing gasoline and alternative fuels, such as methanol, ethanol, and natural gas. Major technical issues to be addressed in this program include advanced catalysts, CO cleanup, transient controls, and reformer startup/shutdown time.

As an extension of the integrated fuel processor, Epyx is developing and testing an advanced 50-kWe PROX device based on proprietary catalyst technology. A major focus of fuel processor development will be gas purity when gasoline and ethanol are used in operation. Epyx supports Plug Power in the development of a 50-kWe fuel cell power system.

OAAT R&D Plan: Tasks 5 and 6; Barriers E, F, G, and H

Approach

- Build and test a brassboard 10-kWe system based on existing reformer design, existing stack hardware, and other available components as a proof of concept (3-atm pressure).
- Test steady-state CO cleanup (study multiple options @ 10-kWe level) – offline on flow reactor.
- Integrate complete 10-kWe system and test at Epyx labs, using our 10-kWe system test facility.
- Aid Plug Power in the development of a test facility for full-scale (50-kWe) system testing.
- Design and build an advanced 50-kWe fuel processor based on Phase I and Phase II testing.
- Continue catalyst refinement from Phase I.
- Test 50-kWe fuel processor/PROX combination, including transients, at Epyx/ADL labs.
- Provide integration assistance for testing at the prime contractor's laboratory for 50-kWe brassboard (Phase III) system demonstration.

- Aid prime contractor/system integrator in the mechanical design and packaging of the Phase III 50-kWe system, focusing on system functionality and efficiency of operation.
- Work with a test facility to perform transient tests of the integrated Phase III system.
- Build and deliver a Phase IV 50-kWe fuel processor subsystem to prime contractor for final integration. The Phase IV system will meet PNGV weight and volume targets for the year 2004.

Accomplishments

- Demonstrated two distinct generations of fuel processor technology.
- Operated fuel processor for 1000+ hours with less than 1% CO output at firing rates between 5 and 65 kWth.
- Exceeded 2004 fuel processor efficiency targets on Phase II RFG, ethanol, methanol, and natural gas.
- Performed testing of the PNNL microchannel fuel vaporizer.
- Demonstrated 10:1 turndown and 8-min startup.
- Operated PROX during steady-state and 17-kW/s step transients with less than 10 ppm CO output.
- Demonstrated integrated 10-kWe fuel cell power system operating on gasoline at 34% efficiency.
- Measured exhaust emission levels at <<ULEV.
- Completed integration of 50-kWe Phase III fuel processor subsystem for delivery to Plug Power.
- SFAA Program – New start in FY 1999.

Fuel Cell Power System

(including fuel processor, stack and auxiliaries; excluding gasoline tank and DC-DC converter)

Characteristic	Status	DOE Technical Target
Net Power (kWe)	50	50
Energy Efficiency @ 25% Peak Power (%)	40 (predicted)	40
Power Density (W/L)	250 (predicted)	250
Specific Power (W/kg)	250 (predicted)	250
Durability (hours)	2000 (predicted)	2000

Future Directions

- Design and build a sub-50-kWe fuel cell system to evaluate and improve system models.
- Conduct extensive endurance testing to evaluate catalyst and hardware lifetime issues.
- Develop advanced catalyst beds and heat-exchanger designs in collaboration with subcontractors.
- Develop high-activity and low-cost catalyst and integrate with advanced heat exchangers.

Experimental Setup and Procedures

On the basis of experimental results of testing carried out in Phase I of this program, a new generation of fuel processor subsystem hardware was designed, built, and tested prior to integration into a complete fuel cell power system (1,2). Three components comprise the fuel processor subsystem: the fuel processor, the CO cleanup device, and the tailgas burner/converter. The fuel processing

subsystem converts a primary fuel to a hydrogen-rich gas stream, the CO cleanup subsystem removes carbon monoxide to levels appropriate for PEM fuel cell operation, and the tailgas burner converter system oxidizes the waste stream from the fuel cell anode to achieve near-zero emissions. On the basis of results from previous integrated testing, the new fuel processor subsystem was designed to be operated over a thermal input power range of

5-65 kW. Upon completion of the fuel processor subsystem testing and verification, a complete fuel cell power system was integrated in the Epyx laboratory, using a Plug Power fuel cell subsystem.

Experimental studies were carried out to permit characterization of the entire system with regard to efficiency, tailpipe emissions, system startup time, thermal balances, pressure balances, hydrogen purity effects, and required control interaction. System sensitivity tests were performed to allow adjustment of critical variables in order to assess the sensitivities of other components to variations.

Fuel Processor and PROX Testing

Figure 1 shows the newly designed “Model B” fuel processor under testing in the Epyx laboratories. As in the previous generation of fuel processor, the Model B contains the partial oxidation reactor (POX) and catalytic reforming section, the water gas shift (WGS) reactor, the sulfur-removal bed, the system steam generator, and the air preheater. The fuel processor assembly is 15 in. in diameter and 15 in. high, and it weighs 125 lb. With a thermal input capacity of 65 kW and operation at 80% efficiency, the fuel processor produces sufficient hydrogen flow to support a 25-kWe fuel cell power system.

Testing was carried out to determine the effect of fuel choice, equivalence ratio, and firing rate on fuel processor efficiency. Equivalence ratio is defined as the actual fuel-air ratio, divided by the stoichiometric fuel-air ratio. Fuel processor



Figure 1. Model B fuel processor.

efficiency is defined as the lower heating value of hydrogen produced, divided by the lower heating value of fuel into the fuel processor. Figure 2 shows that for gasoline, methanol, and natural gas, the fuel processor has a high efficiency over a wide range of operating conditions. In general, in order to achieve the year 2004 efficiency targets, it is necessary to operate the fuel processor at equivalence ratios between 3.5 and 4.5, depending on fuel type. When achieving these efficiency numbers, the hydrogen concentration in the product gas ranges between 40 and 50% (dry basis). Furthermore, fuel conversion was greater than 99% for all cases during testing, which minimizing the amount of hydrocarbon slip through the system. Although not shown in Figure 2, ethanol was tested and showed an efficiency of 84%; a Fischer-Tropsch fuel showed efficiencies of 79-80%.

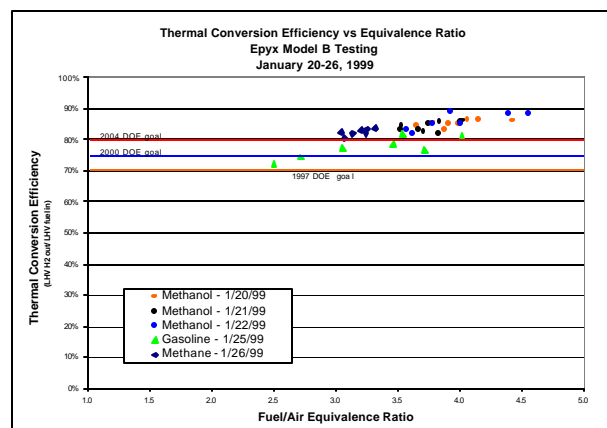


Figure 2. Fuel processor conversion efficiency.

CO cleanup testing was performed in conjunction with the fuel processor testing on a newly designed, two-stage PROX to determine selectivity and performance during both steady-state and transient operation. Figure 3 shows both steady-state performance and performance over a 17-kW/s step decrease and increase. During operation, the fuel processor CO output level did not change significantly, and the PROX outlet CO concentration remained under 10 ppm at all times. The performance was very repeatable over several hundred hours of operation, and the PROX showed excellent selectivity, as depicted in Figure 4. During operation, it was difficult to determine the amount of hydrogen loss, if any, through the PROX reactor.

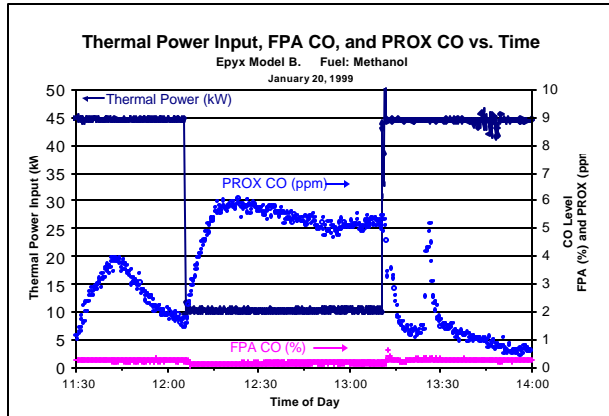


Figure 3. PROX performance.

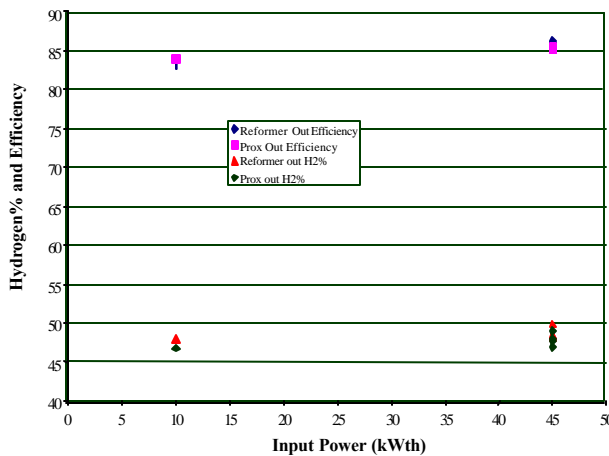


Figure 4. PROX selectivity.

Integrated Fuel Cell Power System Testing

Testing was performed over a wide range of operating conditions to determine efficiency, startup time, and emissions of the system, as well as to define key variables and considerations for the Phase III and IV 50-kWe systems.

Table 1 shows selected results of a 10-kWe system test operating on low-sulfur gasoline. Results show 34% system efficiency over an operational range of 25-100% power. During operation, the fuel processor hydrogen percentage ranged between 36 and 41% on a dry basis, with PROX outlet CO concentrations between 2 and 14 ppm. It is important to note that the efficiency numbers quoted do not take into account parasitic components, such as the compressor/ expander, which would lower the recorded values. Moreover, the current lab system had much higher heat loss than an integrated system would, due to lack of heat integration, which would cause the efficiency

numbers to increase. Overall, the efficiency numbers recorded were as expected; results were well on the way to the Phase IV targets. The integrated fuel cell power system was operated on California Phase II reformulated gasoline, ethanol, methanol, M-85, natural gas, and Fischer-Tropsch fuels.

Also demonstrated during this testing was an 8-min startup to full electric power.

Table 1. Integrated gasoline FCPS performance.

Fuel	Sulfur Free Gasoline				
FUEL			SFG	SFG	SFG
EPA INPUT POWER	(kWe)	13.8	7.4	29.8	
PRESSURE					
	Supply from FPA	(psig)	38.0	38.0	38.0
CALCULATED FLOW RATE					
PROX out					
	H2 flow	(kW)	10.0	5.3	22.9
TEMPERATURE					
	F.C. inlet	(°C)	21	21	21
COMPONENT					
GC SAMPLING POSITION			PROX	PROX	PROX
DRY VOL %					
	H2	(dry mol%)	38.66	36.10	40.57
DRY PPM					
	PROX CO	(dry ppm)	14	11	2
**NOTE: 24.15 standard liters per mole is assumed (70 F, 1 atm)					

Emissions were measured during system operation for all fuels tested, using experimental measuring equipment as previously described (1). Table 2 shows results for system operation on low-sulfur gasoline. GC analysis shows that the major recorded hydrocarbon emission from the system is methane, which would further lower the NMOG emissions from the system. It is anticipated that SULEV emissions should be achievable with a gasoline fuel cell power system. However, tests with a fuel system on the appropriate driving cycles are necessary to confirm these results.

Table 2. Integrated FCPS emissions.

	2.5 kWe (mg/g _{fuel})	5 kWe (mg/g _{fuel})	10 KWe (mg/g _{fuel})
NMHC	—	—	—
NMOG	—	—	—
Total HC	0.090	0.075	0.066
CO	0.063	0.003	0.004
NO _x	0.226	0.093	0.120

Future Work

DOE SFAA: On the basis of our current in-depth understanding of fuel processing and fuel cell systems, Epyx shall perform a three-part program that will yield a fully optimized fuel processing subsystem. In the first part of the program, Epyx will work with Energy Partners to integrate existing hardware into a 10-kWe multifuel power system in order to identify key system-level trade-offs in the design of a fuel processing subsystem and to allow validation of computer models developed both internally and by Argonne National Laboratory. In the second part of the program, Epyx will utilize existing integrated and modular fuel processors to perform endurance testing that will identify and address material and catalyst degradation mechanisms. The output of this work will feed directly into the final fuel processor design in the third part of the program. The major element of this third part will be an in-depth catalysis R&D program designed to identify high-activity, low-cost catalysts. The new catalysts and supports will be integrated into a fuel processor package specifically suited to the optimized catalyst suite. The output of this program will be a fully integrated fuel processing subsystem that meets or exceeds 2004 PNGV targets.

Conclusions

The design and development of a multifuel reformer/fuel cell system for transportation applications has been demonstrated via a 10-kWe brassboard power system comprising a fuel processor, a CO cleanup device, and a 10-kWe PEM

fuel cell. System testing shows that the Epyx multifuel processor establishes efficient, integrated fuel cell power systems operating on multiple fuels. Specific achievements include:

- 1000+ hours of fuel processor operation with less than 1% CO output at firing rates between 5 and 65 kWth.
- Exceeded 2004 efficiency targets on Phase II RFG, ethanol, methanol, and natural gas.
- Demonstrated 10:1 turndown and 8-min start.
- Operated PROX during steady-state and 17-kW/s step transients with less than 10 ppm CO.
- Demonstrated integrated 10-kWe fuel cell power system operating on gasoline at 34% efficiency.
- Measured exhaust emission levels.

References

1. Mitchell, W.L., "Program Research Development Announcement for Integrated Fuel Cell Systems and Components for Transportation and Buildings. Integrated Power System for Transportation – Advanced Fuel Processor Development," Preprints of the Annual Automotive Technology Development Customer Coordination Meeting, U.S. Department of Energy, Office of Transportation Technologies, 1998.
2. Mitchell, W.L., Hagan, M., and Prabhu, S.K., "Gasoline Fuel Cell Power Systems for Transportation Applications: A Bridge to the Future of Energy," SAE Paper No. 1999-01-0535, Society of Automotive Engineers, 1999.

B. Multifuel Processor for Fuel Cell Electric Vehicle Applications

Robert Privette (Primary Contact) and Tom Flynn

McDermott Technology, Inc.

1562 Beeson Street

Alliance, OH 44601-2196

(330)829-7370, fax: (330)829-7293, e-mail: rob.m.privette@mcdermott.com

Jacques De Deken and Dave King

Catalytica Advanced Technologies

430 Ferguson Drive

Mountain View, CA 94043-5272

(650)940-6339, fax: (650)968-7129

DOE Program Manager: Donna Lee Ho

(202)586-8000, fax (202)586-9811, e-mail: donna.ho@ee.doe.gov

ANL Technical Advisor: Walter Podolski

(630) 252-7558, fax: (630) 252-4176, e-mail: podolski@cmt.anl.gov

Contractor: McDermott Technology, Inc., Alliance, Ohio

Prime Contract No. DE-FC02-99EE50586, September 1999-January 2002

Subcontractor: Nextech Materials, Ltd., 720-I Lakeview Plaza Blvd., Worthington, OH 43085

Objectives

- Design, build, and demonstrate a fully integrated, 50-kWe catalytic, autothermal fuel processor system. The fuel processor will produce a hydrogen-rich gas for direct use in Proton Exchange Membrane (PEM) fuel cell systems for electric vehicle applications.

OAAT R&D Plan: Task 5; Barriers E, F, G, and H

Approach

- Develop preliminary design of 50-kWe fuel processor system and performance goals for individual components.
- Evaluate alternative approaches for the major catalytic components (e.g., desulfurizer, reformer, shift reactor, and selective oxidation reactor).
- Conduct subsystem testing of major components, utilizing best catalyst approach.
- Develop final design of overall system and design specifications for individual components.
- Assemble 50-kWe fuel processor system.
- Perform demonstration testing on gasoline, methanol, natural gas, and ethanol.
- Ship fuel processor system to Argonne National Laboratory.

Accomplishments

New start in late FY 1999.

Performance Characteristic	Project Goal	DOE Technical Targets	
		Calendar Year 2000	Calendar Year 2004
Power Density, W/L	280	600	750
Specific Power, W/kg	285	600	750
CO Content, ppm	10	10	10
Lifetime, hours	5000	2000	5000

Future Directions

- Develop preliminary design of 50-kWe fuel processor
- Identify the preferred technical approach for each catalytic component and provide recommendations on the best catalysts.

Introduction

Development of a compact, efficient, and low-cost processor for converting carbon-based fuels to hydrogen is an important aspect of the successful implementation of fuel cells for transportation applications. Advantages of a catalyst-based autothermal reforming approach include lower temperature, faster startup, and better materials compatibility. Coupled with a liquid fuel desulfurizer, the multifuel processor promises to approach the targets established by the Partnership for a New Generation of Vehicles (PNGV).

Background

The fuel processor will consist of a liquid-phase desulfurizer, an autothermal reformer, high- and low-temperature water gas shift units, a selective oxidizing unit, and associated pumps, compressor/expander, heat exchangers, and controls. A general arrangement conceptual drawing of the fuel processor system is shown in Figure 1. The design has been described previously [1].

The liquid fuel desulfurizer will reduce sulfur in gasoline from 30-100 ppm to less than 3 ppm. The autothermal reformer unit, operating at an average temperature of 800°C, will produce a hydrogen-rich gas from the fuel feed. Two reformer approaches will be evaluated during the program – a single packed bed comprising a bifunctional catalyst and a bifunctional monolith catalyst. A shift reactor, consisting of either a single catalyst bed or

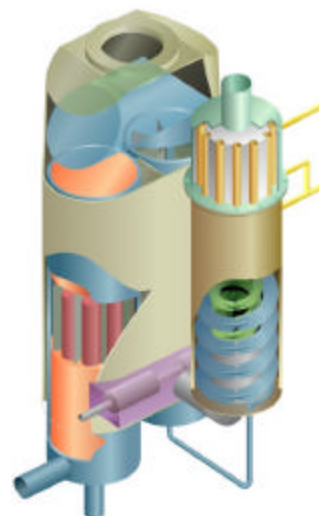


Figure 1. General arrangement drawing.

individual high- temperature and low-temperature catalyst beds, will reduce the CO concentration in the reformed gas to approximately 2000 ppm. Final reduction of CO in the reformed gas will be achieved in a selective oxidation reactor.

McDermott Technology, Inc., will develop the overall system design, including heat integration, mechanical design, auxiliary equipment, and instrumentation/controls. Catalytica Advanced Technologies will develop the catalytic components, including improved catalysts. NexTech, as a major subcontractor and cost-share contributor on the project, will contribute its expertise and technology in the area of shift catalysis.

References/Publications

1. Flynn, T. J., Privette, R. M., Perna, M. A., Kneidel, K. E., King, D. L., and Cooper, M., "Compact Fuel Processor for Fuel Cell-Powered Vehicles," International Congress and Exposition, Detroit, Mich., March 1-4, 1999, SP-1425, pp. 47-53.
2. Privette, R.M., et al., "Fuel Processing to Military and Commercial Fuel Cell Applications," Proceeding of the 1998 Fuel Cell Seminar, Palm Springs, CA, pp. 323-325, November 16-19, 1998.

C. Fuel-Flexible, UOB™ Fuel Processor System Development and Status

Richard Woods (Primary Contact) and John Cuzens

Hydrogen Burner Technology, Inc.

3925 Vernon Street

Long Beach, CA 90815

(562) 597-2442, fax: (562) 597-8780, e-mail: Rwoods@HydrogenBurner.com

DOE Program Manager: Patrick Davis

(202) 586-8061, fax: (202) 586-9811, e-mail: patrick.davis@ee.doe.gov

ANL Technical Advisor: James Miller

(630) 252-4537, fax: (630) 252-4176, e-mail: millerj@cmt.anl.gov

Contractor: Hydrogen Burner Technology, Long Beach, California

Prime Contract No. DE-FC02-97EE50482, October 1997-December 1999

Objectives

- Research, develop, assemble, and test a 50-kWe net fuel-flexible, fuel-processing (F³P) subsystem. Conduct performance mapping of the subsystem on various fuels, including natural gas, gasoline, ethanol, and methanol. Verify the humidified low-temperature-shift (HLTS) concept and assess its applicability to F³P subsystem integration. Coordinate with fuel cell system developers, such as AlliedSignal Aerospace Corporation, in preparation for system-level integration activities.

OAAT R&D Plan: Task 5; Barriers E, F, G, and H**Approach**

- This program includes the process and hardware design of a F³P subsystem, the assessment of alternative materials and catalysts, the fabrication of integrated hardware assemblies, and the evaluation of alternative carbon monoxide (CO) polishing approaches.
 - The design approach selected for the prototype F³P subsystem hardware includes three assemblies – the F³P assembly, the fuel vaporizer assembly, and the CO polishing assembly. A breadboard control package was also included to allow automatic control of the hardware subsystem.
 - The F³P assembly integrates the primary functions required for a fuel processor – UOB™ reactor, thermal management, shift reactors, and integrated steam generation.
 - The fuel vaporizer assembly integrates the function of fuel vaporization and anode off-gas combustion.

- The CO polishing concepts being evaluated include methanation, preferential oxidation (PROX) of CO, and several proprietary configurations in cooperation with AlliedSignal Corporation.
- This program also includes the verification of the HLTS reactor concept, which has encompassed the evaluation of alternative hardware configurations and the development of advanced low-temperature-shift (LTS) catalysts with improved activity at lower temperatures and higher humidity.

Accomplishments

- A process integration and hardware configuration approach was established and modeled. A process model was used to evaluate thermal integration and chemical stability characteristics, while a heat-transfer model was used to assess heat-transfer requirements and hardware dimensions. A preliminary hazardous operations (HAZOP) assessment was completed to assess safety issues.
- A fabrication design package has been completed for the F³P assembly, vaporizer/anode gas oxidizer assembly, and breadboard control assembly. The initial F³P subsystem has been fabricated and assembled.
- These F³P subsystems have been operated to assess functionality, map unit performance, qualify delivery units, and evaluate fuel-flexibility characteristics. Over 120 hours of operation have been completed, including approximately 60 start/stop cycles.
- Three alternative fuels have been tested – gasoline, natural gas, and methanol.
- Advanced high-temperature- and low-temperature-shift catalysts were developed and evaluated in the laboratory and in the F³P assembly hardware.
- The HLTS reactor hardware concept was selected and integrated into a prototype F³P assembly for concept verification testing.
- Fabrication and delivery of three additional prototype F³P subsystems was completed under parallel programs for evaluation by an automotive manufacturer, a fuel cell system integrator, and a national laboratory.

Future Directions

- Complete performance mapping of the UOBTM F³P subsystem.
- Complete the control system logic, which provides for automatic control and shutdown protection.
- Assess operation of the F³P subsystem on ethanol and M-85 (85% methanol, 15% gasoline).
- Complete concept verification testing of the HLTS hardware.
- Develop a precommercial hardware design approach based on the results of the prototype F³P subsystem activities.

Introduction

Fuel cells are considered to be a viable alternative to the internal combustion engine in automotive applications. Debate exists within the automotive and development communities regarding the appropriate fuel for fuel cell vehicles. Hydrogen (H₂) fuel provides the easiest and smallest fuel cell system, but “on-board storage” of H₂, as well as the absence of a H₂ refueling infrastructure, raises many concerns. An alternative approach would be to use existing liquid fuels (such as gasoline) or evolving fuels (such as ethanol, methanol, or any of the many synthetic liquids currently being developed). Any of these fuels would require an “on-board reformer” to

convert the liquid fuel into H₂ gas on demand. Hydrogen Burner Technology, Inc. (HBT), has entered into a cooperative agreement with the U.S. Department of Energy, through the Office of Transportation Technologies, that focuses on the development and testing of a F³P subsystem for automotive applications.

Program Overview

The cooperative agreement focuses on two independent efforts. The greater portion of the activity is related to the design, construction, and testing of a prototype F³P subsystem. The second

effort is related to verification of the humidified low-temperature-shift (HLTS) concept.

Figure 1 identifies the overall program scope and structure, while indicating the progress during FY 1999. In October 1998, HBT was beginning the assembly of the first set of F³P components and hardware. This unit was completed by December, and testing was initiated during January 1999. Activities during FY 1999 include performance mapping of the F³P subsystem, completion of the controller software, and defining of advanced concepts to be incorporated into the precommercial hardware configuration. Initial testing of the F³P subsystem has identified advanced components and concepts that are either being implemented into the prototype to enhance operation or being outlined for the precommercial hardware definition.

F³P Subsystem Design and Hardware

Design of the F³P subsystem is based on HBT’s noncatalyzed, under-oxidized burner (UOB™) technology. The hardware approach uses three separate hardware assemblies to allow for the evaluation testing of alternative components. The three assemblies are the fuel vaporizer/anode gas oxidizer assembly, the F³P assembly, and the CO polishing assembly. Seven of the most critical chemical processes of the F³P subsystem are thermally and physically integrated into the F³P assembly hardware. Figure 2 illustrates these processes. The integrated hardware of the F³P assembly provides close thermal interaction between the UOB™ reaction zone, which operates at 1375-1500°C (2500-2700°F), and the lower-temperature zones of the process air preheater and high-temperature-shift zones, which operate at

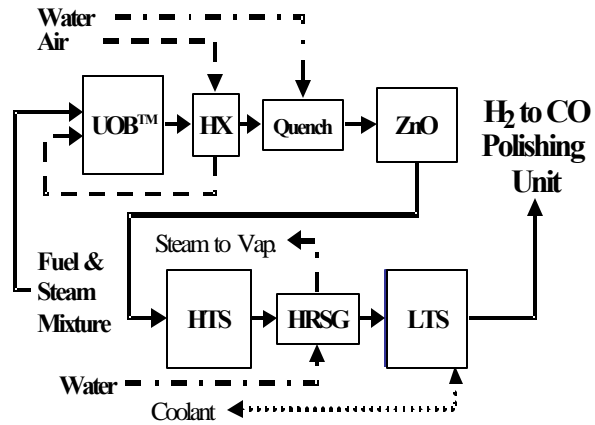


Figure 2. Integrated F³P assembly.

300-800°C (600-1500°F). This configuration minimizes heat loss while maximizing reaction temperatures.

All of the processes identified in Figure 2 are physically integrated into the hardware illustrated in Figure 3. The prototype F³P assembly, with conventional, commercially available catalysts, weighs approximately 104 kg (230 lb), which is approximately 25% greater than its target weight of 83 kg (183 lb). Most of this excess mass comes from high-density commercial catalyst and flange structures used for easy disassembly and inspection.

The volume of the F³P assembly is ~ 85 L (3 ft³). Increasing this size by the volume needed for the vaporizer and CO polishing assemblies indicates that the prototype hardware is approximately 30% greater than its target volume. This experience with the prototype hardware indicates that it should be feasible to package the precommercial components within their target volume of 600 W/L and target mass of 600 W/kg.

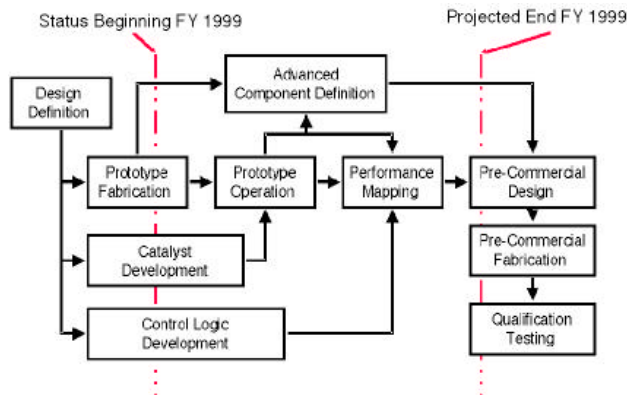


Figure 1. Overall program scope.

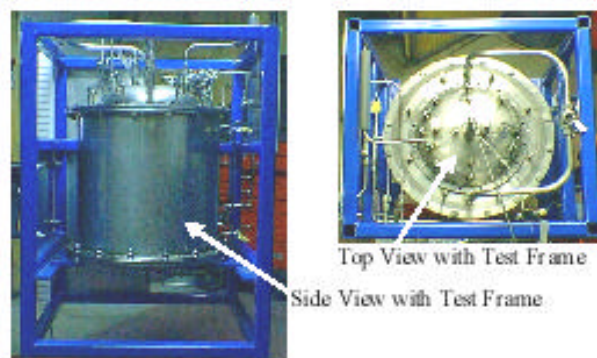


Figure 3. Prototype F³P assembly configuration.

Interest in the concept of an on-board fuel processor is very strong in the automotive and fuel cell development communities. In parallel with our cooperative agreement, HBT also fabricated three additional prototype subsystems for evaluation by others. These include an automotive manufacturer, a fuel cell developer, and a national laboratory supported by DOE. Results from the qualification testing of these units are also discussed.

Subsystem Testing Results

To date, HBT has collected over 120 hours of operational experience on the F³P subsystems fabricated. This experience includes over 60 start-stop cycles and operation on three fuels – gasoline, methanol, and natural gas. Table 1 provides a summary of the operating experience achieved to date. All of this testing has been accomplished using manual control of the subsystem because of delays in completing the automatic sequence control software.

This operating experience has partially mapped the performance characteristics of the F³P subsystem on three fuels. A summary of the achievements to date is indicated in Table 2. Additional testing will establish higher operating capacities on natural gas and gasoline and push the performance envelope to higher efficiencies through operation at a lower stoichiometric ratio.

Testing has indicated the ability to achieve LTS outlet CO concentrations between 1000 and 3000 ppm. Laboratory testing of a methanation reactor has shown the ability to decrease these levels to the 10-ppm specification of the fuel cell. Initial testing of the PROX unit is also promising. Additional characterization is needed to assess the

Table 1. Operating experience summary.

	S/N 001	S/N 002	S/N 003	S/N 004
Customer	HBT/DOE	Auto Mfg'er	LANL	FC Devel
Fabrication	12/30/99	2/20/99	3/9/99	7/1/99
Delivered	1/1/99	3/5/99	5/28/99	9/13/99
Runs	26	11	13	27
Operating	36 hr	18 hr	24 hr	98 hr
Fuels	NG, Gasoline	NG, Gasoline	NG, Gasoline, Methanol	NG

Table 2. Summary performance mapping.

	Methanol	Nat. Gas	Gasoline
Minimum SR	0.33	0.40	0.42 - 0.45
Efficiency	<76%	~70%	~68%
Max H ₂ , %dry	40%	33%	31%
Min CO, (LTS only)	0.3 to 0.1%	0.4 to 0.1%	0.5% to 0.1%
Tested Capacity, kWe**	38kWe	22kWe	15kWe

* Note preliminary performance based on ~120 hrs operation.

** Note Estimated Capacity based on Fuel Consumption and H₂ Concentration.

selectivity of the two hardware concepts and the process efficiency impact.

Due to delays in completing the automatic control software, only manual startup characteristics have been verified. Sample data from liquid-fueled tests are shown in Figure 4. These tests indicate the ability to achieve normal hydrogen production within 15 to 30 min, with a cold start at low to nominal fuel-flow rates. Similarly, hot restarts in less than 5 min have been achieved when the shift beds were warm. During these tests, the CO level out of the LTS never rose above the normal levels.

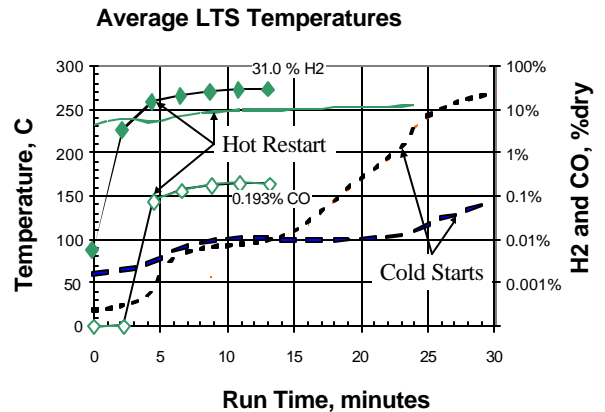


Figure 4. Comparison of startup tests.

Conclusions

Continued performance mapping is required to complete the characterization of the F³P subsystem. To date, the F³P subsystem has successfully demonstrated operation and has approached its performance targets. Fully integrated, advanced design concepts are being developed that offer improved efficiency and reduced mass and volume.

D. Integrated Fuel Processor Development

Shabbir Ahmed, Sheldon H. D. Lee, Candido Pereira, and Michael Krumpelt

Argonne National Laboratory, Argonne, IL 60439

(630) 252-4553; fax: (630) 972-4553

DOE Program Manager: JoAnn Milliken

(202) 586-2480, fax: (202) 586-9811, e-mail: joann.milliken@ee.doe.gov

Objectives

- Demonstrate a fuel-flexible fuel processor suitable for use on-board a fuel cell powered vehicle
 - As a microreactor process train
 - As an engineering-scale integrated reactor

OAAT R&D Plan: Task 3; Barriers F and G

Approach

- Verify fuel processor functions in a microreactor process train and operate a PEFC stack on reformat gas.
 - The process train includes the reformer, H₂S absorber, shift reactor(s), preferential oxidizer, and fuel cell stack.
 - The components can be studied individually or as a group.
 - Alternative scrubbing technologies can be readily installed and studied.
- Design and demonstrate an engineering-scale integrated reformer that converts fuel, steam, and ambient air into a sulfur-free, low-CO reformat gas.
 - Catalyst performance is verified in a self-sustained reactor.
 - Heat effects are integrated to improve hydrogen yields.

Accomplishments

- Completed setup of the microreactor process train and operating parameters for the individual reactors.
 - Demonstrated that the shift reactor with the Argonne catalyst can reduce CO level from 20% to 1.5%.
 - Demonstrated the reduction of CO from 20% to 0.8% by using the Argonne water gas shift and Argonne preferential oxidation reactors.
- Operated a 7-liter integrated reactor with methanol, isooctane, and gasoline.
 - The igniter coil was turned off after start-up.
 - Desirable temperature profiles were achieved in all the catalyst zones.
 - The reactor has been rated for 5 kW_e; higher throughputs may be possible.
 - Hydrogen concentrations of 32% (isooctane) to 47% (methanol) were measured.

Future Directions

- Determine operating parameters for each component in the process train and demonstrate fuel cell operation on reformat.
 - Study the effect of new-generation catalysts for the various components (reactors).
 - Study the effect of alternative scrubbing technologies.
 - Design an integrated fuel processor and demonstrate operation with monolith catalysts, rapid start capability, and transient operation.
-

The objective of this work is to design, develop, and demonstrate fuel-flexible catalytic fuel processors based on autothermal reforming. These reformers will be used to generate hydrogen for fuel cells in light duty vehicles. The catalytic process offers the advantages of greater product selectivity and high activity at relatively low temperatures.

To achieve this objective, the fuel processor is being studied at two levels. First, a microreactor process train has been established, with a series of reactors set up to represent the various unit processes.

This task is designed to obtain the “best” operating conditions of the individual unit operations and processes in a fuel processor. The units are controlled so that the final reformat gas is of sufficient quality for sustained power generation in a polymer electrolyte fuel cell. The information obtained from the process train is then used to develop an integrated fuel processor design, and it is subsequently verified at the engineering scale.

Figure 1 shows a schematic of the microreactor process train, which can operate five reactors in series. Vaporized fuel, steam, and air are fed into the catalytic reformer, from which the product gas passes through the sulfur removal bed, followed by up to two stages of water gas shift reactors, and then through the final CO removal unit. The CO removal unit can be either a catalytic preferential oxidation reactor or a CO sorption unit. The clean reformat gas is then supplied to a polymer electrolyte fuel cell to generate power and obtain polarization curves.

The feeds to each of the reactors can be independently controlled. That is, the feed can be a synthetic reformat gas from a cylinder, or additional feed components can be added to the feed stream from the previous reactor. Since all the

reactors are located within furnaces, the reactor temperatures can be controlled very effectively. Each reactor is also connected to a GC/MS system, allowing careful analysis of both the reactant and product streams.

The microreactor fuel processing train provides the ability to carefully study each component individually and to fine tune its performance. A major benefit of this configuration is the flexibility to evaluate alternative processing stages – for example, a CO-removal process involving a membrane separator can easily be placed anywhere in the sequence.

Table 1 shows some preliminary data comparing the conversion of synthetic reformat gas in a high-temperature water gas shift reactor, a low-temperature shift reactor, and a preferential oxidation reactor. The feed gas composition, on the basis of CO, CO₂, and H₂ only, are as shown in the second column. When this feed gas was passed through a high-temperature shift reactor filled with a commercial FeCr catalyst bed at 325°C, the CO level was reduced to 3.7%. Passing the feed gas directly through a reactor filled with an Argonne shift catalyst bed at 225°C reduced the CO level from 20% to 1.5%. When the product from the Argonne shift catalyst bed was further passed through a reactor filled with a new preferential oxidation catalyst maintained at 200°C, the CO level dropped to 0.8% (on the basis of H₂, CO, and CO₂ only). The H₂O/CO molar ratio in the feed stream was 4, and the O₂/CO ratio in the preferential oxidation unit was 1.

Table 1. The microreactor process train was used to evaluate the CO reduction in water gas shift and preferential oxidation reactors.

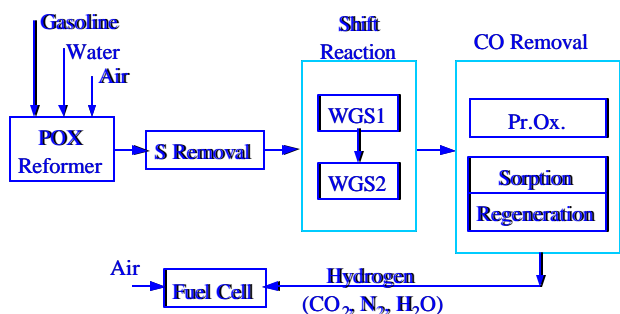


Figure 1. Schematic of the microreactor fuel processing train.

	Feed	Comm. HTS	ANL Shift	ANL (Shift+PrOx)
CO	20.0 ±0.2	3.7 ±2.0	1.5 ±1.1	0.8 ±0.4
CO ₂	21.8 ±0.3	35.6 ±4.0	31.1 ±1.2	34.4 ±5.5
H ₂	58.2 ±0.2	60.7 ±4.0	67.4 ±2.3	64.9 ±5.5

Figure 2 shows a schematic of the integrated autothermal fuel processor. The fuel, air, and steam feeds enter the central cylindrical zone. A small, electrically powered igniter coil starts the reaction. As the exothermic reaction raises the bed temperatures, the igniter coil is turned off. The products from the reformer section are cooled from 700°C to 350°C by injecting a small amount of water before entering the sulfur removal section. This zone is filled with ZnO pellets. The products continue to flow through the shift reactor section, where the gases are gradually cooled to exit at 200°C.

Using GCTool, a mathematical model based on thermodynamic equilibrium, heat transfer, and material and energy balances has been developed for this reactor. The hardware is being used to validate the model, and the data generated will be used to upgrade the reactor design.

Figure 3 shows the temperature profile as the gases flow through the reactor. The first eight thermocouples are located in the reformer section, and the last four are located in the outer annular region. With appropriate heat exchange, this reactor design avoids the sharp temperature rise typically seen when the fuel and oxygen begin to react near the inlet of most autothermal reforming reactors. Varying the amount and method of water injection helps to control the extent of cooling before the ZnO bed.

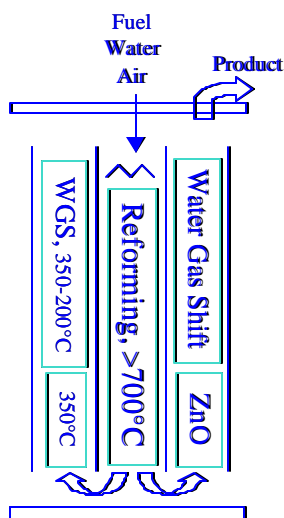


Figure 2. Schematic of the Argonne integrated partial oxidation reformer.

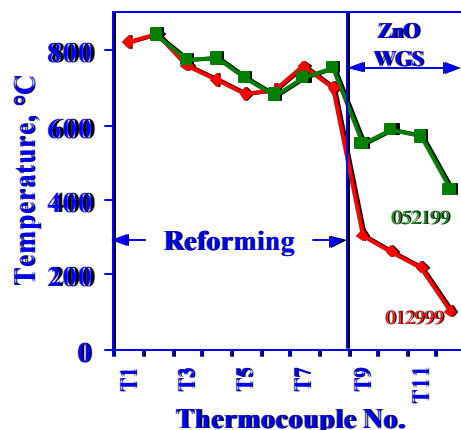


Figure 3. Temperature profiles within the integrated reactor.

The integrated reactor was operated with isooctane, gasoline, and methanol. Figure 4 shows the percentages of hydrogen (30%), carbon dioxide (12%), carbon monoxide (8%), and methane (3%) produced from gasoline. (The balance is mostly nitrogen). The hydrogen percentage is considerably lower than expected because of a leak in the seals that led to part of the reactants bypassing the catalysts. Also, the CO percentage is high because the water gas shift catalyst was not available.

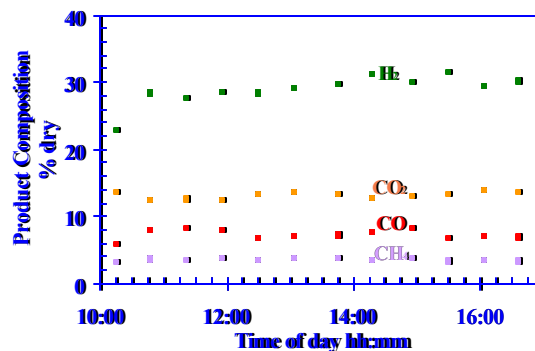


Figure 4. Composition of the product gas obtained from autothermal reforming of California Phase II gasoline. (Fuel=19 mL/min, Air=1.5 scfm, Water=16-24 mL/min).

Figure 5 shows the percentages of hydrogen and carbon monoxide obtained from methanol. For the shift reaction, an auxiliary copper zinc oxide catalyst bed was used. The sharp transitions of the two curves reflect the switching of the reformer gas through the CuZnO bed. After passing through the shift reactor, the product gas contained

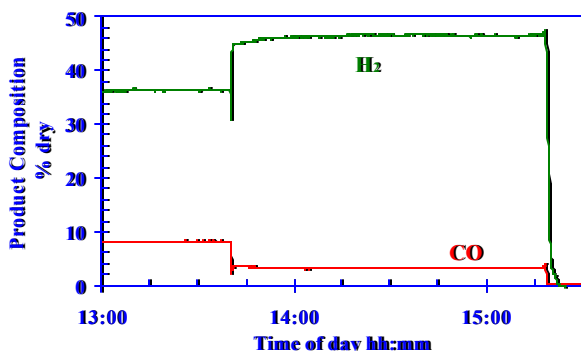


Figure 5. Percentages of hydrogen and CO present in the reformat gas from methanol. CuZnO was used in the water gas shift reactor (Methanol=34 mL/min, Air=0.96 scfm, Water=31 mL/min).

47% hydrogen, 3% carbon monoxide, and 18% carbon dioxide.

The reactor was subsequently operated with isooctane and with the outer annular zone filled with the Argonne water gas shift catalyst. Thirty-seven percent (dry basis) hydrogen and 3% CO were measured in the product gas stream. It is expected that the hydrogen yield will substantially increase after the leaking seals have been welded. It is also anticipated that the CO level can be further reduced by adjusting the temperature profile in the shift zone.

For the future, the microreactor process train will be used extensively to determine “best” operating conditions of the individual reactors and to evaluate the performance of new catalysts and newer reformat clean-up technologies. For the integrated reactor, we will follow the steady-state performance studies with the demonstration of rapid-start and transient operations. Data gathered from this reactor will be used by GCTool to design a more compact reactor.

E. Microchannel Fuel Processor Components

Robert S. Wegeng, Eric A Daymo, Ward E. TeGrotenhuis, Anna Lee Y. Tonkovich, Yong Wang, and Greg A. Whyatt

*Pacific Northwest National Laboratory, P.O. Box 999,
Richland, WA 99352*

(509) 375-3710, fax: (509) 375-6561, e-mail: robert.wegeng@pnl.gov

DOE Program Manager: JoAnn Milliken

(202) 586-2480, fax: (202) 586-9811, e-mail: joann.milliken@ee.doe.gov

Objectives

- Demonstrate compact reactors, separation units, and heat exchangers, based on microsystems technology, for the on-board, automotive production of hydrogen from liquid hydrocarbons.

OAAT R&D Plan: Task 3; Barriers F, G, and H

Approach

- Utilize a newly developed method for process intensification to produce extremely compact hardware with high throughputs, based on the heat and mass transport advantages realizable in engineered microstructures. The key to this effort is the development and application of microfabrication methods for reactors, separations units, and heat exchangers.

Accomplishments

- Development and proof-of-principle demonstration of a single-cell, steam-reforming microchannel reactor was conducted during FY1999. The demonstration included vaporization of isooctane (as a gasoline surrogate) and water in microchannel vaporizers, plus recuperation of the reformat stream in a microchannel recuperative heat exchanger. The unit produces hydrogen in concentrations in excess of 65% (dry gas). Scale-up through the incorporation of multiple cells suggests an overall steam reformer/heat exchanger/vaporizer unit occupying less than 0.25 ft³ volume for the 50-kWe application.
- An R&D 100 Award was received from *R&D Magazine* during FY1999 for the microchannel gasoline vaporizer, identified as one of the 100 most technologically significant new products of the year. This unit consists of microchannel reactor and microchannel heat-exchanger cells that vaporize the gasoline stream for a 50-kW_e fuel processing/fuel cell system. Heat for vaporization is provided through the internal, catalytic combustion of low-concentration hydrogen from the fuel cell anode prior to discharge to the atmosphere. The unit weighs 4 lb and occupies a volume of 0.01 ft³. Validation testing of the microchannel gasoline vaporizer was performed by Epyx at their facilities in Massachusetts during FY1999; similar testing is expected by Hydrogen Burner Technology during late FY1999 and early FY2000.
- Manufacturing studies for microchannel reactors and heat exchangers demonstrate the potential for low hardware cost through mass production. In particular, the microchannel gasoline vaporizer was estimated to cost approximately \$60-70 per unit when manufactured in quantities of 500,000 per year.

Future Directions

- Develop an integral steam reforming system that includes multiple-microchannel reforming reactors, combustors, recuperative heat exchangers, and vaporizers.
- Establish a microchannel fuel processor/fuel cell test loop that provides for the investigation of fuel processing systems, including microchannel reformers, water-gas-shift reactors, heat exchangers, and gas cleanup units. Steady-state and transient operation with a 5-kWe fuel cell is anticipated.
- Continue industrial interactions with the microchannel gasoline vaporizer, as well as with other microchannel reactors and heat exchangers.
- Validate mass-production techniques for microchannel reactors and heat exchangers by fabricating several units, using low-cost mass production methods.
- Operate microchannel reactors and heat exchangers for long-duration tests.
- Adapt the current microchannel steam reformer for transportation fuels.

The development of an on-board fuel processing system to produce hydrogen gas from liquid hydrocarbons for fuel cell use presents a number of technical challenges, including process miniaturization and thermal energy integration. The approach utilized by this project applies a new method of *process intensification*, based on rapid heat and mass transport in engineered microstructures.

Microchannel Fuel Vaporizer

An extremely compact gasoline fuel vaporizer (1.5 in. × 3 in. × 4 in.) for automotive fuel cell/fuel processing systems has been demonstrated (see Figure 1). This vaporizer, which consists of four reactor cells and four heat-exchanger cells, is

fabricated by using micromachining techniques; it exploits the extremely rapid heat and mass transport rates that are possible in engineered microstructures. The unit is able to vaporize gasoline at a sufficient rate for a fuel processing/fuel cell system that provides 50 kW_e of electrical power.

The fuel vaporizer captures and recycles energy from unused hydrogen in the fuel cell waste gas by catalytically reacting it with air and then routing the stream through microchannel heat exchangers, within which gasoline is evaporated. Validation testing of the microchannel gasoline vaporizer was performed by Epyx at their facilities in Massachusetts during FY1999; similar testing is expected by Hydrogen Burner Technology during late FY1999 and early FY2000.



Figure 1. R&D 100 Award-winning microchannel gasoline vaporizer.

The microchannels (shown in Figure 2) are typically 150-300 μm wide and one to several millimeters deep, supporting heat fluxes that exceed 150 W/cm^2 . Despite their small size, microchannels do not present high pressure drops for fluids. Measured pressure drops are consistent with calculations for laminar flow in fluids. As is shown on the graph (Figure 3), the pressure drop through the microchannels is actually less than one pound per square inch (psi). The pressure drop of this vaporizer system is dominated by that across the engineered, monolithic catalyst, which is still quite small (a few pounds per square inch).

The results of this fuel vaporizer project show that catalytic microchannel reactors and heat exchangers can be fabricated and operated in parallel, to realize an extremely compact, lightweight system that produces product streams with appropriate throughput for automotive applications. The current expectation is that a complete microchannel fuel processing system for the 50-kWe fuel cell, including microchannel heat

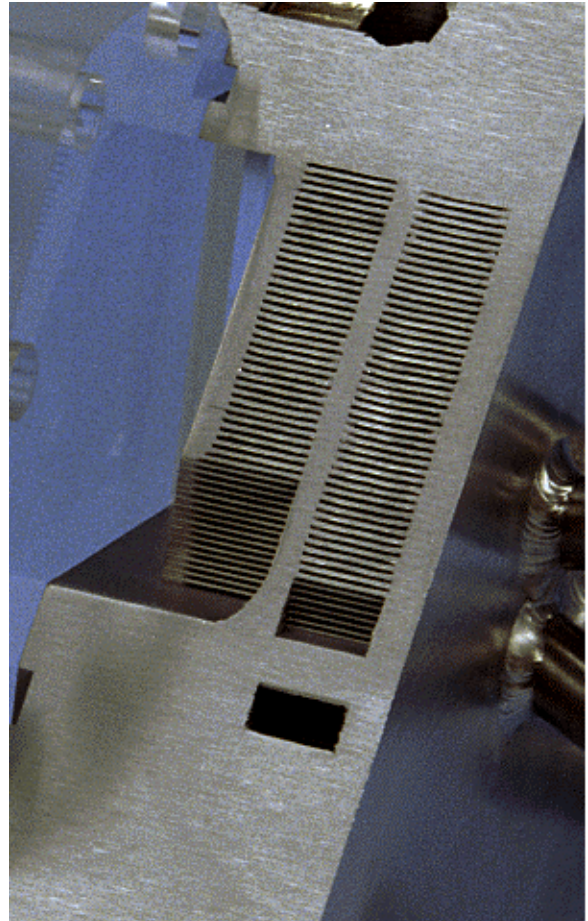


Figure 2. Engineered microchannels, typically 100-300 μm wide, 1-10 mm tall, and 1-10 cm long.

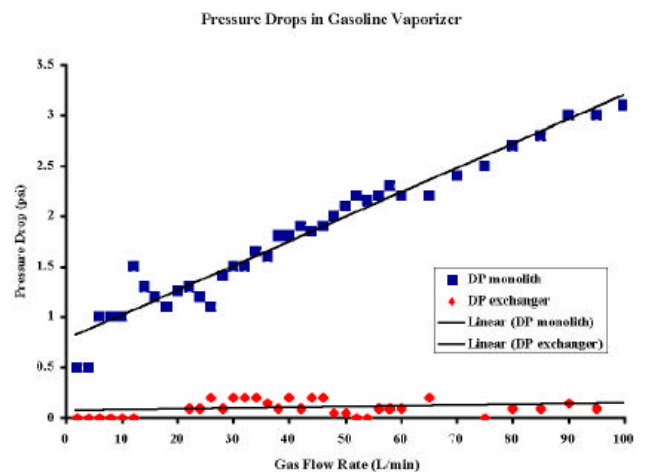


Figure 3. Experimental pressure-drop measurements within microchannels and engineered catalyst for microchannel gasoline vaporizer.

exchangers and reactors, may occupy a volume as small as 0.3 ft³.

Experimental Validation of High Effectiveness in Recuperative Microchannel Heat Exchangers

High thermal efficiency for a fuel processing system requires highly effective recuperative heat exchangers. During FY1999, this project designed, fabricated, and tested microchannel heat exchangers with gas-to-gas recuperation as the objective. Design validation was provided through fabrication and testing of a single-cell unit that operated with high effectiveness. This unit is designed to recuperate the thermal energy content from the reformat stream (as it emerges from a steam reforming reactor).

Proof-of-Principle Demonstration of a Microchannel Steam Reforming Reactor

In general, steam reforming is a more efficient way to produce hydrogen from liquid fuels than other reactions, such as partial oxidation or autothermal reforming. Advantages include higher hydrogen content and the elimination of nitrogen as a diluent in the fuel stream. However, conventional steam-reforming reactors suffer from poor heat and mass transport, resulting in slow reaction rates and low throughput rates per unit hardware volume.

To address the potential application of engineered microstructures to steam reforming, preliminary catalyst screening investigations were conducted during FY1998. These experimental studies confirmed the rapid *intrinsic kinetics* (<50 ms) for the steam reforming of automotive fuels and demonstrated the scientific feasibility of applying this miniaturization approach to steam-reforming reactors.

Efforts during FY1999 included the design, fabrication, and experimental demonstration of a single-cell, microchannel steam reforming reactor. For testing this unit, a breadboard system was assembled that included compact microchannel heat exchangers for vaporizing fuel (isooctane) and water, a very small catalytic combustor, an integral microchannel catalytic reactor/heat exchanger for steam reforming, and a microchannel recuperative heat exchanger for recuperating energy from the reformat stream. As indicated in Figure 4, which

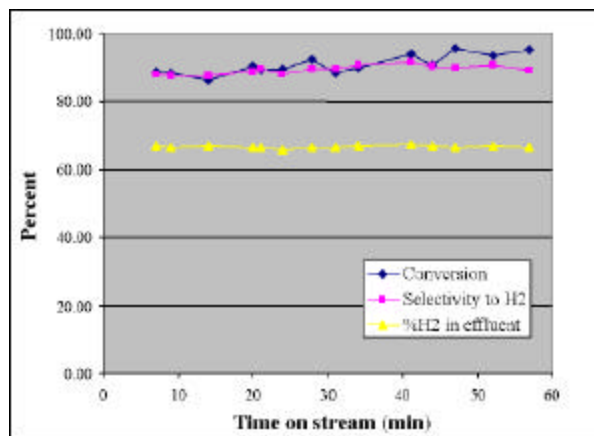


Figure 4. Proof-of-principle demonstration of steam reforming in catalytic microchannel reactor (experimental data, first hour of testing).

shows data from the first hour of testing of this unit, this system was operated at one bar pressure, at 650-700°C, with 100% conversion of the fuel feed. Residence time in the system was quite small, about 2.3 ms, and conversion and selectivity to hydrogen was consistently around 90%. Dry gas content contained >65% hydrogen for all test runs.

Microchannel Fuel Processing System Implications

Current developments suggest that a microchannel fuel processing system, including reformers, water-gas shift reactors, and gas cleanup, could be developed for the PEM fuel cell, with an overall system efficiency of up to 45% and a fuel processing system volume of less than 1 ft³. While high efficiency for a total fuel cell/fuel processor system requires reasonable hydrogen utilization within the fuel cell, system studies have confirmed that overall system efficiency is not strongly sensitive to this parameter, because unused hydrogen can be recycled to the fuel processor to provide for additional reforming. The expectation is that a compact steam-reforming unit can provide high efficiency and high power densities for the overall system.

Publications

Drost, M.K., C.J. Call, J.M. Cuta, and R.S. Wegeng, "Microchannel Integrated Evaporator/Combustor Thermal Processes," *Journal of Microscale Thermophysics Engineering*, Vol. 1, No 4, pp. 321-333, 1997.

Martin, P.M., D.W. Matson, and W.D. Bennett, "Microfabrication Methods for Microchannel Reactors and Separations Systems," Joint AICHE/DECHEMA Special Topical Meeting: *Process Miniaturization – Second International Conference on Microreaction Technology*, March 1998.

Tonkovich, A., C. Call, D. Jimenez, R. Wegeng, and M. Drost, "Microchannel Heat Exchangers for Chemical Reactors," *Heat Transfer – Houston 1996 (AIChE Symposium Series 310)*, pp. 119-125.

Tonkovich, A., J. Zilka, D. Jimenez, M. Lamont, and R. Wegeng, "Microchannel Chemical Reactors for Fuel Processing," Joint AICHE/DECHEMA Special Topical Meeting: *Process Miniaturization – Second International Conference on Microreaction Technology*, March 1998.

Tonkovich, A., C. Call, and J. Zilka, "The Catalytic Partial Oxidation of Methane in a Microchannel Chemical Reactor," Joint AICHE/DECHEMA Special Topical Meeting: *Process Miniaturization – Second International Conference on Microreaction Technology*, March 1998.

Tonkovich, A., J.L. Zilka, M.J. Lamont, Y. Wang, and R.S. Wegeng, "Microchannel Reactors for Fuel Processing Applications. I. Water Gas Shift Reactor," accepted for publication in *Chemical Engineering Science*, 1998.

Wegeng, R., and M. Drost, "Developing New Miniature Energy Systems," *Mechanical Engineering*, Vol. 116, pp.82-85. American Society of Mechanical Engineers, Sept. 1994.

Wegeng, R., M. Drost, T. Ameen, and R. Warrington, "Energy Systems Miniaturization Technologies, Devices, and Systems," *Proceedings of the International Symposium on Advanced Energy Conversion Systems and Related Technologies*, RAN 95, Dec. 1995.

Wegeng, R., C. Call, and M. Drost, "Chemical System Miniaturization," PNNL SA-27317, *AIChE 1996 Spring National Meeting*, New Orleans, La., Feb. 1996. [Also available on the world wide web at: <http://www.pnl.gov/edo/license/programs/fliers/microfly.stm>]]

Wegeng, R., and M. Drost, "Opportunities for Distributed Processing Using Micro Chemical Systems," Invited Plenary Speech, Joint AICHE/DECHEMA Special Topical Meeting: *Process Miniaturization – Second International Conference on Microreaction Technology*, March 1998.

F. On-Board Hydrogen Generation Technology

James Hedstrom, Nick Vanderborgh (Primary Contact), Michael Inbody, Byron Morton, Mike Banaszek, JinKi Hong, Lois Zook, and José Tafoya
MS J576, Los Alamos National Laboratory, Los Alamos NM 87545
(505) 667-6651, fax: (505) 665-6173

DOE Program Manager: JoAnn Milliken
(202) 586-2480, fax: (202) 586-9811, e-mail: joann.milliken@ee.doe.gov

Objectives

- Explore the effects of various fuels and fuel impurities on the performance of on-board hydrogen generation technology integrated into PEM fuel cell systems through
 - Measurement of automotive-scale (50-kW) fuel processor performance and durability
 - Measurement of the effects of real reformat on gas cleanup devices
 - Measurement of fuel cell stack anode performance under realistic operating conditions

OAAT R&D Plan: Task 4; Barriers E and F

Approach

- Develop an automotive-scale fuel processor test facility with the ability to integrate gas cleanup devices and fuel cell stack components
 - Precision measurement of flow, pressure, temperature, and chemical species
 - Transient control and measurement
 - Operation on hydrocarbon and alcohol fuels, with ability to blend test impurities into fuels and fuel mixtures
- Install and characterize the operation of two automotive-scale fuel processors:
 - Integrated fuel processor system from Hydrogen Burner Technology for studies of integrated system performance
 - Modular fuel processor system from Epyx for studies of individual component performance
- Study the effects of fuel processor operation on fuel cell stack anode performance:
 - Measure stack anode CO tolerance with and without air injection
 - Examine the design options and penalties between operation with PROX and/or stack air injection
 - Characterize fuel cell stack anode response to high-concentration CO pulses
 - Characterize effects of fuel processor output on fuel cell stack thermal management

Accomplishments

- Designed and fabricated fuel processor test facility
 - Received Fuel-Flexible Fuel Processor from Hydrogen Burner Technology
 - Awaiting shipment of Modular Pressurized Flow Reactor fabricated by Epyx
- Designed and fabricated 25-kW electrochemical test facility
- Measured fuel cell stack anode CO tolerance with and without air bleed
- Measured fuel cell stack anode response to high-concentration CO pulses
- Examined PROX and stack air injection efficiency options

Future Directions

- Complete installation of test fixtures in fuel processor test facility:
 - Complete experiment automation
 - Complete installation of emissions analysis instrumentation
 - Verify fuel processors and fuel processor test facility with operation on CNG :
 - Verify reactant management, pressure control, and emissions instrumentation to achieve accurate heat and mass balances
 - Verify controls operation
 - Measure CO transients, both normal and within operational stages
 - Study fuel processor operation on petroleum-based fuels to evaluate effects of major constituents:
 - Evaluate requirements to achieve stable and efficient hydrogen generation rates
 - Measure fuel processor transient operation, including startup/shutdown and variations in flow rates
 - Integrate fuel cell stack testing with fuel processor operation to evaluate system integration effects of fuels
-

Introduction

This report describes our FY99 technical progress in on-board hydrogen generation technology research. The goal of this research is to explore the effects of various fuels and fuel impurities on the performance of on-board hydrogen generation devices and consequently on the overall performance of the PEM fuel cell system.

Fuels and fuel impurities may affect fuel processor operation, efficiency, reformat gas composition, transient performance, lifetime, and durability. The effects will be investigated through experiments with fuel processor hardware in a newly developed fuel processor test facility. The effects of fuels and fuel impurities on fuel processor operation cascade to affect the performance and operation of gas cleanup devices integrated with the fuel processor. The performance and operation of gas cleanup devices on real reformat from the installed fuel processors will be investigated. Fuels and fuel impurities ultimately affect the performance and operation of the fuel cell through their effects on the anode feed stream composition and contaminants and their variation with time. These effects are investigated by testing representative fuel cell stacks with simulated reformat streams and also by eventual integration within the fuel processor test facility.

Below we describe our progress on the development of a fuel processor test facility and the installation of two vendor-provided fuel processors, the development of an electrochemical test facility,

and results from testing fuel cell stacks on simulated reformat.

Fuel Processors and Fuel Processor Test Facility

The fundamental tools for our research on the effects of fuels and fuel impurities on on-board hydrogen generation technology are our fuel processor test facilities, beginning with two automotive-scale fuel processors. These two automotive-scale fuel processors will serve complementary roles in our laboratory.

The first fuel processor, the Fuel-Flexible Fuel Processor (F³P) from Hydrogen Burner Technology (Long Beach, CA), is an integrated fuel processor that incorporates a partial oxidation reformer, a high-temperature shift reactor, a zinc oxide sulfur-removal bed, a low-temperature shift reactor, an integral steam generator, and a combustion-driven fuel vaporizer. Control hardware and software are included. This fuel processor will be used to study the effects of fuels and fuel impurities on a thermally integrated system where the interactions between components are close-coupled. Studies involving transient operation, startup and shutdown, and integration with gas cleanup devices and fuel cell stacks are also planned for this system. The fuel processor, shown in Figure 1, was received from Hydrogen Burner Technology in June 1999; it is being installed in the fuel processor test facility, with testing to begin in the last quarter of FY99.



Figure 1. The Fuel-Flexible Fuel Processor (from Hydrogen Burner Technology) at Los Alamos.

The second fuel processor, the Modular Pressurized Flow Reactor (MPR) from Epyx (Cambridge, MA), incorporates the sequential unit operations of a partial oxidation reformer, a steam reformer, a high-temperature shift reactor, a zinc oxide sulfur-removal bed, a low-temperature shift reactor, and heat exchanger components in individual sections. This modular configuration can be seen in the isometric drawing of the reactor (Figure 2). This fuel processor allows for detailed studies of the effects of fuels and fuel impurities within each component. Multiple temperature and gas sample ports allow profiling of each stage. The modular components permit the modification of the configuration and the changing of catalysts. Epyx has completed fabrication of the reactor and conducted initial testing of the reactor components. The reactor is scheduled to be shipped to Los Alamos in the fourth quarter of FY 1999.

The fuel processor test facility was designed to provide the balance-of-plant framework for these fuel processors, together with the necessary analytical instrumentation and supervisory control to characterize their operation and performance. The balance-of-plant systems include the fuel supply and fuel vaporizer, process air supply and preheater, deionized water supply, steam supply, anode off-gas simulation gas supplies, coolant supply for the heat exchangers, and fuel processor exhaust treatment and back pressure system. These systems are

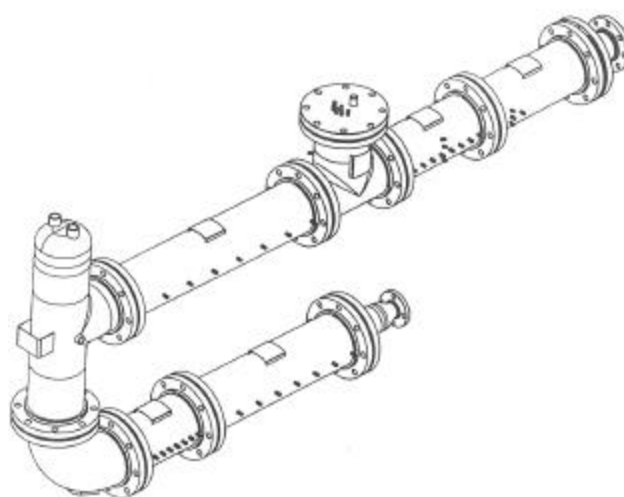


Figure 2. Isometric drawing of the Epyx Modular Pressurized Flow Reactor.

designed for accurate reactant management and emissions management so that accurate heat and mass balances can be measured during operation. Supervisory control hardware and software allow for transient control and operation of the fuel processors.

The next step in this task is to complete the installation of the fuel processors in the test facility and to complete automation of the experiments. The operation of the fuel processors and test facility will be verified through operation on methane and compressed natural gas. The reactant management, pressure controls, and emissions measurements will be verified to obtain accurate heat and mass balances on the systems. Transient behavior will be characterized both for normal operation and for transitions between operating power levels. Following these initial characterizations on natural gas operation, fuel processor operation on petroleum-based fuels will be characterized to evaluate the effects of fuel composition and contaminants. The goals of these tests are to identify fuel processor operating conditions for stable, efficient hydrogen generation and to investigate the effects of fuel composition on durability and lifetime. Future work will involve integrating gas cleanup devices, such as a PROX, with the fuel processor and incorporating a fuel cell stack into the system.

Fuel Cell Stack Anode Performance

Fuel cell stack testing was conducted to identify effects of fuel processor operation on fuel cell stack anode performance. The capabilities of the LANL stack test facility allow testing of stacks on synthetic reformat; the gas flow rate and composition can be varied to replicate fuel processor and gas cleanup device behavior. Trace contaminants such as CO can be introduced in either steady state or transient conditions. Fuel cell stack performance then can be measured for a variety of fuel processor operating conditions, including different fuel options. Alternatively, a stack can be tested on actual reformat, derived from one of the fuel processor units. Because today the scale of the fuel processor is larger than the scale of test hardware, such integration tests require sample splitting, using only a fraction of the fuel processor output for stack testing.

A full fuel cell stack was obtained from a supplier. This 68-cell stack has an active area of 123 cm² and is rated at 4 kW. The bipolar plates are coated stainless steel and have an embossed flow field. Such hardware can lead to low-cost manufacturability. Some testing was completed on the full stack, but most results presented here were obtained with a short (10-cell) stack. This stack was fitted with commercial MEAs. A photograph of the stack as installed in the Fuel Cell Test Stand is shown in Figure 3.

Of particular interest were anode effects that influenced the stack's performance. One such test was a CO tolerance test. The results are shown in Figure 4. With 1.5% air injection, this stack can operate to over 200 ppm CO without a serious loss in cell voltage. With no air injection, this stack can

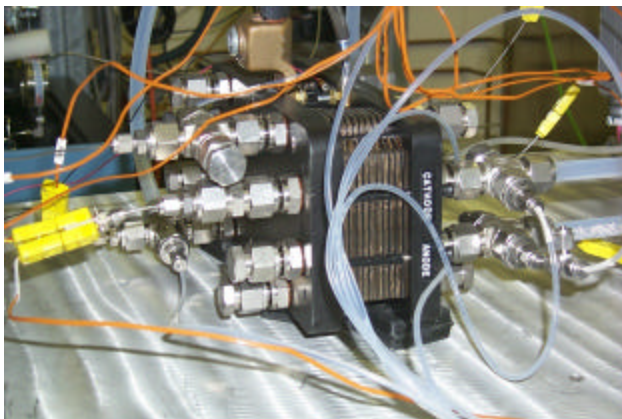


Figure 3. Short stack in test stand.

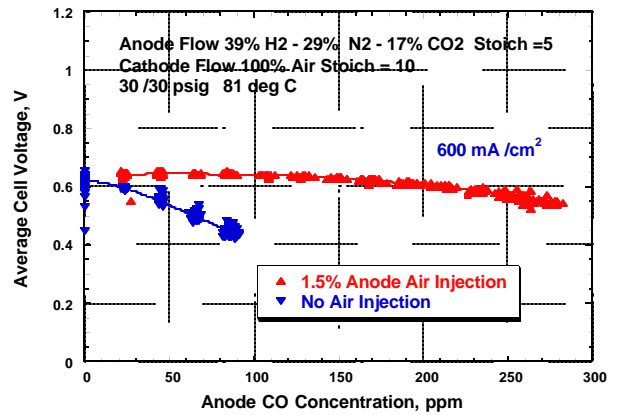


Figure 4. CO tolerance tests on short stack.

tolerate a concentration up to 20 ppm CO. Tests were also completed to determine if CO₂ had adverse consequences (e.g., by flooding the anode structure). Exchanging the same number of moles of N₂ with CO₂ and then reversing the procedure showed no performance loss with carbon dioxide.

Parametric studies were completed to determine the efficiency variation observed with changing the air injection strategy—injecting air into the PROX or into the anode of a particular stack. PROX performance was obtained by testing a PROX built to support Energy Partners (see III H, *Reformat Cleanup Technology*, Figure 2).

The results of the efficiency study are shown in Figure 5. The efficiency presented here is defined as the fuel cell power divided by the LHV of hydrogen in the PROX inlet stream. It is assumed that all oxygen injected into the system and not combined with CO is consumed by hydrogen oxidation, an

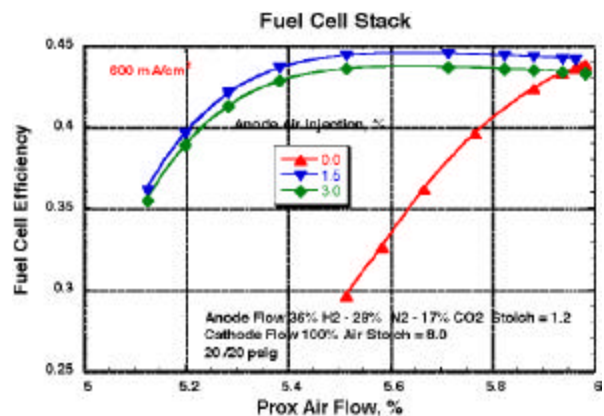


Figure 5. Effect of efficiency caused by changing air injection strategies.

efficiency loss mechanism. The PROX air flow is the total air flow into all stages of the PROX. For this stack, highest efficiency is achieved by injecting 1.5 % air into the anode and 5.65% air into the PROX. The PROX air feed rate results in a PROX outlet CO concentration of 50 ppm. The actual result for any given stack depends on tolerance to CO with a given amount of anode air injection.

The stack supplier indicates that the proper moisture level is essential to obtain good performance. The net water balance for the stack is defined in Figure 6 and plotted as a function of anode stoichiometry for various cathode thermal conditions. The cathode temperature increase within the stack is controlled by setting the inlet temperature (with the inlet steam condenser) and then adjusting the stack coolant temperature to achieve the desired cathode outlet temperature. With a small cathode temperature rise, the stack tends to accumulate water because the difference in absolute humidity between cathode entrance and exhaust ports is small. Likewise, a large cathode temperature rise results in a dry stack exhaust region and a decline in actual relative humidity below 100%. Lowering the anode flow rate maintains more humid conditions because less moisture is removed as part of the anode flow stream.

The stack performance for these same test conditions is shown in Figure 7. The best performance for this stack is seen to occur when the anode stoichiometry is between 1.2 and 2.0 and the cathode temperature rise is between 5 and 10° C. When the stack is very wet (Dt=0) the cell voltage drops rapidly when the anode stoichiometry is

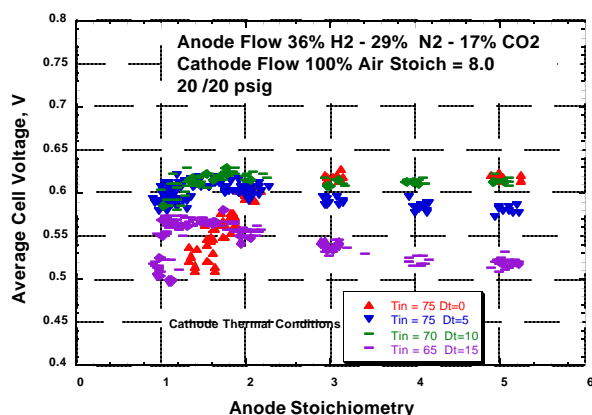


Figure 6. Variation of stack performance with variation in fluid dynamics of anode compartment.

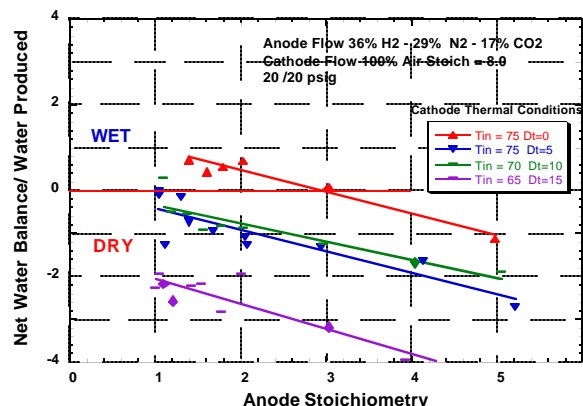


Figure 7. Effect on performance resulting from water management strategies.

decreased below 2.0, as no moisture is being removed from that side of the membrane as well. The dry stack also does not perform well, but it does improve in performance as the anode stoichiometry decreases as less water is being removed.

Contemporary stack design offers two general approaches for reactant delivery control: (1) prescribed flow channels, leading to improved and simplified reactant dynamics at the expense of greater manufacturing complexity; and (2) open flow channels, leading to somewhat more complex requirements for reactant gas dynamics, but probably with far less complex manufacturing. The test article supplied is of this second type.

Several experiments are also reported that use data collected on a test fixture supplied by another company. Tests shown here reflect results when a large-concentration/finite-duration pulse of CO is admitted to the anode compartment. The experiment is to establish stable operating conditions (reformate-air), promptly inject a CO contaminant stream of 600 ppm for 60 s, and then revert to the original CO-free test conditions. (Such an event might replicate an upset in reformer control systems, for example.)

Data are shown in Figure 8. The lower left-hand trace shows the CO introduction. The heavy line shows the computer control signal, and the lighter line represents the measured CO concentration, sampled at the stack anode inlet. The difference in data represents the response time of the reactant control hardware. Two data sets are shown. One is done with a continuous 2% (of the total flow) air bleed—a standard anode test condition. The second shows results with no air injection. As can be seen,

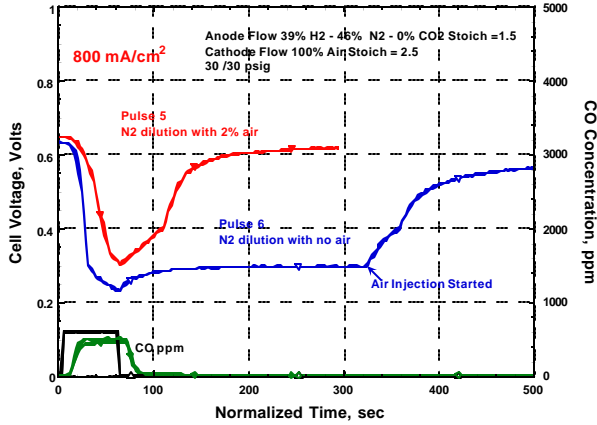


Figure 8. Response of a stack to high-concentration pulses of carbon monoxide. Two experiments are shown, with and without 2% air bleed. The 35-cell stack showed no adverse long-term consequences.

the results are quite different. In both cases, performance loss of approximately 50% is observed. Air bleed results in a case where the performance decay is less rapid and the loss somewhat less severe. At the termination of the pulse, recovery is rapid with air bleed and essentially nonexistent in the absence of air bleed. (The abrupt change in slope of voltage with time data in the recovery plots is an artifact of the cell load control system.)

The LANL team also assembled a new electrochemical-testing fixture, which permits advanced diagnostics of devices up to the 25-kW level. A schematic of this testing instrument is shown in Figure 9. A new feature is a unique digital valve that permits rapid, flexible, computer-controlled pressure-flow metering of hydrogen and hydrogen-containing gaseous mixtures.

In summarizing the anode-performance experiments, the following conclusions are apparent:

1. *CO Control:* An appropriate reactant injection strategy is necessary to achieve the best anode performance. This is a system-level control issue involving the extent of CO tolerance in the anode and the design of the PROX hardware. Optimization is component-dependent.
2. *CO₂ Performance Loss:* A modern MEA shows no adverse consequences with significant, long-term exposure to carbon dioxide.
3. *Reactant Flow:* Successful stack designs can be built with a variety of fluid dynamic solutions,

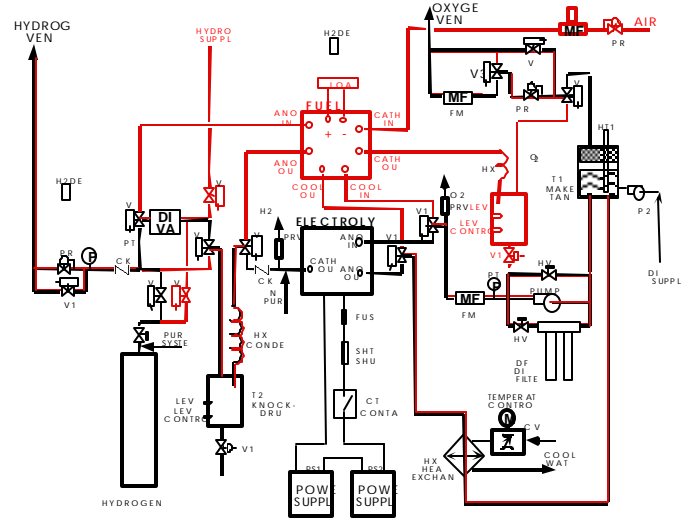


Figure 9. Schematic of new electrochemical test stand.

- including both open flow areas and prescribed (channel) flow areas.
4. *CO Pulse Experiments:* Stacks continue to perform, even in the presence of extraordinary CO contamination levels. Recovery requires thorough removal of CO (e.g., by air oxidation of that species).
5. *Stack Diagnostics:* Data analysis (not shown) of the time response of performance loss can be used to evaluate the quantity of reactive anode catalyst.

Although quality test fixtures (PEM fuel cell stacks) were necessary to achieve these results, it is not the authors' intent to compare performance among different vendors. Both of the test fixtures are prototypical and may or may not represent other hardware from the same vendor. Data are selected to represent the types of experiments now under way at LANL, to support DOE's activities in fuel-cells-for-transportation technology. A more appropriate view is that the stack component is just one element in the overall system—the optimization of the engine is the necessary goal.

FY 2000 Technical Plans

Future activities are focused on stack testing with the use of actual reformat gaseous mixtures generated by means of the fuel processing hardware at Los Alamos. Testing will emphasize documentation of effects of specific components resulting from the fuel processing hardware. Both

large-concentration and trace-concentration constituents will be explored.

We will also experiment with the effects of cold storage temperatures of PEM systems, such as might occur with a vehicle stored outdoors in cold

climates. Studies will examine similar constituent effects and evaluate improved start-up options.

We will continue to advance the technology leading to improved diagnostics of the stack component within these indirect fuel cell engines.

G. R&D on a Novel Breadboard Device Suitable for Carbon Monoxide Remediation in an Automotive PEM Fuel Cell Power Plant

Nguyen Minh (PM) and Tim Rehg (Co-PI)

AlliedSignal Aerospace Equipment Systems

2525 W. 190th Street, MS-36-1-93140

Torrance, CA 90504-6099

Minh: (310) 512-3515, fax: (310) 512-3432, e-mail: Nguyen.Minh@AlliedSignal.com

Rehg: (310) 512-2281, fax: (310) 512-3432, e-mail: Tim.Rehg@AlliedSignal.com

Di-Jia Liu (Co-PI)

AlliedSignal Des Plaines Technology Center

50 E. Algonquin Road

Des Plaines, IL 60017-5016

(847) 391-3703, fax: (847) 391-3750, e-mail: Di-Jia.Liu@AlliedSignal.com

DOE Program Manager: Patrick Davis

(202) 586-8061, fax: (202) 586-9811, e-mail: patrick.davis@ee.doe.gov

ANL Technical Advisor: William Swift

(630) 252-5964, fax: (630) 252-4176, e-mail: swift@cmt.anl.gov

Contractor: AlliedSignal Aerospace Equipment Systems, Torrance, California

Prime Contract No. DE-FC02-99EE50578, September 1999-November 2001

Objectives

- Develop, implement, and demonstrate a new CO-removal system for use in PEMFC systems that provides high CO-removal efficiency, low parasitic hydrogen consumption, and tolerance to CO input variation in an easily controlled manner. The system will be designed for removal of CO from a continuous reformat flow sized for a 10-kW PEMFC stack with a CO input level of 5000 to 8000 ppm.

OAAT R&D Plan: Task 7; Barrier E

Approach

- In a 27-month program, AlliedSignal will research and develop a novel technology to selectively remove CO from reformat fuel for use in PEMFCs. Two approaches to CO removal will be explored and developed. Following the initial 12-month R&D phase, these approaches will be evaluated critically for selection on the basis of efficiency, system compatibility, and cost criteria. A breadboard CO-remediation system sized for a 10-kW PEMFC stack will then be constructed and tested on synthetic reformat, as well as on reformat obtained from a Hydrogen Burner Technology fuel processor.

- The program consists of four major tasks:
 - Research and development on two potentially viable approaches to the in-line removal and treatment of CO.
 - Selection of the most promising technique on the basis of performance and cost.
 - Design and fabrication of a brassboard CO-removal device based upon the selected technology of choice.
 - Testing of the CO-removal system.

Accomplishments

- New start in late Fiscal Year 1999.

Fuel Cell Stack System

(excludes fuel processing/delivery system)

(includes fuel cell ancillaries: i.e., heat, water, air management systems)

Characteristic	Status	DOE Technical Target
Peak Power (kW)	50	50
Stack System Efficiency @ 25% Power (%)	44-55	55
Stack System Efficiency @ Peak Power (%)	45-52	44
Power Density (W/L)	282-322	350
Specific Power (W/L)	295-430	350
Precious Metal Loading (g/kW)	0.9-2.6	0.9

Future Directions

- Conduct in-depth R&D and analysis for approach selection and brassboard application.
- Construct a prototype for performance evaluation.

Introduction

Because of its inherent advantages, including high efficiency, low noise and chemical emissions, and low operating temperature, the PEMFC continues to benefit from intense development efforts for its potential application in automobiles. Hydrogen is the most energetic fuel for the PEMFC, but the lack of an existing infrastructure for the routine handling and distribution of hydrogen severely limits its utility. Therefore, the use of reformers to convert more conventional and readily available hydrocarbon fuels, such as gasoline or methanol, to hydrogen is considered a more viable alternative at present. Unfortunately, a typical reformatte consists of a mixture of gaseous products that includes CO at concentration levels near 1%; the detrimental effect of CO, even at the parts-per-million (ppm) concentration level, on the performance of a PEMFC operating with platinum catalysts is well documented. One approach to the CO problem is to incorporate a pretreatment device

– residing in the fuel line, between the fuel processor and the fuel cell – that significantly decreases the CO concentration in the reformatte. This process can be either by physical removal (as in the case of membrane separation) or by chemical reaction (as in the case of methanation or the use of PROX). These techniques suffer from various disadvantages, including high cost and complexity, high parasitic hydrogen consumption, and intolerance to large CO transients without complicated and expensive control processes.

Objective and Approach

The goal of this program is to develop and demonstrate a novel CO-removal system that provides high CO-removal efficiency with an increased tolerance to CO input variation in an easily controllable manner. This system will be incorporated in a working PEMFC system, between the fuel processor and the PEMFC stack, as shown in Figure 1. The system is based on the use of a

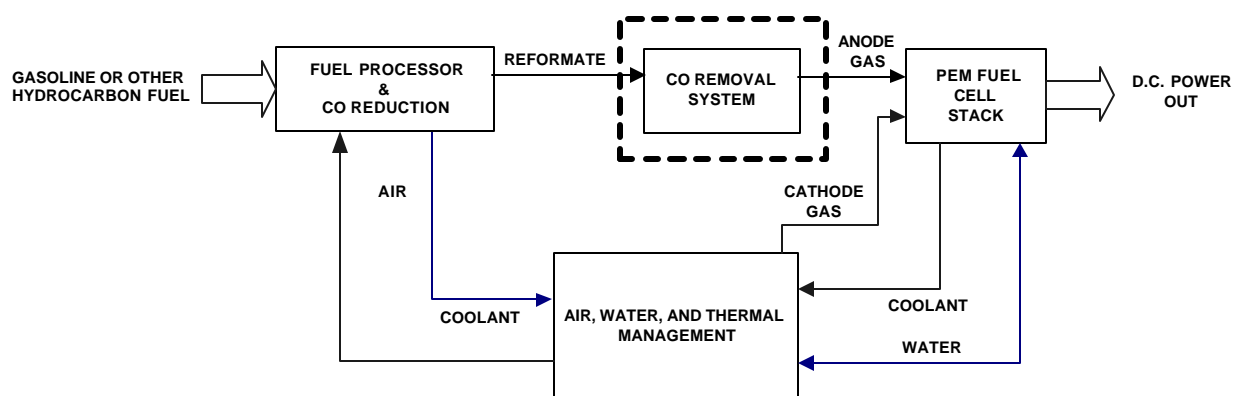


Figure 1. CO removal system in a reformer-fueled PEMFC power system.

selective CO-removal device that can be regenerated periodically when saturated with CO. Potential advantages of this approach include a high tolerance toward variations in CO input with changing load dynamics, low parasitic hydrogen consumption, relative simplicity of operation, and an ability to control and operate during the “cold-start” condition.

Two innovative approaches to selective CO removal and regeneration will be investigated. Initial proof-of-principle experiments for both approaches have been successfully demonstrated in our laboratory. Shown in Figure 2 are preliminary data that confirm our first approach. During the CO-removal phase of the experiment, a synthetic reformat with a CO concentration greater than 1400 ppm was passed through the device and, as shown in the figure, >95% of the CO was removed selectively from the reformat stream. The device regeneration process can be repeated continually with no apparent loss in CO-scrubbing efficiency.

Shown in Figure 3 are preliminary data that demonstrate the underlying concepts of the second approach. Again, CO is selectively removed from the synthetic reformat. As the figure indicates, a CO-removal device based on Approach 2 can be operated in a discrete mode. With an increase in the frequency of operation, a continuous depletion of CO in the reformat can be obtained.

The most promising of the two techniques will be selected for implementation and testing in a brassboard device. The device will be designed for

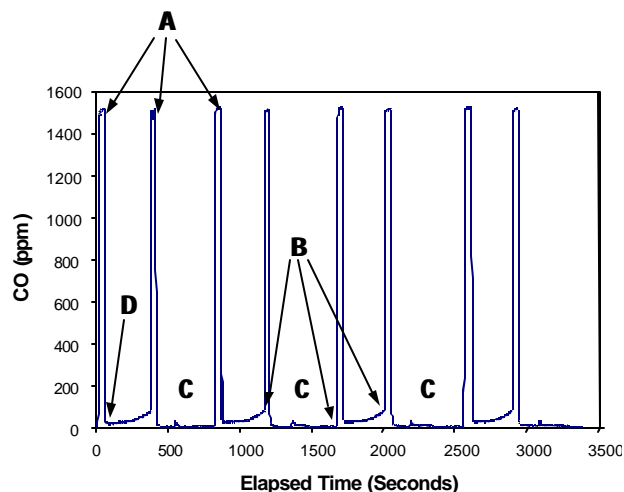


Figure 2. Demonstration of periodic CO removal with rapid device regeneration, using approach #1. At Point A, the CO-containing reformat was directed into the CO removal device prior to reaching the in-line CO detector. Point B denotes the device’s removal from the reformat stream, indicated by the rapid increase in CO concentration. During C, the device was readied for the next cycle (regeneration process not shown). At Point D, no CO was detected; the apparent presence of CO is due to detector offset.

removal of CO from a continuous reformat stream sized for a 10-kW PEMFC stack with an input CO concentration level of up to 8000 ppm. The prototype will later be delivered to Argonne National Laboratory for further testing.

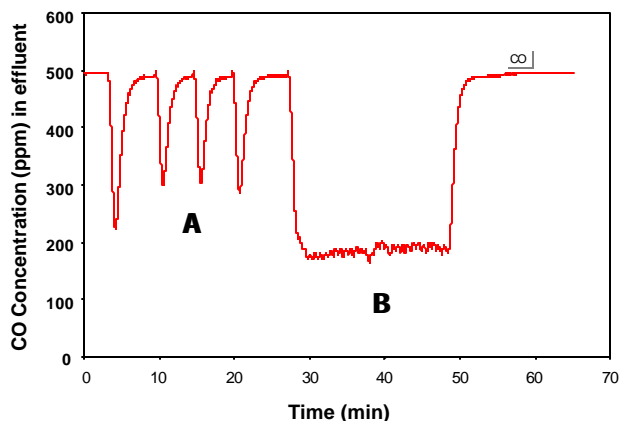


Figure 3. Demonstration of periodic CO removal, using approach #2. The device can be operated in either a discrete (A) or a continuous (B) mode.

Reference

Ferrall, J., et. al., "Parametric Analyses for an Air-Reformate Proton Exchange Membrane (PEM) Fuel Cell Vehicle Application," Proceedings of the 1998 Fuel Cell Seminar, Palm Springs, CA, pp. 323-325, November 16-19, 1998.

H. Reformate Cleanup Technology

Michael Inbody (Primary Contact), José Tafoya, Byron Morton, James Hedstrom, Barbara Zelenay, JinKi Hong, Mike Banaszek, and Nicholas Vanderborgh
 MS J576, Los Alamos National Laboratory, Los Alamos NM 87545
 (505) 665-7853, fax: (505) 665-9507

DOE Program Manager: JoAnn Milliken
 (202) 586-2480, fax: (202) 586-9811, e-mail: joann.milliken@ee.doe.gov

Objectives

- Develop gas cleanup technology for removal of contaminants from the fuel processor outlet stream to optimize fuel cell stack performance
- Develop improved reactor cleanup designs to meet PNGV goals by
 - Improving device efficiency
 - Optimizing for fuel cell engine system
 - Increasing the ability to accommodate automotive transients
 - Improving cost, volume, weight, and durability metrics.

OAAT R&D Plan: Task 3; Barrier E

Approach

- Investigate catalysts, catalyst supports, and catalyst performance for gas cleanup applications
- Refine PROX concept and design
 - Modify reactor design, controls, and sensors for optimal performance and to meet performance requirements
- Test PROX designs and concepts in LANL PROX Experimental Test Facility

- Quantify contaminant removal and transient performance on simulated reformat
- Develop and refine control strategies under simulated operating scenarios
- Test PROX designs and concepts in fuel processing systems
 - Address system integration issues and operation on real reformat streams
 - Develop 10-kWe PROX for Energy Partners PEM system
 - Integration 50-kW PROX with HBT and Epyx fuel processors in LANL fuel processing lab
- Develop modeling and analysis tools
 - Support reactor design, experimental analysis, optimization, and control algorithm development

Accomplishments

- Implemented a new PROX/catalytic reactor design that permits compact operation with a 2% CO inlet stream
- Developed a PROX for the Energy Partners PEM fuel cell system
 - Designed, fabricated, thoroughly evaluated, and delivered
 - Reconfigured reactor design to manage higher inlet CO concentration
 - Demonstrated low outlet CO (< 10 ppm)
 - Demonstrated operation at reduced oxygen stoichiometry and with reduced hydrogen consumption
 - Demonstrated decreased sensitivity to fluctuations in inlet CO concentration
 - Demonstrated ability to accommodate transients
- Conducted catalyst evaluations
- Conducted PROX transient response studies
- Addressed DFMA issues through planned workshop and PROX design and testing

Future Directions

- Continue PROX transient experiments to investigate control strategies and provide modeling data
- Continue catalyst investigation and evaluation
 - Evaluate rugged supports for use in PROX automotive applications
 - Evaluate catalysts for reducing size of the PROX catalyst volume
- Investigate compact devices for controls, gas mixing, sensors, and actuators to reduce overall PROX volume and cost, thereby enabling new, compact fuel processing hardware
- Integrate PROX with fuel processing systems at LANL
 - Operate stacks on “real” vs. synthetic reformat
 - Address PROX/POX system integration issues, including synergy and transients
 - Investigate durability issues
 - Investigate reformat cleanup by processing of additional contaminants in real reformat stream
 - Investigate effects of fuel-processing contaminants on PROX performance
- Explore technology transfer opportunities.

Introduction

This report describes our FY 1999 technical progress in research on reformat gas cleanup technology. The goal is to advance catalytic gas cleanup technology to remove contaminants from the fuel processor outlet stream, thereby improving fuel cell stack performance. The initial focus of research has been the removal of the contaminant,

CO, from reformat streams by preferential oxidation (PROX) cleanup technology. Our research and designs have expanded to implement additional mechanisms for CO removal and to address other reformat contaminants, but we still describe the devices that accomplish this by the generic name “PROX.” To develop a PROX from the current laboratory device into an automotive device requires improvements in efficiency and transient capability,

as well as meeting automotive requirements for cost, volume, weight, and durability.

The approach taken to meet the PROX automotive requirements requires investigating catalysts and catalyst supports, refining the PROX concept and design, and incorporating improved catalysts into a reactor design with the required controls and sensors. We verify these PROX designs through benchmark testing on simulated reformat in our PROX experimental test facility and through integration with fuel processing systems via industrial collaborations or, in the future, integration with prototypical fuel processor systems in LANL laboratories.

Below, we describe our implementation of a new PROX design, development of a PROX for the Energy Partners PEM system and its performance, experiments in catalyst testing and PROX transient studies, and progress toward manufacturability of PROX devices.

Implementation of New PROX Design

Much of the experimental work on gas cleanup has been conducted with a new design of the PROX hardware. The motivation for this new design resulted from new specifications for the Energy Partners natural gas PEM fuel cell system and the need to develop a flexible, modular catalyst test reactor as our laboratory tool for gas cleanup research.

The modular design allows rapid addition and removal of a single stage. The design is compact because of integrated air injection and mixing within



Figure 1. PROX stage components. Outer shell is shown by the two stages in the foreground. A catalyst cartridge is shown in the center background, with a HEX insert in the right background.

a heat exchanger built into the device's exterior. The transient response of the device is improved through reduction of the mass of the internal components and by regenerative heat transfer features. The design incorporates manufacturable components while still maintaining experimental ease and flexibility of use for laboratory investigations.

The parts are fabricated from drawn, precision, thin-wall stainless steel tubing. Only the external tubing has the necessary thickness to achieve the pressure rating; the internal components are lightweight and demonstrate improved transient response.

One key design feature is the use of an easily replaceable catalyst cartridge that can accommodate catalysts in the form of monoliths, pellets, foams, and screens. Another key design feature is the use of a replaceable heat exchanger insert that facilitates quick exchange of different heat exchanger configurations for interstage cooling. The end result is a flexible and multipurpose design in which any stage can be configured as a PROX stage, a filter stage, a shift reactor stage, or a reformer stage. This design serves well for cleanup experiments that use realistic flow rates and process conditions. Importantly, it is fully capable of handling hydrogen-containing gaseous mixtures under a variety of testing conditions.

Development of PROX Subsystem for Energy Partners

We designed, fabricated, thoroughly evaluated and delivered a PROX subsystem to Energy Partners (West Palm Beach, Fla.). The PROX subsystem was designed for integration into a natural-gas-fueled PEM fuel cell system being integrated by Energy Partners. The new PROX design described above was implemented for this PROX device. The initial configuration of the PROX included three active catalyst stages designed to manage a maximum inlet concentration of 1% carbon monoxide at a maximum reformat flow of 45 kWth, based on the LHV of methane.

The modified PROX device, shown in Figure 2, incorporated the balance-of-plant components to make the system self-contained. Air mass flow controllers within the stand control the air injection. Proportional control valves regulate the coolant flow through each interstage heat exchanger. Pressure and temperature instrumentation are also included. The



Figure 2. PROX subsystem for Energy Partners PEM fuel cell system.

data acquisition and control interface uses hardware from National Instruments, and the operating software was written using National Instruments' LabVIEW. Figure 2 shows the test stand framework incorporating the PROX subsystem. The PROX is mounted on the left. The mass flow controllers, flow control valves, and data acquisition hardware are mounted on the right. The open test stand design allows easy access for modifying the hardware and altering the PROX reactor design (for example, to change the catalyst). Thus, this test apparatus is built for experimental convenience rather than compactness.

We conducted proof testing of the PROX subsystem at Los Alamos, during which time we trained personnel from Energy Partners in standard operation procedures. The proof testing served to identify the PROX stage-operating map to meet the design requirements for the Energy Partners fuel cell stack. For the tests, we simulated methane partial oxidation reformat with an inlet CO concentration of 1% at two total flow rates, 35 kWth and 15 kWth, based on the LHV of methane. Figure 3 shows the the

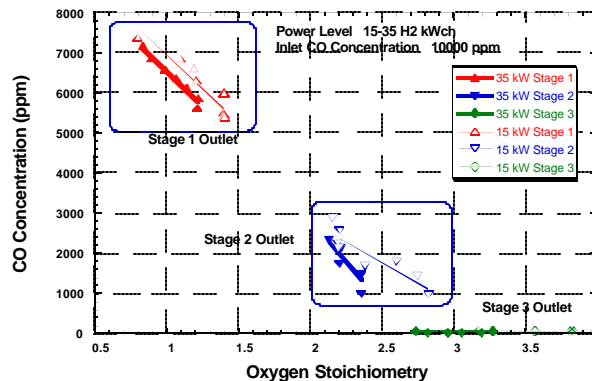


Figure 3. Outlet CO concentration from each stage of PROX as function of overall oxygen stoichiometry.

outlet CO concentration from each stage of the PROX as a function of oxygen stoichiometry. Here we define oxygen stoichiometry as

$$f_{O_2} = 2 \cdot \left(\frac{\dot{N}_{O_2}}{\dot{N}_{CO}} \right)_{actual}$$

where \dot{N}_{O_2} is the oxygen molar flow from the air

injection and \dot{N}_{CO} is the carbon monoxide molar flow at the PROX inlet. An overall oxygen stoichiometry for a PROX stage sums the oxygen molar flows up to and including that stage. The ideal operating point for a PROX would be an overall oxygen stoichiometry of 1, where just enough oxygen is added to oxidize quantitatively the carbon monoxide. Where oxygen stoichiometries are higher than 1.0, operating conditions are such that oxygen consumes hydrogen in addition to carbon monoxide, an efficiency penalty. Figure 4 shows the outlet CO concentration from the PROX as a function of overall oxygen stoichiometry. At the two indicated flow rates, the outlet CO concentration drops below 50 ppm, our target level, for oxygen stoichiometries ranging from 4 to below 3.

The PROX subsystem subsequently was installed in the Energy Partners natural gas PEM fuel cell system, where it was used in the successful demonstration of electricity production from a natural gas system.

Reconfiguration of PROX Subsystem

Results from catalyst testing in a duplicate version of the Energy Partners PROX led to the

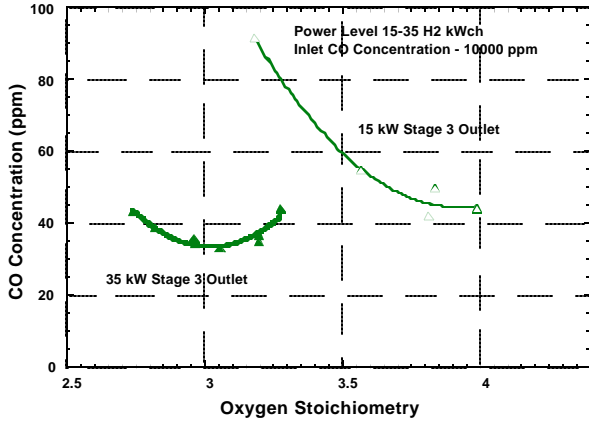


Figure 4. Detail of PROX outlet CO concentration as a function of overall oxygen stoichiometry.

concept for a new approach to reduce both the outlet CO concentration and oxygen stoichiometry. Test data obtained during the Energy Partners experiments showed a new design requirement, to manage higher levels of CO than first planned. Based on these results, the PROX subsystem for Energy Partners was reconfigured and rebuilt for operation with an inlet concentration of 2% CO. The modifications included (1) the addition of a particulate inlet filter to assure dust-free sample inlet flow; (2) addition of a compact low-temperature shift reactor stage; (3) modifying the catalyst design in the PROX reactor stages; and (4) a new code for the control computer.

We conducted benchmark testing of the reconfigured PROX subsystem before shipping it back to Energy Partners. Operating conditions observed during Energy Partners' fuel cell system experiments were reproduced in the LANL PROX Test Facility. Figure 5 shows the resulting outlet CO concentration for each stage of the PROX for simulated methane POX reformate at 4 total flows and specified POX equivalence ratios and steam-to-carbon ratios. A 2% CO inlet concentration was utilized for all of these experiments. PROX operating conditions were determined that led to an outlet CO concentration of less than 10 ppm CO under all test conditions. Note: at the 20-kWth flow rate, three PROX stages are sufficient to achieve the <10-ppm CO level. Figure 6 shows the PROX outlet CO concentration as a function of the overall oxygen stoichiometry and shows greater detail of the low outlet CO concentration (< 10 ppm) for each flow rate. The graph also shows that the overall oxygen

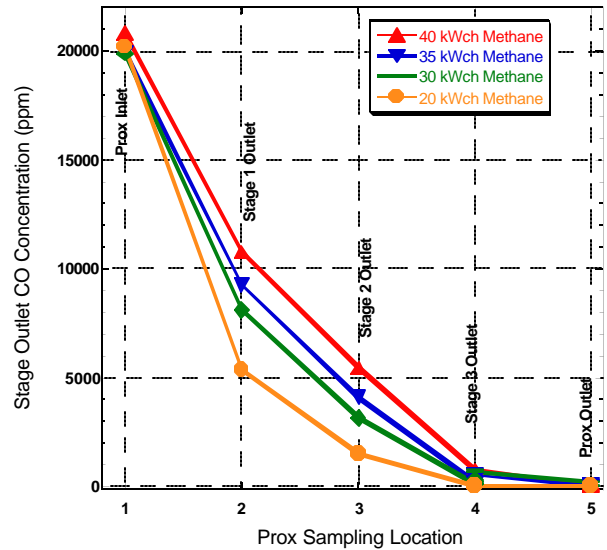


Figure 5. Outlet CO concentration from each stage of the PROX.

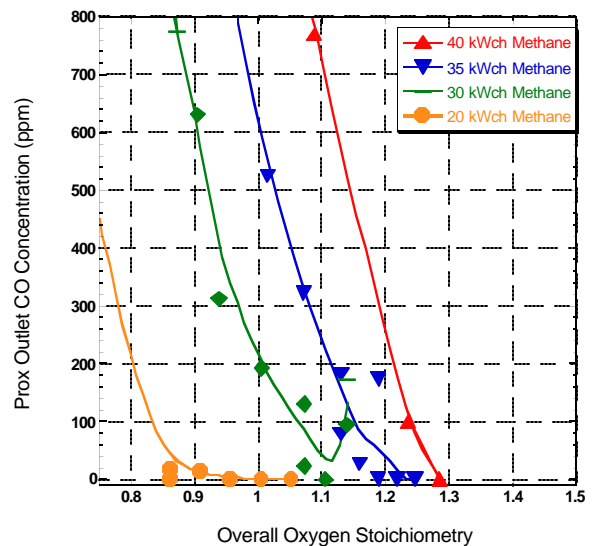


Figure 6. PROX outlet CO concentration as a function of the overall oxygen stoichiometry.

stoichiometry required to achieve these low outlet CO concentration values has been reduced below 1.3 for all four flow rates. This represents a significant reduction in the hydrogen consumption and, thus, an improvement in the overall efficiency of the fuel cell system.

Following the benchmark testing at Los Alamos, the reconfigured PROX was transferred to Energy Partners and again incorporated into their natural gas fuel processor-fuel cell system experiment. Figure 7 shows a data snapshot taken during the initial

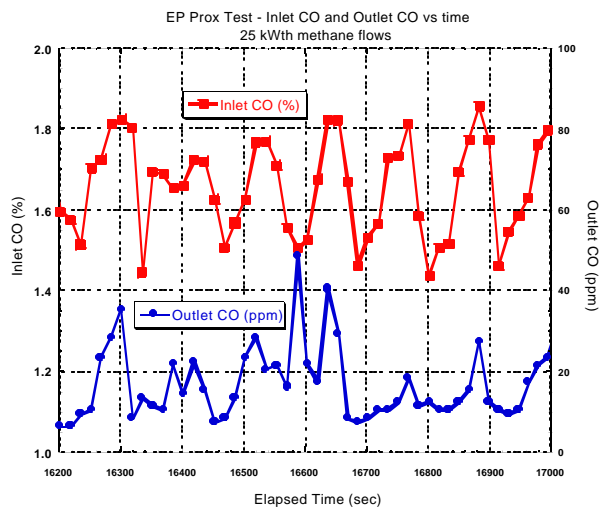


Figure 7. Data snapshot taken of PROX inlet and outlet CO concentrations with the fuel processor operating at 25-kWth total flow rate.

checkout of the PROX in the Energy Partners laboratory. The graph shows the PROX inlet and outlet CO concentrations as a function of time, with the reformer operating at a steady-state 25-kWth total flow rate. During this time snapshot, the PROX outlet CO concentration remains below 50 ppm, even though the inlet CO concentration varies considerably. Here, we are demonstrating that the improved PROX approach results in a greatly reduced sensitivity to fluctuations in the inlet CO concentration. The fuel processor in this system was not fitted with an active low-temperature shift reactor and thus shows periodic variation in the PROX inlet CO concentration. A system with a low-temperature shift reactor would be expected to yield far smaller fluctuations in the PROX inlet CO concentration.

Catalyst Investigations

We continue investigations of catalysts and catalyst supports to document catalyst performance and to generate data for kinetic modeling. These studies provide the research base for improving PROX performance and design. The catalyst evaluation studies utilize the new PROX design in a two-stage configuration—these tests are done using full-scale flow rates. The first stage is a gas mixing and conditioning stage, while the second is the catalyst, which modifies the composition of the sample stream.

Catalysts tested during the year have included formulations made with platinum, ruthenium, and palladium. Catalyst support types have included pellet, monolith, and ceramic foam supports. Also, experiments were instrumented to measure temperature and species profiles throughout the catalyst volume to obtain data for modeling studies.

PROX Transient Operation

We also continue experiments that measure the transient response of the PROX, including new options for faster transient operation. Both the 50-kWe PROX system developed last year and the new, reconfigured PROX design have been used for these transient experiments. The experiments are now focused on the new PROX design because of its demonstrated faster transients, coupled with experimental flexibility.

Experiments in progress study fluctuating inlet CO concentrations and control of those fluctuations, as well as PROX transient response and control during transients in overall reformate flow rates, which occur when fuel cell system power levels change. The goal for these experiments is to develop a simplified control strategy for PROX transients. Work under way seeks new approaches that may eliminate the need for an online CO sensor.

PROX Design for Manufacturing

We are also investigating design-for-manufacturing engineering, where the goal is to cooperate with new partners in the design and prototype fabrication of a compact, transient-capable, durable PROX device. As part of that process, Larry Blair, the Los Alamos Fuel Cells for Transportation Program Manager, will organize a workshop during the year 2000.

Our activities on this task have focused on manufacturable automotive components. This work includes testing manufacturable components in the PROX, designing catalyst components with reduced size and weight and of rugged design, testing LANL PROX concepts in real-world situations (such as within a cooperative activity with Energy Partners), and developing design tools that lead to system design optimization. Also, we are investigating options for transient control, via new concepts built into the reactor design. Here, the goal is to eliminate an online CO sensor, reduce the overall sensor count in the fuel cell system, and reduce the actuator count

for air injection and temperature control. There are several design directions that appear to lead toward such goals.

Future Directions (FY2000)

The future direction for this work on reformat cleanup technology is to improve options for catalytic cleanup technology, moving toward ever more compact, reliable, and cost-effective reactor designs. This includes continuing development of PROX transient experiments, with the goal of investigating control strategies and developing input data for transient modeling. We will continue catalyst investigations and evaluations and will work

with catalyst developers on rugged catalyst structures for more transient-capable and compact hardware. To meet automotive requirements for cost and volume, we will investigate and develop compact devices for controls, gas mixing, sensors, and actuators.

We also plan to integrate the PROX with fuel processing systems in our laboratory. This experimental integration work is aimed at operation of combined Autothermal/Shift/PROX components containing cleanup devices used to provide reformat for PEM stack testing. Such tests will be critical in studying the effects of fuels and fuel composition.

I. Evaluation of Partial Oxidation Fuel Cell Reformer Emissions

Stefan Unnasch

ARCADIS Geraghty & Miller, Inc.

555 Clyde Avenue, P.O. Box 7044

Mountain View, CA 94039

(650) 254-2413, fax: (650) 254-2496, e-mail: sunnasch@acurex.com

DOE Program Manager: Donna Ho

(202) 586-8000, fax: (202) 586-9811, e-mail: donna.ho@ee.doe.gov

ANL Technical Advisor: Walter Podolski

(630) 252-7558, fax: (630) 252-4176, e-mail: podolski@cmt.anl.gov

Contractor: ARCADIS Geraghty & Miller, Inc., Mountain View, California

Prime Contract No. DE-FC02-99EE50585, September 1999-September 2000

Objectives

- Determine the emissions from partial oxidation/autothermal fuel processors for PEM fuel cell systems.
- Determine whether emission standards for automobiles and light-duty trucks can be met by a fuel cell vehicle with a multifuel reformer.
- Evaluate performance of catalytic burners in controlling startup emissions.

OAAAT R&D Plan: Task 5; Barriers F, G

Approach

- Quantify cold startup and normal operating emissions from a partial oxidation reformer before and after anode-gas-burner treatment.
- Test four fuels – gasoline, methanol, ethanol, and natural gas – as well as different catalyst formulations.

- Test both Epyx and Hydrogen Burner Technology, Inc. (HBT), fuel processors.

Accomplishments

- New start in late FY 1999.

Future Directions

- Complete emissions testing in FY 2000.

Introduction

This project will determine the emissions from partial oxidation/autothermal fuel processors for PEMFC systems. Both Epyx Corporation and Hydrogen Burner Technology, Inc. (HBT), fuel processors will be tested. The cold startup and normal operating emissions of NO_x, CO, and CO₂, methane, nonmethane hydrocarbons, carbonyl group compounds (aldehydes), and speciated hydrocarbons (light end hydrocarbon group components and mid-range hydrocarbon group components) from a partial oxidation reformer (POX), before and after treatment by an anode gas burner, will be quantified. Different anode gas burner catalyst formulations and four fuels (gasoline, methanol, ethanol, and natural gas) will be tested. The project will determine whether a fuel cell vehicle with a multifuel reformer can meet emission standards for automobiles and light-duty trucks.

Background

The operating requirements for both the HBT and Epyx systems are similar. Emissions from the fuel cell system arise in two operating modes, startup and normal partial oxidation (POX) operation. During startup, the fuel processor burns fuel at near-stoichiometric conditions. Cold-start emissions from a cold combustor are much higher than those from a system that has been warmed up. Target times for startup are less than 30 seconds. However, the emissions produced during this brief period can be substantially higher than those during the remaining, much longer portion of a driving cycle. Pollutant emissions from startup include NO_x, unburned hydrocarbons and other organic compounds, CO, and formaldehyde. Organic compounds – including hydrocarbons, alcohols, and aldehydes – are referred to in California, and regulated as, “nonmethane organic gases” (NMOG). This distinction is convenient when dealing with

oxygenated fuels, such as reformulated gasoline (RFG), which contains 11 percent methyl tertiary butyl ether (MTBE) or other oxygenated compounds, as well as methanol and ethanol.

During normal operation, the fuel processor operates under very rich conditions, with a stoichiometric air/fuel ratio below 0.4. Under these conditions, virtually no NO_x is formed, although the formation of ammonia is possible. Most hydrocarbons are converted to carbon oxides (or methane, if the reaction is incomplete); however, trace levels of hydrocarbons can pass through the fuel processor and fuel cell. Carbon monoxide in the product gas is reduced by the shift reactors and preferential oxidizer (PROX), so the feed concentration to the fuel cell can be less than 20 ppm. The fuel cell may also convert CO to CO₂, thereby further reducing exhaust CO levels. Of the criteria pollutants (NO_x, CO, and hydrocarbons [NMOG]), NO_x and CO levels are generally well below the most aggressive standards. NMOG concentrations, however, can exceed emission goals if these compounds are not efficiently eliminated in the catalytic burner.

Figure 1 shows estimated NMOG emissions, taken from the ARCADIS Geraghty & Miller study for CARB, for compressed-natural-gas- (CNG-) and gasoline-fueled POX systems. The figure illustrates the importance both of startup emissions in

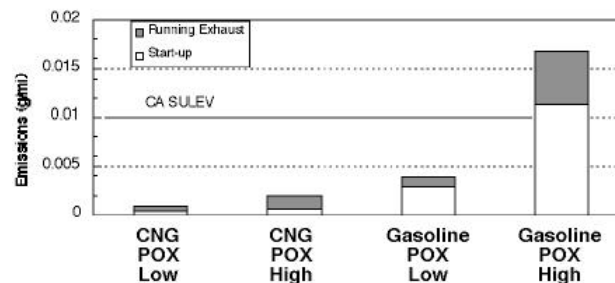


Figure 1. Estimated exhaust emissions for POX/PEMFC systems.

J. Catalytic Partial Oxidation Reforming Materials and Processes

Michael Krumpelt (Primary Contact), S. Ahmed, R. Wilkenhoener, J.D. Carter, Y. Shi
Argonne National Laboratory, Argonne, IL 60439
(630) 252-4553; fax: (630) 972-4553

DOE Program Manager: JoAnn Milliken
(202) 586-2480, fax: (202) 586-9811, e-mail: joann.milliken@ee.doe.gov

Objectives

- Develop catalyst for the partial oxidation reforming of hydrocarbon fuels for fuel cells in transportation
 - Improve catalyst formulation to increase activity and selectivity
 - Elucidate mechanism
 - Support catalyst on monoliths

OAAT R&D Plan: Task 3; Barrier E

Approach

- Catalyst performance is evaluated in microreactors under carefully controlled conditions:
 - Pure hydrocarbons, oxygen/carbon ratio, water/carbon ratio, temperature
 - Elucidate mechanism by studying segments of the reforming reaction sequence
- Explore new materials
 - That have some theoretical basis for promoting the desired reaction
 - That match the properties of catalysts demonstrating high activity and selectivity
- Catalyst technology development:
 - Investigate synthesis techniques that lead to higher activity, promote stability, and are suitable for manufacturing
 - Develop monolith catalysts suitable for transportation applications

Accomplishments

- Developed new catalyst formulation and synthesis technique
 - Increased activity such that 60% (dry, N₂-free) hydrogen was achieved at 600°C
 - Increased catalyst surface area by a factor of 4
 - Demonstrated higher space velocity (10X) capability, leading to compact reformer

Future Directions

- Continue fundamental studies of catalyst to improve performance through the understanding of material effects on reaction mechanism
 - Advance catalyst formulation and preparation
 - Materials, synthesis methods, and structured supports
-

The objective of this work is to develop catalysts for the autothermal reforming of hydrocarbon fuels for use in fuel cell vehicles. It has

been demonstrated that a new class of catalysts developed at Argonne has the ability to convert various hydrocarbon fuels into a hydrogen-rich gas

at temperatures of less than 750°C. This project undertakes to improve the catalyst's activity and selectivity; to elucidate the reaction mechanism, which will lead to better catalysts; and to develop monolith catalysts that are suited for use in mobile applications.

The catalyst development work is pursued from a number of directions. For example, the catalyst formulation is varied to study the changes in catalytic properties that result from different materials, their phases, the proportions and the resulting effects of material interactions, etc. Changing the synthesis technique alters the material properties because of modifications in the phase and structure, as well as in the surface area, of the catalyst.

The concept for the Argonne partial oxidation reforming catalyst was derived from our experience with solid oxide fuel cell materials, where the anode material is chosen on the basis of (among other things) the ability to conduct oxide ions. Also, Vayenas et al. [1,2] showed that when an applied chemical potential exceeded a threshold value, the rate of oxidation reactions jumped several orders of magnitude, as shown in Figures 1 and 2. Extending this phenomenon, called the non-Faradaic Electrochemical Modification of Catalytic Activity (NEMCA), we have demonstrated that catalysts based on these oxide-ion-conducting materials show remarkable activity for the partial oxidation of hydrocarbons and exhibit good selectivity for hydrogen and carbon dioxide in the product.

The Argonne partial oxidation catalyst uses a combination of a metal on the oxide ion conductor (substrate) to achieve the desired reaction. In order to determine the effect of the metal loading on the substrate, experiments were conducted in a

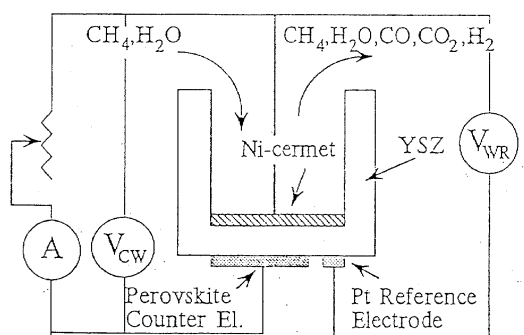


Figure 1. Schematic of the fuel cell reactor.

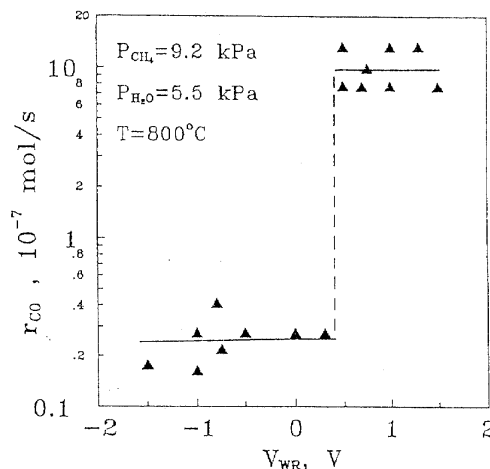


Figure 2. Effect of V_{WR} on the rate of CO formation; Catalyst C4.

microreactor with isooctane as the fuel, oxygen ($O_2/C_8=4$), and steam ($H_2O/C_8=8$), with the reactor maintained at 800°C. Figure 3 shows the product gas distributions obtained by changing the loading of metal A. The hydrogen percentage was found to be maximum at a weight loading of 0.5 wt.%. However, the variations in product distribution with loadings between 0.2 and 1.03 are quite small.

A number of material combinations and synthesis techniques have also been tried to increase the catalyst activity. Figure 4 compares the percentages of hydrogen obtained from a new catalyst material synthesized by a new method to that obtained with a formulation from the previous year. The new method produced a catalyst with a surface area that was 4 times larger, at 30 m²/g.

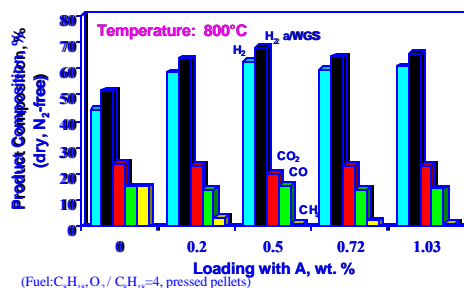


Figure 3. Effect of metal A loading (on a substrate), on product gas distributions during autothermal reforming of isooctane. (H_2 a/WGS means the H_2 percentage after the CO is converted in a water gas shift reactor)

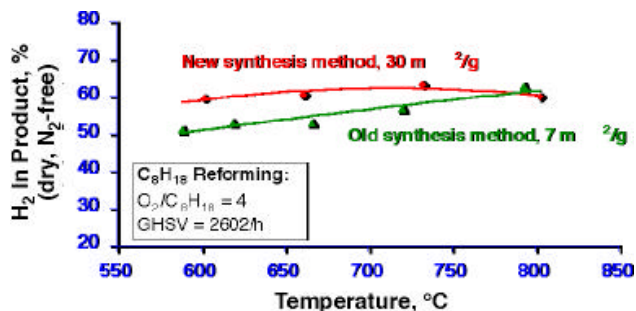


Figure 4. Newer catalyst material and synthesis methods give 60% hydrogen at 600°C.

The combination of new material and higher surface area has led to a more active catalyst. This is demonstrated by the fact that the new catalyst produced 60% hydrogen (dry, N₂-free) at 600°C (Figure 4), compared to the older catalyst, which produced similar H₂ concentrations at over 750°C.

The improved catalyst activity is reflected in the fact that complete conversion can now be achieved at a much higher space velocity. Figure 5 shows the product gas distributions obtained as a function of the gas hourly space velocity (GHSV, based on gaseous reactants at 25°C and catalyst volume). The reactor was maintained at 700°C. At the low space velocity of 3000 hr⁻¹, 62% hydrogen was measured in the product gas. When the space velocity was increased by an order of magnitude, to 30,000 hr⁻¹, the catalyst was still able to complete the conversion of isooctane, although the level of by-product hydrocarbons (mainly methane) was increased and the hydrogen percentage dropped to 55%. It is very likely that the trend toward higher HC and lower H₂ percentages can be reversed by raising the temperature slightly, and this will be investigated further. The fact that the space velocity can be increased 10-fold while maintaining conversion is very promising because it predicts that the reformer volume can be reduced by a factor of 10.

The catalyst development work has led to a new catalyst material that has shown remarkable activity

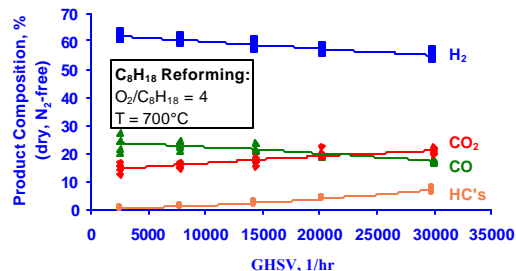


Figure 5. Effect of space velocity on product gas distributions obtained from partial oxidation reforming of isooctane.

and selectivity for the partial oxidation reforming reaction. Fundamental studies in progress have led to advances in the catalyst formulations, and to synthesis methods that indicate more active and selective catalysts are possible. These advances, in turn, point to the ability to reform at lower temperatures and in smaller reformers.

These studies on the fundamental aspects of material interactions and their effects on the reaction mechanism will be pursued further to gain a better understanding of the process. The work on alternative synthesis techniques will be continued to develop faster methods that produce more rugged catalysts with larger surface area.

For transportation applications, it is desirable to use monolithic catalysts. We are investigating several methods (e.g., catalyst monoliths, catalysts supported on monoliths, etc.) to establish the best way to make catalyst forms that achieve the robustness of monoliths without compromising the catalytic properties.

References

1. C.G. Vayenas and S. Bebelis, *Catalysis Today*, **51** (1999), 581.
2. I.V. Yentekakis, Y. Jiang, S. Neophytides, S. Bebelis, and C.G. Vayenas, 2nd European Solid Oxide Forum, Oslo, 1996, p.131.

K. Alternative Water-Gas Shift Catalyst Development

Romesh Kumar (Primary Contact), Deborah J. Myers, Christopher R. Kinsinger, J. David Carter, Theodore R. Krause, and Michael Krumpelt
Argonne National Laboratory, Argonne, IL 60439-4837
(630) 252-4342, fax: (630) 252-4176

DOE Program Manager: JoAnn Milliken
(202) 586-2480, fax: (202) 586-9811, e-mail: joann.milliken@ee.doe.gov

Objectives

- Develop alternative water-gas shift catalysts to:
 - Eliminate the need to sequester catalyst during system shutdown
 - Eliminate the need to activate catalyst *in situ*
 - Increase tolerance to temperature excursions
 - Reduce size and weight of the shift reactor(s)
 - Extend lifetime of the catalyst

OAAT R&D Plan: Task 3; Barriers E and G

Approach

- Develop metal-support combinations to promote bifunctional mechanism of catalyst action:
 - One component to adsorb CO (e.g., metal with intermediate CO adsorption strength)
 - Second component to adsorb and dissociate H₂O (e.g., mixed-valence oxides with redox properties, such as ceria, under reformate conditions)
 - Exploit such reaction pathways as
 - * + CO \rightleftharpoons CO_{ad} * = active surface site
 - M₂O₃ + H₂O \rightleftharpoons 2MO₂ + H₂
 - 2MO₂ + CO_{ad} \rightleftharpoons M₂O₃ + CO₂

Accomplishments

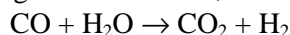
- Improved catalyst activity by a factor of >3 while reducing precious metal content by a factor of 2
- Demonstrated high catalyst activity over the entire conventional HTS and LTS operating temperatures (i.e., from 230°C to 400°C)
- Demonstrated that the catalyst retains high activity even after prolonged exposure to air at 550°C
- Determined kinetic parameters and estimated preliminary reactor sizes to be much smaller than with conventional HTS and LTS catalysts
- Scaled up the supported catalyst fabrication process to synthesize 2-kg batches

Future Directions

- Explore other oxide/metal combinations, such as MnO_x/Mo, for reduced cost, higher activity
- Determine source of poor catalytic activity obtained for nonprecious metals
- Decrease loading of total catalyst and precious metal on high-surface-area support
- Test catalyst under real reformate conditions and investigate potential poisoning by contaminants (e.g., sulfur)

Introduction

The water-gas shift reaction,



is used to convert the bulk of CO in the raw reformat to CO₂ and additional H₂. In the chemical process industry (e.g., in the manufacture of ammonia), the shift reaction is conducted at two distinct temperatures. The high-temperature shift (HTS) takes place at 350–450°C, using an Fe-Cr catalyst. The low-temperature shift (LTS) is carried out at 160–250°C with the aid of a Cu-Zn catalyst.

Commercial HTS and LTS catalysts require activation by careful pre-reduction *in situ*; once activated, they lose their activity very rapidly if they are exposed to air. Further, the HTS catalyst is inactive at temperatures <300°C, while the LTS catalyst degrades if heated to temperatures >250°C.

For the automotive application, with its highly intermittent duty cycle, it is important to develop alternative water-gas shift catalysts that:

- (1) eliminate the need to sequester the catalyst during system shutdown,
- (2) eliminate the need to activate the catalyst *in situ*,
- (3) increase tolerance to temperature excursions, and
- (4) reduce the size and weight of the shift reactors.

Approach

We are developing metal-support combinations to promote a bifunctional mechanism of catalyst action. In this approach, the metal to adsorb the CO is selected as one with an intermediate CO adsorption strength (i.e., an adsorption energy of 20–50 kcal/mol). The support serves to adsorb and dissociate the H₂O. This is typically a mixed-valence oxide with redox properties (such as ceria) under the highly reducing conditions of the reformat. This mechanism may be represented as,

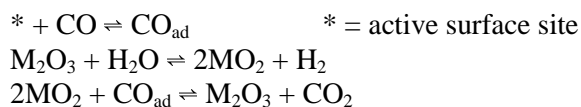


Figure 1 shows the CO adsorption energies of the Periodic Table Group IV to Group XIV metals. The metals with CO adsorption energies of 20 to 50 kcal/mol are shown in Figure 1; these metals were the ones tested as a shift catalyst component. Similarly, the candidate supports with

mixed valence are the oxides of transition metals (Fe, Cr, Mn, V, but not Ni, which is a methanation catalyst and which also forms the volatile nickel carbonyls) and the lanthanides (La, Ce, Sm, etc.). Note that ZnO would not fit this approach, because its role in the commercial Cu-ZnO shift catalyst is not bifunctional. Other non-bifunctional supports could include zeolites, for example.

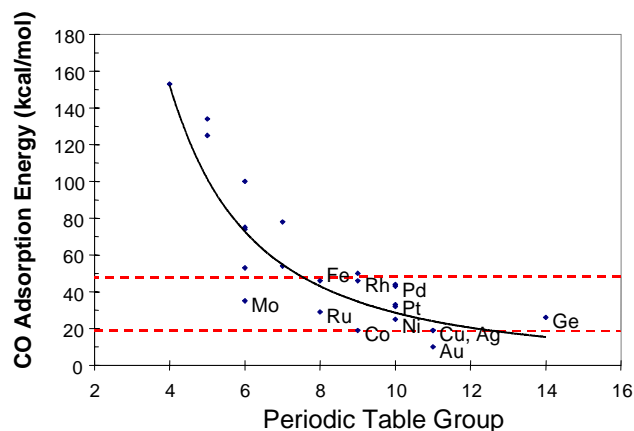


Figure 1. The CO adsorption energy of several Group IV to Group XIV metals.

Recent Progress

Table 1 shows the results of testing the metals identified in Figure 1 with various candidate support materials. High shift activity was observed only with noble metals.

Tests of the candidate catalyst's activity were conducted with simulated reformat, using a microreactor setup as shown in Figure 2.

The reactor was operated as an integral reactor for activity determinations. The logarithm of the change in CO concentration relative to its

Table 1. High catalytic activity was obtained only with noble metals.

Metal	Number of Supports	Relative Activity
Ag	2	Poor
Co	1	Poor
Cu	2	Medium
Fe	1	Poor
Pt	5	High
Ru	2	High (but CH ₄)
Pt-Cu	1	High
Pt-Ru	1	High

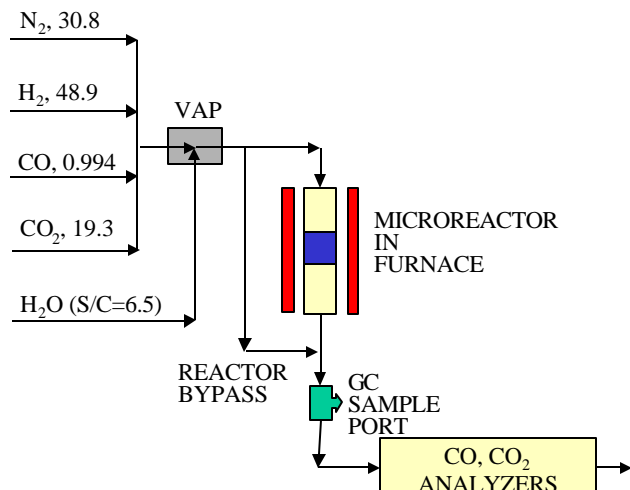


Figure 2. Schematic diagram of the microreactor test apparatus.

equilibrium value, when plotted versus the inverse of the reactant flow rate, shows a linear behavior. The slope of this line is proportional to the reaction kinetics (i.e., the activity of the catalyst). Most of the tests were conducted at 230°C, except the tests to determine activation energies, for which the temperatures ranged up to 400°C.

Figure 3 shows that over the past year we have increased the activity of the catalyst (at 230°C) by more than a factor of 3, while at the same time the catalyst's precious metal content has been reduced by one-half.

The activity of the catalyst was unaffected by exposure to air and to high temperatures in air, as shown in Fig. 4.

The catalyst also showed high activity over the temperature range from 230 to 400°C. The change in product composition as a function of temperature is shown in Figure 5. The product composition

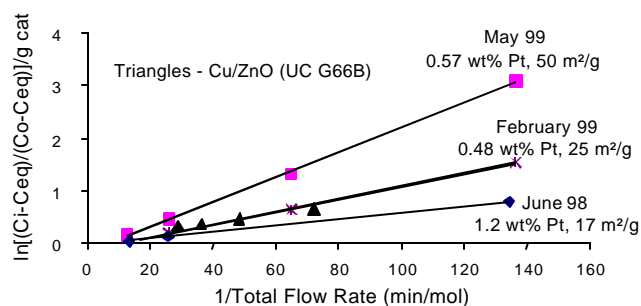


Figure 3. Improvements in catalyst activity from June 1998 to May 1999.

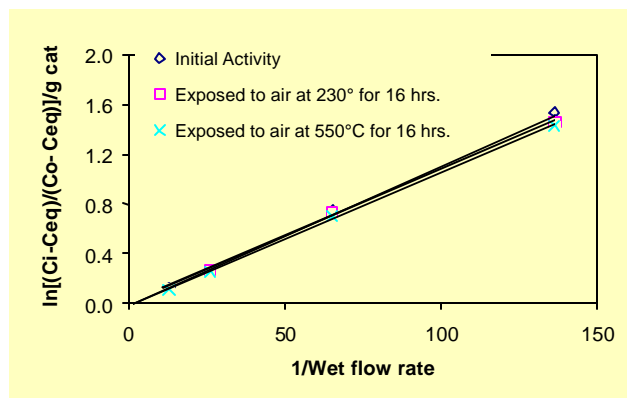


Figure 4. Catalyst retains high activity even after exposure to air at 550°C for 16 h.

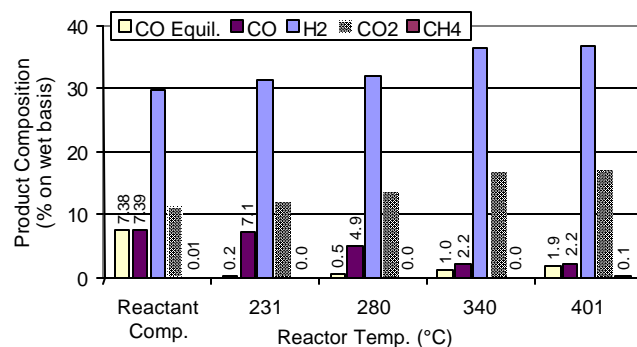


Figure 5. The Argonne catalyst is active from 230°C to 400°C, the range covered by the commercial HTS and LTS catalysts.

approaches the equilibrium CO concentration at higher temperatures, reaching nearly the equilibrium value at 401°C.

The catalysts discussed above were in powder form and were made by the glycine nitrate or like processes. We have also successfully supported the catalyst on high-surface-area γ -alumina, making the catalyst form more rugged while simultaneously reducing the net Pt loading (see Figure 6). Fabrication of the supported catalyst has been reproducibly scaled up to 2-kg batch sizes.

The Argonne catalyst can reduce the shift reactor volumes significantly, if the reactor can be designed to exploit the high intrinsic activity of the catalyst (i.e., to operate with no diffusion limitations). Table 2 shows a comparison of the calculated shift reactor volumes for the commercial HTS and LTS catalysts, as well as for the Argonne catalyst, used at the two distinct temperatures shown in the table. The calculated reactor volumes were

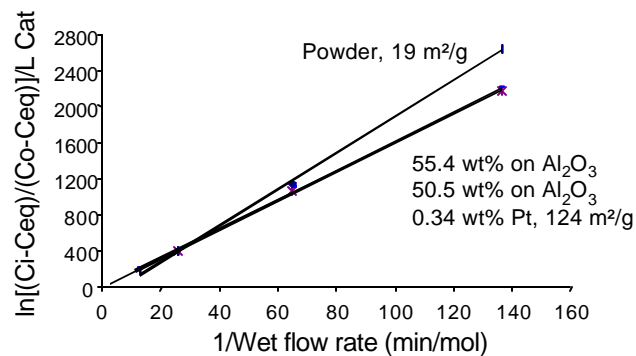


Figure 6. Catalyst retained high activity when supported on γ -alumina, even with reduced Pt loading.

based on the measured intrinsic reaction rates and activation energies for the Argonne catalyst, and on the published kinetic data for the commercial catalysts. The HTS and LTS stages were assumed to operate adiabatically. The calculated amount of catalyst is that needed to reduce the exit CO concentration to 1% (dry basis) from an inlet reformat gas consisting of 10% CO, 10% CO₂, 34% H₂, 33% N₂, and 13% H₂O (wet basis). As shown in Table 2, for the commercial HTS and LTS catalysts operated at 400°C and 200°C, respectively, a total catalyst volume of 19.2 L is needed for a 50-kW fuel cell system. In comparison, with the Argonne catalyst operated at 400°C and 300°C, the total required catalyst volume is 13.5 L, amounting to a 30% reduction.

Table 2. The Argonne catalyst can reduce shift reactor volumes significantly.

	Commercial Catalyst		Argonne Catalyst	
	HTS	LTS	HTS	LTS
T _{in} , °C	400	200	400	300
T _{out} , °C	455	227	455	327
CO _{in} , %	11.4	4.3	11.4	4.3
CO _{out} , %	4.3	1.0	4.3	1.0
Vol., L	5.5	13.7	0.8	12.7
Total, L	19.2		13.5	

Accomplishments

- Kinetic parameters have been determined for the Argonne catalyst to enable reactor design and analysis.
- Preliminary reactor sizing calculations show that significant reductions in reactor volumes may be achievable with the Argonne catalyst.
- Tolerance of the Argonne catalyst to air and to high temperatures in air has been verified.
- The catalyst has been supported on high-surface-area γ -alumina to reduce platinum loading while maintaining high activity.

IV. FUEL CELL STACK SUBSYSTEM

A. R&D on a 50-kW, High-Efficiency, High-Power-Density, CO-Tolerant PEM Fuel Cell Stack System

Tim Rehg (Primary Contact) and Nguyen Minh (Program Manager)

AlliedSignal Aerospace Equipment Systems

2525 W. 190th Street, MS-36-1-93140

Torrance, CA 90504-6099

(310) 512-2281, fax: (310) 512-3432, e-mail: Tim.Rehg@AlliedSignal.com

DOE Program Manager: Patrick Davis

(202) 586-8061, fax: (202) 586-9811, e-mail: patrick.davis@ee.doe.gov

ANL Technical Advisor: William Swift

(630) 252-5964, fax: (630) 252-4176, e-mail: swift@cmt.anl.gov

Contractor: AlliedSignal Aerospace Equipment Systems, Torrance, California

Prime Contract No. DE-FC02-97EE50470, October 1997-December 1999

Objectives

Research, develop, assemble, and test a 50-kW net polymer electrolyte membrane (PEM) fuel cell stack system composed of a PEM fuel cell stack and the supporting gas, thermal, and water management subsystems. The PEM fuel cell stack system will be capable of integration with at least one of the fuel processors currently under development by Hydrogen Burner Technology (HBT) and Epyx Corporation.

OAAT R&D Plan: Task 11; Barriers A, B, C, D, and E

Approach

This phased program includes the fabrication and testing of three 10-kW subscale PEM fuel cell stacks, leading up to the final 50-kW system. Stack technology development and system analysis are iteratively conducted to identify pertinent technology advances to be incorporated into successive subscale stack builds. The final system analysis will define the 50-kW stack and system configuration.

- Phase I:
 - PEM stack R&D to demonstrate multifuel capability and CO tolerance.
 - PEM stack R&D to advance technologies toward DOE targets.
- Phase II:
 - Subscale integration, electronic control system development, transient characteristics and durability testing.
- Phase III:
 - Testing of the 50-kW PEM fuel cell stack system.
 - Hardware delivery of 50-kW PEM fuel cell stack system.

Accomplishments

- Demonstrated two feasible concepts for CO management on a laboratory scale, based on regenerable adsorption bed techniques.
- Characterized a new anode electrocatalyst.
- Demonstrated CO tolerance and MEA performance to meet second 10-kW stack objectives.
- Demonstrated 28 days of stable performance with coated aluminum bipolar plates.
- Upgraded stack system testbed with a reformat simulator.
- The first 10-kW-class stack has been built and tested. This 130-cell stack produced 18 kW on hydrogen/air and 15 kW on 10-ppm CO gasoline reformat/air.
- A 73-cell stack was subjected to a 100-hour life test, running continuously on CO-containing reformat.
- Completed the conceptual system design for a 50-kW fuel cell stack system.
- 50-kW brassboard system design is in process. Component performances have been specified, and major component procurement has begun.
- 50-kW brassboard controls/interfaces work has begun. Dynamic transient data are being collected, and dynamic simulation is under way.
- The stack engineering design and component procurement have been completed for the second 10-kW subscale PEM fuel cell stack.

Fuel Cell Stack System

(excludes fuel processing/delivery system)

(includes fuel cell ancillaries: i.e., heat, water, air management systems)

Characteristic	Status	DOE Technical Target
Peak Power (kW)	50	50
Stack System Efficiency @ 25% Power (%)	44-55	55
Stack System Efficiency @ Peak Power (%)	45-52	44
Power Density (W/L)	282-322	350
Specific Power (W/kg)	295-430	350
Precious Metal Loading (g/kW)	0.9-2.6	0.9

Future Directions

- The second 10-kW-class PEM stack build and test is scheduled for September 1999.
- Brassboard 50-kW net PEM fuel cell stack system to be delivered to Argonne National Laboratory at the conclusion of the project.
- Continue collaboration with Argonne National Laboratory and fuel processor contractors on system integration issues.
- Continue to drive development toward DOE 2000 technical targets for high-volume production costs (\$100/kW for 500,000 units/yr).

Introduction

Fuel cell power plants will become viable substitutes for the internal combustion engine (ICE) in automotive applications only when their benefits of increased fuel efficiency and reduced emissions

are accompanied by performance and cost comparable to that of the ICE. Meeting these requirements is a significant technical challenge that requires an integrated systems approach. This effort encompasses the technical and developmental activities required to incorporate innovations

necessary to develop a 50-kW fuel cell stack system to meet the requirements set forth by the DOE. In this reporting period, AlliedSignal is progressing from Phase I to Phase II of the program.

System Analysis

The PEM fuel cell stack system consists of the fuel cell stack and supporting gas, thermal, and water management systems, as shown in Figure 1. Overall system performance depends on the careful integration of these subsystems.

A conceptual system design for a 50-kW fuel cell stack system has been completed (Figure 2), using ASPEN PLUS and internally developed AlliedSignal modeling tools.

Both pressurized and near-ambient systems have been evaluated. The analysis revealed that a near-ambient system will require a stack with ~200% more electrochemically active surface area than that of a stack in a pressurized system to simultaneously meet the power and efficiency goals. Consequently, AlliedSignal has adopted a pressurized system for the brassboard.

The 50-kW brassboard system design is currently in process. Component performances have been specified, and major component procurement has begun. Dynamic transient data are being collected, and dynamic simulation is under way to support the controls/interfaces work.

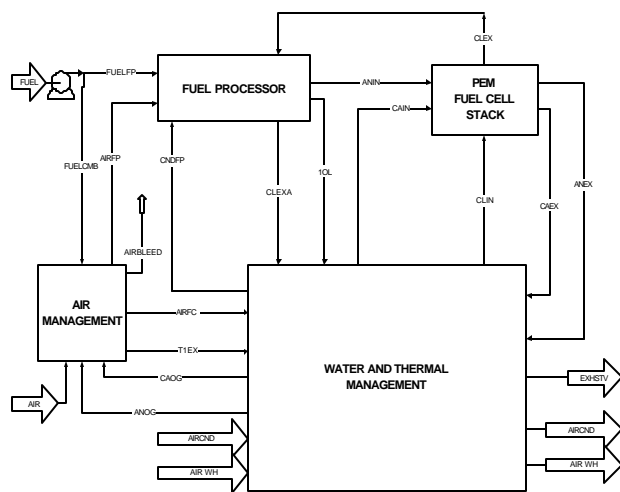


Figure 1. PEM FC stack system diagram.

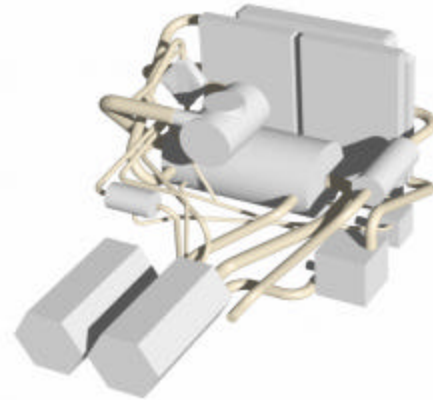


Figure 2. Conceptual system design, preliminary package.

Stack Technology Development

Our technology development efforts are divided into the areas of CO management technology development, MEA technology development, and stack technology development. The CO management technology development has been transitioned to a separate DOE contract, described elsewhere in this report (see III G).

In the area of MEA technology development, we have characterized a new anode electrocatalyst and demonstrated long-term (200+ hours) stability of cell performance with an improved gas diffusion layer (GDL). We have also demonstrated (Figure 3) that our cells can tolerate 100 ppm CO contamination without appreciable performance loss.

A variety of materials are under investigation in our work on low-cost, advanced bipolar plate materials. Among these are coated metals and conductive composites.

A coated aluminum bipolar plate has been tested for 28 days of continuous operation with no observable loss in performance (Figure 4). Fuel cell testing of full-size coated aluminum plates is in progress. We also plan to use conducting composite bipolar plates in our upcoming second 10-kW stack build.

The first 10-kW stack has been built and tested (Figure 5). This stack gave a specific power of 0.69 kW/kg and a power density of 1.32 kW/L.

The stack engineering design and component procurement have been completed for the second 10-kW subscale PEM fuel cell stack (Figure 6).

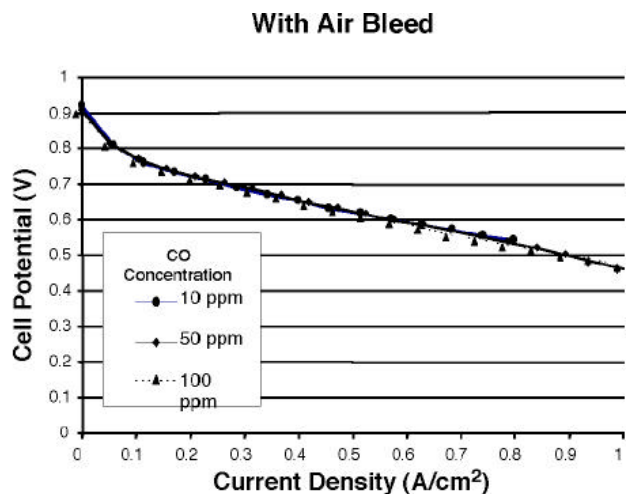


Figure 3. Effect of air bleed on CO poisoning.

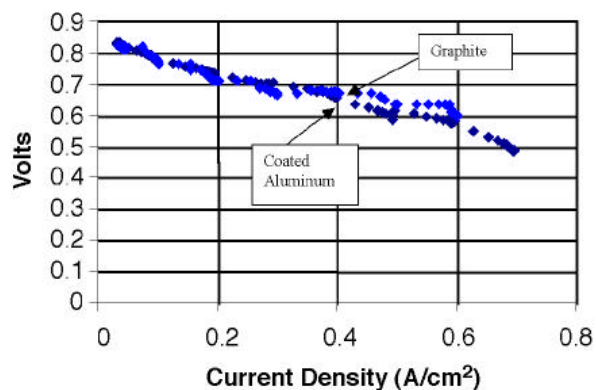


Figure 4. Coated aluminum bipolar plate performance following 28 days of operation.



Figure 5. First 10-kW-class stack.

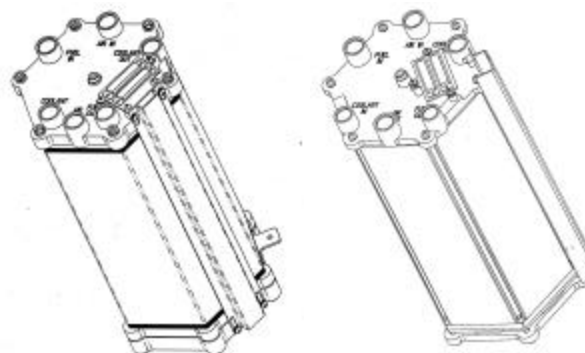


Figure 6. 10-kW stack designs. Comparison of Stack 1 (left) and Stack 2 (right) designs.

Improvements for this second stack build will include a new flowfield with lower stoichiometry capability, conducting composite bipolar plates, 13% increase in active cell area, and substantial improvements in stack weight, volume, and manufacturability.

Conceptual studies on a next-generation stack have also begun.

B. Development of Advanced, Low-Cost PEM Fuel Cell Stack and System Design for Operation on Reformate Used in Vehicle Power Systems

Jay Neutzler (Primary Contact) and Frano Barbir

Energy Partners, L.C.

1501 Northpoint Parkway, #102

West Palm Beach, FL 33407

(561) 688-0500, fax: (561) 688-9610, e-mail: neutzler@energypartners.org

DOE Program Manager: Donna Ho

(202) 586-8000, fax: (202) 586-9811, e-mail: donna.ho@ee.doe.gov

ANL Technical Advisor: William Swift

(630) 252-5964, fax: (630) 252-4176, e-mail: swift@cmt.anl.gov

Contractor: Energy Partners, L.C., West Palm Beach, Florida

Prime Contract No. DE-FC02-97EE50476, September 30, 1997-December 31, 1999

Objectives

- Develop low-cost bipolar collector plates through improvements in materials and processes.
- Evaluate and optimize MEA configurations with enhanced CO tolerance and low platinum loading.
- Achieve stable and usable performance with steady-state CO levels of 10 ppm and transient levels of 100 ppm.
- Attain platinum loading less than 0.5 mg/cm² per MEA.
- Design and demonstrate a reformate-capable fuel cell stack with a 50-kW_{net} power output.
- Integrate and demonstrate a small-scale fuel processor/PROX/fuel cell power system.
- Design, integrate, and demonstrate a reformate-capable 50-kW_{net} automotive fuel cell power system.

OAAT R&D Plan: Task 11; Barriers A, B, C, and D

Approach

- Phase I: Demonstration and delivery of a PEM ten-cell stack with reformate capability and ten additional bipolar plates manufactured by the compression molding process.
- Phase II: Demonstration of a high-efficiency, reformate-tolerant 50-kW_{net} fuel cell stack subsystem utilizing injection-molded bipolar plates (with compression-molded plates as an alternative), excluding power conditioning and fuel processor. Delivery to Argonne National Laboratory for independent testing and verification.

Accomplishments

- Bipolar plates
 - Completed compression-molding development for high performance:
 - Achieved high performance, low cost (< \$10/kW) with new injection molding of advanced molded composite bipolar plates, 100% recyclable, with < 20-sec cycle time/part/machine on 232-cm² plates.

- Demonstrated hydrogen and reformat fuel cell stack performance:
 - Scale-up of 50-kW_{net} automotive reformat design Model NG3000, comparable to previous 20-kW_{gross} Model NG2000.
 - Completed over 1000 hours of endurance testing.
 - Freeze-tolerant testing with coolant temperature down to negative 10°C.
 - “Road- tested” 20-kW Model NG2000 (hydrogen FC stack), concluding with Virginia Polytechnic Institute and State University placing second in the “FutureCar Challenge.”
- Acquired fuel processors and gas cleanup units for subscale system analysis and integration:
 - Epyx POX fuel processor rated at 45 kW_{th} on natural gas
 - Johnson Matthey fuel processor rated at 5,000 L/h hydrogen production on methanol
 - Los Alamos National Laboratory preferential oxidation unit
 - Johnson Matthey Demonox gas cleanup unit (integrated with fuel processor)
- System optimization and analysis:
 - Trade-off studies to increase efficiency of performance at temperature extremes.
 - Reduced componentry with thermally integrated system approach.
 - Water balance achievable.

Fuel Cell Stack System

(excludes fuel processing/delivery system)

(includes fuel cell ancillaries: i.e., heat, water, air management systems)

Characteristic	Status	DOE Technical Target
Peak Power (kW)	50	50
Stack System Efficiency @ 25% Power (%)	55-57	55
Stack System Efficiency @ Peak Power (%)	44-50	44
Power Density (W/L)	350 (predicted)	350
Specific Power (W/kg)	350 (predicted)	350
Precious Metal Loading (g/kW)	1.17	0.9

Future Directions

- Continue evaluations of new MEA materials for reformat performance.
- Injection mold large-scale blank bipolar plates (1000 cm²).
- Injection mold net-shaped bipolar plates with all features (500 cm²).
- Deliver reformat-tolerant 10-cell stack.
- Finish fabrication, assembly, controls, and testing of 50-kW_{net} stack subsystem and prepare it for delivery.

Introduction

Energy Partners’ program objective is to develop a state-of-the-art, reformat-tolerant PEM fuel cell stack and integrate it into a reformat-capable operating system that meets automotive design requirements. The development effort focuses on a systems approach, broken down into three discrete areas: bipolar collector plates, PEM fuel cell stack, and integrated system analysis.

Bipolar Collector Plate Development

An optimal bipolar collector plate should be low-cost, impermeable, highly conductive, chemically inert, lightweight, and easily manufactured. The available choices for PEM fuel cells are metals, graphite, and graphite composite materials. Energy Partners uses compression-molded graphite composite plates in all of its fuel cell stacks. Given the advances made in fillers, binders, and processes, these plates have properties comparable

to those of pure graphite, with the exception of somewhat lower conductance. However, because of its long processing time and high energy consumption, compression molding is not suitable for automotive-style mass production.

Energy Partners is developing the materials and processes suitable for injection molding (patents pending). After computer simulations have shown the feasibility of this concept, we have injection-molded several samples of blank plates as well as a sample with channels embossed on its surface. Figure 1 illustrates a 500-cm² compression-molded plate (lower), a 232-cm² injection-molded plate (left), and a sample of injection-molded flow channels (right and upper left insert).

Preliminary results are very encouraging. A part can be produced in less than 20 seconds (as compared to 40 minutes required for compression molding). Conductivity of the injection-molded plates is somewhat lower than that of compression-molded plates, but still within the DOE specifications. Table 1 presents the bipolar plate status with comparison to the DOE requirements. We were able to produce intricate features (array of channels) with both compression- and injection-molding techniques, while keeping flatness and parallelism within the tolerances. Advanced composites, processes, and equipment have the potential to yield improvements in time/equipment,

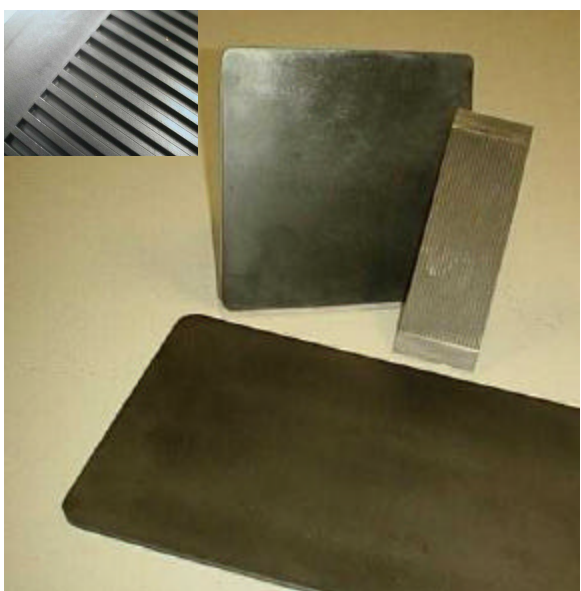


Figure 1. Compression- and injection-molded bipolar plates.

Table 1. Bipolar plate status and properties.

Plate Property	Compression (complete)	Injection (in progress)	DOE Specs.
Bulk conductivity	>320 S/cm	>110 S/cm	> 100 S/cm
Surface resistance	4-point probe method		None
	<30 mΩ-cm ²	<50 mΩ-cm ²	
	<20 mΩ-cm ² (POCO)		
Corrosion rate	< 16 μA/cm ²	< 16 μA/cm ²	< 16 μA/cm ²
H ₂ permeability	<<2 x 10 ⁻⁶ cm ³ /cm ² -sec	<< 2 x 10 ⁻⁶ cm ³ /cm ² -sec	< 2 x 10 ⁻⁶ cm ³ /cm ² -sec
Crush strength	~14,000 psi	>8,000 psi	None
Flexibility (modulus)	1.35 x 10 ⁹ psi	>1 x 10 ⁹ psi	None
Flexural strength	6,000-6,500 psi	6,500-9,000 psi	None
Material cost	~\$7.5/kW	~\$7.5/kW	None
Estimated manu-factured cost	\$146/kW	<\$10/kW	\$10 /kW
Production cycle time	< 40 min	< 20 sec	None
Recyclability	No	100%	None
Durability @ 60°C	>5,000 h	>5,000 h	None
Dimensions:	In Production	Development	None
Total plate	500 cm ²	232 cm ²	
Active area	300 cm ²	150 cm ²	
Thickness	<3.0 mm	<3.0 mm	
Weight	~ 7 oz	< 3 oz	
Material density	2.0-2.2 g/cm ³	1.95-2.0 g/cm ³	None

cost, durability, dimensional stability, and recyclability without sacrificing performance.

PEM Fuel Cell Stack

For the past year, the focus has been on evaluating short fuel cell stacks and full-scale stacks, addressing performance and system integration issues. The program baseline is the advanced hydrogen PEM fuel cell stack NG2000, rated at 20 kW_{gross}. It now has a reformate-tolerant equivalent (NG2000R). The new NG3000 is designed specifically for reformate, with automotive design criteria specified by the program (50 kW_{net}); it has a larger active area (594 cm²) and manifolds designed for the flows required. Testing has shown the performance of the NG2000 and NG3000 designs to be comparable (Figure 2).

Both of these designs are flexible, ranging from 2 to 250 cells. They operate between 0.2 to 3 atm pressure with reformate (40% H₂, 40%N₂, 20%CO₂) and are CO-tolerant to 100 ppm (steady state). Testing has shown durability of over 1000 hours on a 10-cell stack. Figure 3 shows that at a steady state, the stack voltage declines over a period of time (dotted lines). However, this is recoverable by

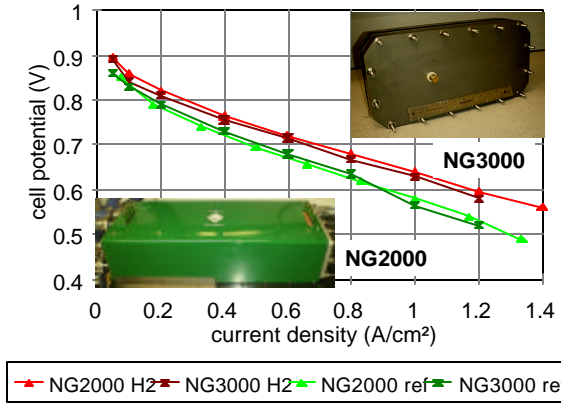


Figure 2. Comparison of NG2000 and NG3000 stacks on hydrogen and on reformat.

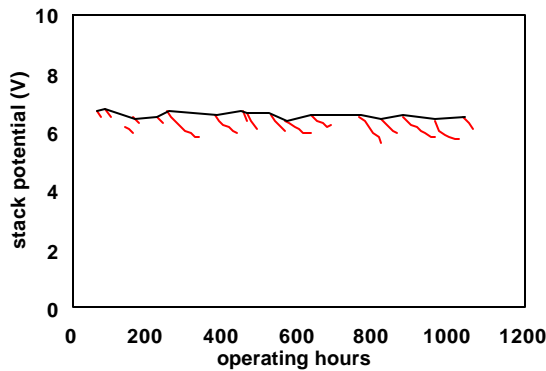


Figure 3. Durability of 10-cell stack @0.80 A/cm² at 60°C and 100% humidification on H₂/air.

simply running a polarization curve (or “exercising” the cell).

In keeping with DOE goals, to prove automotive design concepts on actual hardware, freeze-tolerance testing was performed by reducing the stack liquid coolant temperature down to negative 10°C. The polarization curves, illustrated in Figure 4, show performance when held for 15 minutes at each temperature. The stack was held at negative 10°C for approximately one hour while operating. This preliminary test shows excellent response, which facilitated further systems analysis.

Further understanding and concepts were gained through the “FutureCar Challenge” program with Virginia Polytechnic Institute & State University and Texas Tech University (Figure 5). Virginia Tech placed second in the 1999 competition.

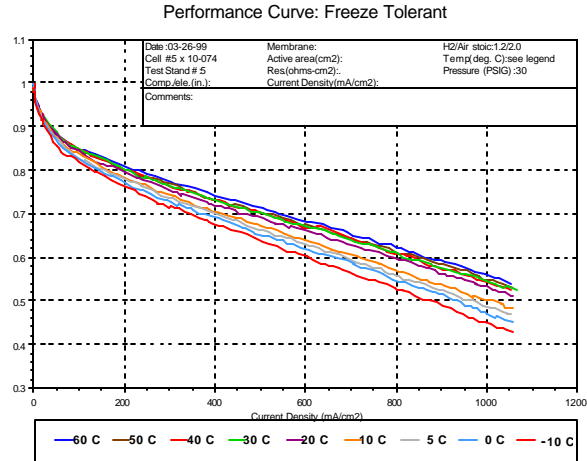


Figure 4. Freeze tolerance performance on H₂/air at 1.2/2.0 stoich.

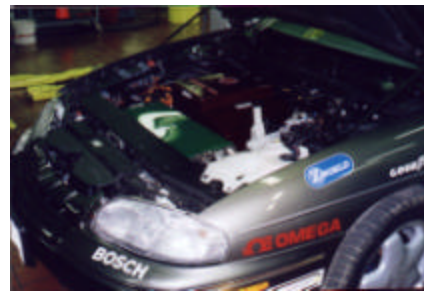


Figure 5. NG2000 stack installed in Virginia Tech’s competition vehicle (Chevy Lumina).

Small-Scale Fuel Processors

Energy Partners has completed over 100 hours of Epyx POX fuel processor testing without any significant drops in performance or efficiency. Operation has been performed at various power levels, from 6 kW_{th} to 45 kW_{th}. A summary of reformat compositions on a dry basis at different operating conditions is presented in Table 2. The thermal output is based on the lower heating value (LHV) of methane. The reformat compositions are presented in volume percent.

Table 2. Reformate composition from Epyx fuel processor (vol%).

kW _{th}	H ₂	CO ₂	O ₂	N ₂	CH ₄	CO*
20	38.2	12.9	0.24	44.3	1.27	2.04
25	40.9	14.2	0.30	41.8	0.67	1.52
30	41.2	14.2	0.18	42.3	0.09	1.92
40	41.9	13.2	0.29	41.3	0.11	2.36
45	40.7	11.9	0.31	42.2	0.96	2.10

* CO concentration before LTS reactor.

Currently, over 50 hours of testing have been conducted on the Epyx fuel processor and the Los Alamos National Laboratory PROX integrated system. Energy Partners has been working closely with Epyx and LANL to reduce the carbon monoxide (CO) concentration to levels below 100 ppm. LANL modified and installed a low-temperature-shift (LTS) reactor into the first stage of the PROX. With the modifications, the PROX was able to operate comfortably with the oxygen stoichiometric ratio well below 3 (~2.7), as illustrated in Figure 6. This leads to very little hydrogen being burned in the PROX. An analysis of reformat at the inlet and outlet of the PROX showed less than 2% of the hydrogen-in was oxidized in the PROX. A photograph of the Epyx fuel processor and LANL PROX integrated test stand is shown in Figure 7.

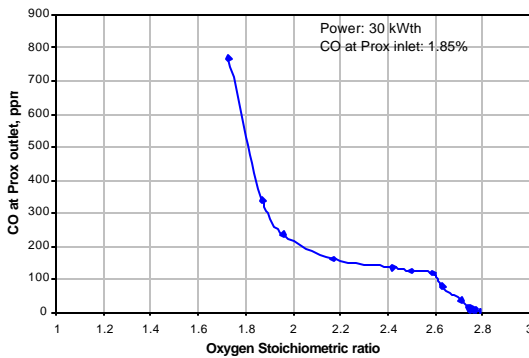


Figure 6. CO concentration at PROX outlet.



Figure 7. Epyx fuel processor and LANL PROX.

In addition to subscale testing of the natural gas fuel processor from Epyx, testing of a methanol fuel processor from Johnson Matthey was also conducted at Energy Partners over the past year. Currently, over 60 hours of durability testing have been performed without a significant drop in performance. The Demonox™ gas cleanup unit, developed by Johnson Matthey, performed flawlessly — virtually no CO was detected during steady operations. CO levels of less than 10 ppm were detected during transient operations.

Integrated System Analysis

Over a thousand simulations were conducted, using various system configurations and operating conditions. Optimization included such factors as operating pressure, which affects system power density; achieving a zero system water balance; resolving thermal dissipation needs; and maximizing system controls and integration and overall system efficiency. Simulation information was exchanged with Arthur D. Little, and realistic values of the compressor-expander efficiency were used in the simulation to estimate net fuel cell system efficiency. Based on DOE-PRDA efficiency targets, the maximum allowable parasitic power consumption (radiator fan, pumps, etc.) was estimated from simulations and components were subsequently identified, resulting in a fuel cell system exceeding DOE performance goals, as shown in Table 3.

Table 3. Energy Partners’ status vs. DOE program goals.

Characteristic	EP Status (7/99)	DOE Goals
System efficiency		
@50 kW _{net} (wo/FP)	44-50%	>=44%
@12.5 kW _{net} (wo/FP)	55-57%	>=55%
Net power density	350 W/l (est.)	350 W/l
Net specific power	350 W/kg (est.)	350 W/kg
Cost (\$)	<100/kW (est.)	100/kW
Durability	>1000 h	2000 h
Emissions	<<Tier 2	<<Tier 2
Transient performance (10% to 90%)	~0 s	3 s
Precious metal loading (anode + cathode)	0.6 mg/cm ² 1.17 g/kW	0.5 mg/cm ² 0.9 g/kW
Cold start-up to full power		
-40°C	<5 min	5 min
20°C	97% in ~0 s	1 min
CO tolerance (<20 mV loss at 0.7 V) (steady state)	~0 mV with 2% air bleed	>10 ppm
CO tolerance (<20 mV loss at 0.7 V) (3-s transient)	~0 mV with 2% air bleed	>100 ppm

Operating conditions were optimized to result in the smallest heat-exchanger equipment size while maintaining water balance. The resulting system is shown in Figure 8. A control strategy has been developed to maintain neutral water balance over the entire system operating range (kW) and under different ambient conditions (patent pending). Simplified humidification techniques based on optimized thermal integration (from simulations) are being verified experimentally.

Rapid start-up from an extreme ambient temperature of -40°C is possible under Energy Partners' system design. As shown in Figure 9, the system is almost up to full power in 2-3 minutes. Experimental results from freeze-tolerance tests (explained earlier) were used in the simulations. The quick start-up feature is the result of optimum utilization of feed gas thermal energy and fuel cell stack thermal dissipation (patent pending).

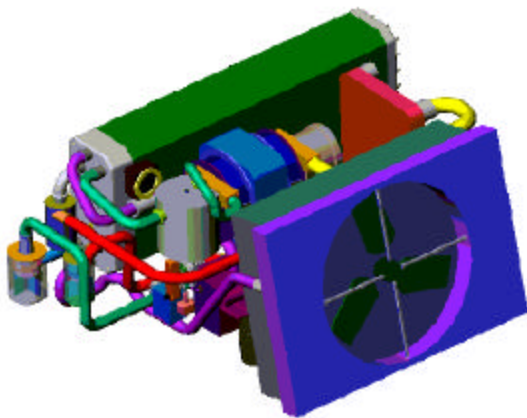


Figure 8. Resulting 50-kW_{net} automotive system.

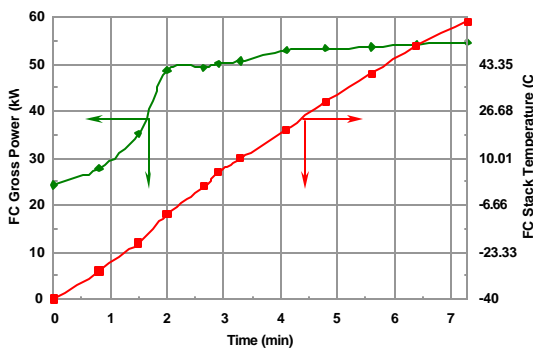


Figure 9. Cold start-up simulated response of Energy Partners' 50-kW_{net} system.

Conclusion

Energy Partners is developing an automotive fuel cell power system that will meet the DOE performance goals. Significant progress has been made in development of mass-producible bipolar plates, in stack and system design, and in development of a control strategy that will result in neutral water balance over the entire system operating range and under different ambient conditions.

Presentations/Publications:

F. Barbir, B. Balasubramanian, and J. Neutzler, Trade-off Design Study of Operating Pressure and Temperature in PEM Fuel Cell Systems, Symp. on Thermodynamics and the Design, Analysis and Optimization of Energy Systems, ASME Winter Annual Meeting, Nashville, Tenn., Nov. 1999.

F. Barbir, B. Balasubramanian, and J. Neutzler, Optimal Operating Temperature and Pressure in PEM Fuel Cell Systems in Automotive Applications, accepted for the 218th National Meeting of the American Chemical Society, New Orleans, La., Aug. 1999.

F. Barbir, J. Braun, and J. Neutzler, Properties of Molded Graphite Bi-Polar Plates for PEM Fuel Cells, presented at the 3rd International Symposium on New Materials for Electrochemical Systems, Montreal, Canada, July 1999.

F. Barbir, J. Braun, and J. Neutzler, Effect of Collector Plate Resistance on Fuel Cell Stack Performance, in *Proton Conduction Membrane Fuel Cells II*, S. Gottesfeld and T.F. Fuller (eds.), Proc. Vol. 98-27, pp. 400-406, The Electrochemical Society, Pennington, N.J., 1999.

V. Gurau, F. Barbir, and H. Liu, Two-Dimensional Model for the Entire PEM Fuel Cell Sandwich, in *Proton Conduction Membrane Fuel Cells II*, S. Gottesfeld and T.F. Fuller (eds.), Proc. Vol. 98-27, pp. 479-503, The Electrochemical Society, Pennington, N.J., 1999.

F. Barbir, J. Neutzler, W. Pierce, and B. Wynne, Development and Testing of High Performing PEM Fuel Cell Stack, Proc. 1998 Fuel Cell Seminar, Palm Springs, Calif., pp. 718-721, 1998.

F. Barbir, Trade-offs in Ambient/Pressurized PEM Fuel Cell Systems, presented at the SAE Fuel Cells for Transportation TOPTEC, Cambridge, Mass., March 1998.

J. Braun, M. Fuchs, J. Neutzler, and R. Ross,
Development of Bipolar Collector Plates for Mass
Production PEM Fuel Cells, presented at the SAE

Fuel Cells for Transportation TOPTEC, Cambridge,
Mass., March 1998.

C. Direct Methanol Fuel Cells

*Piotr Zelenay, Xiaoming Ren, Sharon Thomas, Huyen Dinh, John Davey, and Shimshon Gottesfeld
(Primary Contact)*

*Los Alamos National Laboratory, Los Alamos, NM 87545
(505) 667-6832, fax: (505) 665-4292*

DOE Program Manager: JoAnn Milliken

(202) 586-2480, fax: (202) 586-9811, e-mail: joann.milliken@ee.doe.gov

Objectives

Develop materials, components, and operating conditions for direct methanol fuel cells (DMFCs) that would prove the potential of DMFCs for transportation applications in terms of power density, energy conversion efficiency, and cost. Specifically,

- Continue to optimize anode catalyst layers to enhance cell performance;
- Prove that low fuel utilization can be resolved with combination of ionomeric membrane of good protonic conductivity and optimized stack operation conditions; and
- Prove stability of all cell components – primarily anode catalyst – in longer-term operation under these combined requirements.

OAAT R&D Plan: Task 14; Barriers B, F, H, and I

Approach

- Operate DMFC cells and stacks near 100°C with a variety of membrane/electrode assemblies, using optimized catalyst layers to demonstrate performance and stability.
- Optimize other cell components, including backing layers and bipolar plate/flow fields, to maximize demonstrated performance in DMFC short stacks operating near 100°C.

Accomplishments

- Five-cell methanol/air LANL stack, originally built by LANL for portable power applications (with DARPA's support), was reconfigured to operate at 100°C and 30 psig air, generating power density on the order of 1 kW per liter of active stack volume.
- Fuel utilization near 90% was demonstrated in the five-cell DMFC stack at the expected design point of 0.45V.

Future Directions

- Further lowering of precious catalyst loading.
 - Possible (budget permitting) scale-up of stack to the 0.5-1.0 kW level.
-

The objective of the direct methanol fuel cell effort at LANL, sponsored by DOE/OAAT, has been to develop materials, components, and operating conditions for such cells and small stacks, to prove their potential for transportation applications in terms of power density, energy conversion efficiency, and cost. Introduction of a DMFC as a primary power source for transportation has the potential to offer the combined attractive properties of a liquid fuel of good potential availability, high system simplicity (“liquid fuel + air in, DC power out”), good potential for packaging as required to achieve 350-mile range in a passenger vehicle, and good potential for zero-emission vehicle (ZEV) characteristics.

In our work this year, we have focused on the first demonstration of a DMFC short stack, based on LANL unique stack hardware, operating near 100°C on methanol and (30-psig) air. Our demonstrated five-cell stack (45 cm² active area), shown in Figure 1, had a pitch of only 1.8 mm per cell, at the same time allowing operation with pressure drops across the stack as low as a few inches of water. Figure 2 demonstrates the performance achieved

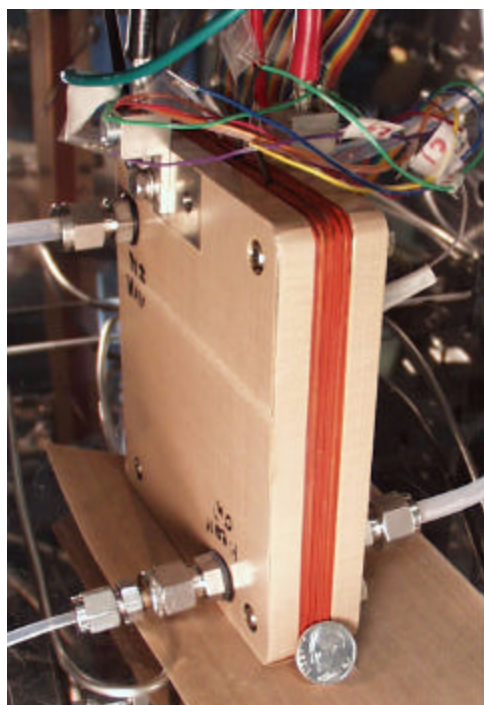


Figure 1. Five-cell DMFC stack, built this year utilizing novel LANL hardware that enabled, together with optimized MEAs, achievement of maximum power output of 1 kW per liter of active stack volume.

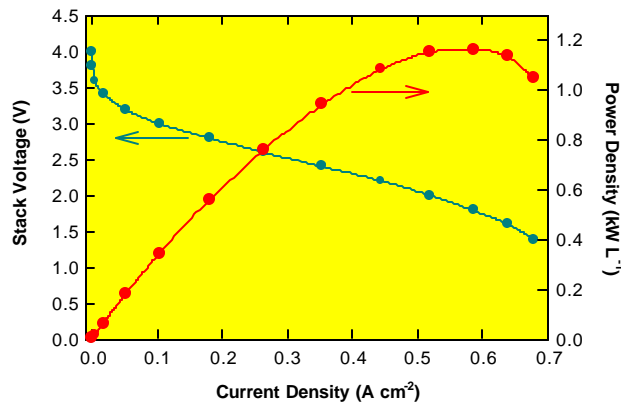


Figure 2. Five-cell DMFC stack: methanol/air performance at 100°C (active area 45 cm², cell width 1.8 mm).

from that five-cell stack in terms of voltage-current and power-current characteristics. Maximum power generated by the stack under these conditions was 50 W. The active part of the stack volume was close to 40 cm³; thus, maximum power density exceeded 1 W cm⁻³, or 1 kW L⁻¹. This is certainly a respectable level, reaching an order of power density similar to those achieved from reformate/air PEM fuel cell stacks.

Table 1 highlights the other highly important feature we have demonstrated for this small DMFC stack. The table provides details of methanol mass-balance measurements performed for the stack in operation at 0.45 V per cell. In contrast to a prevailing perception that fuel utilization in DMFCs is low (because of significant methanol crossover through the membrane electrolyte), Table 1 reveals methanol utilization of 82% with an anode feed of 1 M methanol, and as high as 99% (5% error bar) when the methanol feed concentration is lowered to 0.75 M. This high fuel utilization was achieved by optimizing electrode structure, rather than by any significant membrane modification. Therefore, high fuel utilization can be reached in DMFC stacks even before development of alternative membrane technology. This is an important insight regarding prospects and the potential time line for demonstrating and implementing DMFC technology in transportation applications, where energy conversion efficiency is of prime significance.

Finally, to address the issue of cost, this year we have further pursued the target of lowering catalyst loading in DMFCs while maintaining performance. Figure 3 illustrates results obtained with relatively

Table 1. Fuel utilization, *i.e.*, (cell current)/(cell current + crossover current), derived from a detailed methanol balance in a LANL five-cell methanol/air stack. (The table shows that, in this stack, which utilized a commercially available ionic membrane, fuel efficiencies as high as 99% could be achieved when operating at 0.45 V per cell. The high fuel utilization is achieved with appropriate electrode design.)

C_{FEED} (M)	C_{EXHAUST}^* (M)	M_{FEED} ($\mu\text{mole s}^{-1}$)	M_{EXHAUST} ($\mu\text{mole s}^{-1}$)	M_{OX} ($\mu\text{mole s}^{-1}$)	$M_{\text{X-OVER}}$ ($\mu\text{mole s}^{-1}$)	$I_{\text{X-OVER}}$ (A cm^{-2})	ϵ (%)
0.75	0.57	385.5	234.0	150.9	0.6	0.002	99 \pm 5
1.00	0.79	522.8	334.3	154.0	34.5	0.089	82 \pm 4

* Determined in the electrochemical crossover measurement in a separate cell.

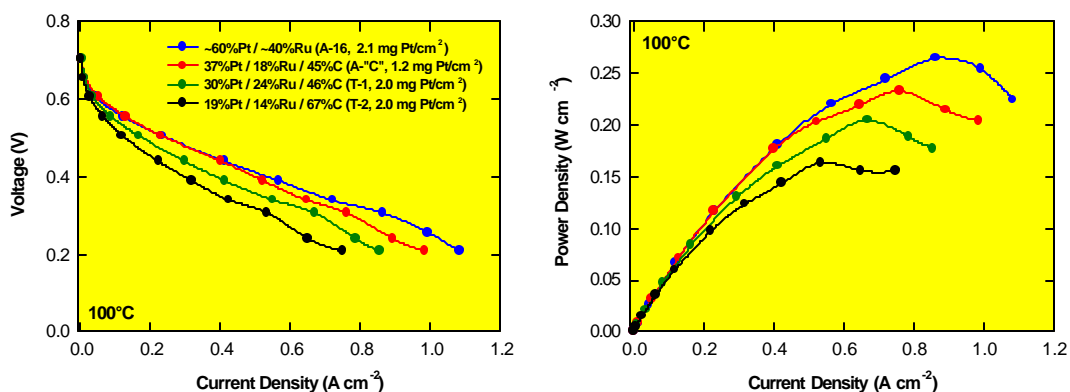


Figure 3. Voltage–current and power–current plots for single cell DMFCs utilizing lower Pt loading. The best DMFC result obtained this year with our MEAs was 5 mgPt W⁻¹ (5 gPt kW⁻¹), at 100°C, for operation on methanol/water feed to the anode and 30 psig air to the cathode.

low loading of Pt. The highest effective catalyst activity demonstrated was 5 mg Pt W⁻¹ (5 g Pt kW⁻¹), counting the total loading in the cell (*i.e.*, anode + cathode Pt loading). This is better by a factor of two than our demonstrated catalyst activity in DMFCs last year and thus constitutes a further step toward lowering the DMFC catalyst cost. In our estimate, the state of the art can be roughly summarized as a ratio of about 3 between DMFC loading and (overall system) reformat/air precious metal loading. While certainly significant, and a target for further effort, this gap in precious metal loadings is smaller than is usually perceived.

The technical achievement of the DOE/OAAT-sponsored efforts at LANL, targeting potential transportation applications of DMFCs, is substantial.

On the basis of short stack results, in terms of power density and energy conversion efficiency, the DMFC is today comparable with an on-board methanol reforming system. There is a remaining gap in precious-metal catalyst demand, with the DMFC requiring 5 g Pt kW⁻¹ vs. about 2 g Pt kW⁻¹ needed today for an on-board reforming system. However, we believe that this gap can be narrowed, and we will devote a significant part of our DMFC effort in FY 2000 to this goal. Our effort will focus on further optimization for higher-temperature cell operation and further anode catalyst work. We also plan, budget permitting, to extend our DMFC work in FY 1999 to fabrication and testing of stacks in the range of 0.5-1 kW, operating near 100°C.

D. Efficient Fuel Cell Systems

Mahlon S. Wilson, Steffen Moeller-Holst, Daniel M. Webb, and Christine Zawodzinski

Materials Science and Technology Division, MST-11, MS D429,

Los Alamos National Laboratory, Los Alamos, NM 87545

(505) 667-6832, fax: (505) 665-4292, e-mail: mahlon@lanl.gov

DOE Program Manager: JoAnn Milliken

(202) 586-2480, fax: (202) 586-9811, e-mail: joann.milliken@ee.doe.gov

Objectives

- Develop a high-performance, simple, low-parasitic-power, low-cost fuel cell system.

OAAT R&D Plan: Task 13; Barriers B, C

Approach

- Utilize direct liquid water hydration of the membrane electrode assemblies (MEAs).
- Operate the cathodes at near-ambient pressures to minimize parasitic power losses.
- Operate the stack in an “adiabatic” configuration.

Accomplishments

- Designed new 300-cm² active-area cell hardware to optimize operation of the “adiabatic” stack configuration.
- Scaled up to a 26-cell, 300-cm² active-area near-ambient-pressure stack that supplies more than 1.5 kW under nominal load.
- Demonstrated system efficiencies, using the 1.5 kW stack, that exceed 55% (LHV of hydrogen). Parasitic power losses are only 1.4% of the stack output (does not include the fan for water recovery from the condenser, which is expected to be approximately 1%).
- Attained stack volumetric power densities of 365 W/L (based on the area of the graphite bipolar plates and a 55% efficiency level).

Future Directions

- Refine and optimize system, stack components, and operation/control.
- Demonstrate a water self-sufficient system (incorporate condenser, etc.).
- Determine performance enhancement with sea-level operation).
- Increase power density to 500 W/L (on a bipolar plate area basis).

Historically, most fuel cell system development efforts have emphasized the use of pressurized reactants, primarily because of the improved performance with the increase in the oxygen partial pressure on the cathode. However, a relatively powerful and sophisticated compressor is then required to supply the pressurized air for the fuel cell stack. To partially offset the substantial power

requirements of the compressor, an expander located on the cathode effluent can be used to recover some of the compression work. Even so, the parasitic power draw on the system can be significant. For example, a hydrogen fuel cell system with a compressor/expander, recently demonstrated by a major fuel cell developer, incurred parasitic power losses of about 20%, primarily due to the 30-psig

compressor. Naturally, a 20% power loss profoundly affects the overall system efficiency.

Therefore, one of our major objectives is to operate the air-side of the fuel cell stack at near-ambient pressure, because even relatively modest pressures can result in a surprisingly high power requirement. This is illustrated in Figure 1, which depicts the parasitic power losses incurred with an ideal adiabatic compressor as a function of the cathode inlet air pressure. Even a seemingly modest 2 psig incurs a 3% loss in this example; in reality, a loss as high as 10% might be expected because of blower inefficiencies.

For this reason, it is desirable to operate at air pressures of only several inches of water. This precludes the ability to humidify the air before the fuel cell stack, because of the additional pressure drop due to a humidification module and an air flow-field design that can tolerate two-phase flow. However, introducing dry air to the fuel cell stack requires the use of an alternative membrane humidification scheme; here, we adapt a method that was developed previously in this program to directly humidify the fuel cell membrane electrode assembly (MEA) with liquid water.¹ The humidification is accomplished by the introduction of an anode wicking backing that conveys liquid water in the anode flow-field plenum directly to the membrane, as depicted in Figure 2.

The technique of using direct liquid hydration of the MEAs has a number of advantages for a simple, low-cost fuel cell system; it utilizes “ordinary” MEAs and bipolar plate technologies and eliminates

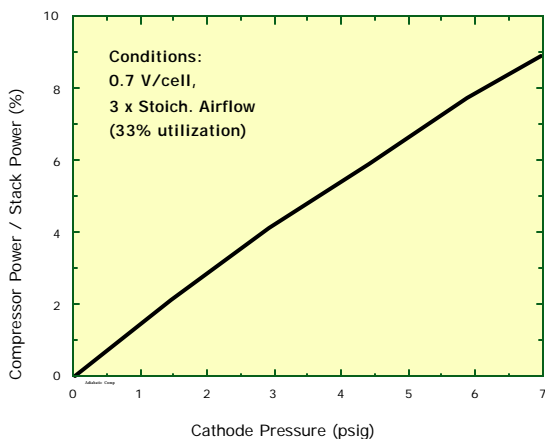


Figure 1. Contribution of an ideal adiabatic compressor to the parasitic power loss as a function of cathode inlet pressure.

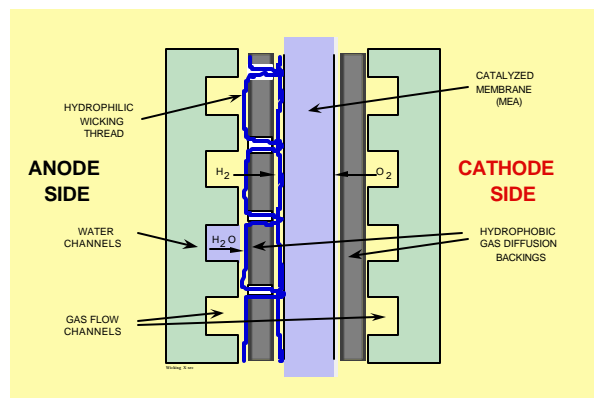


Figure 2. Schematic depicting the use of an anode wicking backing to convey water from the anode flow-field directly to the MEA.

the need for a number of auxiliary components. The approach supplies liquid water to all regions of the MEA to improve performance at higher stack temperatures and/or at lower cathode air pressures. Direct liquid hydration also separates the functions of gas supply and membrane hydration, which substantially simplifies the overall system as well as its control. The fine wicking threads are simply sewn into a conventional hydrophobic carbon cloth backing, using a computer controlled embroidery machine to accurately place the wicking thread in the desired configuration.

One benefit of operating a well-humidified fuel cell stack with a dry, cool cathode air inlet is that the airstream becomes heated and water vapor becomes saturated as it passes through the cells. This configuration then provides *in situ* evaporative cooling of the stack, which eliminates the need for a separate cooling system or cooling plates within the stack. Evaporation is a very effective heat-transfer mechanism, and the waste heat is transferred to the air as generated and where generated. Since the air inlet is at room temperature and the effluent is at 60-70°C, a large temperature gradient develops across the stack. This differs from most fuel cell stack designs, which typically strive to attain isothermal conditions. In our case, the stack is designed to encourage a monotonically increasing temperature as the air passes through the stack, thereby preventing condensation from occurring within the flow-field channels. This general scheme of nonisothermal operation with *in situ* evaporative cooling has been appropriately described as an “adiabatic” stack in Argonne National Laboratory’s system modeling efforts.

This past year, 300-cm² active area cells were designed for an adiabatic stack based on 6" × 10.5" graphite bipolar plates. New design features were a narrower active area and external manifolding of the reactants. The narrower width decreases the span between tie-bolts, and hence the deflection of the endplates, while also providing shorter cathode channels. Externally manifolding the reactant supply simplifies plate design and fabrication, as well as sealing and alignment.

A number of single cells were assembled and tested in an effort to optimize performance. Of paramount interest was obtaining a cathode-side pressure drop of about 4" H₂O at three times stoichiometric air flow. At much less pressure, the air supply did not appear to be uniform, but at much more the airflow through the anticipated 1.5-kW stack would not be sufficient with the 12-V blowers we had on hand. Naturally, a single cell would not heat up as much as a stack; nonetheless, it was desirable to optimize around realistic stack temperatures. To compensate, the end plates were heated to 60 or 70°C, although the temperature profile would undoubtedly be different than that which would be attained in the midst of a stack. A configuration was settled upon that provided the target 300 mA/cm² at 0.7 V/cell and three times stoichiometric air flow at 4" H₂O for the single cell. Cell resistances were about 0.13 Ω-cm².

A 26-cell stack was assembled using this plate design. A small 12-V diaphragm pump was used to supply the hydration water to the anode side of the stack, and a slightly larger version was used to recirculate the hydrogen to flush out accumulated water. A picture of the system is provided in Figure 3. Shown are all of the relevant components: stack, blower, water trap/reservoir, and hydrogen and water pumps. Manifold pressures were higher than anticipated from the single-cell results, even

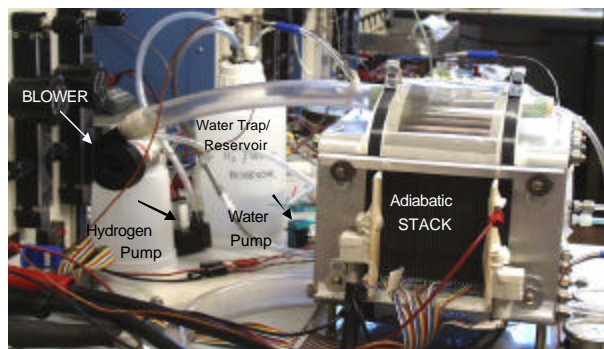


Figure 3. Components of the 1.5-kW adiabatic stack fuel cell system.

though adequate compression of the stack was not achieved, as indicated by hydrogen leakage from the plates and cell resistances that were about 0.02 Ω-cm² too high. Nevertheless, the stack was operated sufficiently long for some degree of break-in.

A data set obtained at that point indicated a stack voltage of 17.41 V (0.67 V/cell, or a voltage efficiency of 57% based on LHV of hydrogen) and a current of 87 A, for 1.51 kW gross power. The water balance indicated that 25.5 mL/min of water was evaporated to the air-stream, which corresponds to about 1000 W of evaporative cooling (260 W lost to ambient). The water-vapor-saturated effluent air was at 61°C, which yields a stoichiometric flow of only 2.2. The 6" H₂O manifold pressure was already at the limit of the capabilities of the blower. For whatever reason, the pressure drop was higher than anticipated by the single-cell work, so we could not attain the target 3X stoichiometric flow. Nevertheless, since our parasitic power load for the blower and hydrogen and water pumps was only 21.6 W (1.43% parasitic power), the system efficiency still met the target of 55% (LHV) while providing a net system power of 1.49 kW.

These numbers, however, do not include the parasitic power requirements for a fan to cool a condenser to enable water self-sufficiency. Based on last year's effort, this would incur roughly an additional 1 % parasitic power. Also, the hydrogen leakage (approximately 10% of the total flow) may have influenced the heat balance to some degree.

The specific power of the adiabatic stack at these performance levels is about 365 W/L on a graphite plate area basis and about 490 W/L on an active area basis. These numbers are not dramatically different from those attained with pressurized systems. From a balance-of-plant perspective, the adiabatic system would appear to have significant cost and simplicity advantages over a pressurized system.

The next step was to increase the compression of the stack to eliminate the leaks and attain single-cell resistance levels. This was achieved by retorquing the tie-bolts while clamping the stack in a large press. As hoped, leakage and cell resistances dropped to the desired levels and stack performance increased correspondingly (about 20 mV per cell), but so did the manifold pressure, to about 10" H₂O, well beyond the desired pressure range. As a result, the next step will be to dismantle the stack and machine down the air-flow channels further to

decrease the pressure drop and allow three times stoichiometric flow at an efficient pressure drop. It is hoped that this will provide the 300 mA/cm^2 current densities at 0.7 V/cell that would provide a comfortable cushion to accommodate the condenser fan parasitic power and still attain 55% net system efficiency.

Elements of the full 1.5-kW system require further refinement. The current stack sealing materials are readily available but do not appear to be the best choice. Other operating conditions need to be investigated, and the system has not been refined or tuned to any degree.

The purpose of operating the stack at or below three times stoichiometric air flow is to elevate the temperature of the water-vapor-saturated air to a level that facilitates water recovery in a condenser. Roughly two-thirds of the water vapor needs to be condensed and recovered for system self-sufficiency. Last year, we assembled a plastic flat-plate condenser that we demonstrated to provide overall heat-transfer coefficients and fan power requirements similar to those of a conventional water/air radiator for equivalent amounts of heat transfer. Next, we need to integrate a similar flat-plate condenser (last year's is too large for a 1.5-kW stack) into the stack system in order to demonstrate water self-sufficiency for the full system while achieving the target system efficiency.

All of the above results were obtained in our laboratories, which are at an altitude of 7,300 ft above sea level (2,250 m), where the ambient pressure is only 0.76 atm. Because of the compounding effect of the water vapor pressure, oxygen partial pressures within the stack can be as much as 60% lower than at sea level. Furthermore, blowers etc. are only about half as effective as at sea level. As a result, determining sea-level performance and efficiency is of interest because of the possibly substantial improvements. The results are also of more relevance than our high altitude data for most potential applications.

Finally, power density is of considerable interest for transportation applications. The simplest method of realizing increases is by decreasing the thickness of the bipolar plate. Currently, our web thicknesses are rather generous. Time permitting, an interesting exercise would be to see if about one-third thinner plates could be used, which should push the specific power over 500 W/L (although sea-level operation alone may also achieve this).

Reference

1. M.S. Wilson, C. Zawodzinski, and S. Gottesfeld, "Direct Liquid Water Hydration of Fuel Cell Membranes," in *Proton Conducting Membrane Fuel Cells II*, Vol. 98-27, pp. 424-434, The Electrochemical Society, 1998.

V. PEM STACK COMPONENT COST REDUCTION

A. High-Performance, Low-Cost Membrane Electrode Assemblies for PEM Fuel Cells and Integrated Pilot Manufacturing Processes

Mark K. Debe (Primary Contact) and Judith B. Hartmann

3M Co.

3M Center, Building 201-2N-19

St. Paul MN 55144-1000

(651) 736-9563, fax: (651) 737-2590, e-mail: mkdebe1@mmm.com

DOE Program Manager: JoAnn Milliken

(202) 586-2480, fax: (202) 586-9811, e-mail: joann.milliken@ee.doe.gov

ANL Technical Advisor: James Miller

(630) 252-4537, fax: (630) 252-4176, e-mail: millerj@cmt.anl.gov

Contractor: 3M Company, St. Paul, Minnesota

Subcontractor: Energy Partners, Inc., West Palm Beach, Florida

Prime Contract No. DE-FC-02-97EE50473, September 1997-December 1999

DE-FC02-99EE50582 (Proposed), September 1999-December 2001

Objectives

- Demonstrate the feasibility for continuous manufacture of high-performance, high-quality membrane electrode assemblies (MEAs) for polymer electrolyte membrane (PEM) fuel cells, based on a nontraditional catalyst support system.
- Develop highly CO-tolerant anode catalysts based on the proprietary catalyst system.
- Develop a continuously produced, low-cost electrode backing medium with optimized properties for use with the proprietary MEA.
- Develop a set of high-performance, matched PEM fuel cell components and integrated manufacturing processes to facilitate high-volume, high-yield stack production (New Contract).

OAAT R&D Plan: Task 13; Barriers A and B

Approach

- Phase I (primary contractor only) had five primary areas of development:
 - Demonstration of the continuous manufacturing feasibility of the nanostructured thin film support,
 - Demonstration of a continuous process for Pt catalyst deposition on the nanostructured supports,
 - Development of a continuous process for forming 3-layer membrane electrode assemblies with the proprietary catalyst and commercial membranes,
 - Development of new multicomponent catalyst compositions and structures for highly CO-tolerant anodes, based on the nanostructured support, and
 - Development of conductive, porous web-based electrode backing materials with optimized properties for use with the 3-layer membrane electrode assemblies.
- Phase II consists of demonstrating scale-up potential for fabricating the CO-tolerant anode catalysts and targeting performances of prototype manufactured MEAs in subcontractor fuel cell stacks.

- Phase I of the new contract will focus on the development of high-performance, matched components and pilot manufacturing processes, building on the results of the first contract. Tasks include:
 - Develop anode catalyst compositions and structures with higher reformate tolerance,
 - Investigate catalyst compositions and structures to produce higher activity cathodes,
 - Scale up the pilot manufacturing process for continuous fabrication of catalyst-coated membrane assemblies,
 - Develop continuously produced electrode backing media, and
 - Develop integrated manufacturing processes for fabrication of membrane electrode assemblies.
- Phase II of the new contract will involve stack fabrication and testing of matched component systems, in cooperation with the subcontractor. The primary tasks are:
 - Evaluate matched component system performance in subcontractor stack tests and
 - Fabricate and deliver a 10-kW stack.

Accomplishments

- Completed multiple deposition coating runs, producing over 1700 ft of proprietary catalyst support material, which exceeded target limits for process control.
- Completed conversion of the proprietary catalyst support material to the nanostructured form on 500 m of web material and coating with Pt.
- Demonstrated feasibility for continuous formation of 3-layer catalyst-coated membrane material, producing 15 meters with <0.7% of nontransferred catalyst and excellent down-web uniformity.
- Prepared and tested over 25 new catalyst anode compositions for CO tolerance, including a new ternary composition with CO tolerance similar to that of PtRu.
- Completed assessment of 24 new porous conductive composite materials produced by continuous web processing means for use as diffuser current collectors.
- Evaluated multiple membrane electrode assemblies in subcontractor prestack tests.
- Demonstrated feasibility for continuous manufacturing of optimized anode catalyst coatings on proprietary catalyst support films.

Future Directions

- Complete Phase II of existing contract, evaluation of full-sized MEAs in subcontractor stacks.
- Work on Phase I of the new contract is expected to begin in September 1999.

Introduction

The membrane electrode assembly (MEA) is the core component set of a PEM fuel cell stack. For large-scale volume fabrication at the costs and quality targets required by transportation applications, very high yields and in-line control of continuous processes based on cost-effective materials will be required. The objective of this work has been to demonstrate the feasibility of high-volume manufacturing of a novel 5-layer MEA for PEM fuel cells, based on a proprietary thin-film catalyst and support system. Specifically, the targets are to demonstrate a continuous process with low cost and high volume potential for fabrication of

MEAs with ultra-low loadings of catalyst on commercial membranes, develop anode catalyst compositions and structures optimized for CO tolerance, and develop continuously produced, low-cost carbon-containing electrode backing media with properties optimized for use with the thin-film catalyst support. In the FY 1998 Contractors' Program Report, the proprietary thin catalyst support system was discussed, a batch-processed 3-layer MEA with ultra-low (0.04 mg/cm² total anode and cathode) catalyst loadings was illustrated, and polarization curves were presented that demonstrated cathode-specific activities of the proprietary catalyst of 150 A/mg-Pt at 0.5 V under 60 psig O₂.

Process Scale-Up Feasibility

During the current period, the Phase I tasks were completed that demonstrated the feasibility for scaling up the fabrication of the proprietary thin-film catalyst and catalyst-coated membrane as a continuous process.

The first development task area focused on scale-up of the nanostructured support film. Figure 1 illustrates an example of continuously coated material prior to conversion to the nanostructured phase. Multiple coating experiments totaling over 1700 feet of coated substrate were conducted that met or exceeded the target thickness control of $\pm 5\%$ at the targeted web speeds.

Conversion of the support material in Figure 1 to the nanostructured support film phase was also demonstrated as a continuous process by two methods. In one method, over 1500 feet of web was converted and the target conversion rate achieved. Task 2 of Phase I, to demonstrate coating of the catalyst onto the thin-film proprietary support as a continuous process, was also concluded in this period.

Figure 2 shows a scanning electron micrograph of a cross-section of the continuously produced catalyst-coated nanostructured films.

The third task of Phase I was to demonstrate feasibility for the continuous fabrication of a catalyst-coated membrane (CCM), using a commercial membrane and the proprietary nanostructured catalyst film material from the first and second tasks. The work completed under this

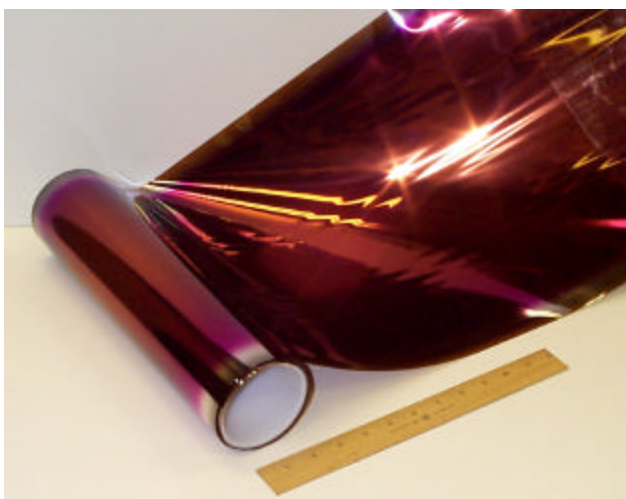


Figure 1. Roll-good coated nanostructure support material.

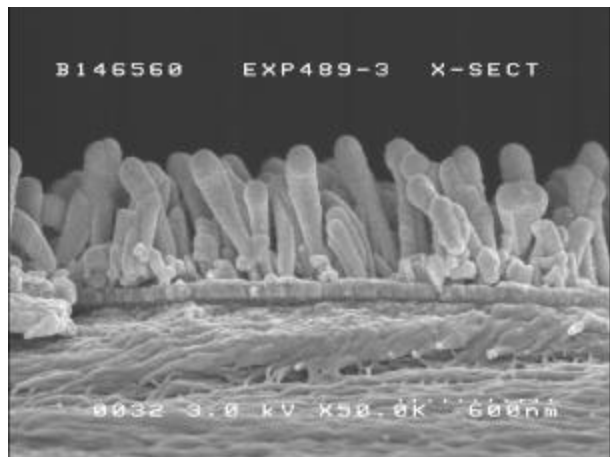


Figure 2. SEM cross-section of nanostructured catalyst film.

task included five catalyst transfer experiments with Nafion 115. Approximately 50 meters of 3-layer CCM was produced at the target speed while obtaining data on the catalyst transfer parameters. Approximately 15 meters of 3-layer CCM was produced with excellent results, with $< 0.7\%$ untransferred catalyst. Figure 3 is a photograph of CCM produced in the successful transfer run.

Down-web uniformity of the 3-layer CCM shown in Figure 3 was examined by cutting 50-cm² electrode area samples from the web at approximately 10-ft intervals (between 5 ft and 45 ft) and measuring fuel cell performance. Figure 4



Figure 3. 3-layer catalyst-coated membrane as a roll-good.

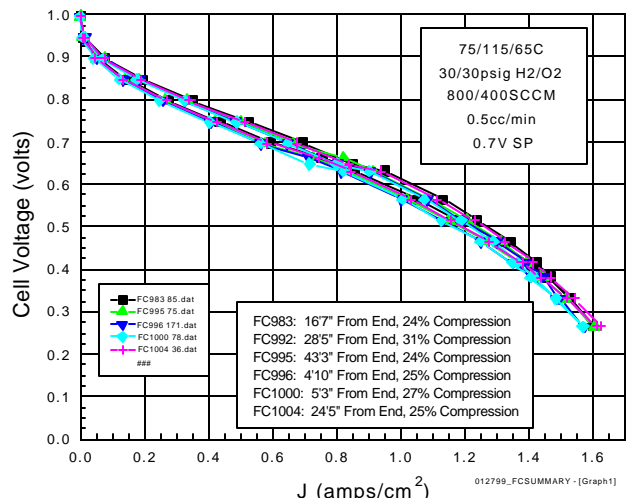


Figure 4. Fuel cell performance versus down-web position.

shows a superposition of the potentiodynamic polarization curves obtained from the sampling process. The very good reproducibility of the fuel cell performance validates the uniformity of the continuous roll-good produced CCM.

The fourth task of Phase I of the current contract has been directed at development of proprietary catalysts based on nanostructured films for optimized CO tolerance. The new type of catalyst support and facile catalyst deposition methods allow the obtaining of new catalyst stoichiometries and physical structures. The ability to control the composition and structure, then rapidly characterize and evaluate fuel cell performance, has allowed fast screening of multiple material and process parameters. Over the course of the current contract, 40 binary, 120 ternary, and 14 quaternary compositions have been made and tested for CO tolerance in some 200 MEAs. The target was to demonstrate less than 20 mV loss at 0.7 V under 100 ppm CO, compared to pure hydrogen/air (30 psig) for 16 hours with no air bleed and low anode catalyst usage. This was nearly demonstrated for a PtRu-based system. Performance was further improved with 0.5% air bleed and 50 ppm CO, as shown in Figure 5. Under 24 psig H₂/air, the pure-H₂ and CO-containing polarization curves are identical, with only 0.12 mg/cm² anode loading.

The materials for the above task were produced by a batch process. The second task of Phase II of the current contract was directed at demonstrating the feasibility of scaling up the process to

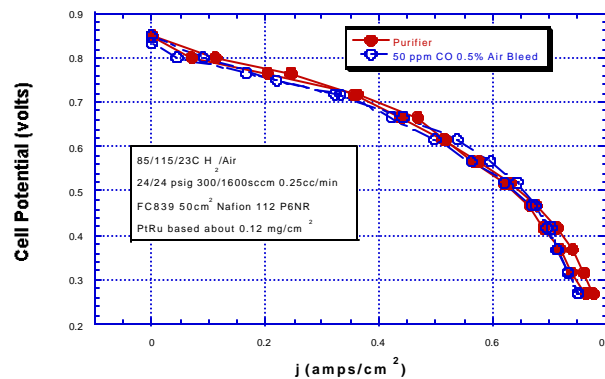


Figure 5. Comparison of 50-ppm CO and pure H₂.

fabricate the CO-tolerant anode catalyst developed in the batch process. During this period, a scale-up in the process rate by a factor of 100 was successfully demonstrated as feasible. The process parameters were studied in over 100 deposition runs to determine sensitivity of fuel cell performance and material properties to process conditions. It has been found that CO tolerance is a strong function of one process parameter variation, and the effect of this parameter on material properties has also been determined. Similarly, it has been found that CO or reformat tolerance is very dependent on water management and operating pressure conditions.

The fifth task under Phase I was directed at developing a continuously produced porous, conductive composite material for use as a diffuser current collector (DCC). In this reporting period, work continued on material and process screening of a proprietary technology (7 new composites), selected fuel cell evaluations (20), and evaluation of a new composite approach (17 composites fabricated). Of all the new composite constructions, one has demonstrated performance equivalent to that of a preferred commercial DCC, producing 0.6 A/cm² at 0.6 V on ambient-pressure air with Nafion 112. Transfer of this composite approach to a continuous process remains to be done.

Testing of MEAs prepared with CCMs made by continuous processes like that in Figure 3 has begun at our subcontractor, Energy Partners. The first task of Phase II of the current contract is directed at evaluating 150-cm² MEAs in single cells. Initial testing of MEAs has focused on understanding “fit and function” parameters and test station/protocol differences that affect measured fuel cell performances. The proprietary 3M catalyst

electrodes have different water management properties from conventional dispersed carbon particle supported catalysts. Understanding how to optimize their performance with the subcontractor's proprietary flow fields is necessary before proceeding to full-sized stack testing. These first tasks are nearly completed.

New Contract Work

Our development program has been driven by assessment of the significant manufacturing challenges that must be met to achieve the PNGV goals. Considering the 5-layer MEAs, bipolar plates, and gaskets/seals, a 50-kW stack may involve as many as 3,000 layers produced by a variety of process steps. With this many components and process steps, the yield requirements can only be met with a philosophy of six-sigma quality throughout the entire set of manufacturing processes. Furthermore, the processes must be high-volume. For example, if we assume 10 m² of MEA per 50-kW stack and a target of 500,000 units/year, the MEA production rate would have to be ~150 ft²/minute. The manufacturing approach must be capable of cost-effectively providing such levels.

The new contract effort will build on the feasibility demonstrations of the first contract and will focus on the development of cell and stack component sets matched for optimum performance and high-volume production by well-understood, integrated manufacturing processes to meet these challenges. It includes further development of nanostructured anode catalyst compositions and structures with higher reformate tolerance and of continuously produced electrode backing media. Catalyst compositions and structures to produce higher-activity cathodes will be investigated. The pilot manufacturing process for continuous fabrication of catalyst-coated membrane assemblies will be scaled up, and integrated manufacturing processes for fabrication of membrane electrode assemblies will be developed. The best candidates for the matched components system will be selected at the end of the first phase of the new contract, on the basis of component characterization and cell performance tests and manufacturability. In the second phase, the performance of the selected matched component systems will be evaluated in subcontractor stack tests, and a 10-kW stack will be fabricated and delivered to ANL.

B. Low-Cost, High Temperature, Solid Polymer Electrolyte Membrane for Fuel Cells

Robert Kovar (Primary Contact) and Richard M. Formato

Foster-Miller, Inc.

350 Second Avenue

Waltham, MA 02451-1196

(781) 684-4114, fax: (781) 290-0693, e-mail: bkovar@foster-miller.com

DOE Program Manager: JoAnn Milliken

(202) 586-2480, fax: (202) 586-9811, e-mail: joann.milliken@ee.doe.gov

ANL Technical Advisor: James Miller

(630) 252-4537, fax: (630) 252-4176, e-mail: millerj@cmt.anl.gov

Contractor: Foster-Miller, Inc., Waltham, Massachusetts

Prime Contract No. DE-FC02-97EE50478, July 1998-June 1999

Objectives

- Demonstrate a new class of low-cost, high-temperature solid polymer electrolyte composite membranes, which are useful in automotive (PNGV) applications.

OAAT R&D Plan: Task 13; Barrier B

Approach

The following tasks are required to develop and qualify the composite membrane and membrane/electrode assemblies (MEAs):

- Identify and develop a qualifying ion-conducting polymer (ICP). The ICPs employed must show less than 10% ionomer degradation in accelerated fuel cell life testing.
- Identify and develop qualifying microporous polymeric substrates. The substrates employed must be dimensionally stable, thin, and pinhole-free structures.
- Develop fabrication methods for the high-temperature composite membranes (using the selected ICP and substrate). The ICP and substrate must be combined to form an interpenetrating network (IPN).
- Develop an appropriate electrode structure and corresponding processing methods for MEA fabrication.
- Evaluate and refine the MEA structure for use in HTSPEM fuel cell systems.

Accomplishments

- Selected methods for synthesis and scale-up of ICPs, using the most promising commercially viable candidate base polymer, polyphenylsulfone (PPSU, Radel R).
- Selected methods for synthesis and characterization of poly-p-phenylene benzobisoxazole (PBO) polymer, identified as the most promising polymeric substrate material.
- Continued to develop and refine the processing methods (imbibition/pressing etc.) for fabrication of the ICP/substrate combination into microcomposite membranes.
- Developed first-generation MEAs, using the above microcomposite membranes.
- Conducted single-cell PEM fuel cell testing. The Foster-Miller HTSPEM-based MEAs have already demonstrated performance curves similar to state-of-the-art perfluorinated ionomers.

Future Work

- Continue development of low-cost, high-temperature aromatic-based ICPs that show long-term fuel cell stability.
- Continue development of substrates with microstructure suitable for IPN formation.
- Continue development of electrode structure and corresponding application method(s).
- Continue single-cell fuel cell testing, including analysis of fuel cell performance curves to optimize operating conditions.
- Supply high-temperature MEAs for independent testing (LANL, ANL, etc.)

Introduction

The objective of this work is to develop a low-cost, high-temperature solid polymer electrolyte membrane (HTSPEM) for use in fuel cells. This advanced membrane is designed to address the shortcomings of today's Nafion-based solid polymer

electrolyte fuel cells (SPEFC, H₂/O₂-driven). The HTSPEM will cost less, improve power density, and reduce sensitivity to carbon monoxide in hydrogen fuel. It may also alleviate water-management problems, which limit the efficiency of present-day Nafion-based fuel cells. Utilizing this new

membrane technology will provide a clean, quiet, efficient, lightweight, and high-density power source useful over a wide range of applications, from portable computers to next-generation vehicles.

Fabrication and Evaluation of HTSPEMs

Both the ICP and PBO components selected to make the composite membranes were scaled up to allow batch-type membrane production methods. Composite membranes were prepared by Foster-Miller (as discussed in last year's annual summary report) by using selected PBO/ICP combinations. Sulfonated PPSU (by Foster-Miller) was used as the ICP, and PBO (by Foster-Miller) was used as the substrate material. Once fabricated, the HTSPEMs were fully characterized, and the most promising specimens were made into MEAs. These MEAs were then evaluated at various operating conditions in single-cell test hardware.

The composite membranes prepared by Foster-Miller were sent to Giner, Inc., to determine selected transport and physical/chemical properties. Properties of the Foster-Miller membranes were measured and compared with those of Nafion 117 as a baseline. Recent composite membrane results are listed in Table 1. The most important properties are high ionic conductance (low area specific resistance) and limited fuel crossover. The low-cost, high-temperature (aromatic) ICPs do not yet exhibit acceptable long-term stability. The issue of stability is being addressed through a newly awarded program sponsored by the DOE fuel cells for buildings program (Ron Fiskum). The composite membranes were evaluated for the following set of properties:

- Thickness (dry and wet).
- Ion exchange capacity (IEC, meq/g).
- Water content (%).
- Area specific resistance (ASR, $\Omega\cdot\text{cm}^2$).
- N_2 gas permeability at 23°C ($\text{cm}^3\cdot\text{mil}/\text{ft}^2\cdot\text{h}\cdot\text{atm}$).
- Dimensional stability.

The most important of these properties are discussed below, including a summary of recent results in ionic conductivity, area specific resistance, and nitrogen gas permeability. Table 1 results confirm that by varying the processing methods, we can achieve the composite membrane target values:

IEC > 1.5 meq/g, ASR < 0.20 $\Omega\cdot\text{cm}^2$, and gas permeability (GTR) < 150 $\text{cm}^3\cdot\text{mil}/\text{ft}^2\cdot\text{h}\cdot\text{atm}$. Note, however, that the water contents of the composite membranes are much higher than the target value (target < 50%, currently >>100%). Future work has been proposed to reduce the ICP water content while maintaining low resistance. It is important to note that, even at these high water contents, our crossover values are similar to (or lower than) that for Nafion 117 membranes. Therefore, reducing water content will result in significantly lower GTR, with the added benefit of improved hydrated mechanical strength.

Ion Exchange Capacity and Water Content

As shown in Table 1, we have developed several composite membranes that have exceeded the target IEC of 1.5 meq/g, which is considered necessary for adequate ionic conductance. Some composite membranes showed very low resistance values, even at IECs of less than 1.5 meq/g. The water content of our composite membranes, which are based on SPPSU ICP (measured IEC = 1.9 meq/g, measured water content = 174%) normally ranges from 100 to 150%. This is far in excess of the target value of 50% or lower. In future programs, Foster-Miller will work to develop ICPs (new and modifications of existing ones) that show the required combination of low resistance and reduced water content. If successful, this approach will result in a number of synergistic improvements in composite membrane properties.

Ionic Conductivity and Area Specific Resistance

Foster-Miller continues to generate composites with low values of area specific resistance. However, we have not yet been able to obtain the theoretical composite conductivity values. The best samples fabricated (to date) exhibit two to five times higher ASRs than expected. Clearly, the fabrication method for producing the composites must be improved if we are to realize the full combination of substrate benefits (strength and thin cross-section). The ASR value for FMI 167-19CW of 0.119 $\Omega\cdot\text{cm}^2$ is almost one-half (48%) that of Nafion 117! Work continues on developing composites with improved ASR by improving ICP/PBO synthesis and composite membrane processing methods.

Table 1. Data from Foster-Miller's composite membrane.

Serial Number	Thickness (mil)		IEC (meq/g)	Water Content (%)	Resistance ($\Omega \cdot \text{cm}^2$) ^a	N ₂ , Permeability @ 23°C (cm ³ ·mil/ft ² ·h·atm)	Dim. Stability (% area change)
	Dry	Wet					
Nafion Control	7.1	8.7	0.90	38	0.229	148.3	-20
FMI 126-AY2	1.9	3.0	1.69	139	0.220	NT ^b	nil
FMI 126-AY3	1.4	2.4	1.56	111	0.230	NT	nil
FMI 126-82BE	1.0	1.5	0.91	143	0.140	15% of N117; 1 M Me(OH)	nil
FMI 167-11CR	1.3	2.0	1.26	118	0.125	43.2	nil
FMI 167-15CU	2.5	5.8	1.52	164	0.150	161.0	nil
FMI 167-19CW	1.1	2.0	1.70	131	0.119	154.2	nil
FMI 167-36DS	1.5	2.5	1.06	108	0.208	89.2	nil
FMI 167-52EV	2.5	3.5	0.84	121	0.285	76.2	nil
FMI 167-55EX	2.0	3.0	1.00	127	0.285	61.4	nil

^a Contact pressure = 500 psi, bonded Pt black electrodes (H⁺ form, 23°C).

492-DOE-97210-1

^b NT = Not tested/no data available.

Gas Permeability [Nitrogen]

Nitrogen (N₂) gas diffusion measurements were obtained on all film samples, as well as on baseline controls (N117). Testing was performed according to ASTM tests D-1424 and D-618(A) at a differential pressure of 25 psi and a temperature of 73°F. Prior to measurements, all samples were fully hydrated by boiling in DI water for 1 h. As shown in Table 1, sample FMI167-11CR shows both an improved ASR (45% less of N117) and an improved GTR (71% less than N117). The other samples, although not as good, show similar trends. Optimization of the SPPSU (Radel R) ICP water content (currently 174%!) will certainly reduce the GTR even more, as well as having the added benefit of improved mechanical properties (when hydrated).

Dimensional Stability

The dimensional stability (in plane area change of the fully hydrated composite membrane) of all the PBO-based composites is outstanding. No samples tested showed any noticeable dimensional changes in the plane of the membrane! This is impressive, considering that the sulfonated Radel R films (no substrate used) showed excessive swelling and dimensional change (ranging from 84 to 153%). Foster-Miller remains confident that, given the exceptional strength of the PBO substrate, the mechanical properties of the composites will be well in excess of state-of-the-art fuel cell membranes (e.g., Nafion 112, Gore-Select).

Produce HTMEAs and Complete Single-Cell Fuel Cell Tests

After property evaluations, the composite membranes were developed into MEAs, which were used in single-cell fuel cell tests. Standard platinum black electrodes (4 mg/cm² Pt loading) were thermally bonded onto the FMI films and tested in an H₂/air fuel cell. To date, the best performance was obtained on sample 167-55EX. The MEA fabricated with FMI sample 167-55EX was placed in fuel cell hardware, and performance data were collected initially at 80°C, and subsequently at 90°C and 100°C. Hardware limitations prevented data collection above 100°C. Testing at these temperatures was completed at a pressure of 30 psig, even though minor cross-cell leakage was detected. The data were compared with those for an MEA fabricated with Nafion 117, which had the same electrode structures as the 167-55EX-based MEA. At temperatures above 100°C, the Nafion MEA began to lose its mechanical properties, and measurements were difficult to obtain, in agreement with LANL experience (1).

Performance data collected at each temperature range are shown individually in Figures 1-3. The gradual increase in cell resistance with temperature increase indicates a loss of water in the films during operation. FMI sample 167-55EX exhibited higher performance than that of the baseline Nafion 117 film. At a temperature of 80°C, the FMI sample exhibited a 50-mV improvement in H₂/O₂

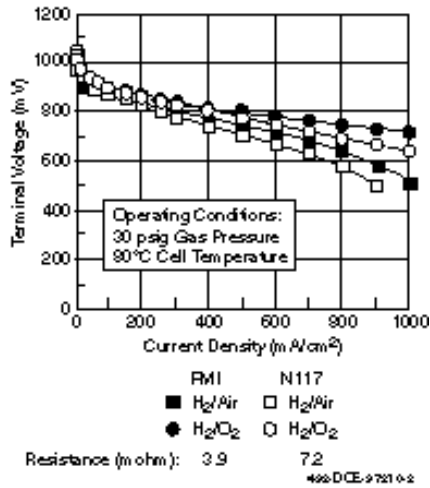


Figure 1. Comparative FMI membrane performance at 80°C (iR-included).

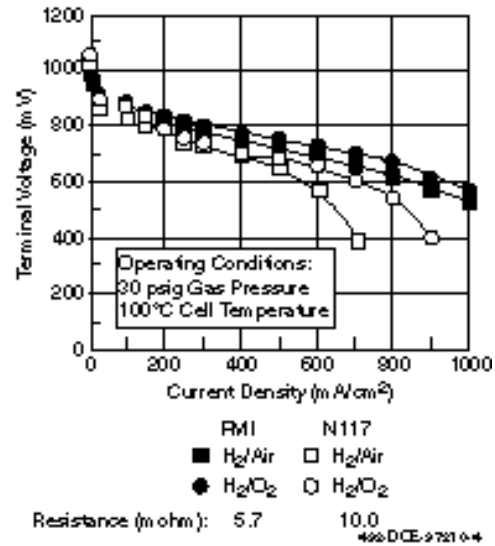


Figure 3. Comparative FMI membrane performance at 100°C (iR-included).

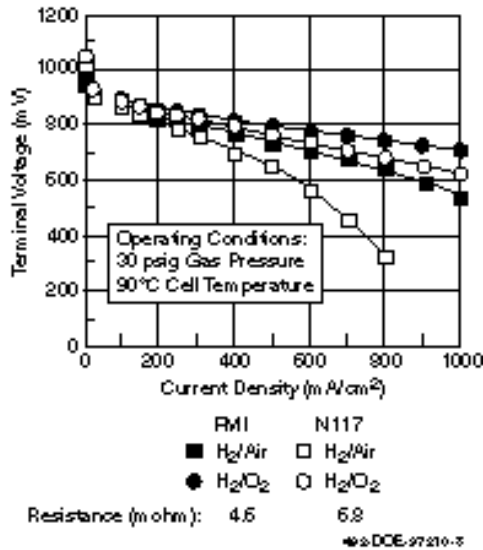


Figure 2. Comparative FMI membrane performance at 90°C (iR-included).

performance at a current density of 1000 mA/cm²; at 90°C, ~100 mV. At an operating temperature of 100°C, the performance of the FMI film at a current density of 1000 mA/cm² was 558 mV. The Nafion MEA did not sustain its performance at this current density and temperature.

Reference

1. T. Zawodzinski, Los Alamos National Laboratory, personal communications (undated).

FY1999 Publications/Presentations

1. R. Formato, R. Kovar, P. Osenar, and N. Landrau, "Composite Solid Polymer Electrolyte Membranes," U.S. Patent Pending.
2. J.E. McGrath, J. Mecham, W. Harrison, S. Mecham, R. Kovar, and R. Formato, "Sulfonated Poly(arylene ether)s as Potential Proton Exchange Membranes," Virginia Polytechnic Inst. and State Univ., Blacksburg, Va., accepted for publication by ACS, 1999.
3. R. Formato, R. Kovar, P. Osenar, and N. Landrau, "Novel Ion Conducting Materials Suitable for Use in Electrochemical Applications and Methods Related Thereto," U.S. Patent Pending.

C. Nanopore Inorganic Membranes as Electrolytes in Fuel Cells

Marc A. Anderson

Water Chemistry Program

University of Wisconsin – Madison

660 North Park Street

Madison, WI, 53706

(608) 262-2674, fax: (608) 262-0454, e-mail: nanopor@facstaff.wisc.edu

DOE Program Manager: Patrick Davis

(202) 586-8061, fax: (202) 586-9811, e-mail: patrick.davis@ee.doe.gov

ANL Technical Advisor: Robert Sutton

(630) 252-4321, fax: (630) 252-4176, e-mail: sutton@cmt.anl.gov

Objectives

- Develop inorganic membranes with high proton conductivity.
- Develop methods for depositing platinum on mesoporous ceramic electrolytes.
- Deposit crack-free films of ceramic electrolyte membranes on mesoporous electrodes.
- Fabricate and test an entire proton exchange ceramic membrane fuel cell (PECMFC).

OAAT R&D Plan: Task 13; Barriers A and B

Approach

- Develop and characterize ceramic membranes with high proton conductivity.
- Support these membranes on catalytically active porous supports.
- Design and construct a fuel cell prototype based on these materials.

Accomplishments

This work started in late FY 1999. To date, we have studied a number of candidate ceramic materials and have selected a few, which have been characterized with respect to proton conductivity and pore structure.

Future Directions

Prepare supported thin ceramic films, using porous conductive media that have been coated with a catalyst.

Introduction

Proton exchange membrane (PEM) fuel cell technologies based on organic polymer membranes (perfluorosulfonated polymer, sold under the trade name of “Nafion”) are unlikely to meet system requirements for PEM fuel cell cogeneration systems. The lower operating temperatures required in using these perfluorosulfonic membranes leads to increased costs because of excess platinum

requirements and the tendency of the cell anodes to be fouled by CO poisoning. Also, as operating temperatures are raised, organic polymer membranes are unable to retain water, leading to poor proton conductivity.

Proton Conductivity

In the first phase of our project, we have studied the temperature and relative humidity (RH)

dependence of conductivity in three different ceramic membrane materials: SiO₂, TiO₂, and Al₂O₃. [1].

Proton conductivity was determined as a function of both RH and temperature. Figure 1 shows the impedance spectra of the TiO₂ chip at 25°C for different RH values. The membrane resistance was considered to be the intersection of the arc with the Z(Real) axis, a value that was independent of the different applied bias voltages, applied on top of the oscillating potential. Similar behavior was obtained for Al₂O₃ and SiO₂. Data in Figure 2 show that the conductivity for all three oxides improves with increasing relative humidity. The conductivity of SiO₂ and TiO₂ improves by three orders of magnitude when the RH increases from 33% to 97%. However, between 58% and 81% RH, the conductivity increases sharply, by two orders of magnitude. The conductivity of alumina has a linear dependence on relative humidity; from 33% to 81% RH, it increases by only one order of magnitude. At 25°C, the largest value of conductivity, $1.1 \times 10^{-3} \Omega^{-1} \cdot \text{cm}^{-1}$, is observed in the TiO₂ sample. Concerning the ability of our ceramic materials to hold water, the results listed in Table 1 show that conductivity values do not correlate with water content under the conditions of 81% RH and 25°C. This is true whether our results are considered

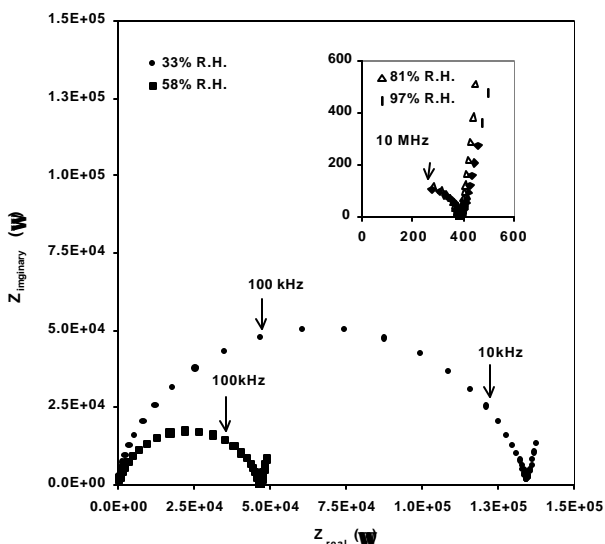


Figure 1. Dependence of conductivity on relative humidity. This example corresponds to TiO₂. Both Al₂O₃ and SiO₂ show the same behavior. (● 33% RH; ■ 58% RH; △ 81% RH; ◆ 97% RH).

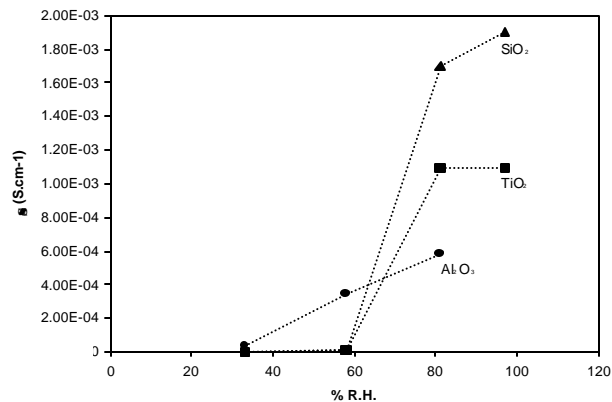


Figure 2. Dependence of conductivity on relative humidity. Data obtained at 25°C.

Table 2. Water content and stability in samples hydrated at 25°C under 81% RH. Data obtained from thermogravimetric analysis.

Sample	% Weight Loss ^(a)		Temp. of DTG min. (°C)	Water Content	
	100 °C	200 °C		Molec./nm ² ^(b)	mmol/cm ³ ^(c)
SiO ₂	23.7	0.6	76	22	20
TiO ₂	21.2	1.8	80	64	26
Al ₂ O ₃	18.2	4.8	85	23	25
Nafion	13.2	2.8	60	--	15
Nafion ^(d)	29.5	--	--	--	21

- (a) Samples equilibrated at 81% RH.
- (b) Internal specific surface area.
- (c) Volume of chip.
- (d) 100% RH Nafion.

on the basis of sample volume or specific surface area. The only correlation that we find with conductivity among all of these materials, including Nafion, is the degree of surface acidity, which can be related to the pK of surface protonation. Surface acidity is also reflected in the isoelectric pH (pH_{iep}) of the material: SiO₂ = 2.0 < TiO₂ = 4.5 < Al₂O₃ = 9.0. Nafion, on the other hand, has very acidic functional groups.

Figure 3 shows that, at 81% relative humidity, the conductivity for all three oxides increases with temperature in the range of 10 to 92°C. At the higher temperatures, the conductivity still increases in the order $\sigma \text{ Al}_2\text{O}_3 < \sigma \text{ TiO}_2 < \sigma \text{ SiO}_2$. The observed values are 2.0×10^{-3} , 3.9×10^{-3} , and $4.0 \times 10^{-3} \Omega^{-1} \text{ cm}^{-1}$ for Al₂O₃ (92°C), TiO₂ (80°C), and SiO₂ (92°C), respectively. In our experiments, the RH is

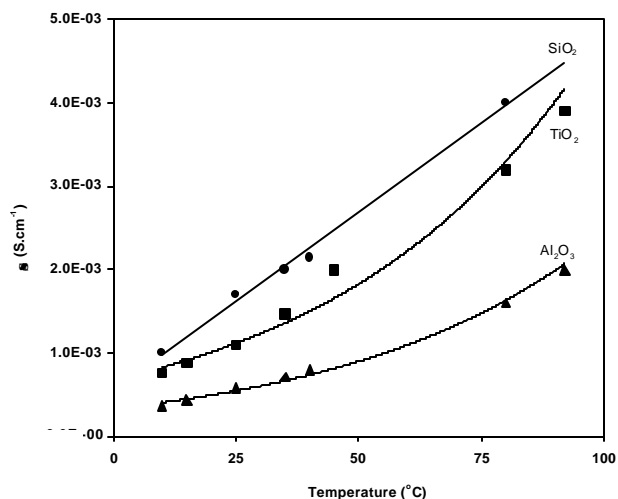


Figure 3. Dependence of conductivity with temperature. Data obtained at 81% RH.

controlled by using saturated salts and the % RH for these salts depends on temperature, so the conductivity for the systems at 80 and 92°C may correspond to a RH value lower than 81%, and it is probably underestimated. Figure 3 also shows that, in the case of SiO₂, the conductivity increases linearly with temperature, while for TiO₂ and Al₂O₃, it increases exponentially. However, the activation energies calculated from these data are very similar for the three materials: 15.8, 17.0, and 17.1 kJ·mol⁻¹ for SiO₂, TiO₂, and Al₂O₃, respectively. Reported values of activation energy for Nafion range from 17 to 29 kJ·mol⁻¹. [2-4].

Following Sumner [5] and Zawodzinski [6], the conductivity of Nafion does not depend as strongly on RH as does that of our ceramic materials. At room temperature, the values reported by Sumner [5] range from $1 \times 10^{-2} \Omega^{-1} \text{ cm}^{-1}$ at 45% RH to $4 \times 10^{-2} \Omega^{-1} \text{ cm}^{-1}$ at 70% RH. At higher temperatures, the conductivity does not increase at the same rate as it does with relative humidity; the value reported for Nafion at 79°C and 42% RH is $1.3 \times 10^{-2} \Omega^{-1} \text{ cm}^{-1}$. Moreover, Zawodzinski [6] reported that the water content in Nafion, in terms of water molecules per sulfonate group, does not change significantly when the temperature is raised from 30 to 80°C in samples equilibrated with water vapor, and that the membrane takes up less water as the temperature is raised. We therefore assume that the same behavior can be expected under conditions

of higher temperature and relative humidity. If we extrapolate Sumner's data to the same conditions used in our study, we find that the conductivity of Nafion is not higher than $3.7 \times 10^{-2} \Omega^{-1} \text{ cm}^{-1}$. In the case of our ceramic chips, the conductivity increases significantly with both RH and temperature. Our values at higher RH and temperature are less than an order of magnitude lower than that observed for Nafion, but our materials can be easily obtained as 0.5- μm thin supported films, whereas Nafion membranes are about 160 μm thick. Therefore, the actual ohmic resistance of such films would be of the same order of magnitude as that of Nafion, or lower, in a given device.

Conclusions

Monolithic, self-supporting ceramic chips can be prepared from different materials via the sol-gel route. These chips are mesoporous and present surface areas ranging from 120 to 489 $\text{m}^2 \text{ g}^{-1}$, and they have high porosities. These ceramic chips retain more water than do Nafion membranes, and they lose this water at higher temperatures. The proton conductivities of these chips are highly dependent on relative humidity, being 1 to 2 orders of magnitude lower than that of Nafion. Because the chips can be obtained as supported thin films that are at least 300 times thinner than Nafion, we believe that they are a potential candidate for electrochemical applications in fuel cells.

References

1. F.M. Vichi, M.T. Colomer, M.A. Anderson, *Electrochem. Solid State Lett.*, **2**, 313 (1999).
2. K.D. Kreuer, *Solid State Ionics*, **97**, 1 (1997).
3. F.N. Büchi and G.G. Scherer, *J. Electroanal. Chem.*, **404**, 37 (1996).
4. K. Uozaki, K. Okazaki, and H. Kita, *J. Electroanal. Chem.*, **287**, 163 (1990).
5. J. Sumner, S. Creager, J. Ma, and D. DesMarteau, *J. Electrochem. Soc.*, **145**, 107 (1998).
6. T.A. Zawodzinski, Jr., and S. Gottesfeld, *Extended Abstr. of the Electrochemical Society Meeting Canada*, Fall 1992.

D. Development and Optimization of Porous Carbon Papers Suitable for Gas Diffusion Electrodes

Gerald J. Fleming, Principal Investigator

Spectracorp Ltd.

599 Canal St.

Lawrence, MA 01840

(978) 682-1232, fax: (978) 682-3253, e-mail: spectragjf@aol.com

DOE Program Manager: Donna Lee Ho

(202) 586-8000, fax: (202) 586-9811, e-mail: donna.ho@ee.doe.gov

ANL Technical Advisor: James Miller

(630) 252-4537, fax: (630) 252-4176, e-mail: millerj@cmt.anl.gov

Contractor: Spectracorp Ltd., Lawrence, Massachusetts

Subcontractor: Energy Partners, West Palm Beach, FL

Prime Contract No. DE-FC02-97EE50474, September 1997 – December 1999

Objectives

- Improved performance and cost reduction in polymer electrolyte membrane (PEM) fuel cells through the optimization of the carbon-based gas diffusion electrode (GDE) material. A matrix of numerous variations in the composition and processing of carbon-fiber-based papers will be fuel-cell-tested and analyzed to determine the effect of performance-enhancing, lower-cost materials and processes. Base paper properties will be correlated with fuel cell performance, and a manufacturing feasibility study and limited production runs will be conducted on the most promising materials in terms of cost and performance.

OAAT R&D Plan: Task 13; Barrier B

Approach

- Change the various parameters in carbon/carbon GDE, such as pore size distribution, electrical and thermal conductivity, and physical strength, by varying fiber types and lengths, heat treatment temperatures, density, and thickness (over 30 variants).
- Correlate the variants to fuel cell performance by using cell testing and analysis – first short-term, and then long-term for the more promising variants.
- Produce the optimized paper(s) in production volumes and make them available for evaluation by laboratory and industry partners.

Accomplishments

- All variants of the GDE were manufactured and tested for physical and electrical properties, as well as pore size, pore size distributions, and gas flow. Correlation of these properties (such as air flow vs. density, resin content, thickness, and pore size) was performed.
- Numerous fuel cell testing parameters (stoichiometries, temperatures, humidification levels, pressures, membranes, electrode treatments) were investigated to obtain a high-performance baseline cell using current state-of-the-art papers.
- Initial cell screening demonstrated very strong performance by several low-cost variants and eliminated nonperforming variants.

- Combinations of the most promising material variants were produced to explore the limit of potential cost reduction while maintaining excellent cell performance.

Future Directions

- Long-term testing on the best-performing GDE variants from initial screening will commence shortly.
- Large-volume cost and manufacturing analysis (including possibility of continuous manufacturing) is under way for the most promising GDE variants.
- A small production run of the best-performing GDE variants will be made.

Introduction

The objective of this program is to optimize the physical structure of porous carbon papers for use as gas diffusion electrodes in membrane electrode assemblies for fuel cells. This optimization will be directed toward maximizing cell and stack performance with regard to such characteristics as mass transport (H₂O removal), appropriate electrical conductivity, and reduced cost versus current state-of-the-art materials.

Manufacture and property characterization was conducted on the full GDE matrix (30+ variants), a fuel cell baseline was established, and initial cell screening was conducted on the GDE variants. Representative cell testing results can be seen in Figure 1.

As can be seen in Figure 1 (and as was expected), some variants exhibited excellent performance, while other variants (stretching the limits on several paper variables in order to define the performance envelope) exhibited quite poor performance.

Figure 2 shows the performance of the baseline material (1N) at several different pressures. Excellent performance is maintained at lower pressure, demonstrating the feasibility of lower-cost materials used in atmospheric-pressure fuel cells.

Much of the expense of existing carbon fiber paper GDEs derives from the processes used in the manufacture of the finished product. In particular, the high heat treatments (>2,000°C) – carried over from phosphoric acid fuel cell technology – add considerable expense to the material and may not be

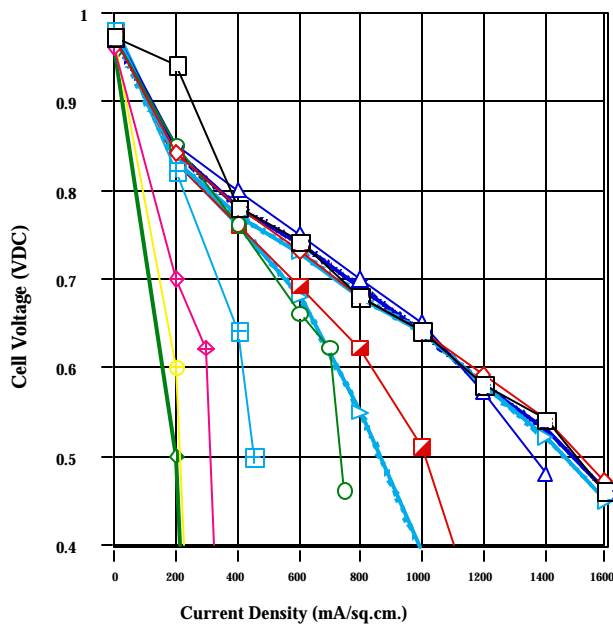


Figure 1. Representative polarization curves from GDE matrix.

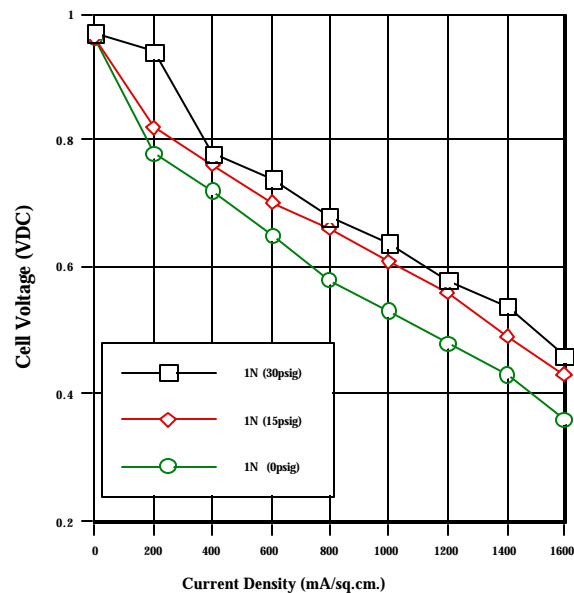


Figure 2: Polarization curves at different cell pressures.

necessary, because of the less caustic environment of the PEM cell. Figure 3 shows promising results from a preliminary examination of lower-cost treatments.

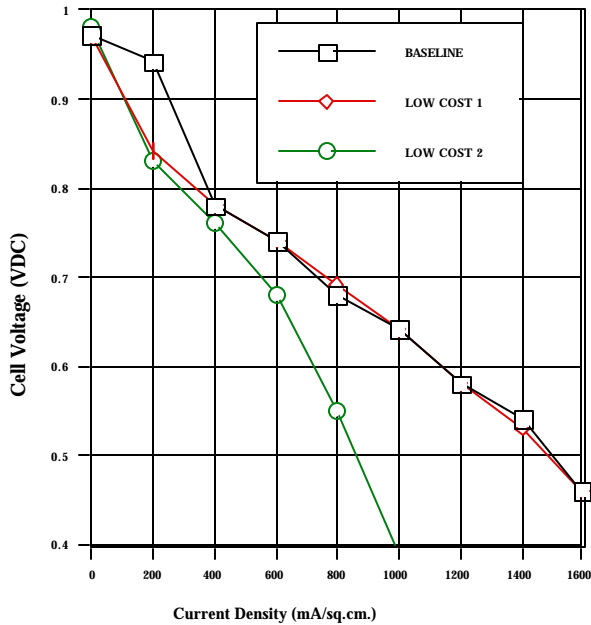


Figure 3. Polarization curves for low-cost GDE.

Combinations of the best-performing and lowest-cost GDE variants from the initial cell screening have been manufactured and will be included in long-term testing at Energy Partners, which is to commence shortly.

Initial cost reductions present no manufacturing hurdles; small production-run quantities will be produced. Long-term cost reductions will require changes in the manufacturing process (possibly to continuous manufacturing). Analysis of the manufacturing possibilities, based on examination of the cell testing data, has begun and should yield a paper cost of <\$10/m² in large volumes, a reduction of over 50% from current cost figures.

E. Optimized Electrodes for PEM Operation on Reformate/Air

Thomas A. Zawodzinski (Primary Contact), Francisco Uribe, Jayson Bauman, Tommy Rockward, Bernd Mueller, Markus Vogt, Thomas Springer, Judith Valerio, and Shimshon Gottesfeld

Electronic and Electrochemical Materials and Device Research Group

Los Alamos National Laboratory

(505) 667-0925, fax: (505) 665-4292, e-mail: zawod@lanl.gov

DOE Program Manager: JoAnn Milliken

(202) 586-2480, fax: (202) 586-9811, e-mail: joann.milliken@ee.doe.gov

Objectives

To achieve maximum performance in PEFCs under conditions appropriate for reformate/air operation, via methods that allow cost and efficiency targets to be met for transportation

OAAT R&D Plan: Task 13; Barrier A

Approach

Simultaneously achieving the following cell characteristics, through applied R&D:

- Minimum air injection for CO cleanup
- Minimum catalyst loading
- Minimum losses due to dilution at high fuel utilization
- Highest possible performance at 0.8 V

Accomplishments

- *Dilution effects.* Achieved improved operation at high utilization, in line with predictions from new diagnostics.
- *CO tolerance.* Reduction in both precious metal loading ($0.5 \rightarrow 0.2$ mg/cm²) and in air bleed (2.5% or lower vs. 4% for 100 ppm) since July 1998 review.
 - New catalyst in reconfigured anode shows promise for reaching full tolerance with <5% air bleed to 500 ppm in reformate, using 0.3 mg/cm² anode catalyst.
 - New, reconfigured MEA allows us to tolerate 100 ppm in reformate with only 0.5% air bleed.
 - Testing of transient response of cells under various conditions; improved recovery from transient increase in CO, using air bleed.
 - Testing with segmented cell indicates stepwise propagation of poisoning down the channel.
- *Impurities other than CO.* Effects of ammonia, methane, olefins, and hydrogen sulfide on performance were studied. Ammonia and hydrogen sulfide caused substantial performance loss. However, in each case, a cleanup method was demonstrated.
- *Cathode Performance.* The cell performance at 0.8 V was studied. Performance improvements, relative to that obtained at steady state in cells using Pt, were obtained with different alloy catalysts and using low duty cycle pulsing of the cell voltage to lower voltages.

Future Directions

- Change emphasis to reflect need to increase cell voltage – more cathode work.
- Cathode work: overall goal is to increase achievable current density at 0.8 V.
- Improve cathode catalysts.

- Vary catalyst layer and backing compositions to improve hydration.
- Experiment with elevated temperature operation/alternative hydration methods.
- Obtain guidance from cathode modeling.
- Anode work: overall goal is to minimize effects of dilution and CO.
- Improve anode catalysts, reconfigure anodes, and increase effectiveness of air injection for ever higher CO tolerance.
- Improve catalyst layer composition to further minimize dilution effects, increase fuel utilization.
- Further clarify long-term effects of higher levels of CO.
- Practical studies: break-in effects, cold start, new fabrication approaches.

Introduction

The requirements for overall polymer electrolyte fuel cell (PEFC) performance include operation under conditions of maximum fuel utilization efficiency, as well as the best possible performance using gasoline-derived reformat. These requirements are tightly coupled, because the former entails higher cell voltages (and thus, some focus on the PEFC cathode); higher cell voltages also may provide some “relief” in the context of the stringency of CO-tolerance requirements. The scope of this project has broadened slightly to include both of these items. We seek to address these needs by developing an understanding of electrocatalysis and transport issues related to reformat feed and by using this understanding to guide the development, testing, and demonstration of improved electrodes for reformat operation. We test the single cells under steady-state and transient exposure to various levels of CO. We have also tested cells exposed to various other impurities expected in a reformat stream. Finally, we have carried out preliminary work aimed at improving fuel cell cathode performance.

Dilution Effects

We encountered substantial performance losses in 50-cm² single cells as we lowered the anode stoichiometric flow rate below 1.3 (approx. 77% fuel utilization). Operation of a fuel cell using a feed stream with 40% hydrogen under the target conditions of 90% utilization results in a hydrogen concentration of 6% near the cell outlet. Accordingly, we investigated the effect of dilution of the anode stream on cell performance. To decouple the dilution effect from utilization effects,

we operated in small single cells, using high flow rates, to approximate a “zero utilization” condition. Results of such tests for a series of different dilutions are shown in Figure 1.

We also include a result for which the humidification was varied. The improved performance at lower humidification led us to believe that gas access to the electrode could be a decisive factor. Accordingly, we systematically varied the gas diffusion layer (GDL), looking at several thicknesses and hydrophobicities, and tested the deviation of the cell response from the ideal, Nernstian behavior expected for simple dilution effects. We found, surprisingly, that the best performance was obtained for a GDL with a thick microporous layer on one side of the backing. On the basis of this finding, we tested a larger cell under high utilization conditions and found that this enabled good performance on simulated reformat with 83% utilization (Figure 2), thus overcoming a previously observed barrier.

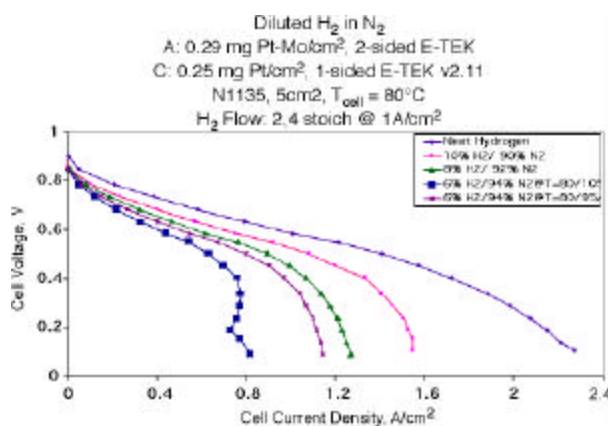


Figure 1. Polarization curves showing the effect of diluting the anode feedstream under “zero utilization” conditions.

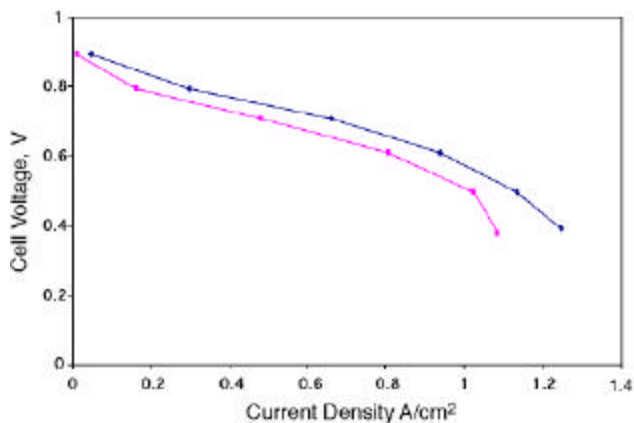


Figure 2. Polarization curves comparing operation on neat H₂ (upper curve) and 40% H₂ (lower curve). Cell conditions: 0.2 mg/cm² Pt each on anode and cathode, other operating conditions as in Figure 1.

CO Tolerance

We have continued to progress toward the simultaneous goals of enhanced CO tolerance with minimum air injection and minimum catalyst loading. We showed that certain new catalysts allowed us to approach a high level of tolerance to 500 ppm CO. Figure 3 shows this result.

We also showed that the effects of 100 ppm CO in reformat could be eliminated by as little as 0.5% air bleed with an optimized MEA (reconfigured anode, 0.6 mg/cm² anode Pt loading). In short-term tests, we can simultaneously lower catalyst loading to 0.2 mg/cm² and achieve complete tolerance to

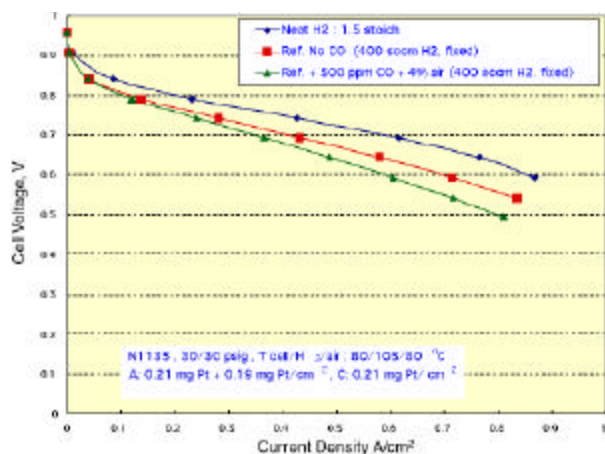


Figure 3. Polarization curves showing the combined effects on new catalyst and reconfigured anode, providing near complete tolerance to 500 ppm CO in reformat.

100 ppm CO with <2.5% air bleed. Our best results to date, shown in Figure 4, indicate that we can reach full tolerance to 100 ppm in reformat with 0.5% air. Industrial collaborators are currently testing our reconfigured anodes.

In another set of tests, we have extensively studied the effects of transient excursions in CO levels, characterizing the response of cells as a function of flow rate, temperature, catalyst loading, and type. Perhaps the most technologically significant result is our finding that injection of air can dramatically improve the recovery, from excursions in CO level from 20 to 100 and back to 20 ppm CO, as shown in Figure 5.

Impurities Other than CO

Various impurities or products of the reforming process could be present at the fuel cell anode. We demonstrated the deleterious effects of hydrogen sulfide (Figure 6) and ammonia on fuel cells, together with methods of cleanup. We also showed that the presence of methane and ethylene in the anode flow stream had little effect on the cell performance.

Cathode Performance

To meet efficiency requirements for operation on reformed gasoline, the cathode performance must be improved at high cell voltages. We began a serious investigation of this problem with several studies, two of which are highlighted here.

Operation at high cell voltages necessarily implies operating with little water production at the

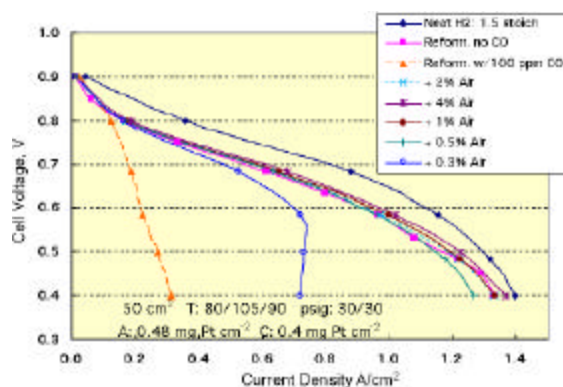


Figure 4. Series of polarization curves with various levels of air injection used to achieve CO tolerance.

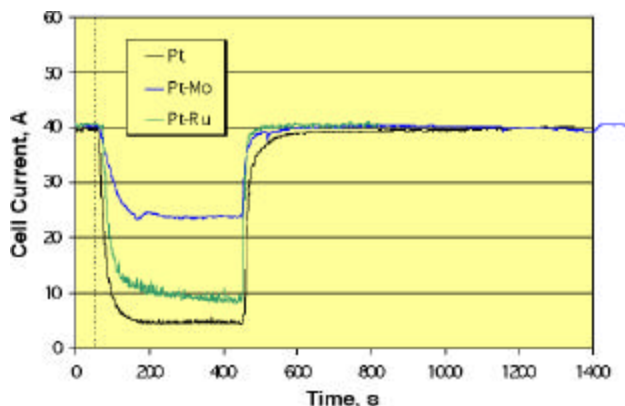


Figure 5. Rapid recovery from a transient increase in CO level, achieved with air injection. Plot shows response of 3 different anode catalysts to CO in H₂ varied from 20 ppm to 100 ppm and back to 20 ppm. Other cell conditions as in Figure 1.

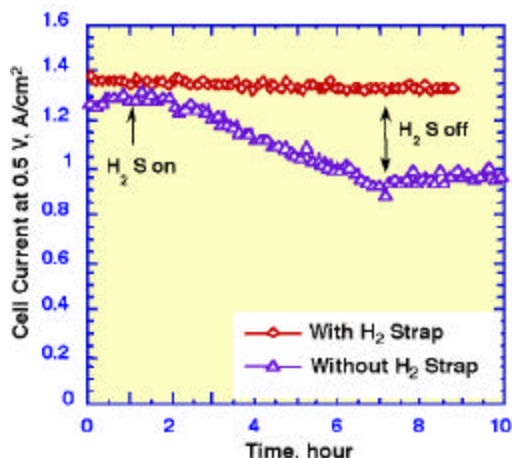


Figure 6. Plot showing effect of exposure of cell to 3 ppm H₂S as a function of time, with and without upstream trapping method. Other cell conditions as in Figure 1.

cathode. We previously showed that dry conditions led to poorer oxygen reduction reaction (ORR) kinetics. Figure 7 shows the decline in steady-state current with time after changing cell voltage from 0.6 to 0.8 V. We tried to overcome this problem by “pulsing” the cell to lower voltages, thus generating more water. The results of such an operation mode,

with a 1% duty cycle at the lower cell voltage, are shown in Figure 7. Clearly, the application of such a pulse provided improved steady-state performance. The nature of the improvement is under investigation.

We also studied the relative ORR activity of various alloy catalysts in the cell. Results are shown in Figure 8. Thus far, PtNi and PtCr cathode catalysts have been the most active.

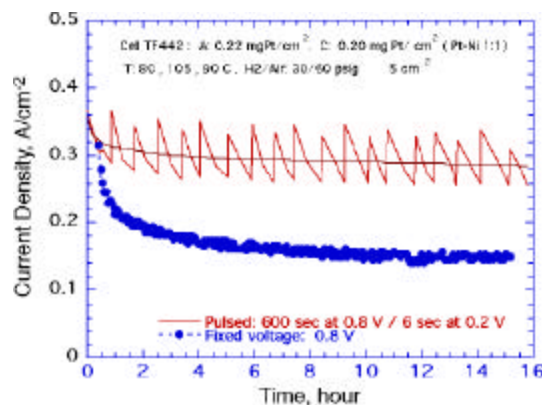


Figure 7. Response of the cell with time (bottom curve) after changing the cell voltage from 0.5 V to 0.8 V and effect of pulsing the cell voltage (top curve) between 0.8 V (99% of the time) and 0.2 V (1%).

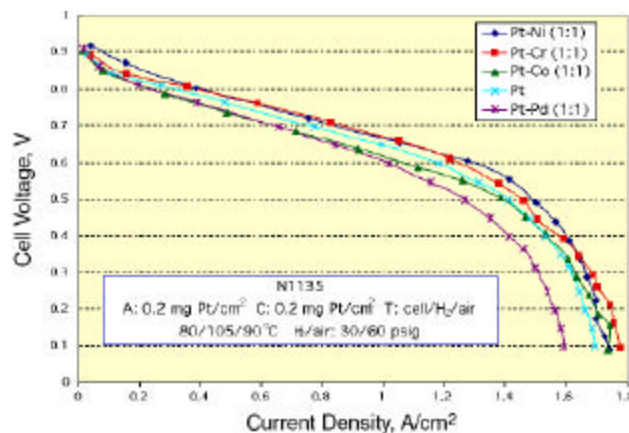


Figure 8. Polarization curves for a series of different cathode catalysts.

F. New Alloy Electrocatalysts and Electrode Kinetics

Philip N. Ross, Jr.

Materials Sciences Division, Lawrence Berkeley National Laboratory

University of California

Berkeley, CA 94720

(510) 486-6226; fax: (510) 486-5530; e-mail: pnross@lbl.gov

DOE Program Manager: JoAnn Milliken

(202) 586-2480, fax: (202) 586-9811, e-mail: joann.milliken@ee.doe.gov

Objectives

- Conduct research on the kinetics and mechanism of the electrode reactions in low-temperature fuel cells.
- Develop new electrocatalysts, using a materials-by-design approach.

OAAT R&D Plan: Task 13; Barrier A

Approach

- Study the kinetics of fuel cell electrode reactions by means of modern electroanalytical methods. Study the reaction mechanisms by using state-of-the-art *in-situ* spectroscopic techniques.
- Use ultra-high vacuum methods of surface preparation and surface analysis to form tailored surfaces, and synthesize nanoclusters to have the tailored surface. Characterize the microstructure of the nanoclusters by high-resolution electron microscopy.
- Transfer technology to catalyst developers/vendors.

Accomplishments

- Collaborated with LANL and BNL in testing of the prototype E-TEK Pt-Mo alloy catalysts in PEM fuel cells fed with simulated reformat. Achieved milestone of 50–100-mV higher cell voltage than with Pt-Ru catalyst with reformat containing 20 ppm carbon monoxide (no air bleed).
- Obtained the first results for a Pd-based catalyst.

Future Directions

- Determine CO tolerance of tailored electrodes consisting of thin films (1-10 monolayers) of Pd on the close-packed single crystal surfaces of Nb, Ta, and Mo.
- Pursue Pt-skin structures as novel air cathode electrocatalysts.

Introduction

During the past fiscal year, we collaborated with E-TEK to synthesize a carbon-supported Pt-Mo catalyst having performance approaching that predicted for alloy nanoclusters that have the Pt₇₅Mo₂₅ bulk alloy surface. We established a performance milestone for prototype Pt-Mo catalyst: less than 50 mV loss at 0.6 A/cm² (80°C, 3 atm) with

H₂/25%CO₂/20 ppm CO, using 0.5 mgPt/cm². We collaborated with Los Alamos National Laboratory (LANL) and Brookhaven National Laboratory (BNL) in testing the prototype E-TEK Pt-Mo alloy catalysts in PEM fuel cells fed with simulated reformat. Prototype carbon-supported Pt-Mo catalyst from E-TEK met the performance milestone by the end of the 1st quarter. We determined the CO tolerance of ternary Pt_{4-x-y}M_xM'_y electrodes prepared

by plasma immersion ion-implantation (PIII) of M' in Pt-M binary alloy. The systems to be studied were $M = \text{Ru}, \text{Mo}$, and $M' = \text{Sn}$. The results with Sn implanted in $\text{Pt}_{75}\text{Ru}_{25}$, $\text{Pt}_{77}\text{Mo}_{23}$, and $\text{Pt}_{85}\text{Mo}_{15}$ to the levels of 10–15 at.% Sn were disappointing; the presence of Sn in the surface either had no effect or actually decreased the CO tolerance. We decided not to continue the study of ternary $\text{Pt}_{1-x-y}\text{M}_x\text{M}'_y$ systems at this time, meeting our milestone of a Go/No Go decision by mid-year.

Thin films of Pd on early-period transition metals (e.g., Nb, Ta, W) are reported to have dramatically reduced binding of CO when adsorbed in UHV, probably because of strong intermetallic bonding between Pd and the transition metal substrate. Electrochemical properties of these systems have never been investigated. This electronic interaction may create a “weakly adsorbed” state of CO on the Pd that can be oxidized at low potentials, thus producing a CO-tolerant surface. Pd metal itself is essentially as active a catalyst for H_2 electrooxidation as is Pt. Electronic effects in electrocatalysis are frequently postulated but rarely proven to exist. In theory, however, such effects present an important opportunity that we must seek to utilize.

Preliminary results in the study of Pd thin-film (1–10 ML, 1 ML = 1 monolayer) electrodes appear promising. We were able to control the film thickness in the 1–10-ML region. As shown in Figure 1, a 1-ML film of Pd on Pt(111) showed slightly increased activity [with respect to that for clean Pt(111)] for H_2 electrooxidation, and significantly greater activity than a multilayer Pd film [i.e., bulk Pd(111)]. Pt(111) was chosen as a “control” substrate, but even in this case, an electronic effect was observable. The theoretically more interesting substrates, the hexagonal close packed (hcp) surfaces of Ta and W, have been prepared and are ready for use.

In previous research directed toward improved air electrodes for phosphoric acid fuel cells, we had sought to utilize what we termed a “skin effect” to produce a more active state of Pt for oxygen reduction. The skin effect arises from strong surface segregation of Pt in certain alloys — in particular, Pt_3Co and Pt_3Ni . At equilibrium (in vacuum), the surface of these alloys is *pure Pt* (i.e., a monolayer “skin” of Pt), with the second layer nearly pure Co

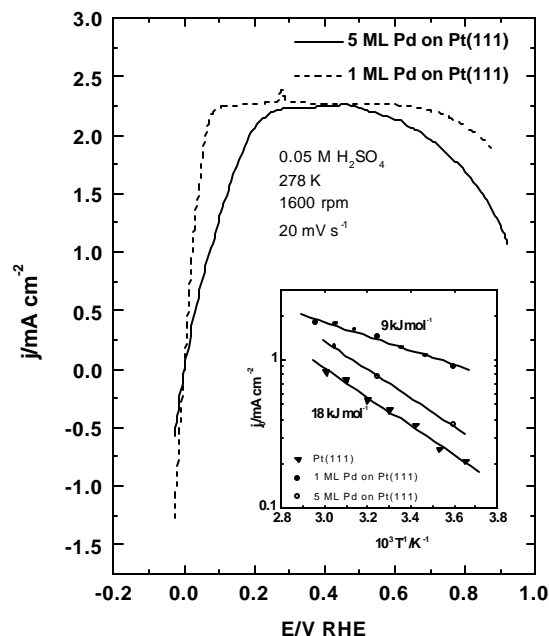


Figure 1. H_2 oxidation/evolution polarization curves on Pt(111) and epitaxial thin films of Pd on Pt(111). Note uniquely lower activation energy for the 1-ML Pd film vs. either bulk Pt(111) or epitaxial multilayer Pd.

or Ni. The electronic state of the Pt skin is shifted from that of a bulk Pt surface, which results in enhanced oxygen reduction kinetics with respect to pure Pt. However, in hot phosphoric acid fuel cell cathodes, the skin structure of the alloy nanoclusters was found to be unstable, and the enhanced activity was lost relatively quickly (after about 100 hr). At lower temperatures, and in the less aggressive medium of polymer electrolyte, the skin structure may be more stable.

Studies of the oxygen reduction activity and stability of the skin structure on Pt_3Co and Pt_3Ni bulk alloys in polymer electrolyte are in progress, using our unique rotating ring-disk electrode methodology coupled with *ex-situ* surface analysis techniques. It is fundamentally important in the pursuit of this concept to determine the stability of elements like Co and Ni in PEM, even when they are covered by a “skin” of Pt. We have also initiated studies of other possible skin-effect bimetallic systems for Pt, using thin films (<4 ML) of Pt evaporated onto a metal M that — in the Pt-M alloy — is predicted (from *ab initio* calculations) to form a Pt-skin structure.

Publications

Refereed Journals

1. Grgur, B., N. Markovic, and P. Ross, "Electro-oxidation of H₂, CO and H₂/CO Mixtures on a Well-Characterized PtRe Bulk Alloy Electrode and Comparison with Other Pt Binary Alloys," *Electrochim. Acta* **43** (1998) 3631.
2. Markovic, N., B. Grgur, C. Lucas, and P. Ross, "Electrooxidation of CO and H₂/CO Mixtures on Pt(111) in Acid Solutions," *J. Phys. Chem. B* **103** (1999) 487.
3. Mukerjee, S., S. Lee, E. Ticianelli, J. McBreen, B. Grgur, N. Markovic, P. Ross, J. Giallombardo, and E. De Castro, "Investigation of Enhanced CO-Tolerance in PEM Fuel Cells by Carbon Supported PtMo Alloy Catalyst," *Electrochem. and Sol. State Lett.*, **2** (1999) 12.
4. Grgur, B., N. Markovic, and P. Ross, "The Electrooxidation of H₂ and H₂/CO Mixtures on Carbon Supported Pt-Mo Alloy Catalysts," *J. Electrochem. Soc.*, **146**, 1613, 1999.

Books, Book Chapters, and Refereed Conference Proceedings

1. Ross, P., "The Science of Electrocatalysis on Bimetallic Surfaces," in *Electrocatalysis*, J. Lipkowski and P. Ross, Eds., J. Wiley and Sons, New York, N.Y., 1998, pp. 43-74.

2. Grgur, B., N. Markovic, and P. Ross, "On the Mechanism of CO-Tolerance of Pt-Mo Alloy Electrocatalysts," in *Proton Conducting Membrane Fuel Cells II*, S. Gottesfeld and T. Fuller, Eds., The Electrochemical Society, Pennington, N.J., Proc. Vol. 98-27, 1999, pp. 176 – 187.

Other Publications

1. Markovic, N., Grgur, B., and P. Ross, "Electro-oxidation of H₂, CO and H₂/CO Mixtures on Well-Characterized Pt-Ru, Pt-Sn, and Pt-Mo Alloy Surfaces," in *9th Int. Conf. Sol. State Protonic Conductors.*, Bled, Slovenia (Aug. 17-21, 1998), Extended Abstracts, pp. 243-44.
2. Ross, P., J. Giallombardo, and E. De Castro, "Preparation and Testing of a New CO-Tolerant Electrocatalyst for PEM Fuel Cells," *1998 Fuel Cell Seminar Abstracts*, Courtesy Assoc., Washington, D.C., 1998, pp. 560-61.

G. Cathode Catalysts

Dan DuBois (Primary Contact) and Jim Ohi
Basic Sciences Center, National Renewable Energy Laboratory
1617 Cole Boulevard
Golden, CO 80401
(303) 384-6171, fax: (303) 384-6150, e-mail: dan_dubois@nrel.gov

DOE Program Manager: JoAnn Milliken
(202) 586-2480, fax: (202) 586-9811, e-mail: joann.milliken@ee.doe.gov

Objectives

- Develop new electrocatalysts for oxygen reduction.
- Develop rapid throughput method for electrocatalyst discovery.

OAAT R&D Plan: Task 13; Barrier B

Approach

- Synthesize libraries of bimetallic complexes in which the coordination environment of the metals and the distance between the metals are systematically varied:
 - Synthesize bridging ligands (triphosphine and carboxylate for 1999).
 - Develop rapid throughput synthesis of bimetallic complexes.
- Adapt screening method used in previous work to study oxygen reduction.

Accomplishments

- Prepared bridging ligands containing tridentate phosphine and carboxylate groups.
- Developed rapid throughput synthetic methods for preparing bimetallic complexes.
- Integrated rapid screening method (using cyclic voltammetry) with rapid throughput synthetic method. This integrated approach permits rapid identification of active catalysts from reaction mixtures. Screening method is both general and quantitative.
- Prepared more than 1200 bimetallic complexes and screened them for oxygen reduction. Approximately 20 hits were observed, which indicates that bimetallic complexes are a promising class of compounds for further study.

Future Directions

- Now that the feasibility of the basic approach has been demonstrated, increased emphasis will be placed on the design of the bridging ligands.
 - Two classes of bridging ligands will be studied in the next year, bis (diphosphine) and bis(Schiff base) compounds.
-

Introduction

The major objective of this research is to use a rapid throughput approach to identify new electrocatalysts for oxygen reduction. The

electrochemical reduction of O₂ to water is an important reaction in all low-temperature fuel cells. In hydrogen fuel cells, it is the oxygen electrode that has the largest overpotential. For methanol fuel

cells, highly selective oxygen reduction catalysts could also reduce or eliminate the energy loss associated with methanol crossover. For these and other reasons, the development of new catalysts for oxygen reduction is important for efficient and practical low-temperature fuel cells. Although significant effort has been devoted to development of better oxygen reduction catalysts than platinum-based catalysts, none have been found.

In the research outlined below, we describe the application of a new experimental approach, called "combinatorial" or "rapid throughput" chemistry,^{1,2} to the discovery of new catalysts for oxygen reduction. The main difference between the rapid throughput approach and more traditional catalyst discovery methods is the use of rapid synthetic methods, coupled with rapid screening methods. The objective is to be able to prepare and evaluate large numbers of compounds for evaluation as catalysts. Compared to more traditional approaches, the rapid throughput approach should permit at least 100 times as many compounds to be evaluated.

In the past year, we began a study of bimetallic homogeneous compounds that will permit a systematic approach to catalyst development. Bimetallic complexes were chosen because it is known that such complexes facilitate the four-electron reduction of oxygen to water more readily than do mononuclear complexes.³ The rapid synthesis of arrays of bimetallic complexes was demonstrated. This was accomplished by adding two weakly solvated metal complexes to ligands specifically designed and/or selected to promote the binding of two metals. These reaction mixtures were screened by cyclic voltammetry without separation of the different complexes that resulted from this synthetic approach. Proper analysis of the resulting data permitted the complexes responsible for catalytic activity to be identified from reaction mixtures.

Bridging ligand syntheses

Figure 1 shows ligands that we prepared and used to synthesize bimetallic complexes. The two ends of the first three bridging ligands are tridentate binding units, which can be the same (e.g., **L3**) or different (e.g., **L1**). Different ends result in different coordination environments around each metal center, allowing features that control redox potentials and reaction pathways to be varied. The

ligands in Figure 1 also permit variation of the distance between the two metal sites. This distance is thought to be important in oxygen reduction.

Library synthesis

Synthesis of the bimetallic complexes consisted of adding a stoichiometric amount of mixtures of two weakly solvated metal ions (shown in Table 1) to solutions of the bridging ligands. For example, we followed the reaction of one equivalent of $[\text{Ni}(\text{CH}_3\text{CN})_6]^{2+}$ and one equivalent of $[\text{Fe}(\text{CH}_3\text{CN})_6]^{2+}$ with one mole of the symmetrical bridging ligand, **L3**, by ³¹P NMR spectroscopy. The result was the formation of a mixture of three compounds, Fe-**L3**-Ni, Fe-**L3**-Fe, and Ni-**L3**-Ni, in a roughly statistical 2:1:1 ratio, as expected. Whenever two different metals are used with a symmetrical bridging ligand, three bimetallic

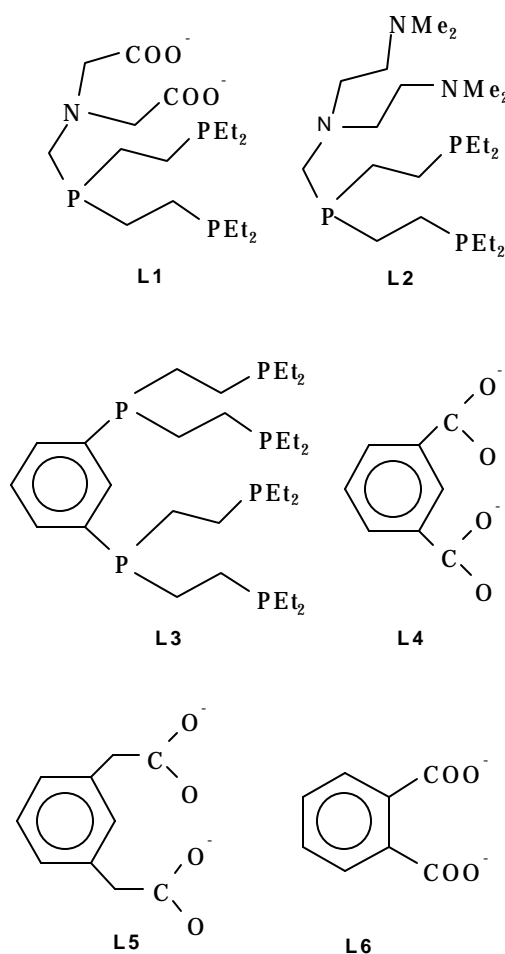


Figure 1. Bridging ligands.

Table 1. Metal complexes.

[M(CH ₃ CN) ₆](BF ₄) ₂ M = V, Cr, Mn, Fe, Co, Ni, Ru
[Cu(CH ₃ CN) ₄](PF ₆)
[Pd(CH ₃ CN) ₄](BF ₄) ₂
[Pt(COD)(CH ₃ CN) ₂](BF ₄) ₂
[V(O)SO ₄] ₃ H ₂ O
Mn(NO ₃) ₂
In(NO ₃) ₃
Ag(BF ₄)

compounds should result. This situation is shown schematically in Table 2.

The number three in this matrix indicates those reaction vessels expected to contain three bimetallic compounds. If the two aliquots of the same metal solution are added to L, then pure M-L-M complexes will be obtained. This result has also been confirmed by NMR spectroscopy. These pure compounds are indicated by the numeral 1 for the diagonal elements of the matrix. It is clear that the array contains all possible M-L-M' compounds, where M and M' can either be the same or different. Most of the reaction vessels will contain mixtures. We have used approximately 20 different metal complexes for preparing arrays of compounds. This results in 210 different bimetallic complexes [(N+1)!/(N-1)!2! where N = 20] for each symmetrical bridging ligand (e.g., **L3**) and 400 compounds (N²) if the two ends of the bridging ligand are different (e.g., **L1**). To date, we have prepared more than 1200 compounds by using this approach.

Table 2. Reaction matrix.

	M1	M2	M3	M4
M1	1	3	3	3
M2	3	1	3	3
M3	3	3	1	3
M4	3	3	3	1

Screening of bimetallic complexes

The screening process consisted of performing multiple cyclic voltammograms on the arrays of reaction vessels discussed in the preceding paragraph. A cyclic voltammogram was performed on each reaction mixture (or reaction vessel) under (1) nitrogen, (2) oxygen, (3) oxygen and acid, and

(4) acid with nitrogen purge. A positive result or "hit" has one criterion: for acidic solutions, the ratio of the catalytic current in the presence of oxygen (i_c) to the current observed for the complex under study in the absence of oxygen (i_d) must be greater than 4 ($i_c/i_d > 4$). This corresponds to a second-order rate constant of approximately 20 M⁻¹ s⁻¹ under our screening conditions. For example, if compound M3-L-M3 is active, then all of the reaction mixtures shown in column 3 and row 3 of Table 2 should show catalytic activity, with the diagonal elements having approximately twice the activity of the off-diagonal elements in row and column 3. These matrix elements are highlighted with light gray. If a mixed compound, say M1-L-M2, is active, then the two off-diagonal elements, M1M2 and M2M1 (dark gray) will show activity, but no diagonal elements will be active. Using this screening approach, it is possible to screen between 50 and 100 compounds per day, obtaining quantitative information under a variety of reaction conditions. More than 1200 compounds have been evaluated, and it is possible to unambiguously identify the species responsible for the catalytic activity. Approximately 20 of these 1200 compounds have demonstrated sufficient catalytic activity to be classified as hits. The rapid throughput approach has allowed us to confirm that bimetallic complexes are an active class of compounds for oxygen reduction, and for a broader range of compounds than had been previously studied.

Compounds selected for further study or so-called "promising candidates" must meet two criteria. The i_c/i_d ratio must be greater than 4, and the onset potential of the catalytic wave must be within 0.5 V of the thermodynamic potential. The compounds studied to date operate at onset potentials too negative to meet our second criterion. We will continue to apply this approach in searching for promising candidates for oxygen reduction.

The rate-determining step in the rapid throughput approach is the synthesis of bridging ligands that allow for a systematic variation in the coordination environments and the distance between the metals. The careful design of such ligands is important for a systematic search of these bimetallic complexes using the rapid throughput approach. Such a systematic search of bimetallic complexes would not be feasible in a reasonable time frame, using more traditional synthetic approaches.

References

1. Baum, R. *Chem. Eng. News* 1996, 74(7), 28-73.
2. Reddington, E.; Sapienza, A.; Gurau, B.; Viswanathan, R.; Sarangapani, S.; Smotkin, E. S.; Mallouk, T. E. *Science* 1998, 280, 1735.
3. Collman, J. P., Rapta, M., Bröring, M., Raptova, L., Schwenninger, R., Boitrel, B., Fu, L., and L'Her, M. J. *Am. Chem. Soc.* 1999, 121, 1387-1388.

H. Development of a \$10/kW Bipolar Separator Plate

Michael Onischak, Leonard G. Marianowski (Primary Contact), Scott Thielman, and Qinbai Fan
Institute of Gas Technology, Des Plaines, IL 60018
(847) 768-0590, fax: (847) 768-0916

DOE Program Manager: Donna Lee Ho
(202) 586-8000, fax: (202) 586-9811, e-mail: donna.ho@ee.doe.gov

ANL Technical Advisor: Walter Podolski
(630) 252-7558, fax: (630) 252-4176, e-mail: podolski@cmt.anl.gov

Contractor: Institute of Gas Technology, Des Plaines, Illinois 60018
Prime Contract No. DE-FC02-97EE50477, September 1997-March 2000

Subcontractors:

PEM Plates, LLC, Elk Grove Village, IL 60007

AlliedSignal Inc., Torrance, CA 90504

Stimsonite Corporation, Niles, IL 60714

Superior Graphite Corporation, Chicago, IL 60638

Objectives

- Evaluate the IGT molded graphite bipolar separator plate's performance and endurance in fuel cell stacks.
- Evaluate mass production of molded plates by building a pilot production molding line with a capacity of 5 plates per hour.

OAAT R&D Plan: Task 13; Barrier B

Approach

- Design, build, and operate the 5-plate-per-hour pilot production molding line at PEM Plates, LLC.
- Produce molded bipolar plates from the pilot line for the IGT and AlliedSignal fuel cell stack tests.
- Assemble fuel cell stacks at IGT to establish the functional performance and endurance of molded plates in stack environments.
- AlliedSignal to test the molded plates from PEM Plates in fuel cell stacks of their design

Accomplishments

- Built pilot production line facility and equipment, producing plates for IGT and samples for several fuel cell stack developers.

- IGT operated multiple cell stacks (4-, 7-, and 20-cell stacks) with molded plates from PEM Plates.
- A 20-cell IGT stack, with plates produced by PEM Plates, has remained in operation for over 2200 hours, with excellent performance.
- Confirmed that \$10/kW cost target is within reach with cost of separator plate materials at \$4/kW; however, molding costs under \$6/kW depend upon bipolar plate design.

Future Directions

- Demonstrate operational functionality of molded plates as part of multicell fuel cell stack for heat management, sealing, stacking stability, and water management.
- Design higher-capacity production molding line with process modifications.
- Prepare to supply commercial fuel cell stack developers with molded separator plates of their bipolar plate designs.

Introduction

The overall objectives of this program are to develop a \$10/kW-manufactured-cost, molded bipolar separator plate and to advance the technology to commercial production rates. On the basis of the performance success of the IGT molded composite graphite bipolar separator plate, PEM Plates, LLC, was formed to mold plates for developers worldwide. PEM Plates, LLC, is a joint venture of Stimsonite Corporation and ENDESCO Services.

In the first phase of the DOE program completed last year, several resins, graphite types, and additives were evaluated for their fuel cell property enhancement characteristics. Several types of graphite blends were evaluated; the hydrophilic graphite blend selected was a proprietary blend supplied by our subcontractor, Superior Graphite Corp. This blend, molded into the IGT IMHEX[®] bipolar plate, yielded volume conductivities that were three times the DOE-specified target of 100 S/cm. The criteria for all components were chemical inertness, low cost, long-term availability, low flammability, and no leachates to poison the catalyst or membrane.

Bipolar Plate Measured Properties

Dies for IGT bipolar separator plate molds were made with flow fields for an anode and with water-cooling channels on the opposite side for a cathode (Figure 1). Measurements of the electrical, chemical, and physical properties of the molded plates have met or exceeded DOE’s specified targets, as shown in Table 1.

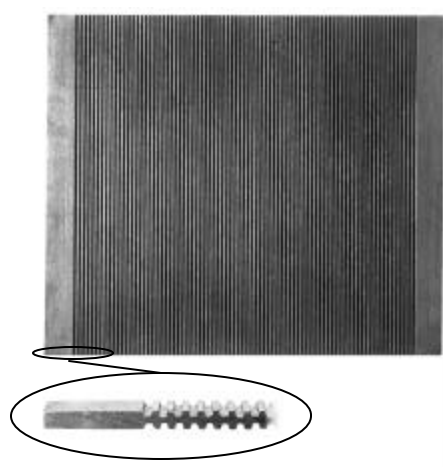


Figure 1. Typical molded graphite plate flow field.

Table 1. Bipolar plate properties.

Property	Measured Value
Conductivity (goal >100 S/cm)	250–350 S/cm
Corrosion (goal <16 μA/cm ²)	<5 μA/cm ²
H ₂ permeability	<2 x10 ⁻⁶ cm ³ /cm ² -s (dry, nonporous plates); bubble pressure >15 psig (wet, porous plates)
Crush strength	>3000 psi
Flexibility	3–6% deflection at mid-span
Total creep	~1% @ 200 psi, 100 °C
Material cost	~ \$4/kW
Manufactured cost	<\$10/kW

The DOE target of 100 S/cm for conductivity, measured by ASTM C-661, was typically exceeded by a factor of three. The corrosion-rate target of 16 $\mu\text{A}/\text{cm}^2$ in hydrogen, air, and oxygen atmospheres was determined in an aqueous solution of 2 ppm fluoride, using ASTM G5, at 90°C, pH~4. The IGT molded composite blend yielded measured rates below 5 $\mu\text{A}/\text{cm}^2$. Hydrogen permeability was measured as a function of molding pressure for either dense, nonporous molded plates or plates molded with some degree of porosity. The hydrogen permeability rate for the dense, non-porous plates was $2 \times 10^{-6} \text{ cm}^3/\text{cm}^2\text{-s}$ at 90°C and 30 psi, well below the specified 16×10^{-6} value.

In addition, IGT measured the strength, flexibility, and creep characteristics of the plates, anticipating a magnitude of 200 psi for fuel cell holding forces, nonuniformity of gasketing and stack assembly, plus handling and packaging actions from the production line. These values (Table 1) are expected to be within a reasonable safety factor. The plates also have retained their properties after being subjected to immersion in boiling water and to freeze-thaw cycles.

Multicell Fuel Cell Stack Performance

In Phase 1 of the DOE program, IGT molded bipolar separator plates with active areas of 50 cm^2 and 300 cm^2 for property measurements, as well as for single-cell performance testing. The single fuel cell performance was compared to operation in state-of-the-art machined graphite plates under identical conditions. Performance was nearly identical to that of the state-of-the-art machined graphite (about 3% lower performance, ~15 mV @ 400 mA/cm^2 , mainly due to the slightly higher surface resistance of the present molded plates, as shown in Figure 2).

The performance shown in Figure 2 was very stable over the 2000 hours of testing that was conducted as a continuous, 24-hour-per-day test. In this period, weekly diagnostic and open-circuit measurements were made.

Following the 50- cm^2 testing, full-size 300- cm^2 active area plates were tested, and the same performance and endurance were obtained, thereby confirming the scaleup of the molded graphite plates.

In Phase 2 of the DOE program, the molded graphite plates were evaluated in a short-stack

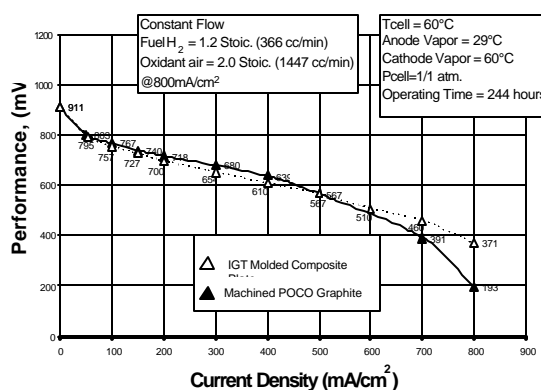


Figure 2. Comparison of IGT molded graphite cell with machined graphite.

environment. The single-cell tests established excellent molded plate performance, but these cells operate isothermally. Operation of fuel cell stacks involves non-isothermal conditions, with attention to active cooling, proper sealing, type of seals, and clamping forces. All of these functionality issues address the durability of the molded bipolar plate.

Full-size anode and water-cooled cathode molded bipolar plates were molded for IGT by PEM Plates. These plates were assembled and tested at IGT in 4-, 7-, and 20-cell fuel cell stacks. AlliedSignal will test the molded plates in their design later in 1999.

The operating performance of the 20-cell IGT stack, 1.5 kW, is shown in Figure 3 up to 2200 hours of operation. The stack was operated at near ambient pressure and at a temperature of 60°C for most of the 2200 hours of operation. Another period to establish endurance at 80°C is planned.

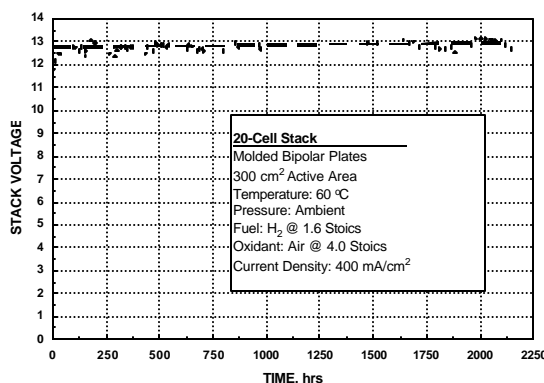


Figure 3. Life test of IGT 20-cell molded bipolar plate fuel cell stack.

Cost Studies and Commercial Production

The updated cost analysis indicates that the materials used in the molded plate in commercial quantities comes to about \$1.46 per pound. Using the DOE goals for power density and active area per kilowatt, this cost translates to about \$4.10/kW. Manufacturing costs are judged to be within \$6/kW, so that the total molded separator plate cost should be under \$10/kW, depending on the complexity of the design.

The molded separator plate information developed in this work is applicable to almost any size and shape of bipolar plates; that is, molding to any final net shape is possible, with no finishing

steps necessary. However, designs with complicated features may cost more to manufacture.

PEM Plates, LLC, has built the pilot production line, with a molding capacity of 5 plates per hour, to evaluate the steps in molding. The pilot line addresses the key steps of preparation of the composite blend, transferring to the mold, forming of the plates, releasing from the molds, post-molding operations, and QA/QC operations.

Several fuel cell stack developers have evaluated the quality of the molded graphite bipolar plate and have requested bipolar plates to be molded. PEM Plates operates on a strictly confidential basis with developers independent of IGT.

I. Layered PEM Stack Development

Michael Pien, Ph.D.

ElectroChem, Inc.

400 W. Cummings Park

Woburn, MA 01801

(781) 938-5300, fax: (781) 935-6966

DOE Program Manager: Donna Lee Ho

(202) 586-8000, fax: (202) 586-9811, e-mail: donna.ho@ee.doe.gov

ANL Technical Advisor: James Miller

(630) 252-4537, fax: (630) 252-4176, e-mail: millerj@cmt.anl.gov

Contractor: ElectroChem, Inc., Woburn, Massachusetts

Prime Contract No. DE-FC02-97EE50475, October 1, 1997-September 30, 1999

Objectives

- Develop a low-cost bipolar PEM separator plate design for light vehicle transportation applications, on the basis of a layered structure composed of low-cost, commercially available, mass-produced materials.

OAAT R&D Plan: Task 13; Barrier B

Approach

- Perform a stepwise development of a layered bipolar plate structure that incorporates stainless steel, porous graphite, and polycarbonate in a reliable and easy-to-manufacture structure:
 - Select materials and fundamental fabrication technologies that are inherently low-cost yet have suitable precision to guarantee reliable stack assembly.
 - Develop bonding techniques between dissimilar materials that are compatible with the environment associated with PEM fuel cell and light vehicle applications.

- Validate the plate design and continued improvements through the construction and testing of a series of laboratory-scale fuel cell stacks:
 - Develop and test several 50-cm² stacks that validate the basic design and materials compatibility.
 - Scale up and test several 232-cm² stacks that validate the best designs for full-scale applications.
- Perform a manufacturing cost and performance analysis in support of the suitability of this technology for light vehicle transportation applications.

Accomplishments

- Developed and tested an inherently low-cost, layered bipolar plate design that uses commercially mass-produced materials. Projected plate costs are estimated to be \$10/kW or less when produced in volume.
- The bipolar plate design exhibits a low internal resistance loss, leading to a potential loss of only 8 mV at a current density of 1 A/cm². This leads to only a 1% loss resulting from internal resistance.
- Validated corrosion resistance of the design by prolonged operation and chemical testing of the product water. No significant corrosion was observed.
- Endurance testing (over a period of six months) demonstrated performance equivalent to conventional low-porosity graphite plates.
- Established reliability and performance of gasket-free design and assembly process for 232-cm² stack.
- Extended layered plate design to successful operation and extended testing of 232-cm² bipolar and cooling plates. Prolonged testing has already passed 6300 A·h, with no signs of degradation.

Future Directions

- Maximize cost savings from the design by using molded graphite and polycarbonate components.
- Develop molded components and automated handling processes to validate cost projections.

Introduction

The principal hardware element in a PEM fuel cell is the bipolar separator plate, which in conventional designs also constitutes the largest single cost item in a fuel cell system. The bipolar separator plate must perform a number of important tasks simultaneously and still remain lightweight and low-cost. It must provide excellent electrical conductivity; keep the gaseous reactants separated; be leak-free; support intricate gas flow patterns to uniformly distribute reactants and water vapor and remove waste products from the membrane electrode assembly (MEA); permit stack cooling; and be fabricated to relatively high tolerances in volume production. Finding a single material from which to inexpensively produce monolithic separator plates remains a challenge. Long experience has shown that graphite has the chemical stability to survive the fuel cell environment, but producing nonporous graphite is a long and expensive industrial process.

Our Approach

Our approach has been to fabricate separator plates from several materials, thereby relaxing performance requirements for any one material. Our basic design approach is shown in Figure 1, where a single monolithic plate design (a) is compared with a layered design (b). The principal components of the new design are porous graphite, polycarbonate plastic, and stainless steel.

Porous graphite is used in this design because the gas impermeability of the completed plate is provided by the stainless steel and polycarbonate. Because the graphite can be porous, the basic material cost is greatly reduced. Commercially available processes exist for the rapid fabrication of porous graphite parts by molding. Alternatively, porous graphite blocks can be produced at modest cost and easily machined with gang cutters.

Polycarbonate is the most chemically resistant of the high-volume manufactured plastics. With a safe operating temperature well above that of PEM

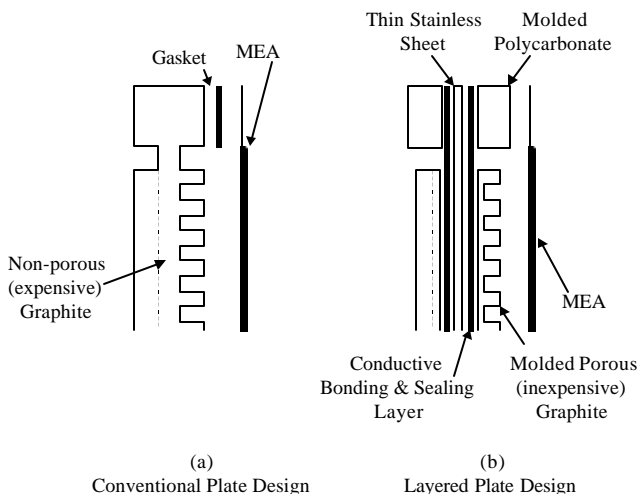


Figure 1. Schematic comparison of conventional fuel cell separator plate vs. ElectroChem’s layered structure. Monolithic plate is made of expensive nonporous graphite or composite. ElectroChem design uses 3 primary materials chosen for low cost, high performance, and ready availability.

fuel cells, its chemical resistance to attack is sufficient for many years of operation. It is easily molded into the shapes necessary to provide reliable gaskets and manifolds. This permits efficient channeling of the reactants and coolants to each of the cells throughout the stack.

Stainless steel (SS) has been examined repeatedly as a primary material for separator plate fabrication. The steel surface is intentionally spaced from the highly reactive surface region of the MEA by the porous graphite plate. Furthermore, the steel sheet is kept flat and stress-free (not stamped to form gas channels), which reduces the tendency for corrosion. Using the steel as a flat featureless surface, with only a few holes for manifolding of reactants, makes its fabrication by a low-cost shearing/stamping process efficient. It also lets the thickness of the steel, the heaviest component of the plate, be minimized for weight reduction.

Because the bipolar plates are now fabricated from several components, the required intricate gas flow channels are easier to design in. Post-mold machining is avoided entirely; the gas manifolding channels can be more easily introduced in several components and then assembled, while sealing surfaces are reliably maintained.

The Technical Challenges

The primary technical challenges in this approach were

1. Providing a reliable, low-resistance contact between the graphite and stainless steel, with minimal stress and long life.
2. Achieving reliable seals, to avoid crossover and leakage.
3. Minimizing corrosion and contamination to maintain stack performance and life.

Initial Test Results: Initial testing of the basic design on small, 50-cm² cells worked well, and the three primary materials selected all performed well under extended life testing. These early tests were accomplished using relatively thick components to enable passive cooling. Extended life test results are shown for the stacks tested, indicating that the materials selected provided performance that matched that of conventional solid graphite plates. No corrosion was observed.

Sealing and Bonding: These small initial cells all used fairly rigid conductive adhesives to make the contact between the graphite and stainless steel. Furthermore, a strong adhesive was used to enable bonding between the polycarbonate and stainless steel. The process required several steps, but the results were encouraging, and the fundamental cost of the materials was acceptably low. However, as the design was scaled to 232-cm² active area,

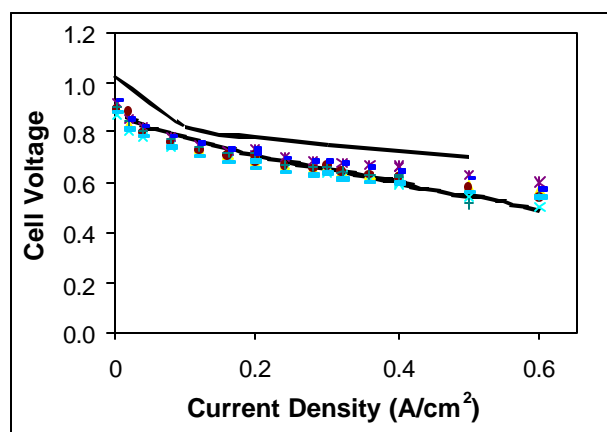


Figure 2. Comparison of 50-cm² layered cell’s performance (data points) with standard performance range obtained from solid graphite separator plates (solid lines). All data were collected at 50 psi.

thermally induced stresses between components became more evident. The larger pieces showed significant curling, and the separation between contact layers was unacceptable.

Stress Analysis: The stress problem was analyzed by means of computer modeling. As expected, the thickness of the components strongly influenced the stress level, with the thinner components generating lower stress. Unexpectedly, it was found that the stress did not scale significantly with part size between 50 and 232 cm². We concluded that the contact layer between the graphite and SS needed to be far less rigid.

Improved Design: A new approach was taken to making a contact layer that has provided superior results. Besides being stress-free, the electrical contact between the graphite and SS has very low resistance. This same contact layer also provides an adequate seal between the polycarbonate and SS to avoid leakage and crossover. Part thickness was also dramatically reduced, so that the total separator plate thickness is now 3.6 mm. This design was assembled and tested at the full-scale 232-cm² size, complete with 6 active cells and 2 cooling plates, with test results shown below.

Plate Resistance Measurements: To verify that the plate design is of low resistance, high DC current (0.5 A/cm²) was passed through the plates, and the potential drop was measured. From these measurements, the internal resistance of the separator plates was determined to be 8.2 mΩ/cm².

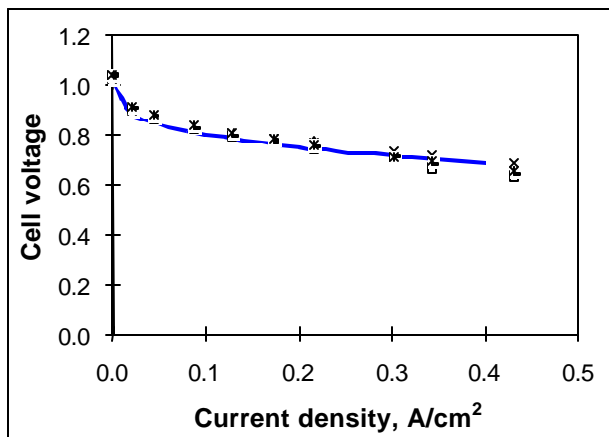


Figure 3. Comparison of 232-cm² layered cell’s performance (data points) compared with standard performance data obtained from solid graphite separator plates (solid line). All data were collected at 30 psi.

This translates into a resistive loss during high power operation (1 A/cm² at 0.8 V/cell) of approximately 1%, thereby meeting the requirements for light vehicle applications.

Corrosion Resistance: All testing was performed with pure oxygen, both to demonstrate high-power-density performance and to maximize corrosion effects. Our results indicated that no significant corrosion occurred, as evidenced either by visible effects on the SS or by ion content of the product water.

Manufacturing Technology: The process for fabrication of the layered bipolar plates lends itself to low-cost mass production using techniques, equipment, and processes used across several industries. Although the plates comprise several pieces that require individual fabrication and handling, each step is quite low-cost and rapidly executed. As part of this program, a cost analysis is being carried out and continuously refined, specifically for volume production associated with the auto industry.

Some of the results of this analysis are shown in Figures 4 and 5. Of primary interest to the vehicle manufacturer is that the fuel cell separator and cooling plates (one cooling plate for every two active cells) meet the simultaneous requirements of low weight and low cost. The layered separator plate design readily meets both of these requirements, using commercially available materials, with reasonable assumptions made about cost savings from volume production techniques.

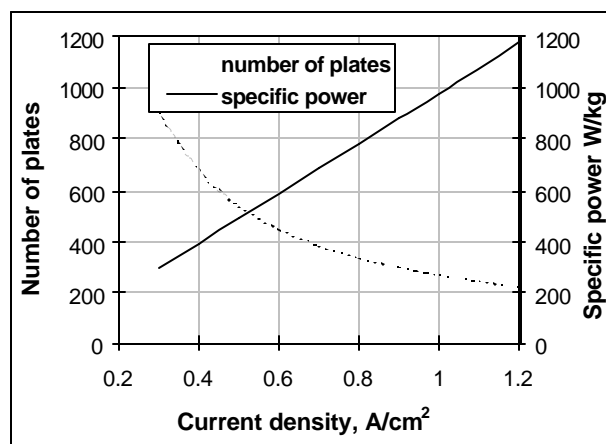


Figure 4. Specific power analysis of layered separator plus cooling plates for a 50-kW stack operating at 0.8 V/cell.

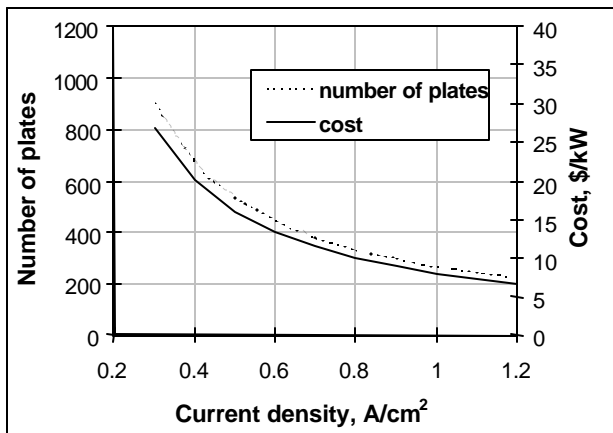


Figure 5. Cost analysis results of layered separator plates plus cooling plates for a 50-kW stack operating at 0.8 V/cell (based on production of 100,000 units/yr).

Future Challenges

A key element in our design involves looking toward the progressive commercialization of fuel cells. The approach taken permits us to adapt these

materials to a wide range of designs that may vary between fuel cell manufacturers. This successful separator plate design is quite generic and can be adapted to a wide range of flow-field patterns. These materials are already produced in bulk and are well-engineered, and economies of scale can be achieved rapidly with minimal investment.

Meanwhile, this material combination can also be obtained in small volumes at modest cost and can be machined inexpensively to provide parts that already cost less than their nonporous graphite equivalents. These less expensive parts can be readily introduced into fuel cells when manufacturing volumes are still small, yet they can provide substantial cost savings at every level of production volume.

Full exploitation of the cost savings from this design will be provided by the use of molded graphite and polycarbonate components. Future work should include the development of molded components and automated handling processes to validate cost projections.

J. Corrosion Test Cell for Metallic Bipolar Plate Materials

Kirk Weisbrod, Don Prier II, and Nick Vanderborgh*

Los Alamos National Laboratory, MS J576

Los Alamos, NM 87545

(505) 665-7847, fax: (505) 667-0600

(Southern University, Baton Rouge, LA 70813)*

DOE Program Manager: JoAnn Milliken

(202) 586-2480, fax: (202) 586-9811, e-mail: joann.milliken@ee.doe.gov

Objectives

Develop tools to characterize the corrosion characteristics of metallic bipolar plate materials:

- Perform potentiometric measurements to rapidly characterize dissolution behavior.
- Design, build, and evaluate a test cell that adequately mirrors the environment encountered by bipolar plate material in a PEM cell.

OAAT R&D Plan: Task 13; Barrier B

Approach

- Use potentiometric scans to characterize dissolution behavior.
- Develop and demonstrate a corrosion test cell that adequately evaluates performance.

Accomplishments

- Performed initial screening of readily available metallic materials.
- Developed and tested a corrosion test cell.

Future Directions

- Test sample materials, as requested by the fuel cell community.
- Provide the corrosion test cell design to potential users, as requested.

Introduction

Development of low-cost bipolar plate materials is a significant challenge for commercialization of PEM fuel cells for transportation applications. Some of the key constraints for selection of bipolar plate materials were outlined by Borup.¹ For metallic options, manufacturing cost is generally minimal. Corrosion resistance is a major challenge. Primary objectives of the test cell are to (a) measure the change in electrical resistance across the bipolar plate and (b) characterize the soluble ions formed that may be absorbed by the ionomer membrane.

Experimental Approach

The interfaces between a large number of cells in a stack may be represented by the two cells given schematically in Figure 1.

Figure 2 illustrates a cross section of the corrosion test cell. The ionomer membrane is replaced with a 0.001 N H₂SO₄ solution containing 2 ppm F. The catalyst layer, an ELAT electrode (0.5 mg Pt/cm², 20% Pt on C), establishes an

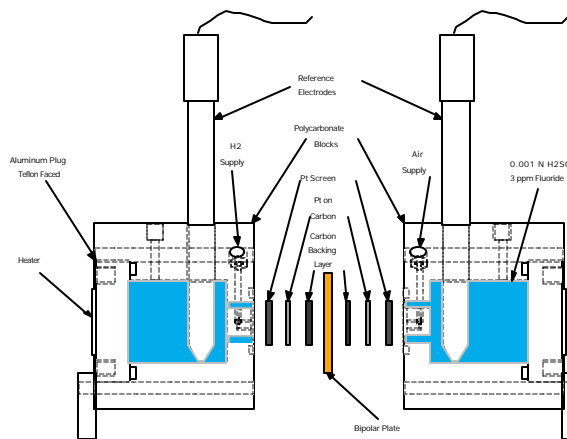


Figure 2. Operating schematic of the bipolar plate corrosion test cell.

electrochemical potential between the metal components and the electrolyte. Platinum screens pass electric current through the backing layers and bipolar plate. Electrical potential between components is recorded to monitor oxide growth. Hydrogen and air are supplied to the anode and cathode faces, respectively.

Results and Discussion

Potentiometric studies were performed at a pH of 3. The dissolution rate of aluminum is quite high, as expected (Figure 3). POCO graphite (AXF-5Q) also has a high dissolution rate at 1 V vs. NHE. Sealing the plate decreases the rate of dissolution to the equivalent of 150 μM/10,000 h. Since the test pH is lower than that expected in a fuel cell, the dissolution rate is higher than expected in actual operation.

Titanium nitride coatings on titanium and nitride implanted in titanium both decrease the corrosion rate to the lowest rate observed in this study. Figures 4 and 5 illustrate how the addition of nickel and chromium to stainless steel alloy did not

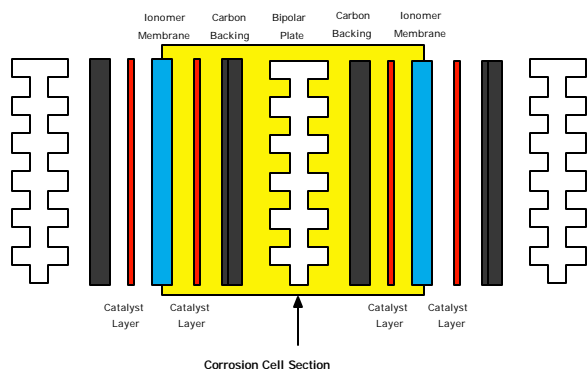


Figure 1. Two-cell cross-section. The central region represents components in the corrosion test cell. The cell is a two-membrane test fixture designed to establish reproducible test conditions surrounding the central plate.

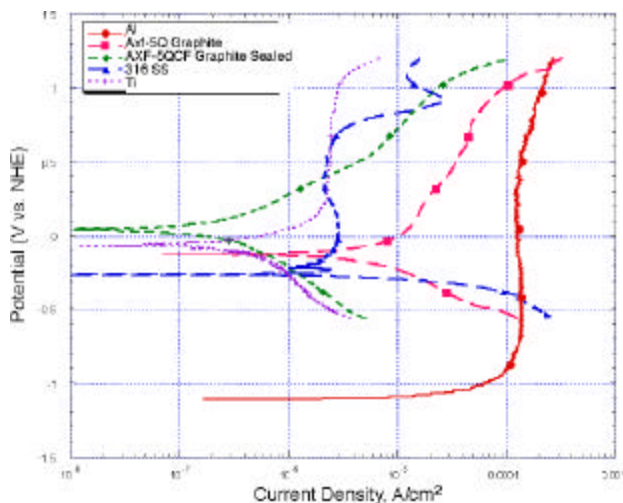


Figure 3. Polarization curves for aluminum, 316 SS, and titanium: 0.001 N H₂SO₄, 2 ppm F⁻, 80°C, deaerated with N₂, 0.1 MV/s scan rate.

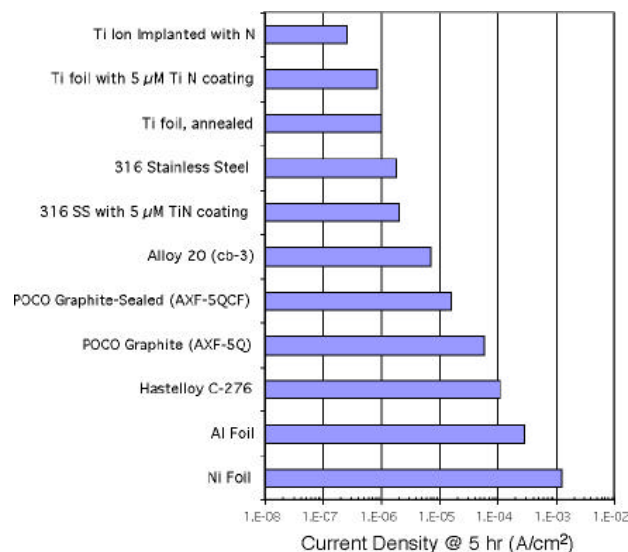


Figure 5. Electrodisolution rate for selected metal samples at cathode potential: 0.96 V vs. NHE after 5 h: 0.001 N H₂SO₄, 2 ppm F⁻, 80°C, deaerated with N₂.

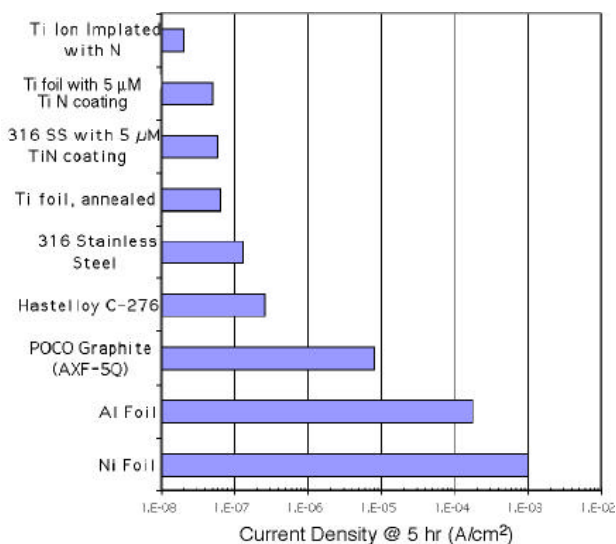


Figure 4. Electrodisolution rate for selected metal samples at anode potential: 0.1 V vs. NHE after 5 h: 0.001 N H₂SO₄, 2 ppm F⁻, 80°C, deaerated with N₂.

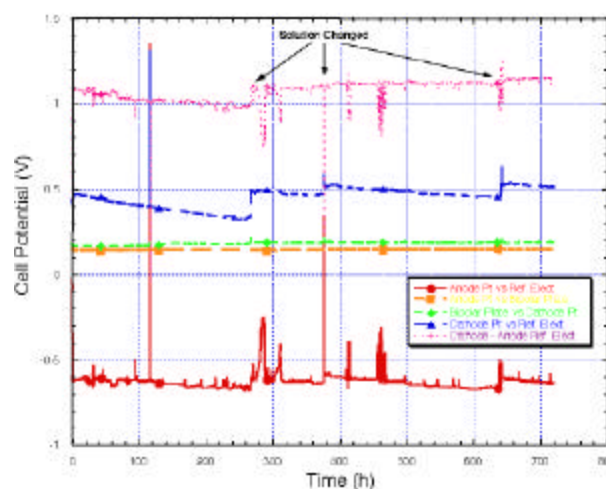


Figure 6. Cell potential transients with 316 SS bipolar plate: 0.001 N H₂SO₄, 2 ppm F⁻, 80°C; anode - H₂ at 1 atm, cathode - air at 1 atm.

decrease the corrosion rate at a pH of 3. Nickel dissolution at low pH appears to enhance the overall dissolution rate. At a pH of 5-6, the effect may not be as significant.²

Corrosion test cell results were obtained for aluminum, 316 SS, titanium, and Hastelloy C-276. Reference electrode potentials indicated that the bipolar plate was exposed to conditions similar to those within an operating fuel cell (Figure 6).

Changes in pH with time are reflected by the reference potential. High dissolution rates for aluminum led to high contact resistance and soluble ion concentrations. 316 SS experienced intermediate performance and may be acceptable for shorter-term applications.³ Titanium and Hastelloy C-276 both showed minimal increases in contact resistance against carbon paper. Lower cation concentrations were measured in solution for C-276 than for 316 SS.

Table 1. Change in anode and cathode bipolar plate resistance in corrosion cell at 1 A/cm².

Bipolar Plate Material	Time (h)	Voltage Change (mV/1000 h)
Aluminum		
Anode	87	172.4
Cathode	87	839.1
316 SS		
Anode	700	8.6
Cathode	700	30.0
Titanium		
Anode	1546	-0.6
Cathode	1546	-1.3
Hastelloy C-276		
Anode	740	-9.5
Cathode	740	0.0

Testing to date indicates that the corrosion test cell is a useful tool in characterizing the change in oxide resistance and formation of soluble ions under conditions that closely represent fuel cell conditions at the anode and cathode. Confirmation of trends in actual fuel cell operation is desirable.

References

1. R.L. Borup and N.E. Vanderborgh, "Design and Testing Criteria for Bipolar Materials for PEM Fuel Cell Applications," *Mat. Res. Soc. Symp. Proc.*, Vol. **393**, pp.151-155 (1995).
2. C. Zawodzinski, Los Alamos National Laboratory, personal communication (undated).
3. S. Cleghorn, X. Ren, T. Springer, M. Wilson, C. Zawodzinski, and S. Gottesfeld, "PEM Fuel Cells for Transportation and Stationary Power Generation Applications," *Hydrogen Energy Progress XI, Proc. WHE Conf.*, Stuttgart, Germany, June 23-28, 1996, pp. 1637-45.

VI. AIR MANAGEMENT SUBSYSTEMS

A. Turbocompressor for PEM Fuel Cells

Mark K. Gee

AlliedSignal Aerospace Equipment Systems

2525 W. 190th Street, MS-36-2-93084

Torrance, CA 90504

(310) 512-3606, fax: (310) 512-4998, e-mail: mark.gee@alliedsignal.com

DOE Program Manager: Patrick Davis

(202) 586-8061, fax (202) 586-9811, e-mail: patrick.davis@ee.doe.gov

ANL Technical Advisor: Robert Sutton

(630) 252-4321, fax (630) 252-4176, e-mail: sutton@cmt.anl.gov

Contractor: AlliedSignal Aerospace Equipment Systems, Torrance, California

Prime Contract No. DE-FC02-97EE50479, October 1997-May 2000

New Start FY 1999, July 1999-February 2001

Objectives

Design, develop, and demonstrate a low-flow turbocompressor for PEM light-duty vehicles powered by PEM fuel cells.

OAAT R&D Plan: Task 13; Barrier D

Approach

- Use of automotive and aerospace turbomachinery technology for low cost and low weight/volume.
- Use of contamination-free and zero-maintenance compliant foil air bearings.
- Use of a high-efficiency, low-cost two-pole toothless motor.

Accomplishments

- Numerous start/stop cycles with no appreciable wear.
- Stable operation at full turbine temperature.
- Compressor and turbine mapping showed performance close to predicted values.
- Compressor mapping with inlet guide vanes and vaneless diffuser showed improved performance at lower flow rates.

Compressor/Expander Turbocompressor Subsystem

(compressor/expander subsystem includes the compressor and expander units; excludes heat exchangers, motors, and controllers); status presented below is based on a 250°C flow inlet temperature to the expander

Characteristic	Status	DOE Technical Target
Flow Rate at 50 kW _e (g/s)		
Compressor	76	64-76
Expander	82	68-82
Peak Efficiency at 80% Flow Rate (%)		
Compressor	71	80
Expander	80	90
Pressure Ratio as a Function of Flow Rate	Below DOE Guidelines	1.3 @ 10% to 3.2 @ 100% flow
Net Shaft Power Required at Max. Flow (kW _e)	5.1 @ 85% flow, est. 7-8 at full flow	4.3
Subsystem Volume (L)	10 (includes motor)	4
Subsystem Weight (kg)	8.1 (includes motor)	3

Future Directions

- Complete power consumption evaluation.
- Complete layout design, incorporating components for optimal performance across the full fuel cell operating range.
- Complete analysis, design, fabrication, and testing of components for increased turbine inlet temperature.
- Perform a test study of performance vs. cost, using the compressor mapping results with the inlet guide vanes and vaneless diffuser, to determine if variable compressor and turbine geometry is viable.
- If the above trade study warrants, complete analysis, design, fabrication, and testing of turbocompressor with variable compressor and turbine geometry.
- With the turbocompressor, complete analysis, design, fabrication, and integrated testing of a vehicle-ready motor controller.

The objective of this work is to develop an air-pressurization system to pressurize a light-duty vehicle fuel cell system. The turbocompressor (Figure 1) is a motor-driven compressor/expander that pressurizes the fuel cell system and subsequently recovers energy from the high-pressure exhaust streams. Under contract to the U.S. Department of Energy, AlliedSignal has designed and developed a motor-driven compressor/expander and evaluated performance, weight, and cost projection data. Compared to positive displacement technology, the turbocompressor approach offers potential for high efficiency and low cost in a compact, lightweight package.

As shown in Figure 2, the turbocompressor consists of a compressor impeller, an expander/turbine wheel, and a motor magnet rotor incorporated on a common shaft; the system operates at a maximum design speed of 104 krpm on compliant foil air bearings. The air bearings are



Figure 1. Photograph of turbocompressor.

lubrication-free, in addition to being lightweight, compact, and self-sustaining; no pressurized air is required for operation. The turbocompressor works

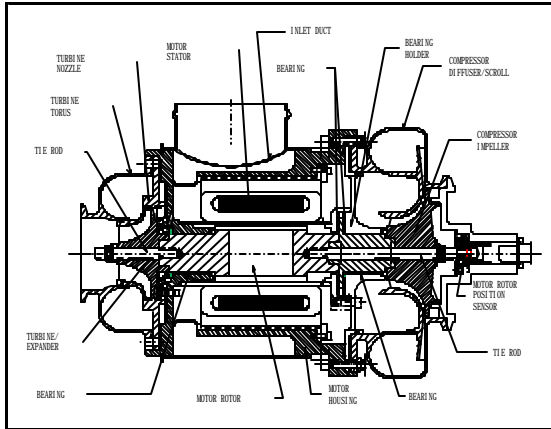


Figure 2. Turbocompressor details.

by drawing in ambient air through the motor/bearing cavities, where it is pressurized by the compressor, delivered to the fuel cell stack, and then expanded through the turbine to enhance the overall turbocompressor/fuel cell system efficiency.

The turbocompressor has operated for more than 200 hours at varying conditions, with and without motor operation. To date, the full design speed of 104 krpm has been reached with the motor.

Other work completed includes the analysis, design, fabrication, and testing of compressor inlet

guide vanes and a vaneless diffuser to widen the compressor operating range. The testing shows progress toward meeting the 1.6 pressure ratio at 2 lbm/min, in addition to a more constant pressure ratio and efficiency for a given corrected speed. Future work will include completion of the motor consumption measurements with the compressor low-flow components. A layout incorporating the compressor inlet guide vanes and vaneless diffuser and an increased-inlet-temperature turbine are also to be completed. From the layout, a detailed design of the increased-inlet-temperature turbine will be completed, fabricated, and tested.

Awarded in March 1999, the new program for a turbocompressor with variable geometry for PEM fuel cells includes four tasks. The first task is a trade study to define the optimal turbocompressor configuration, based on earlier work noted above. Next, the existing turbocompressor will be modified to the preferred configuration, as determined by the trade study. In the previous programs, an industrial controller was utilized. For a vehicle demonstration, a more compact, variable-speed controller will be developed. Testing of the optimal turbocompressor/motor controller also will be performed.

B. Development of a Scroll Compressor/Expander Module for Pressurization of 50-kW Automotive Fuel Cell Systems

Detlef Westphalen, Ronald Forni, William Murphy, and John Dieckmann

Arthur D. Little, Inc.

20 Acorn Park

Cambridge, MA 02140

(617) 498-5821, fax: (617) 498-7213, e-mail: Westphalen.D@ADLittle.com

John McCullough

Scroll Corporation

Carlisle, MA 01741-1553

(978) 287-4407

DOE Program Manager: Patrick Davis

(202) 586-8061, fax (202) 586-9811, e-mail: patrick.davis@ee.doe.gov

ANL Technical Advisor: Robert Sutton

(630) 252-4321, fax (630) 252-4176, e-mail: sutton@cmt.anl.gov

Contractor: Arthur D. Little, Cambridge, MA

Prime Contract No. DE-FC02-97EE50487

Objectives

Design, develop, and demonstrate a scroll compressor-expander module (CEM) suitable for pressurization and energy recovery for a 50-kW automotive fuel cell system.

OAAT R&D Plan: Task 13; Barrier D

Approach

- The second-generation design concept was developed through hardware testing of our first-generation CEM.
- To meet the flow requirements for 50-kW fuel cells, the second-generation design has increased displacement and higher speed with respect to the first-generation CEM.
- A second-generation prototype has been fabricated and is undergoing testing.
- As a final step in the development, the CEM will be integrated with a fuel cell system.

Accomplishments

- Designed and demonstrated first-generation CEM and double-ended compressor based on first-generation design.
- Demonstrated key design components of second-generation CEM:
 - Improved extended-life oil seals that involve no direct surface-to-surface contact
 - Two central drive design concepts that eliminate drive belts
 - Improved orbiting drive with rolling-element bearings for better orbiting scroll alignment.
- Second-generation CEM has been designed, fabricated, and successfully tested up to 80% of design flow.

Compressor/Expander Scroll Subsystem

(compressor/expander subsystem includes the compressor and expander units; excludes heat exchangers, motors, and controllers); status presented below is based on a 150°C flow inlet temperature to the expander

Characteristic	Status	DOE Technical Target
Flow Rate at 50 kW _e (g/s)		
Compressor	76	64-76
Expander	82	68-82
Peak Efficiency at 80% Flow Rate (%)		
Compressor	71	80
Expander	81	90
Pressure Ratio as a Function of Flow Rate	Exceeds DOE Guidelines	1.3 @ 10% to 3.2 @ 100% flow
Net Shaft Power Required at Max. Flow (kW _e)	5.2 (est.)	4.3
Subsystem Volume (L)	27	4
Subsystem Weight (kg)	36	3

Future Directions

- Demonstrate compressor-expander in a fuel cell system.
- Develop hybrid compressor technology for size/weight reduction while maintaining superior performance characteristics.

Phase I of the scroll compressor-expander module (CEM) development culminated in the successful demonstration of a scroll CEM capable of pressurization and energy recovery for a 28-kW fuel cell.

The first-generation prototype, shown in Figure 1, is powered through the orbiting drive, which transforms rotational motion to orbiting motion.

The compressor and expander are mounted on either side of the drive. Expander power is transferred to the compressor mechanically through

the drive. The orbiting drive is oil-lubricated; however, oil is prevented from being introduced into the compressor airflow by two sets of oil seals with vented intermediate space.

The first-generation prototype was tested at flow rates up to 42 g/s and compressor discharge pressures up to 32 psig, operating at a peak efficiency (taking drive losses and parasitic loads into consideration) of 70%. The expander peak efficiency was 80% (see Figure 2).

The main goals of the Phase II work are to:

- Increase flow rate.
- Improve integration of oil and cooling systems.
- Eliminate belt drive.
- Further demonstrate reliability.
- Integrate CEM with a fuel cell system.

The work included construction of a “back-to-back” (BTB) compressor based on the first-generation design: The expander side was replaced with a second compressor. The BTB unit was used for evaluation of individual CEM component efficiencies and durability testing. It has been operated without incident at flow rates up to 46 g/s and pressures up to 30 psig for a total of 130 hours.

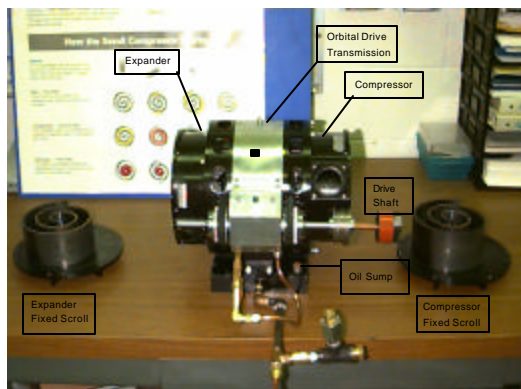


Figure 1. First-generation scroll compressor-expander module.

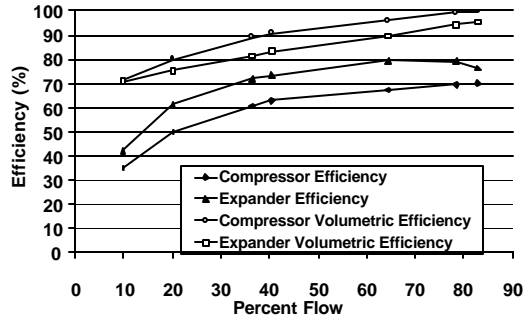


Figure 2. Compressor and expander efficiencies (Phase I).

In addition, the first prototype CEM was modified to demonstrate (1) integration of the oil pump into the orbiting drive and (2) a new orbiting oil-seal system that involves no surface-to-surface contact at the seal point. Both of these modifications to improve CEM reliability have been demonstrated successfully.

Extended reliability testing has been done to verify durability of the first-generation orbiting drive design. About 500 test hours have been accumulated without incident at machine speeds up to 3,450 rpm.

The second-generation CEM has been designed and fabricated, and testing of the machine is proceeding. The second-generation CEM is shown in Figure 3. Design changes, compared with the first generation, include:

- Larger displacement and higher speed in order to achieve 76-g/s flow, suitable for a 50-kW fuel cell.
- Improved thrust bearing to improve scroll alignment.
- Better integration of the oil pump and cooling fans.
- Central-drive design, rather than belt drive, to improve reliability, reduce parasitic losses, and reduce size.
- Additional orbiting drive design changes that will improve reliability and reduce drive losses.
- Magnesium alloy scrolls to reduce weight and reduce bearing loads.

Initial testing of the second-generation machine up to 80% of design flow is complete. This initial testing has verified the performance projections of Figures 4 and 5.



Figure 3. Second-generation scroll CEM.

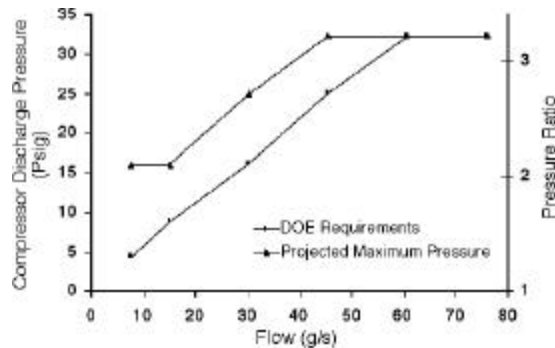


Figure 4. Second-generation scroll CEM operating envelope.

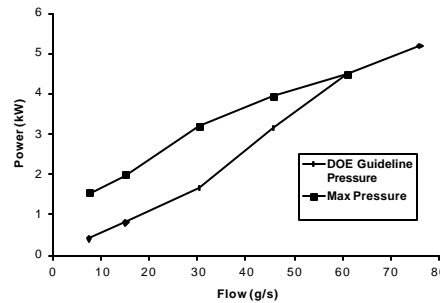


Figure 5. Second-generation scroll CEM projected shaft power.

Demonstration of the CEM integrated into a fuel cell system is currently in process. This work is being done with Energy Partners. The work will show the viability of the scroll compressor for automotive fuel cell applications and allow testing of system control issues.

The performance envelope of the second-generation scroll CEM is shown in Figure 4. The scroll technology allows for a wide flow range while maintaining system pressure level.

The efficiency of scroll technology for fuel cell pressurization is shown in Figure 5. The figure

shows shaft power projections for DOE Guideline pressures and for the projected maximum pressure curve of Figure 4. When operating according to DOE Guidelines, the scroll CEM uses a very modest amount of the net fuel cell stack power over the entire flow range.

C. Fuel Cell Power System - Critical Components for Transportation Development of Compact Air, Heat, and Water Management Systems: Variable Delivery Compressor/Expander Development

Jeremiah J. Cronin, Principal Investigator

VAIREX Corporation

Boulder, CO 80301

(303) 444-4556, fax: (303) 444-6150, e-mail: vairex@vairex.com

DOE Program Manager: Patrick Davis

(202) 586-8061, fax (202) 586-9811, e-mail: patrick.davis@ee.doe.gov

ANL Technical Advisor: Robert Sutton

(630) 252-4321, fax (630) 252-4176, e-mail: sutton@cmt.anl.gov

Contractor: VAIREX Corporation, Boulder, Colorado

Prime Contract No. DE-FCO2-98EE50481, December 1997-December 1999

Objectives

The primary objective is to develop a second-generation integrated compressor expander motor suitable for installation in 50-kW fuel cell vehicles.

- Expand, through research and development, the performance envelope of the variable delivery piston technology for use as a fuel cell air compressor and expander. Focus performance improvements in the areas of operating speed, compressor power consumption, and expander power recovery, as well as the volume and weight of both devices.
- Define development pathway for an application-specific integrated compressor expander motor (ICEM) that will satisfy cost, weight, and volume as well as performance goals for a fuel-cell-powered production vehicle.

OAAT R&D Plan: Task 13; Barrier D

Approach

The phased approach to the development of a satisfactory air system for use in an automotive environment is in its second phase. In the initial phase, the concept of independent control of pressure across a fuel cell power range was demonstrated. The hardware demonstrated the ability to select any pressure ratio at will, from 1.0 to 3.2. The 3.2 pressure ratio was also demonstrated over a 10:1 turndown in mass flow.

Moving beyond demonstration of variable-delivery piston machinery capability, this phase will:

- Compare alternative technology approaches (piston vs. screw) across a representative air delivery requirement for an automotive fuel cell. Use real device data as input to a hypothetical fuel cell stack and examine where differences occur.
- Compare each compressor’s characteristic efficiency behavior.
- Provide air systems in support of the FutureCar Program
- Design a Generation 2 variable-delivery compressor and expander. Build upon the results of testing and evaluation of the first-generation ICEM. Model and optimize the various sub-entities that are required for a successful Generation 2 air system.

Accomplishments

- Demonstrated approximately 30% more mass flow from approximately two-thirds the previous compressor’s volume.
- Demonstrated a 25-30% reduction in compressor power consumption from the previous-generation compressor for comparable pressure settings and mass deliveries.
- Designed a drive core that is common to both compressor and expander devices.
- Modeling of Generation 2 alternative designs has resulted in a reduction in both volume and dynamic mass by one-third, from the previous generation. It has also resulted in approximately 50% parts count reduction.
- Established (a) that both piston (zero clearance device) and screw compressors (clearance device) can have similar efficiencies, but in very different operating regimes, and (b) determined that the optimal application of either technology depends upon the duty cycle of the fuel cell as used in a vehicle.
- Demonstrated the ability of the Generation 1 piston compressor design to handle large amounts of liquid water, not just vapor.

Compressor/Expander Piston Subsystem

(compressor/expander subsystem includes the compressor and expander units; excludes heat exchangers, motors, and controllers); status presented below is based on a 250°C flow inlet temperature to the expander

Characteristic	Status	DOE Technical Target
Flow Rate at 50 kW _e (g/s)		
Compressor	76	64-76
Expander	82	68-82
Peak Efficiency at 80% Flow Rate (%)		
Compressor	70	80
Expander	50	90
Pressure Ratio as a Function of Flow Rate	Variable; can exceed DOE Guidelines	1.3 @ 10% to 3.2 @ 100% flow
Net Shaft Power Required at Max. Flow (kW _e)	5.4 (est.)	4.3
Subsystem Volume (L)	48-65	4
Subsystem Weight (kg)	27	3

Future Directions

- Demonstrate a compressor operating envelope that supports a 50-kW net fuel cell power system.
- Continue to reduce power consumption.
- Continue to reduce dynamic mass, inertia(s), overall component weights, and costs.
- Conduct testing of expander configuration and demonstrate energy-recovery strategies.
- Complete thermal analysis and identify areas for reduction of heat in the compressor and retention of heat in the expander.

- Determine pathway to manufacture, achieving technical targets within cost constraints acceptable to automotive industry.

The Generation 1 compressor/expander demonstrated that pressure ratios in excess of 3.5 could be generated in one stage. The Generation 2 compressor has successfully demonstrated the same performance, but it has done so at a consistent 25-30% lower power consumption.

Figure 1 shows the Generation 2 compressor's power consumption data to date for representative pressure ratios from 1.5 to 3.2. Figure 2 shows the projected power consumption of the Generation 2 ICEM while following the DOE guidelines for pressure and temperature at the respective mass flow.

Means to reduce friction in various parts of the system are being evaluated in this phase. Test fixtures (see Figure 3) have been fabricated and used extensively for examining parts and materials performances before incorporation into the individual assemblies.

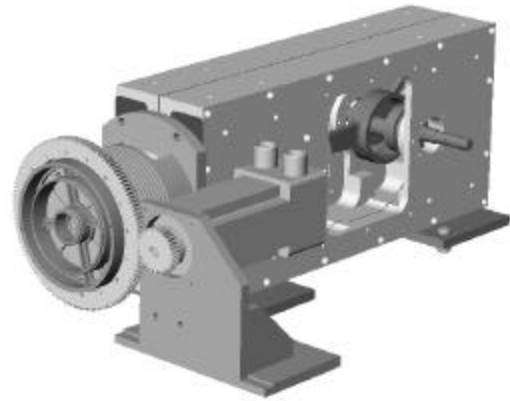


Figure 3. Test fixture.

With the use of advanced seal materials, the zero clearance piston devices are being operated without lubrication.

Modeling, testing, and design efforts on the Generation 2 ICEM have reduced the volume and mass of the compressor and expander hardware by one-third. Figure 4 shows the previous and current generations of compressors, for size comparison.

Development work on the expander has resulted in developing a unique valving configuration. A nationally renowned laboratory has tested it over a large range of Reynolds numbers prior to implementation. The results of this testing have provided a high degree of confidence in the projected expander performance.

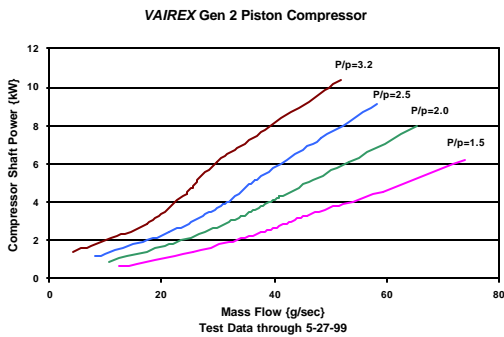


Figure 1. Power consumption data to date, Gen. 2 ICEM.

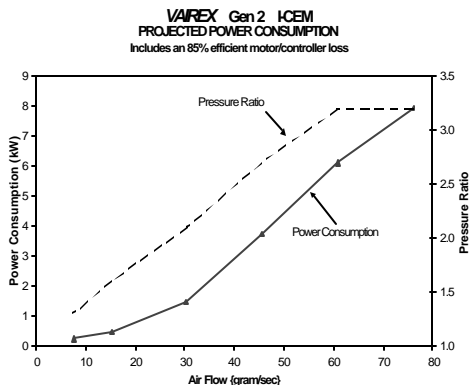


Figure 2. Projected power consumption.

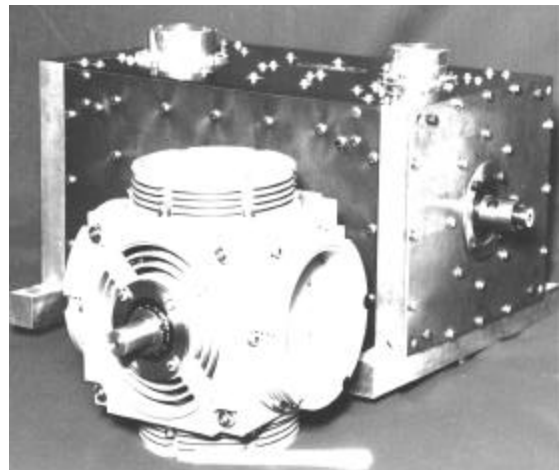


Figure 4. Compressor size comparison, new generation vs. old.

The study of zero clearance compressors vs. clearance compressors determined that the pressure ability of the VAIREX piston compressor device has the capability to provide higher pressure at low mass-flow rates. This would allow an appropriate match to automotive duty cycles, resulting in lower power consumption in the region where the automobile spends the majority of its time. Since the air system is parasitic to the fuel cell, this would be a significant advantage in vehicle power system architecture trades. Figure 5 compares the maximum pressure capability of the two different technologies when configured as a compressor/expander air system. The Federal Urban Driving Schedule (FUDS) indicates that U.S. automotive vehicles spend the vast majority of their life (70%+) below the 30% load level. The majority of their time is spent within the bracketed area shown in Figure 5.

To optimize vehicle fuel efficiency, the automotive fuel cell and all of its support hardware must maximize its collective performance in this same region while remaining able to achieve maximum performance when needed.

Evaluation of the two technologies, configured as an integrated compressor and expander air system, was performed to investigate power consumption differences for a hypothetical fuel cell. The pressure vs. mass flow of the twin screw with throttling (TSCE w/Throttle), indicated in Figure 6, was duplicated by the VAIREX piston compressor/expander. Using test data from this phase, the power consumption of both air systems, at the same mass flow and pressure, is expressed as a percentage of the hypothetical fuel cell's gross power output. For example, if the 30% output point of the fuel cell was 30 kW and one air system used 10 kW to operate at that powering level, that would represent a specific power consumption of 33%. If another air system required 20 kW to operate at that

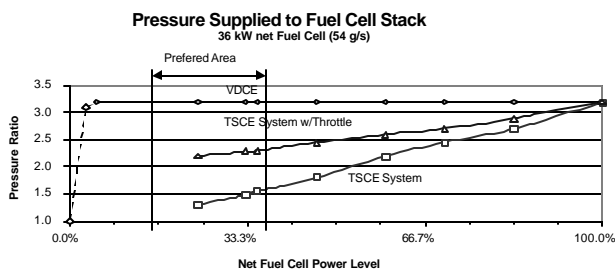


Figure 5. Pressure capability, twin screw vs. VAIREX piston.

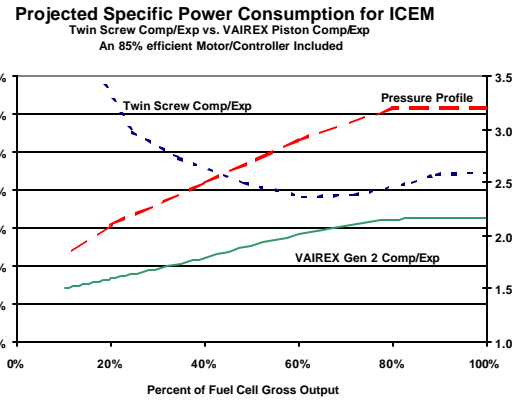


Figure 6. Power consumption, twin screw vs. VAIREX piston.

same point, it would have a specific power consumption of 66%. The piston approach is clearly appropriate in terms of power consumption for the predominant automotive cycles. (See Figure 6.)

Figure 7 shows the Generation 2 compressor component being tested and delivered at the end of this development phase. The manifold configuration shown in Figure 7, in addition to its normal functions of intake and exhaust of compressed air, also provides a shroud for highly effective forced cooling of the piston chambers. The expander configuration is exactly the same as the compressor's. Only the valving accommodating the variable-pressure control function will be different. Current efforts involve the implementation and testing of the expander valving system.



Figure 7. Compressor with manifolds.

The compressor and the expander will be integrated with an available drive motor, as shown in Figure 8, and tested in this phase.



Figure 8. Motor/compressor/expander integrated for testing.

References and Publications

1. Cronin, J. "Assessment Report – Twin-Screw Compressor vs. VDCE™," May 1998.
2. Cronin, J., and S. Milburn, "Relationship between Vehicle Duty Cycle and Air Systems," presented at the Fuel Cell Vehicle Technology Conference, The Institute of Transportation Studies, University of California, Davis. April 28-29, 1998.
3. Cronin, J. "Variable Displacement Compressor Development," Poster Presentation at the Automotive Technology Development Customers' Coordination Meeting. Oct. 27-30, 1997.

D. Electrically Boosted Gas-Bearing Turbocompressor for Fuel Cells

G. Fonda-Bonardi and P. Fonda-Bonardi

*Meruit, Inc., 1450 23rd St., Santa Monica, CA 90404-2902
(310) 453-3259, fax: (310) 828-5830, e-mail: fbarch@concentric.com*

Eric Sonnichsen

*Test Devices, Inc., 6 Loring St., Hudson, MA 01749
(978) 562-6017, fax: (978) 562-7939, e-mail: esonic@testdevices.com*

DOE Program Manager: Patrick Davis

(202) 586-8061, fax (202) 586-9811, e-mail: patrick.davis@ee.doe.gov

ANL Technical Advisor: Robert Sutton

(630) 252-4321, fax (630) 252-4176, e-mail: sutton@cmt.anl.gov

Contractor: Meruit, Inc., Santa Monica, CA 90404-2902

Prime Contract No. DE-FC02-97EE-50480, August, 1998-July, 1999

Subcontractor: Test Devices, Inc., Hudson, MA 01749

Objectives

- Develop and test a Rayleigh step gas-bearing set for small turbomachinery.
- Develop a 70-g/s PEM cell turbocompressor with an integral, high-speed electric motor to supply any required boost.

OAAT R&D Plan: Task 13; Barrier D

Approach

- Design and manufacture a gas-bearing test object modeling a turbocompressor.
- Test the gas-bearing test object according to established test protocol.
- Design the 70-g/s turbocompressor.
- Choose the matching high-speed electric boost motor and power supply.
- Manufacture and test the boosted turbocompressor test object.

Accomplishments

- Designed and fabricated the gas bearing test object; created the test protocol.
- Modeled bearing performance in static, steady-state, and transient conditions.
- Predicted performance to be extremely stiff with an idle stiffness of about 20,000 lb/in., strong damping of oscillations, and no harmful resonant frequencies.
- Statically tested gas bearings, verifying the predicted zero-speed stiffness of 2,500 lb/in.
- Designed an efficient compressor wheel with extended turndown ratio.

Future Directions

- Continue dynamic testing of the gas bearing.
- Continue turbocompressor design concurrently with the bearing testing program.

Introduction

To use the warm (~180°F), low-pressure (~30 psia) PEM cell exhaust flow to achieve a fuel cell air compression of ~45 psia requires very efficient bearings to support the rotor of a small, efficient turbocompressor. Accordingly, the PRDA DE-FC02-97EE-50480 PRDA contract has two major tasks: the first task is to build and test an experimental gas thrust bearing designed to represent the bearing in a turbocompressor for the DOE standard 50-kW automotive fuel cell; if, and only if, the proposed thrust bearing performs as expected, the second task is to design, build, and test a complete turbocompressor for 50-kW fuel cell service, including a built-in electric motor for makeup power (if needed) and presumably for startup.

Meruit proposes to use proprietary radial (journal) and thrust gas bearings that would use less than 1% of the compressor mass flow for lubrication and cooling. Meruit has modeled the gas bearing's performance under static, steady-state, and transient conditions; designed and built a bearing test object; and statically tested the bearings. Dynamic testing will proceed in August and September of 1999; here, we present some of the computed findings.

Technical Progress and Accomplishments to Date

Meruit, Inc. has completed the following subtasks as part of Task 1:

1. Preliminary design of a turbocompressor suitable for the DOE 50-kW target fuel cell; the bearing test object simulates the size, mass, and moments of inertia of the shaft, bearings, turbine and compressor wheels, and integral electric motor (collectively, the “rotor”).
2. Determination of the parameters relevant to the design of the test article, which are:

Maximum speed:	85,000 rpm
Idle speed:	55,000 rpm
Radial bearing	
Diameter:	20.73 mm (0.8165 in.)
Rubbing speed:	121.5 m/s (398 ft/s)
Thrust bearing	
Diameter:	62.25 mm (2.451 in.)
Tip speed:	277.1 m/s (909 ft/s)
Rotor weight:	1,115 g (2.45 lb)

3. Modeling bearing performance: The computation of the expected thrust bearing stiffness at several running speeds is shown in Figure 1. As the rotor moves in its clearance, the thrust bearing creates a restoring force toward the center of its clearance, which in the case of the small turbocompressor designed here is on the order of 0.001 inches per side. Because the air pressure expected from the compressor varies with speed, the bearing's stiffness also varies: it is stiffer at higher air pressures (i.e., at higher speeds). In Figure 1, expected force and stiffness developed by the gas bearing in the test object at different speeds are shown. The X-axis represents displacement Z from dead center as a proportion of the clearance B2; for example, when the rotor has traveled to 90% of the available clearance, the restoring force generated by the gas bearing is about 21 lb at 55,000 rpm (turbo idle) and 48 lb at 85,000 rpm (full speed).

The predicted forces and displacement allows for calculation of a spring constant, or stiffness: it turns out that air in the recesses of the Meruit gas bearing is quite stiff, with a k-factor of about 2,500 lb/in. at zero speed, at least 18,000 lb/in. of displacement at idle, and 41,000 lb/in. at full speed. Since the rotor is expected to weigh about 2.45 lb, the gas bearing should be stiff enough to support the rotor in normal automotive service.

When "floating" in the gas bearing, the rotor may be thought of as a mass suspended on very stiff springs, and it may be subject to resonance frequency effects that might make the bearing unstable in a critical speed range or when subjected to transient accelerations. Although Meruit predicts that the proposed gas bearing will strongly damp any reasonable vibration, collisions must be considered.

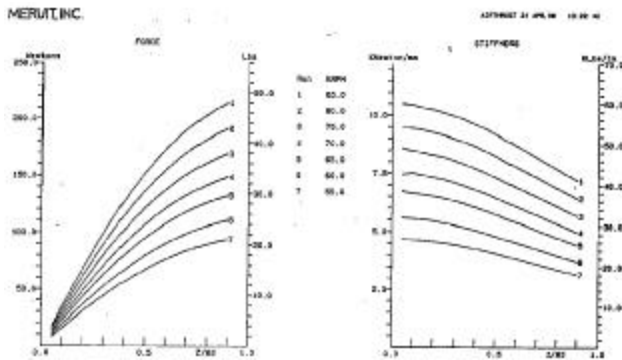


Figure 1. Computed thrust bearing stiffness.

Figure 2 shows a typical response of the suspended mass to a sudden deceleration of the housing from a collision speed of 5 mph to zero in a distance of 0.5 ft (corresponding to the crumpling of the bumper and perhaps some sheet metal) for various rotating speeds of the turbocompressor (resulting in various values of the stiffness). The deceleration is assumed to occur with a sine-like variation, as shown on the lower curve. The top curve shows the displacement of the mass from the center of the stroke toward contact with the thrust bearing face, where the displacement is initial clearance B2. A collision of this strength will not cause contact for all speeds above 30% of the design speed of 85,000 rpm (i.e., never, if the idling speed of the turbocompressor is higher than this). The curves are spaced by intervals of approximately 10% of maximum stiffness, which is not linear with displacement or rotating speed.

If contact occurs, the natural frequency of the spring-mass system is excited, causing oscillations after contact is released; the oscillations decay with a characteristic damping coefficient. We have not yet investigated the details of the release of contact, which depends on the characteristics of the contacting surfaces; an experiment recommends itself.

4. Modeling turbocompressor rotor dynamics: In the steady-state case, the natural frequency for small amplitudes is $\omega_n = \sqrt{k / m}$ (see Table 1), where rpm and ω_n are converted into comparable units of frequency (Hertz): $f = \text{RPM}/60$, and $f_n = \omega_n / 2\pi$, and $r = f / f_n$.

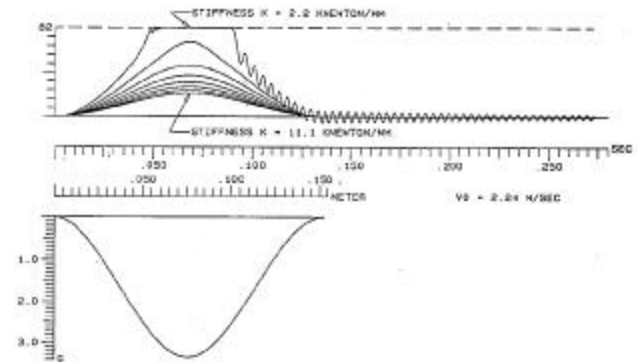


Figure 2. Computed response to 5-mph collision.

Table 1. Turbocompressor rotor dynamics.

rpm	f	fn	r
85,000	1416.67	412.92	3.43
80,000	1333.33	392.42	3.39
75,000	1250.00	371.94	3.36
70,000	1166.67	350.22	3.33
65,000	1083.00	329.05	3.29
60,000	1000.00	302.03	3.32
55,000	916.67	275.64	3.33

The ratio r is large and almost constant, meaning that if the housing is made to vibrate in the axial direction with amplitude Z , the rotor will respond synchronously with the spin with an amplitude of approximately $1.1 Z$, and the relative displacement will be approximately $0.1 Z$. It is exceedingly unlikely that the spinning rotor could ever induce an axial vibration of the housing of any amplitude comparable with $B2$; therefore, the steady-state response appears to be entirely satisfactory. It is equally unlikely that any external excitation of the housing by vehicle (e.g., engine) vibrations and associated harmonics would have components near the natural frequency f_n . Hence, all natural frequencies appear to be far from the corresponding running speed, so that no resonances are expected.

5. Designed and fabricated the bearing test object.
6. Defined the test protocol for the measurement of static and dynamic characteristics of the test article.
7. Tested the bearing statically, finding the predicted zero-speed stiffness.
8. Designed an efficient compressor wheel with the desired pressure ratio and extended turndown performance.

Future Activities

Meruit will:

1. Continue dynamic testing of the gas bearing.
2. Continue modeling compressor and turbine wheels to find a matched set for the best overall performance.
3. Build and test (when bearing wheel performance issues are settled) the turbocompressor test object. For further information, please refer to the cited references.

References

1. G. Fonda-Bonardi, "Gas Bearing for High-Speed Turbomachinery," paper presented at the July 1999 ASME Fluids Engineering Conference, San Francisco, Calif. (FEDSM99-7327).
2. G. Fonda-Bonardi, "Meruit Turbocompressor PRDA: Gas Bearing Experimental Results," DOE PRDA FC02-97EE-50480, June 20, 1999.
3. G. Fonda-Bonardi, "Meruit Turbocompressor PRDA: Turbocompressor Design and Test," DOE PRDA FC02-97EE-50480, June 2, 1999.
4. G. Fonda-Bonardi, "Gas Bearing for High-Speed Turbomachinery," paper presented at the July 1998 ASME Fluids Engineering Conference, Washington, D.C. (FEDSM98-5120).
5. G. Fonda-Bonardi, "Meruit Turbocompressor PRDA: 1998 Program Review," DOE PRDA FC02-97EE-50480, June 20, 1998 (includes Apps. A, B, and C).

VII. HYDROGEN STORAGE¹

A. High-Pressure Conformable Hydrogen Storage for Fuel Cell Vehicles

Richard Kunz (Primary Contact) and Andy Haaland

Thiokol Propulsion

P.O. Box 707, M/S 254

Brigham City, UT 84302-0707

(435) 863-8799, fax: (435) 863-6223, e-mail: kunzrk@thiokol.com

DOE Program Managers: Sigmund Gronich and JoAnn Milliken

(202) 586-1623, fax: (202) 586-5127, e-mail: sigmund.gronich@hq.doe.gov

(202) 586-2480, fax: (202) 586-9811, e-mail: joann.milliken@ee.doe.gov

ANL Technical Advisor: Walter Podolski

(630) 252-7558, fax: (630) 252-4176, e-mail: podolski@cmt.anl.gov

Contractor: Thiokol Propulsion, Brigham City, Utah

Prime Contract No. DE-FC02-97EE-50484, September 30, 1997-March 31, 2000

Subcontractors: Aero Tec Laboratories, Ramsey, NJ, and Southern Research Institute, Birmingham, AL

Objective

Develop and demonstrate key enabling technologies for on-board conformable high-pressure hydrogen storage for fuel-cell-powered light vehicles.

OAAT R&D Plan: Task 1; Barrier I

Approach

Phase I: Component Development and Integration

- Composite structural capability development
 - Demonstrate required pressure capability of conformable tanks for high-pressure hydrogen storage
 - Optimize design, materials, and processes to enhance structural efficiency
- Liner technology development
 - Develop materials and processing capability for plastic liners for conformable hydrogen tank
 - Design and fabricate liners for integration and testing
- Integration and testing
 - Integrate liner and composite technology development through fabrication of plastic-lined, composite overwrapped conformable prototype tanks
 - Perform burst and permeation testing

Phase II: Safety and Durability Testing

- Fabricate 12 full-scale conformable hydrogen tanks
- Perform qualification safety testing

¹ The Hydrogen Storage System Development projects are co-funded by the DOE Office of Transportation Technologies and the Office of Power Technologies Hydrogen Program.

Accomplishments

- Completed liner process development and fabricated full-scale conformable liners for tank fabrication
- Fabricated full-scale tanks on plastic liners and validated tank structural capability through hydroburst testing
- Performed liner material permeation testing at high and low temperature and under biaxial strain
- Performed mechanical property testing of candidate liner materials to determine processability and estimate cycle life capability
- Identified and tested additional candidate liner materials
- Fabricated subscale and full-scale tanks with candidate liner materials to verify processability and burst/cycle performance
- Initiated subscale and full-scale tank cycle testing and integrated leak testing

Future Directions

- Down-select to one baseline liner material and one backup liner material
- Fabricate twelve full-scale tanks and perform Phase II qualification safety testing.

Introduction

Several challenging technical issues confront on-board high-pressure hydrogen storage for fuel cell powered vehicles. Because the energy density of hydrogen is significantly less than that of conventional fuels, larger tanks are required for equivalent range. Furthermore, because the geometry of traditional high-pressure cylinders generally does not conform to the available space on the vehicle, packaging issues arise. Tank cost and weight also significantly influence the amount of fuel that can be carried.

Thiokol is addressing these issues through the development of high-pressure conformable tanks for on-board hydrogen storage. The lightest-weight approach uses high-strength filament-wound carbon fiber composite for structural efficiency, with plastic liners to act as permeation barriers. Thiokol’s conformable storage concept (Figure 1) uses multiple cells, the number and shape of the cells being tailored to maximize internal volume within a rectangular envelope while maintaining membrane loading for structural efficiency. Each cell is filament-wound with a combination of hoop and helical layers, followed by a hoop overwrap over the assemblage of cells. Depending on the shape of the envelope, up to 50% more storage is possible with a conformable tank than with cylinders.

The tanks are designed for a service pressure of 5,000 psi with a burst safety factor of 2.25, consistent with existing standards for high-pressure

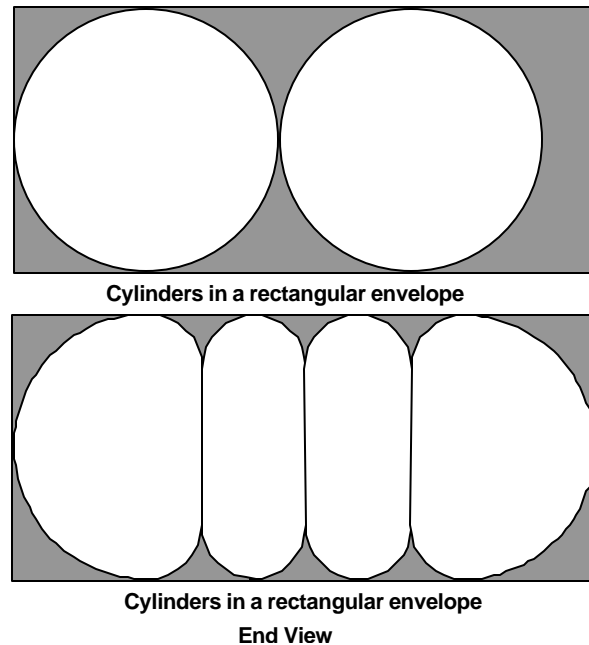


Figure 1. Thiokol’s conformable storage concept.

vehicle fuel tanks. The full-scale tank under development is a two-cell configuration that fits in an envelope 12.8 in. x 21.2 in. x 27.9 in. The tank has a water volume of 17.9 gal and a capacity of 3.4 lb of hydrogen at a nominal service pressure of 5,000 psi. The conformable tank provides 23% more capacity than would two cylinders in the same-volume envelope. An optional third cell would increase the tank width to 29.6 in. and the capacity to 4.8 lb of hydrogen. Tank envelopes were defined

in cooperation with Ford Motor Co. and Directed Technologies, Inc., and are consistent with space constraints on Ford's P2000 fuel cell vehicle.

Structural Capability Development

Successful structural tests of subscale prototype tanks during FY 1998 led to design, fabrication, and testing of full-scale tanks during the current fiscal year. The plastic liners for the full-scale tanks (Figure 2) were designed by Thiokol and fabricated by Aero Tec Laboratories (ATL) by using the rotational molding process. Cross-linked polyethylene (XLPE) was used for the initial liners. Fabrication process development was performed to optimize filament winding on the non-cylindrical plastic liners. Winding patterns and tow tensions were determined to minimize fiber slippage at the dome transitions, ensuring adequate load transfer.



Figure 2. Full-scale plastic liner with aluminum polar boss.

The tanks were designed for a minimum burst pressure of 11,250 psi, consistent with a 5,000-psi service pressure and a 2.25 burst factor, based on finite element analysis of the tank configuration. Two tanks were filament-wound using Toray's M30S carbon fiber with Thiokol's TCR® prepreg resin system (Figure 3). Both tanks were hydroburst-tested; they burst at 11,600 psi and 12,150 psi, respectively. Structural failure initiated in the hoop overwrap and cell sidewalls (Figure 4), consistent with the designed failure mode.

A third tank was fabricated to the same composite design, using liners composed of Kynar Flex, a PVDF polymer formulated for rotational



Figure 3. Full-scale conformable tank.

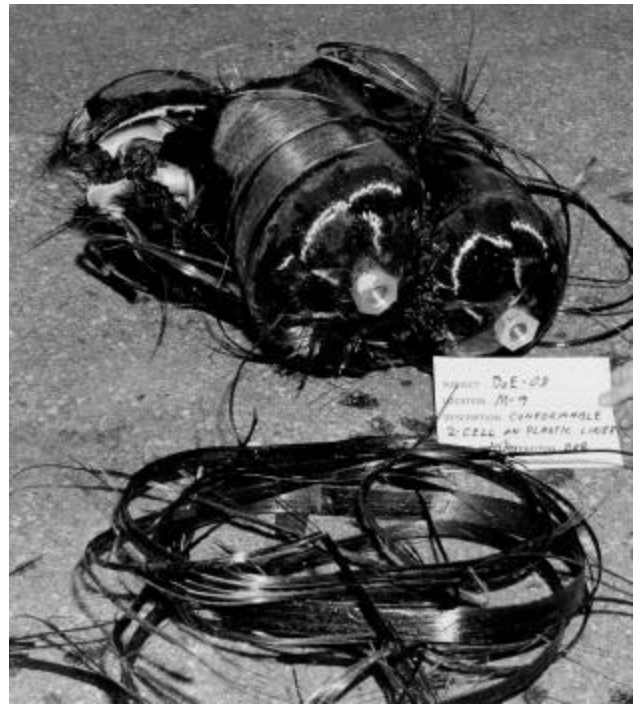


Figure 4. Full-scale conformable tank following hydroburst test.

molding. This tank, which was hydroburst at a pressure of 13,725 psi, also exhibited the desired hoop failure mode.

The above-described testing validates the capability of the conformable tanks to meet the pressure requirements for hydrogen storage. Refinements to the design and fabrication of the full-scale tanks are being developed to improve overall carbon fiber structural performance. Advanced analytical techniques are under development to more accurately predict structural response to pressure

loading. This will lead to the ability to optimize the tank structure within the constraints imposed by the filament-winding process.

Liner Material Selection

Current tank development efforts are focused on material and processing issues relevant to the development of plastic liners. The liner serves as a permeation barrier to the stored hydrogen, as well as a mandrel for filament-winding the load-carrying composite overwrap. Rotational molding was selected as the processing method for prototyping and low-volume liner production. ATL initially conducted an extensive liner material assessment, considering key properties of permeability, processability, density, mechanical properties, material compatibility, and cost of 35 polymer formulations. Based on this evaluation and on preliminary data, three polymer classes – XLPE, nylons, and PVDF – were chosen for further screening.

Because hydrogen permeation is a key selection criterion for the liner material, Southern Research Institute (SRI) developed a unique permeation test fixture for this program. The setup can test permeability of sample coupons to a pressure differential of 5,000 psi at ambient, high, and low temperatures, as well as under biaxial strain. Initial permeability screening tested unstrained, rotationally molded coupons at ambient temperature for XLPE, Nylon, and PVDF (Figure 5). A permeability value of 10^{-14} mol/(m·s·Pa) is estimated to provide a tank half-life of 6 months for a 0.15-in.-thick liner.

Permeation testing at high and low temperatures and under biaxial strain has been performed on Nylon-6 at SRI to evaluate the effects of in-service conditions on permeation. At 180°F, the permeability increased by approximately one order of magnitude above ambient; at -40°F, permeability declined by one order of magnitude. No measurable influence was observed with the specimen under 1% biaxial strain, which is representative of strain conditions at service pressure. A full-scale conformable tank with an XLPE liner is now undergoing integrated leak testing to determine the correlation with coupon permeability data.

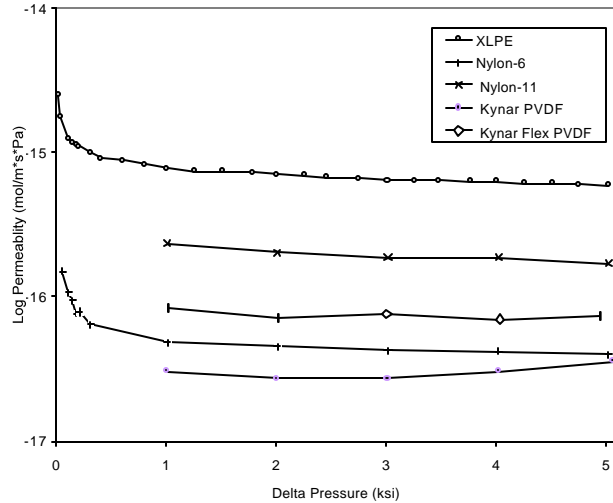


Figure 5. Hydrogen permeability of candidate polymers at ambient temperature.

The liner also largely limits tank cycle life. Fatigue failures are generally characterized by leakage at a liner through-crack. Mechanical property testing of rotationally molded coupons for candidate liner materials is ongoing to estimate tank cycle life. Tensile data collected over a range of strain rates are used in a viscoelastic cumulative damage model.¹ Tank finite element analysis results are then used with the damage model to estimate liner cycle life (Figure 6). This approach has been

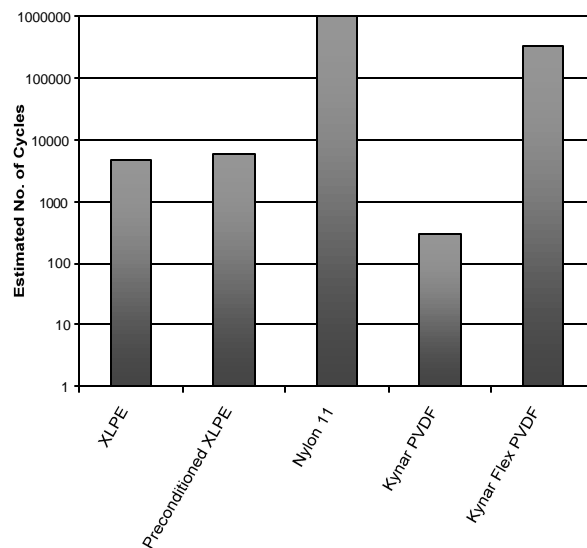


Figure 6. Cycle life estimates for various liner materials.

effective in screening candidate liner materials and in identifying the material property parameters that most influence cycle life. Subsequent pressure cycle testing of both cylindrical and conformable tanks has demonstrated excellent correlation with model predictions.

Liner Evaluation

Coincident with material screening via permeation and mechanical property testing, liner evaluation has been conducted by fabrication and testing of both subscale cylindrical and full-scale conformable tanks with candidate liner materials. Tanks fabricated using both Nylon-6 and Kynar developed liner cracks at low pressure following composite cure. The Nylon-6 liners exhibited brittle-type behavior and a large degree of porosity. The Kynar liners were apparently degraded by the composite cure cycle.

XLPE-lined tanks have performed well in both burst and cycle testing. It was found that the mechanical properties and cycle life behavior of XLPE liners could be improved by preconditioning to the composite cure temperature prior to tank fabrication (see Figure 6). The Kynar flex tanks have also performed very well in both burst and cycle testing. Evaluation of Nylon-12 as a potential liner material is still in progress.

Future Plans

On the basis of analysis and testing to date, XLPE, Kynar Flex, and Nylon-12 remain potential candidates for liner materials. Further evaluation of these materials will lead to the selection of one baseline and one backup to carry into Phase II qualification testing. Because of the lack of a current industry standard for safety, durability, and

performance testing of hydrogen tankage for fuel cell vehicles, qualification tests will be based on the current NGV2² standard for natural gas vehicles. Performed using full-scale two-cell conformable tanks, the tests will include burst, pressure cycling, environmental cycling, flaw tolerance, drop impact, accelerated stress rupture, and bullet impact.

Previous test results on both subscale cylinders and full-scale conformable tanks will be used to guide the material selection and design of tanks for qualification testing. In supporting programs, conformable tanks have been successfully tested to the NGV2 standard for burst; pressure cycling at ambient, high, and low temperature; and flaw tolerance. Drop impact testing has revealed the need for additional damage protection because of the inherent sensitivity of carbon fiber composites to impact damage. An external foam protection system is currently under development and will be incorporated into the design.

Publications/References

1. K.L. Laheru, "Development of a Generalized Failure Criterion for Viscoelastic Materials," *J. of Propulsion and Power*, AIAA, Vol. 8, No. 4, July/August 1992.
2. "Basic Requirements for Compressed Natural Gas Vehicle (NGV) Fuel Containers," American National Standard ANSI/IAS NGV2-1998.
3. R.K. Kunz, R.P. Golde, and B.M. McQuivey, "High Pressure Conformable Hydrogen Storage for Fuel Cell Vehicles," *Proceedings, 10th Annual U.S. Hydrogen Meeting and Exhibition*, Vienna, Va., April 7-9, 1999, sponsored by National Hydrogen Association.
4. R.P. Golde, R.K. Kunz, and M.J. Warner, "The Shape of Things to Come," *SAMPE Journal*, March/April 1999.

B. Advanced Chemical Hydride Hydrogen Generation/Storage System for PEM Fuel Cell Vehicles

Dr. Ronald W. Breault, Christopher A. Larsen, Jonathan Rolfe, and Andrew W. McClaine

Thermo Power Corporation

45 First Avenue

Waltham, MA 02454-9046

(781) 622-1046, fax: (781) 622-1025, e-mail: rbreault@tecogen.com

DOE Program Managers: Sigmund Gronich and JoAnn Milliken

(202) 586-1623, fax: (202) 586-5127, e-mail: sigmund.gronich@hq.doe.gov

(202) 586-2480, fax: (202) 586-9811, e-mail: joann.milliken@ee.doe.gov

ANL Technical Advisor: Walt Podolski

(630) 252-7558, fax: (630) 972-4430, e-mail: podolski@cmt.anl.gov

Contractor: Thermo Power Corporation, Tecogen Division, Waltham, MA

Prime Contract No. DE-FC02-97EE50483, October 1997-April 2000

Objectives

The objective of this program is to develop a prototype, 50-kW electric power equivalent hydrogen supply system utilizing an innovative chemical hydride/organic slurry technology. The system goals are to construct a hydrogen storage system with a gravimetric power density of greater than 3355 W·h/kg and a volumetric power density of greater than 929 W·h/L.

OAAT R&D Plan: Task 1; Barrier I

Approach

The program covers a 30-month period that comprises two phases. During the first 15-month phase, Thermo Power optimized the hydrogen generation efficiency of the proposed process, utilizing a laboratory-scale reactor unit (1-kW equivalent). In the second phase, Thermo Power will be fabricating and evaluating the performance of a prototype hydrogen supply system for 50-kW fuel cell systems. The approach we are following to accomplish the objectives of this program is to:

- Investigate and select metal hydride and organic slurry materials to achieve maximum specific energy.
- Optimize the hydride/organic selection for minimum weight and high stability.
- Develop a system for quick, complete activation of the hydride with minimum weight.
- Establish a thermal management design for a prototype system, including heat dissipation and use.
- Design and fabricate a 50-kW-equivalent prototype system.
- Evaluate and optimize performance of the prototype system.
- Complete hydrogen supply system integration into simulated power sources and performance evaluation.

Accomplishments

The accomplishments of this program during its first year, beginning in October 1997, are as follows:

- Evaluated a wide selection of chemical hydrides and oils to use as slurries.

- Selected lithium hydride for the chemical hydride and a light mineral oil as the slurry liquid. With the use of some carefully selected dispersants, Thermo Power developed a procedure to form a slurry of the mixture. The slurry is transportable and stable, and it protects the chemical hydride from accidental or incidental contact with moisture in the air.
- Developed a hydrogen generation system that produces hydrogen from the chemical hydride slurry and water. The generator is reliable, controllable, and capable of supplying hydrogen under moderate pressures. It produces hydrogen on demand and can be scaled to larger sizes as required.

During the second year of the program, through June 1999, Thermo Power has:

- Completed the design of a thermal management system to handle the heat released during the reaction between the chemical hydride and water.
- Completed the design and fabrication of a prototype 50-kW electric-power-equivalent hydrogen generator.

Future Directions

The balance of Year 2 will see the production and testing of the prototype reactor. The system will provide actual operating experience and an in-depth understanding of the realistic and practical application of the technology, as well as revealing areas that require further efforts in design, selection of materials, and process control. Work will be done to optimize the system and to improve subsystems requiring additional attention. The design will be specifically for a PEM fuel cell application.

Introduction

To supply high-purity hydrogen for fuel-cell-powered vehicles, Thermo Power Corporation is working on the use of a chemical hydride/organic slurry as the hydrogen carrier and storage medium. At the point of use within the vehicle, high-purity hydrogen will be produced by reacting the hydride slurry with water. The chemical hydride slurry approach for hydrogen storage is attractive because:

- The organic slurry system can moderate the reaction rate of the hydrolysis process, minimizing the possibility of runaway reactions such as had occurred in other efforts. In the event of a spill, the reaction of the chemical hydrides with environmental moisture would result in slow release of hydrogen. This would be a hazard comparable with a spill of liquid hydrocarbons for today's vehicles.
- The pumpable organic slurry can be accurately metered, depending on hydrogen demand, pressure, and temperature, to provide safety and reaction control not otherwise possible.
- The use of a simple low-pressure chemical hydride slurry storage system provides volumetric densities approaching that of cryogenic hydrogen storage.

During the past nine months, the program has focused on the issues of (1) developing a thermal management design and (2) designing and fabricating a prototype 50-kW_e equivalent hydrogen generator.

Thermal Management

During the hydrolysis reaction, heat evolves that is equivalent to 37% of the energy contained in the hydrogen stream. Thus, when the reactor is working at its full 50-kW electrical output, it evolves 37 kW of heat. Unfortunately, because of the mineral oil in the slurry, the temperature of this heat energy must be limited to near 100°C to prevent damage to the mineral oil and contamination of the hydrogen product. Disposing of this heat is a difficult problem given the size and weight restrictions for the system. Care must be taken to create a small, lightweight heat exchanger for the system.

In accomplishing this task, Thermo Power evaluated four systems:

1. The direct heat-exchange system considers heat exchange from the reactants through the reactor wall to a water jacket surrounding the heat exchanger. This first design weighs too much, and it is bulky.
2. The water-bathed reactor directly mixes the reactants with the cooling water. The advantage

of this system is that heat is not transferred through a fixed surface, reducing the weight of the heat-exchange system. Unfortunately, the cooling water cannot be separated from the waste products with a reasonable weight or volume.

3. The auger-aided, water-vaporizing reactor accomplishes the cooling water/ waste product separation thermally. Excess water is injected into the reaction zone to be vaporized by the heat of reaction. The water is then condensed in water-vapor-to-air heat exchangers. This system works, but the heat-exchanger size is a bit larger than desired. The design of the 50-kW reactor will be based on this design (see Figure 1).
4. The packed-bed vapor-condensing design focuses on the condensation of water vapor. It uses a dense packed bed to extract heat and water from the hydrogen stream. The packed bed is cooled by water pumped through a water-to-air heat exchanger. This system may have some benefits, but it is expected to weigh more than the third design with direct vapor-to-air heat exchangers.

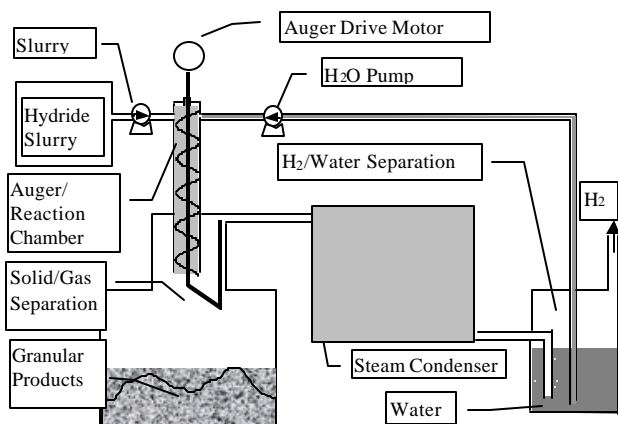


Figure 1. Auger-aided water-vaporization heat-transfer system

Design and Fabricate Prototype System

The goal of Task 5 is to design and fabricate a high-purity 50-kWe H₂ system capable of operating for 15 min at 50 kWe (3 kg H₂/hr). From the results of the previous tasks, Thermo Power has selected the mixed reactor, water-vaporizing reaction system for its simplicity and ability to satisfy weight and volume goals of 3350 W·h/kg and 930 W·h/L. This

design evaporates water to absorb the heat of reaction. During operation, pumps meter slurry and water into the reaction zone. An auger continually clears the injection zone and mixes the two reactants to ensure a quick, complete reaction. A short paddle section of the auger ensures an adequate residence time in the reactor, allowing heat to transfer from the hot products to the excess water used for cooling. The dry products of the reaction are pushed into a hydroxide storage tank. Hydrogen and water vapor produced by the reaction are cooled in the vapor-to-air heat exchanger. This exchanger condenses the water vapor and returns it to the water tank. The product hydrogen stream is filtered and dried before use in a fuel cell. Figure 2 is a picture of the completed hydrogen generator.



Figure 2. 50-kWe hydrogen generation system.

The system mass and volumetric design summary are provided in Table 1. The pilot system is compared with the design system. The differences between the pilot and the ultimate design are caused by the need to design for additional safety for the prototype system.

Table 1. System design summary.

	Ultimate Design		Pilot Design	
	Wt.	Vol.	Wt.	Vol.
	(kg)	(L)	(kg)	(L)
Hydride	103	76	103	76
Hardware	76.5	374.2	141.5	379.2
	W·h/k g	W·h/ L	W·h/k g	W·h/ L
Value	3362	1341	2468	1326
Goal	3355	929	3355	929

Publications/References

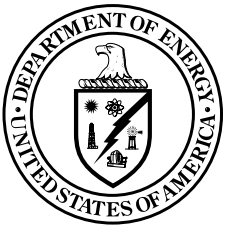
1. R.W. Breault, J. Rolfe, and A. McClaine, "Hydrogen Transmission/ Storage with a Chemical Hydride/ Organic Slurry," 9th Canadian Hydrogen Conference, Vancouver, B.C., Feb. 7-10, 1999.
2. R.W. Breault, J. Rolfe, and A. McClaine, "Hydrogen for the Hydrogen Economy," 24th Coal Utilization and Fuel Systems Conference, Clearwater, Fla., March 8-11, 1999.
3. R.W. Breault and J. Rolfe, "Chemical Hydride Hydrogen Storage Canisters for DOD Fuel Cell Applications," 10th National Hydrogen Association Conference, Tysons Corner, Va., April 7-9, 1999.
4. R.W. Breault, C. Larson, and J. Rolfe, "Hydrogen for a PEM Fuel Cell Vehicle Using a Chemical-Hydride Slurry," 10th National Hydrogen Association Conference, Tysons Corner, Va., April

APPENDIX A: ACRONYMS, INITIALISMS, AND ABBREVIATIONS

ADL	Arthur D. Little, Inc.
AIAA	American Institute of Aeronautics and Astronautics
ANL	Argonne National Laboratory
ANSI	American National Standards Institute
APOR	Argonne Partial Oxidation Reformer
ASR	area specific resistance
ASTM	American Society for Testing and Materials
ATL	Aero Tec Laboratories
ATR	autothermal reformer
BNL	Brookhaven National Laboratory
BOP	balance-of-plant
BTB	back-to-back
CARB	California Air Resources Board
CCM	catalyst-coated membrane
CEM	continuous emission monitor or compressor expander module
CNG	compressed natural gas
CO	carbon monoxide
CSA	Cell Stack Assembly
DARPA	Defense Advanced Research Projects Agency
DCC	diffuser current collector
DI	deionized
DMFC	direct methanol fuel cell
DOE	U.S. Department of Energy
ELAT™	solid polymer electrolyte electrode
FC	fuel cell
F ³ P	fuel-flexible, fuel-processing or fuel-flexible, fuel-processor
FPS	fuel processing system
FUDS	Federal Urban Driving Schedule
FY	Fiscal Year
GC	gas chromatographic or gas chromatography
GC/MS	gas chromatography/mass spectroscopy
GDE	gas diffusion electrode
GDL	gas diffusion layer
GHSV	gas hourly space velocity
GTR	gas transmission rate, gas permeability
H ₂	hydrogen
HAZOP	hazardous operations
HBT	Hydrogen Burner Technology
HLTS	humidified low-temperature shift
HTS	high-temperature water-gas shift reactor or high-temperature shift
HTSPEM	high-temperature solid polymer electrolyte membrane
IAS	International Approval Services
ICE	internal combustion engine
ICEM	integrated compressor expander motor
ICP	ion-conducting polymer
IEC	ion exchange capacity

IFC	International Fuel Cells
IGT	Institute of Gas Technology
IPN	interpenetrating network
LANL	Los Alamos National Laboratory
LHV	lower heating value or low heat value
LMTD	log-mean temperature difference
LTS	low-temperature water-gas shift reactor or low-temperature shift
LTSC	low-temperature shift converter
M-85	85% methanol and 15% gasoline
MEA	membrane electrode assembly or membrane/electrode assembly
MPR	Modular Pressurized Flow Reactor
MTBE	methyl tertiary butyl ether
NEMCA	non-Faradaic Electrochemical Modification of Catalytic Activity
NG	natural gas
NGV	natural gas vehicle
NMOG	nonmethane organic gas(es)
NMR	nuclear magnetic resonance
NO _x	oxides of nitrogen
NREL	National Renewable Energy Laboratory
OAAT	Office of Advanced Automotive Technologies (DOE)
ORR	oxygen reduction reaction
PBO	poly-p-phenylene benzobisoxazole
PC	personal computer
PECMFC	proton exchange ceramic membrane fuel cell
PEFC	polymer electrolyte fuel cell
PEM	polymer electrolyte membrane or proton exchange membrane
PEMFC	PEM fuel cell
PIII	plasma immersion ion-implantation
PNGV	Partnership for a New Generation of Vehicles
PNNL	Pacific Northwest National Laboratory
POCO	a subsidiary of UNOCA, originally the graphite division of Pure Oil Company
POX	partial-oxidation reformer or partial oxidation reactor
PPSU	polyphenylsulfone
PRDA	program research and development announcement
PROX	preferential oxidizer or preferential oxidation
PVDF	polyvinylidene fluoride
QA/QC	quality assurance/quality control
R&D	research and development
RFG	reformulated gasoline
RH	relative humidity
SAMPE	Society for the Advancement of Material and Process Engineering
SFAA	solicitation for financial assistance application
SOTA	state-of-the-art
SPEFC	solid polymer electrolyte fuel cell
SPPSU	sulfonated PPSU
SRI	Southern Research Institute
SS	stainless steel
SULEV	super-low-emission vehicle (California standard)
TCR®	Thiokol Composite Resin
THC	total hydrocarbon(s)

TSCE	twin-screw compressor expander
UHV	ultrahigh vacuum
ULEV	ultralow-emission vehicle
UOB™	Under-Oxidized Burner
UOP	formerly known as Universal Oil Products
USCAR	U.S. Council for Automotive Research
WGS	water gas shift
XLPE	cross-linked polyethylene
ZEV	zero-emission vehicle



THE ENERGY CONVERSION TEAM SERIES OF 1999 ANNUAL PROGRESS REPORTS

- Advanced Automotive Technologies
- Fuel Cells for Transportation
- Advanced Combustion and Emission Control
- Advanced Petroleum-Based and Alternative Fuels
- Propulsion Materials

www.ott.doe.gov/oaat



Printed on recycled paper